UNIVERSITÀ DEGLI STUDI FIRENZE

DOTTORATO DI RICERCA IN
AREA DEL FARMACO E TRATTAMENTI INNOVATIVI

CICLO XXX
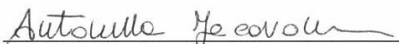
COORDINATORE Prof.ssa Elisabetta Teodori

DESIGN AND SYNTHESIS OF HUMAN NEUTROPHIL ELASTASE (HNE) INHIBITORS

Settore Scientifico Disciplinare CHIM/08

Dottorando   **Tutore**

Dott.ssa Antonella Iacovone   Prof.ssa Maria Paola Giovannoni

(firma)   *(firma)*

Coordinatore

Prof.ssa Elisabetta Teodori

(firma)

Anni 2014/2017

TABLE OF CONTENTS

1. INTRODUCTION

Polymorphonuclear neutrophils (PMN) represent a large percentage of the circulating leukocytes population and are the most abundant type of white blood cells in human blood. They are also known as granulocytes since they contain numerous granules within the cytoplasm and are characterized by a particular morphology of the nucleus, which is segmented into three or five lobes joined together by a thin membrane. These cells play a fundamental role in immune defense against pathogen organisms and are the first mediators in the inflammatory response (Korkmaz, B. et al. 2010). In particular, they perform the antimicrobial activity through two main mechanisms: oxidative and non-oxidative. The first one consists in the production through NADPH-oxidase of the phagolysosomes of many reactive oxygen species, which are extremely toxic for bacteria. Instead, in the non-oxidative mechanism the fusion of cellular phagolysosomes with the primary granules of neutrophils is followed by the release of proteases and peptidases in the same phagolysosome (Faurschou, M. et al. 2003). Recently, in addition to this type of activity, it was discovered a further extracellular defense mechanism through the formation of the so-called NETs, or neutrophil extracellular traps. The main NETs components are DNA, histones, antibacterial granular proteins, and other nuclear and cytoplasmatic proteins, which together play an important role not only for their ability to trap bacteria and fungi but also in immune response, recruiting a large number of neutrophils in the damaged site so increasing the harmful effect on bacteria (Agraz-Cibriana, J. M. et al. 2017) (**Fig. 1**).

Azurophilic (also known as primary) granules:
BPI, neutrophil elastase, cathepsin G, protease 3, azurocidin, myeloperoxidase

Myeloperoxidase

Nets that trap bacteria and neutrophil elastase

Specific and tertiary granules:
Lactoferrin, lipocalin, lysozyme, LL37, MMP8, MMP9 and MMP25
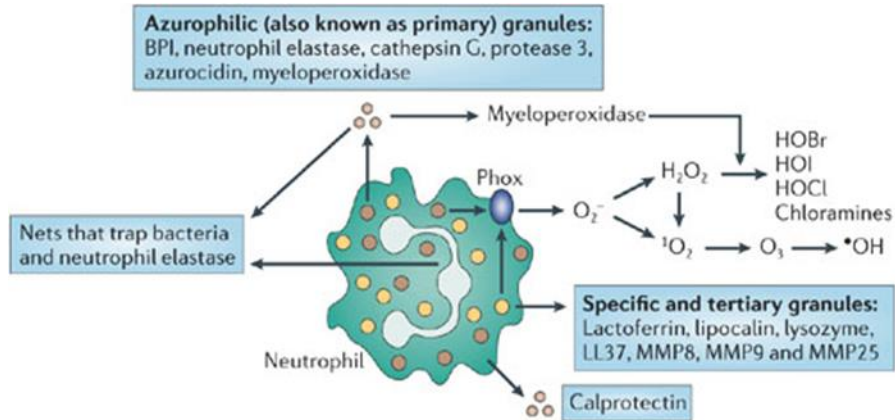
Neutrophil

Calprotectin

Fig. 1: Neutrophil component involved in the immune response

Coming back to the non-oxidative intracellular mechanism, the PMN granules involved in this process can be classified into four different classes according to their protein content and the different ability to be released after pro-inflammatory stimuli by external microorganisms. The granules are divided into primary or azurophil, secondary or specific, tertiary or gelatinase and secretory (Pham, C. T. 2006) (**Fig. 2**).
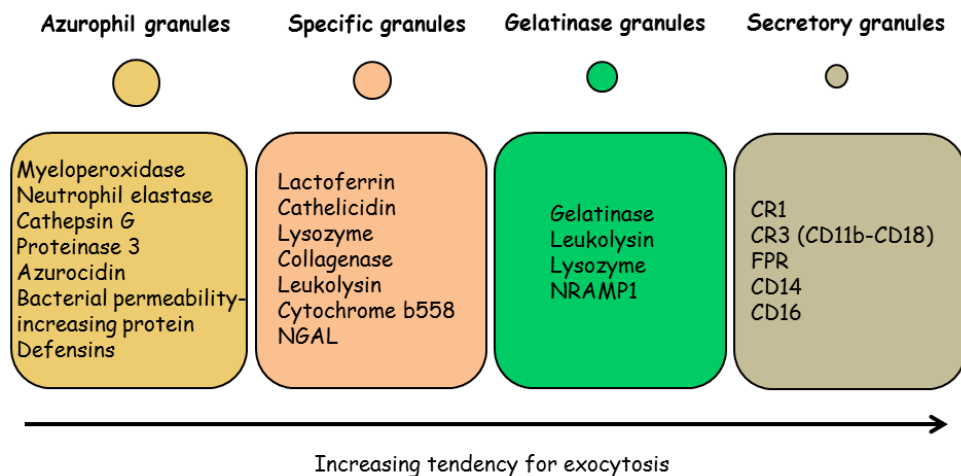

Azurophil granules	Specific granules	Gelatinase granules	Secretory granules
Myeloperoxidase Neutrophil elastase Cathepsin G Proteinase 3 Azurocidin Bacterial permeability-increasing protein Defensins	Lactoferrin Cathelicidin Lysozyme Collagenase Leukolysin Cytochrome b558 NGAL	Gelatinase Leukolysin Lysozyme NRAMP1	CR1 CR3 (CD11b-CD18) FPR CD14 CD16

Increasing tendency for exocytosis

Fig. 2: PMN cytoplasmatic granules

The azurophil granules contain myeloperoxidase, some bactericidal proteins and three serine proteases: *Proteinase 3* (PR3), *Cathepsin G* (CG) and *Neutrophil Elastase* (NE).

1.1 HUMAN NEUTROPHIL SERINE PROTEASES (NSP)

Human Neutrophil Serine Proteases (NSP) are enzymes with high homology belonging to the chymotrypsin family. NSP are stored in azurophil granules as zymogens associated with proteoglycans, which are activated after inflammatory stimuli by the hydrolysis of the N-terminal extremity by the enzyme Dipeptidyl Peptidase 1, also known as Cathepsin C.

The main enzymes belonging to the NSP class, in addition to the Human Neutrophil Elastase, which will be discussed in detail in the next paragraph, are:

- *Cathepsin G*, a protein of 28.5 kDa consisting of 235 amino acids residues and belonging to a family of cysteine cathepsins and aspartic acid proteases. The gene responsible for encoding this enzyme is CTSG, located in the chromosome 14q. Its main function is the degradation of the structural components of the extracellular matrix of pathogens (Turk, V. et al. 2012).

- *Proteinase 3*, an enzyme of 29 kDa consisting of 222 amino acids residues and expressed by PRTN3, a gene located in the chromosome 19. It contributes to the degradation of the chemokine resulting in a truncated form with more potent neutrophil chemoattraction activity (Van den Sten, P. E. et al. 2000).

- *Neutrophil Serine Protease 4*, recently discovered and sharing 30% of identity for other proteases. The peculiarity of this enzyme is its ability to hydrolyze a particular peptide bond involving an arginine residue (Perera, C. N. et al. 2013).

1.2 HUMAN NEUTROPHIL ELASTASE (HNE)

HNE is an enzyme belonging to the chymotrypsin super-family and it is stored in the azurophil granules of polymorphonuclear neutrophils. It is a globular glycoprotein with a molecular weight of 29-33 kDa, consisting of a single polypeptide chain of 218 amino acids and two asparagine-linked carbohydrate side chains at Asn95 and Asn144 (Lucas, S. D. et al. 2011). It is stabilized by four disulfide bridges and it shows basic properties due to the presence of 19 arginine residues affording a value of the isoelectric point around 10-11. HNE is encoded by the ELA2 gene, located in the chromosome 19 and consisting of 5 exons and 4 introns; it is synthetized as inactive zymogen of 267 amino acids representing the so-called pre-proform (Korkmaz, B. et al. 2008). This pre-proform undergoes various consecutive steps that lead to the mature enzyme. The signal peptide, consisting of 29 amino acids, is removed to yield the proform, which is glycosylated on the amino acids Asn109 and Asn159. Subsequently, the cleavage by Cathepsin C of the N-terminal fragment affords a structural rearrangement of the N-terminal region, which inserted into the protein core, leads to the enzyme catalytically active (Hajjar, E. et al. 2010) (**Fig. 3**).
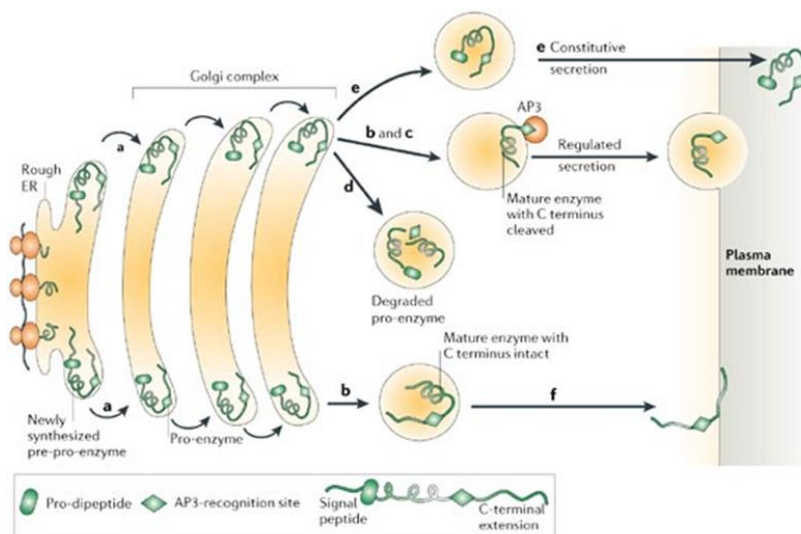

Fig. 3: Enzyme activation

The X-ray crystallographic analysis shows the tridimensional HNE structure, that adopts a fold consisting of two β-barrels made each of six anti-parallel β-sheets, analogously to all chymotrypsin-like serine proteases. There are also two α-helix structures and one of this shows a C-terminal extremity (**Fig. 4** yellow cylinders); it is also possible to identify the two asparagine residues (Asn109 and Asn159) corresponding to the two N-glycosylation sites (**Fig. 4** yellow stars). Finally, it is possible to highlight the three amino acid residues indispensable for the proteolytic activity and constituting the active site of the enzyme (**Fig. 4** green stars) (Hajjar, E. et al. 2010).
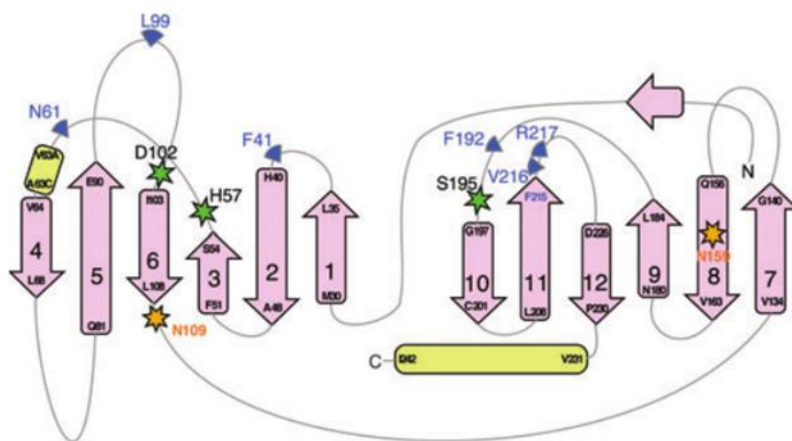

Fig. 4: HNE structure

This last one represents the so-called catalytic triad consisting of Ser195, Asp102 and His57 (Fujinaga, M. et al. 1996). The HNE proteolytic activity occurs through three fundamental steps: interaction with the substrate, acylation of Ser195 and deacetylation. The OH group of the Ser195 is a potent nucleophile and activated by the transfer of an electron from the carboxylic group of the Asp102 and able to attack a specific carbonyl group of the substrate. Once the nucleophilic attack occurred, the generated tetrahedral intermediate evolves in the formation of the acyl-enzyme complex through the cleavage of the peptide bond. The acyl-enzyme complex is then attacked by a water molecule to generate a new tetrahedral intermediate that collapses,

assisted by general acid catalysis from His57. This results in the release of the substrate as acid (COOH form) and in the regeneration of the enzyme (**Fig. 5**) (Kelly, E. et al. 2008) (Korkmaz, B. et al. 2008).
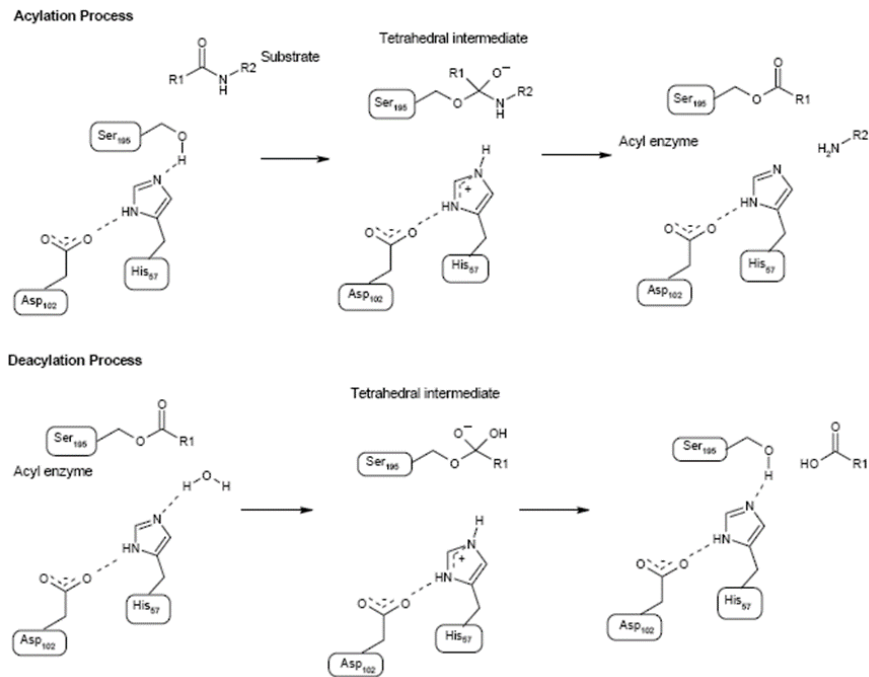

Fig. 5: HNE action mechanism

1.3 HNE PHYSIOLOGICAL ROLE

Analogously to other NSPs, HNE plays an important role in physiological condition and it is considered a multifunctional enzyme able to operate in pathogens killing, inflammatory processes and maintenance of tissue homeostasis (Pham, C. T. 2006). Furthermore, it is implicated in the chemotaxis and migration of inflammation mediators by the hydrolysis of adhesion molecules (**Fig. 6**) (Cepinskas, G. et al. 1999) (Hermant, B. et al. 2003).
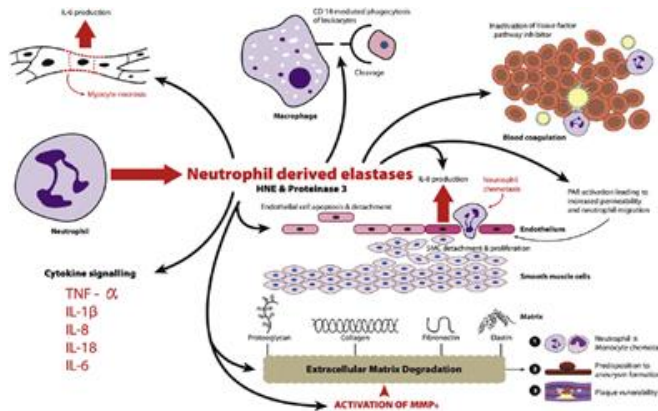
Fig. 6: HNE physiological role

HNE release occurs through a series of intracytoplasmatic reactions, which afford the entry of calcium ions into the granules. This event entails the beginning of the degranulation process in which all the contents of the various granules are released in the neutrophils. In particular, the increase of the intracellular calcium ions concentration allows the interaction of the protein (t)-SNARE of the membrane with the granules protein (v)-SNARE; this interaction leads to their fusion resulting in the release of HNE into the extracellular environment. However, although the most part of HNE is released externally, a certain percentage remains bound to the plasma membrane surface so increasing the catalytic activity and resistance to inactivation by endogenous inhibitors (Lee, W. L. et al. 2001).

1.3.1 Antimicrobial activity

This function can be performed by HNE both intracellularly and extracellularly. As regard HNE intracellular antimicrobial activity, it is synergic with the oxygen reactive species, ROS, and takes place after the pathogen phagocytosis by azurophil granules. In particular, the fusion of the plasma membrane with the phagosome membrane triggers the reduction of molecular oxygen to superoxide anion by the enzyme NADPH-oxidase. This phenomenon leads to the formation of a gradient inducing the entry of H^+ and K^+ ions, which mediate

the NSPs release from their matrix. Additionally, intraphagous myeloperoxidase (MPO) allows the oxidation of the Cl^- to ClO^-, a potent antimicrobial agent (**Fig. 7**) (Pham, C. T. 2006) (Nauseef, W. M. 2007). These phenomena, together with HNE proteolytic activity, produce a synergistic effect for the pathogen kill.
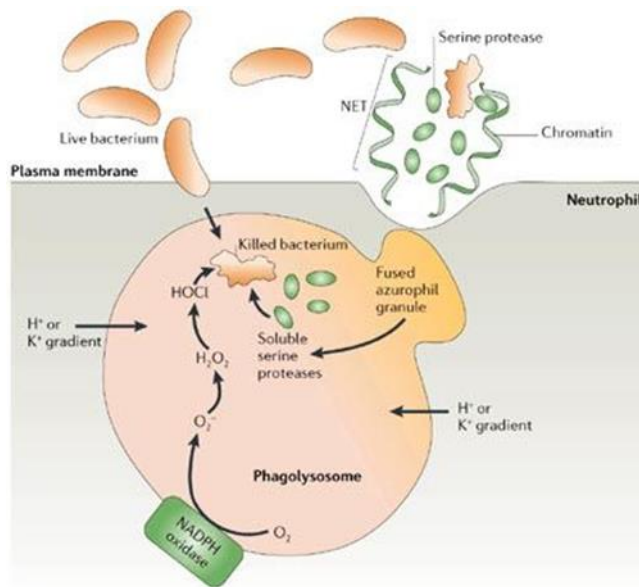

Fig. 7: Intracellular antimicrobial activity

Instead, the extracellular antimicrobial activity can be both indirect and direct. In the first case, HNE produces antimicrobial proteins by hydrolysis of serum proteins, as well as breaking the bacterial virulence factors (Weinrauch, Y. et al. 2002). About the direct action, HNE is able to trap and destroy pathogens through the formation of the neutrophil extracellular traps (NETs). These particular structures are mainly composed by chromatin and cationic proteases that are released into the extracellular environment after the activation of the neutrophils by specific stimuli such as bacterial endotoxins or other pathogenic factors. Following activation, ROS accumulation generates a cellular response that destroys the structural components of the ECM,

resulting in cell flattening that allows the translocation of NSPs in the nucleus with subsequent proteolytic action against histones which leads to the DNA decondensation (**Fig. 8**) (Briukmann, V. et al. 2004).
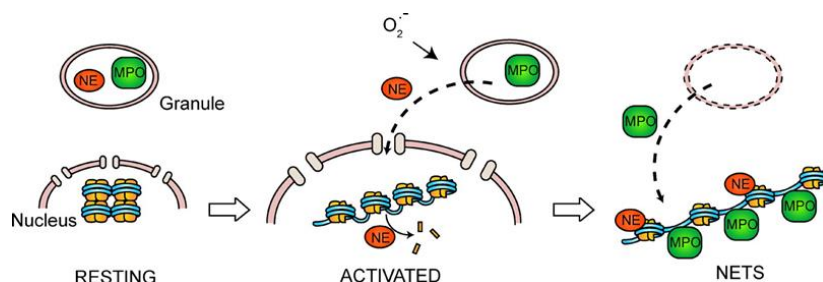

Fig. 8: NETs formation

1.3.2 Anti-inflammatory activity

In addition to its bactericidal properties, HNE is also an important regulator of the local inflammatory response. The role that HNE plays in the inflammatory processes is very complex and still not entirely clear. It plays a double role that leads to modulate the chemokine action. Chemokines are a family of small peptides involved in the recruitment of leukocytes to the inflammatory sites; they are released by various inflammatory cells and they bind to their receptors on the leukocyte surface (Pham, C. T. 2006). Removal of peptide fragments by NSPs of certain chemokines produces an increase in the receptor affinity. In particular, the hydrolysis of the N-terminal portion of Interleukin-8 (IL-8) by HNE leads to a species with higher chemotactic activity (Padrines, M. et al. 1994). Likewise, the hydrolysis of the C-terminal portion by HNE allows a greater recall of macrophages and dendritic cells (APC cells), which possess receptors similar to this peptide (Wittamer, V. et al. 2005). In contrast, not all modifications of these proteins by HNE lead to an increase in their anti-inflammatory activity. For example, the hydrolysis by HNE of CXCL12 and CCl3 proteins, also known as SDF1α and MEP1α respectively, leads to a loss of their chemotactic activity (Ryu, O. H. et al. 2005) (Rao, R. M. et al. 2004).

Recent studies highlight a correlation between HNE and Tumor Necrosis Factor alpha (TNFα), even if the nature of this correlation is still unclear. Some studies affirm that there is a loss of activity after the interaction between the enzyme and TNFα; others show that there is the formation of biologically active small soluble peptides (Kormaz, B. et al. 2010). A further physiological role in the inflammatory processes is related to the interaction with the Tool-Like Receptor 4 (TLR-4), a transmembrane glycoprotein that contributes to the defense against pathogens and participates in the innate immune response (Walsh, D. E. et al. 2001).

1.3.3 HNE and tissue homeostasis

HNE is able to maintain tissue homeostasis in our body since it repairs damaged tissues as well as it degrades the structural proteins (Bieth, J. G. 1986). On the Extracellular Matrix (ECM), HNE performs a proteolytic action degrading elastin, collagen, fibronectin, laminin and proteoglycans (Barret, A. J. et al. 1986). Finally, HNE is able to activate the complement cascade in plasma, as well as it degrades some coagulation factors and it interacts with the immunoglobulins IgG, IgA and IgM (Havemann, K. et al. 1978).

1.4 HNE ENDOGENOUS INHIBITORS

The proteolytic activity of serine proteases, essential for the maintenance of important functions in our organism, can be dangerous if not properly maintained under control (Von Nussbaum, F. et al. 2016). The first fundamental regulatory mechanism is the inactivation of these enzymes through the storage into specialized compartments, such as azurophil granules for serine proteases. However, only this mechanism is insufficient to regulate their proteolytic activity, so the presence of endogenous inhibitors that completely inhibit the activity of proteases (Von Nussbaum, F. et al. 2015a) is of great importance. These inhibitors can be grouped into three main classes: serpins (serine protease inhibitors) (Ekeowa, U. I. et al. 2009), TIMPS

(tissue proteins of metalloproteases) (Gipson, T. S. et al. 1999) and cystatin (cysteine protease inhibitors) (Turk, V. et al. 2008). In particular, HNE activity is mainly regulated by **α1-antitrypsin** (AAT) (also known as **α1-proteinase inhibitor**, **α1-PI**), **monocyte and neutrophil elastase inhibitor** (**MNEI**) (also called **Serpine B1**), belonging to the family of canonical inhibitors including also the **leukoprotease secretion inhibitor**, **SLPI** and **elafin**, and finally **α2-macroglobulin**. Several studies demonstrated that these inhibitors, in addition to the regulation of the inflammatory processes by controlling the proteolytic activity of enzymes, could directly affect other processes such as leukocyte chemotaxis and release of pro-inflammatory mediators, contributing to defending the organism against pathogens attack (Groutas, W. C. et al. 2011).

α1-Antitrypsin is a water-soluble glycoprotein with a molecular weight of 53 kDa, mainly produced by the liver, but in small quantities also by monocytes, macrophages, pulmonary alveolar cells and intestinal and corneal epithelium. It is released into the bloodstream, where it has a concentration of 0.9-1.75 g/L, and through this reaches the lungs. At the level of the lower airway, it regulates not only the activity of HNE, the main substrate of this inhibitor, but it is also active against other targets such as PR3 (Janciauskiene, S. M. et al. 2011). It has a three-dimensional structure consisting of three β sheets and a reactive mobile central ring (RCL) in which there is a particular amino acid sequence that acts as a binding site for target proteases (Lomas, D. A. et al. 2004). Its blood concentration increases considerably in response to inflammatory stimuli or infections, allowing to maintain the correct proteolytic activity of elastase (Janciauskiene, S. M. et al. 2011). A deficiency of α1-PI can significantly increase the risk of COPD (Chronic Obstructive Pulmonary Disease) in the lower airway and may cause liver disease, including cirrhosis and hepatocellular carcinoma (Heutinck, K. M. et al. 2010) (**Fig. 9**).
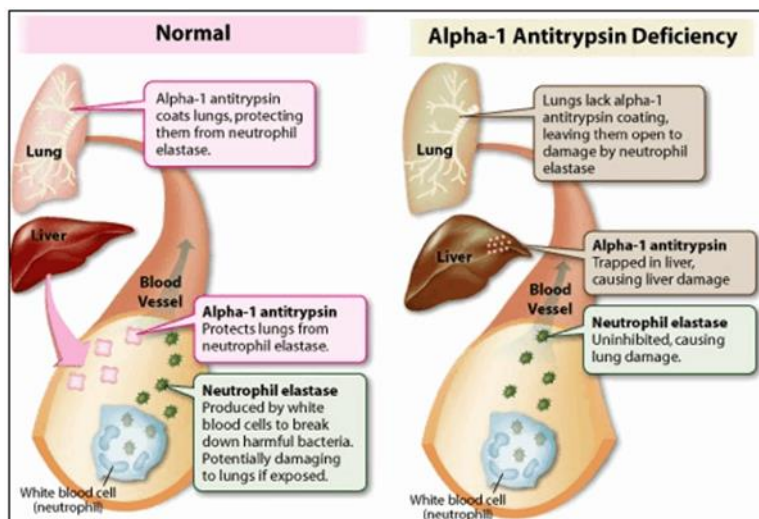
Fig. 9: Physiological and pathological roles of α1-PI

MNEI, or **Serpin B1**, contained within the neutrophil granules, acts not only on elastase, but also on PR3 and CG, performing a similar function, as above reported. In particular, it is involved in the regulation of lung inflammatory processes, such as cystic fibrosis and chronic pathologies due to excessive protease activity of neutrophils (Benarafa, C. et al. 2002).

SLPI, or inhibitor of leukoprotease secretion, is another important serine protease inhibitor, which, unlike MNEI, does not inhibit PR3 activity (Thompson, R. C. et al. 1986). It belongs to the family of chelonianin and it is present in all body fluids, including tears, saliva, seminal fluid, bronchial secretions and intestinal mucus. It is a non-glycosylated protein with a molecular weight of 11.7 kDa and with strong basic characteristics (pI = 11) (Quabius, E. S. et al. 2015). It is produced in the lungs by epithelial tracheal and bronchial cells and by the alveolar cells of type II (Sallenave, J. M. 2002) and its concentration is superior in the higher airways with respect to the deepest ones. Although its role is not yet fully understood, it has recently been shown to have an important function in the regulation of the immune response

and in the control of inflammatory and septic shock processes (Zhong, Q. Q. et al. 2017).

Elafin, or elastase specific inhibitor (ESI), is a non-glycosylated protein of 6 kDa, originally isolated from the skin of patients with psoriasis but also present in pulmonary secretions (Wiedow, O. et al. 1990). Unlike α1-PI, classified as a "systemic" inhibitor because it is synthesized in the liver and then spilled into the bloodstream, elafin and SLPI too are called "alarm" inhibitors because they are directly produced and released into the epithelium of the airways in response to the release of cytokines such as interleukin IL-1β and the tumor necrosis factor (TNFα), together with the HNE (Zhong, Q. Q. et al. 2017) (Pfundt, R. et al. 2000). As SLPI, elafin has tracheo-bronchial origins and it is synthesized by pneumocytes of type II (Sallenave, J. M. 2000). It is a basic protein (pI = 9.7), stable at acid medium and its amino acid sequence as well as its active site share 40% of identity for SLPI (Wiedow, O. et al. 1990). It is a powerful inhibitor of HNE and PR3, while it has no activity against CG (Zani, M. Z. et al. 2004). It shows similar functions to SLPI because it performs anti-inflammatory, immunomodulatory and antibacterial activities. This last one is due to its positive charge, which causes destabilization of the pathogen membrane (Scott, A. et al. 2011). Consequently, an altered expression of this protein seems to be crucial for the development of inflammatory airways disease, but also skin diseases such as psoriasis (Wiedow, O. et al. 1990).

Finally, **α2-macroglobulin** is a polyvalent homotetramer protein with a molecular weight of 725 kDa present in high concentration in human blood (2mg/L) (Petersen, C. M. 1993). It inhibits plasma serine, cysteine and metal proteases (Janciauskiene, S. M. et al., 2011) through a mechanism of action completely different from those previously described for other inhibitors. In fact it traps the enzyme, causing loss of its proteolytic activity only towards the macromolecules but not for small peptides, which can be hydrolyzed in the catalytic site (Travis, J. et al. 1983). In addition, due to its high molecular

weight, α2-macroglobulin is not able to spread outwardly to the endothelium, so it has been hypothesized that its main role is to control the proteases activity only at the level of the blood circulation (Sottrup-Jensen, L. 1989).

All the enzymes above reported may lose their activity due to oxidative agents or to the same proteases. Primarily, HNE is able to hydrolyze some of these inhibitors, such as elafin. Moreover, other proteases, such as MMPs (Taggart, C. C. et al. 2001) or cytyl cathepsin (Geraghty, P. et al. 2007), are able to inactivate endogenous inhibitors. In other cases, it may also occur that the adhesion of the neutrophils to the extracellular matrix relegates proteases, released from the granules, into the periplasmic space. So that endogenous inhibitors are no longer able to reach and hydrolyze the enzymes that continue to carry out its proteolytic activity (Pham, C. T. 2006).

1.5 PATHOLOGIES RELATED TO HNE

Neutrophils represent the first indispensable line of defense during the inflammatory processes. However, as described in the previous paragraph, HNE activity needs to be strictly controlled, as its imbalance can contribute to the development of very serious diseases with a very negative impact on tissue integrity (Heutinck, K. M. et al. 2010). The involvement of HNE and other NSPs in the development of chronic pulmonary inflammatory diseases is widely documented and correlated with an imbalance between HNE and endogenous inhibitor activity, which causes an increase of the proteolytic activity and an infiltration of neutrophils following a massive inflammatory response (Korkmaz, B. et al. 2010) (**Fig. 10**).
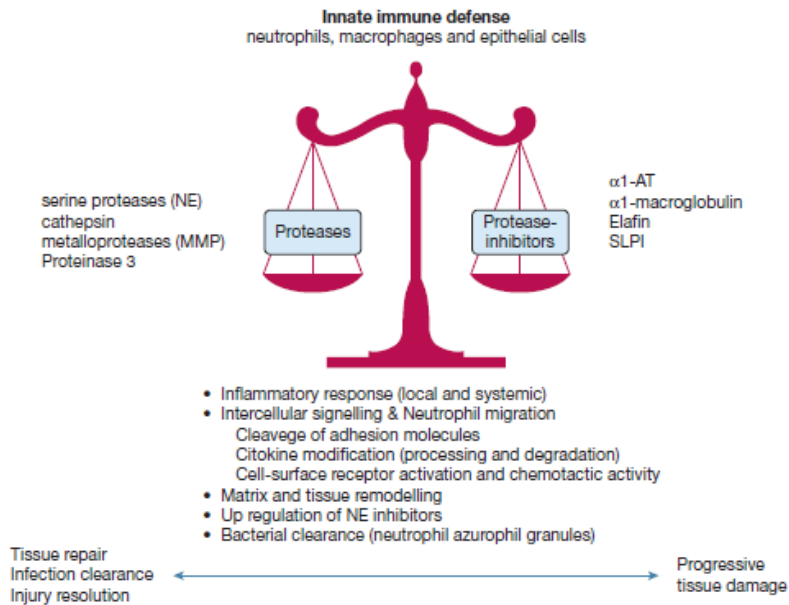
Fig. 10: HNE-anti-proteases balance

There are numerous chronic inflammatory pathologies affecting the respiratory system caused by this type of imbalance: chronic obstructive pulmonary disease (COPD), acute lung injury (ALI), acute respiratory distress syndrome (ARDS) and cystic fibrosis (CF) (Korkmaz, B. et al. 2010).

COPD, or chronic obstructive pulmonary disease, is a pathology characterized by chronic bronchitis and emphysema, responsible for the alteration of normal respiratory activity, since they are characterized by a limited inflow of air into the pulmonary tree (Barnes, P. J. et al. 2005). The World Health Organization (WHO) estimates that 210 million people are affected by COPD and in 2020 it will become the fourth leading cause of death. The primary cause of COPD is tobacco smoke but other risk factors include indoor and outdoor air pollution, occupational dusts, and chemicals or frequent lower respiratory infections during childhood, as well as genetic α1-PI deficiency (Lucas, S. D. et al. 2011). The α1-PI absence affects about 2% of cases and it is due to a genetic mutation that makes the individual not able to synthetize a sufficient

amount of α1-PI, resulting in an uncontrolled HNE proteolytic activity in the pulmonary tissue and thus increasing the risk of premature pulmonary emphysema (Wewers, M. D. et al. 1987). As regards the tobacco smoke, an epidemiologic study conducted on smokers affected by COPD found an enlargement of the air space caused by the breakdown of the alveolar cells in 10% of patients (American Thoracic Society, 2003). Tobacco smoke activates macrophages of the airways, which in turn stimulate the release of chemotactic factors such as IL-8 and leukotriene B4, inducing pulmonary neutrophil accumulation and subsequent secretion of their proteases, HNE and MMPs (Barnes, P. J. et al. 2005). Therefore, there is a strong imbalance between proteases and anti-proteases, followed by an increase of the release of TNF-α and other pro-inflammatory mediators that cause the destruction of pulmonary parenchyma and extracellular matrix (Houghton, A. M. et al. 2006). All these factors cause an epithelial damage, increased microvascular permeability, mucus hypersecretion and mucosal dysfunction (Hoenderdos, K. et al. 2013) (**Fig. 11**).
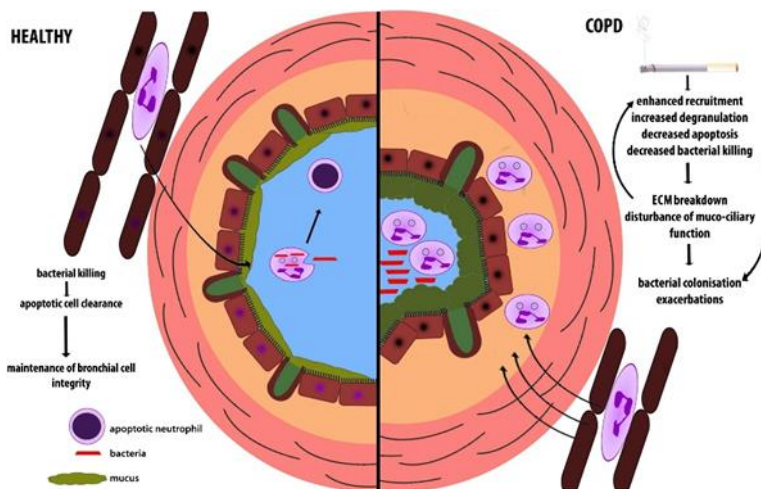

Fig. 11: Neutrophils role in healthy conditions and in COPD disease

However, the available COPD therapeutics are limited to a few classes of agents such as glucocorticosteroids, bronchodilators, anticholinergics,

phosphodiesterase inhibitors and supplemental oxygen. These therapeutics only help to control its symptoms and increase quality of life for the patients, as no currently available treatment reduces the progression of COPD or suppresses the inflammation in small airways and lung parenchyma (Matera, M. G. et al. 2012).

ARDS, acute respiratory distress syndrome, and ALI, acute lung injury, are two pulmonary inflammatory pathologies caused by trauma and sepsis (Tsushima, K. et al. 2009). ARDS and ALI are characterized by an increase in hypoxemia and alveolar-capillary permeability, whose severity, greater in ARDS, is the main element distinguishing these two pathologies (Korkmaz, B. et al., 2010).

→ ARDS is characterized by the inflammation of the lung parenchyma, which causes an alteration of normal gaseous exchanges with concomitant release of pro-inflammatory mediators. Various studies showed that this pathology is caused by a strong increase in oxidative stress levels, but especially by an alteration in the balance between proteases and anti-proteases, in particular a down regulation of synthesis of elafin, a specific and potent HNE inhibitor (Wang, Z. et al. 2009).

→ ALI is a pathology caused by a variety of factors including Gram-negative bacterial infection and it is characterized by interstitial and alveolar edema, associated with an increase in neutrophil infiltration at this level. Also in this case, the overproduction of HNE in the plasma and the absence of a sufficient amount of inhibitors is the main cause of this disorder (Kawabata, K. et al. 2002).

Generally, during the initial phase of both pathologies, neutrophils are massively accumulated in vascular tissue and they are responsible for microvascular damage, which in turn results in epithelial damage, increased capillary permeability, and interstitial edema. After the formation of the edema, HNE also generates powerful chemiotactic peptides, which increase

inflammatory response in the lungs and favor mucus production (Leavell, K. J. et al. 1996).

Cystic fibrosis (CF) is an inherited condition with an incidence rate of approximately 1 in 2500 new born babies (Tizzano, E. F. et al. 1992); it is prevalent in Europe and in the United States and it is the most common fatal genetic disease in Caucasian populations till now (Wagner, C. J. et al. 2016). CF is an autosomal recessive genetic disorder caused by loss of expression or functional mutations of the cystic fibrosis transmembrane conductance regulator (CFTR), which encodes for an ionic channel involved in the flow of chloride and sodium ions across epithelial membranes leading to increased and dehydrated mucus secretions in the lungs. Consequently, a mutation of this gene has significant abnormalities in the function of the exocrine glands, resulting in alteration of ionic composition and increased viscosity of epithelial secretions. In particular, mucus becomes dense and sticky, preventing the proper passage of air through the respiratory airways (Buchanan, P. J. et al. 2009). The sweat glands and salivary glands, the small intestine glands, the pancreatic glands and the bile ducts, the mammary glands and the deferent duct can be also affected by this pathology (Voynow, J. A. et al. 2008) (**Fig. 12**).
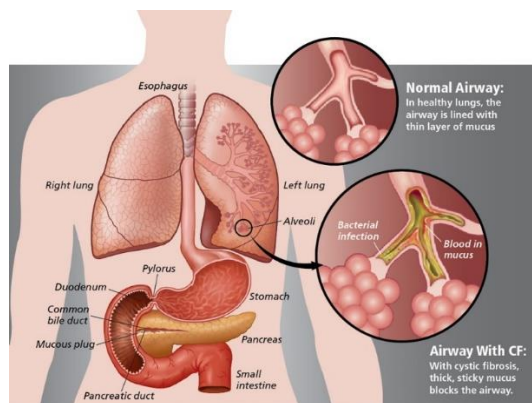

Fig. 12: Organs affected by CF

The alteration of the normal characteristics of the respiratory airways surface results in an increase in susceptibility to the attack of bacterial agents and the activation of a vigorous inflammatory response as a result of increased mucus production which, in healthy individuals, is released during an infection (Nichols, D. P. et al. 2015). However, in patients affected by cystic fibrosis the fundamental problem lies in the high concentration of lung neutrophils, which rises up to 70% compared with 1% in healthy individuals (Buchanan, P. J. et al 2009). Neutrophil are recruited to these sites of infection by increased expression of chemoattractants such as IL-8 by lung epithelial tissue. The increase of IL-8 promotes a further increase in HNE levels released by the same neutrophils, thereby creating a state of chronic infection (Devaney, J. M. et al. 2003). The damage can result in the destruction of the cellular epithelium, in the alteration of the ciliary beat and increased mucus secretion, affording decreased mucus clearance, alteration of the characteristics of the same mucosal secretion and particularly dangerous, the failure to protect the organism against the action of pathogens (Nichols, D. P. et al. 2015) (**Fig. 13**).
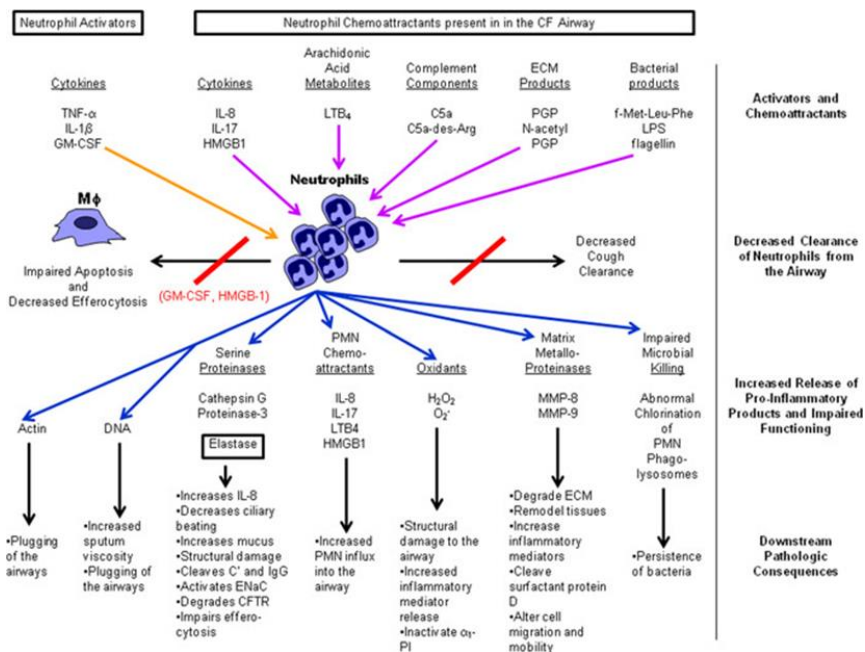

Fig. 13: Neutrophils role in Cystic Fibrosis

Introduction

In addition to all these pathologies, it has been observed that HNE is also involved in the development and progression of breast and lung cancer. In fact, it was demonstrated that many types of cancer originate from bodily districts affected by chronic inflammatory conditions (Coussens, L. M. et al. 2002) and that PMN neutrophils and their proteases are greatly involved in the progression of the diseases (Demaria, S. et al. 2010). It has been observed that tumor cells form metastases through a series of consecutive events that recall those whereby neutrophils act at the level of inflammation sites or fight an infection (Sato, T. et al. 2006). The tumor cells are also able to release proteases to favor their invasion process in host tissues, because they need to overcome a variety of elastin, collagen and proteoglycan tissue barriers (Lu, P. et al. 2012). In addition, it was also demonstrated that the deterioration of elastic fibers caused by HNE could favor the diffusion of other cancer cells or the generation of elastin fragments with cytokine-like properties, such as elastokines (Antonicelli, F. et al. 2007). These last ones favor the tumor progression in different ways:

- o they increase the phlogistic phenomenon and therefore the chemotactic activity of monocytes and neutrophils;
- o they increase the expression of some MMPs in fibroblasts;
- o they act as potent angiogenic agents and stimulate the production of IL-8 by endothelial cells;
- o they amplify the expression of tumor cell growth factors (Hornebeck, W. et al. 2005).

Among the other pathologies not related to the respiratory system where HNE seems to be involved, we can mention rheumatoid arthritis (Capsoni, F. et al. 2005), dermatitis and psoriasis (Wetzel, A. et al. 2006) and atherosclerosis (Henriksen, P. A. et al. 2008).

Rheumatoid arthritis is characterized by the articular infiltration of neutrophils and monocytes, which contribute to the degradation of cartilage tissue by the production of reactive oxygen species (Capsoni, F. et al. 2005)

and enzymes with proteolytic activity. In particular, HNE is able to destroy important proteins constitutive of cartilage tissue, such as type II collagen and proteoglycans (Wiedow, O. et al. 1992).

Psoriasis and some types of **dermatitis**, such as contact dermatitis and atopic dermatitis, are skin infections caused by a defect in skin cohesion, resulting in formation of micro-abscesses, papules and erythematous plaques (Dhanrajani, P. J. 2009). The loss of contact of keratinocytes seems to be due to the lysis of the adhesion proteins normally forming the desmosome junctions, suggesting a possible role of HNE in this pathology (Brown, R. S. et al. 1993) (Wiedow, O. et al. 1992).

Finally, **atherosclerosis** is a chronic inflammatory disease of the arteries characterized by the progressive formation of atherosclerotic plaques, which can cause obstruction of the vessels due to their breakup or detachment and their transport to the plasma (Garcia-Touchard, A. et al. 2005). This multifactorial inflammatory process results in cerebral and cardiovascular complications associated with an increase in the morbidity and mortality and its major clinical manifestations are acute heart attack, stroke and peripheral artery damage (Hartwig, H. et al. 2015). Several studies confirmed that HNE is involved in plaque formation (Dollery, C. M. et al. 2003) since endothelial cells, after activation, synthesize adhesion molecules and chemotactic factors of neutrophils such as cytokines and IL- 8 (Naruko, T. et al. 2002) (Fig. 14).
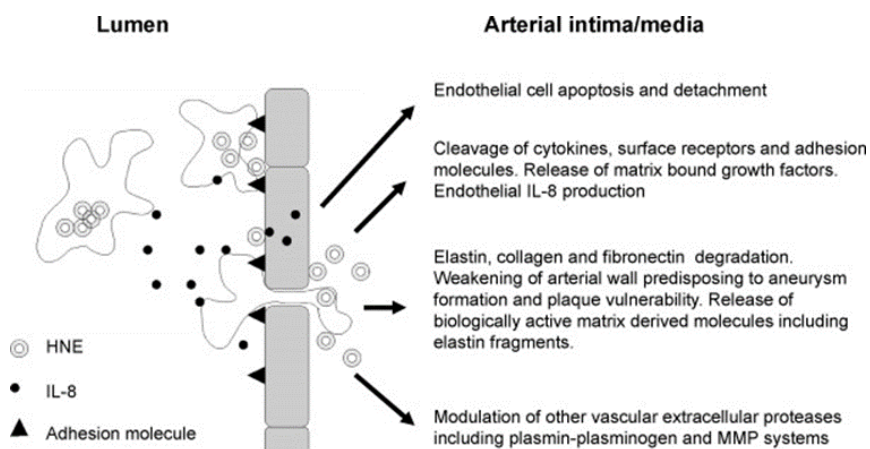
Fig. 14: Atherosclerosis and HNE

1.6 HNE INHIBITORS

In the last three decades, many stakeholders in academia and the pharmaceutical company have discovered a variety of innovative elastase inhibitors. We will briefly summarize this evolution of HNE inhibitors along five generations: 1st generation, 2nd generation, 3rd and 4th generation, 5th generation (Von Nussbaum, F. et al. 2015a).

1.6.1 *1st generation*

Peptide inhibitors

Peptide inhibitors are high molecular weight proteins, consisting of a variable number of amino acid residues (350-500) and they are able to work as highly specific suicidal substrates against HNE. An important class of the peptide inhibitors is represented by the serpins, endogenous HNE inhibitors already described, which can be obtained either by purification of natural compounds or by genetic engineering techniques. However, despite being characterized by a highly specific activity, these types of inhibitors have two major disadvantages. The first one concerns the route of administration, since they can be administered only intravenously or by inhalation. The second one is

due to low stability, which increases in particular pathophysiological conditions or oxidative stress. Pathogenic agents and/or microbial proteases may partially degrade these inhibitors and thus block their function (Sallenave, J. M. 2010) (Guyot, N. et al. 2008), or the inhibitor may be inactivated due to the oxidation of its methionine residues (Nobar, S. M. et al. 2005).

1.6.2 *2nd generation*

In contrast to the first generation, these small molecules (SMOLs) are also able to reach and inhibit membrane-bound elastase. Of further importance, such inhibitors might be able to enter neutrophils cells and thereby interfere with the host defense function of elastase (Von Nussbaum, F. et al. 2015a). Compounds belonging to the 2nd generation can function as acyl-enzymes or the transition state analogues.

Acyl-enzyme inhibitors
The acylating inhibitors afford a tetrahedral transition state analog, which collapses with the displacement of a leaving group to afford a very stable acyl-enzyme complex that can also irreversibly inactivate the enzyme (**Fig. 15**). The main concern related to acyl-enzyme inhibitors is its hydrolysis to regenerate the free enzyme and this phenomenon depends upon the acylating power of the inhibitor. This ability is evaluated by its acylating and deacylating power rates, K_{on} and k_{off}, respectively, and the main goal has been to develop acylating agents which generate a stable acyl-enzymes complex (Lucas, S. D. et al. 2011).
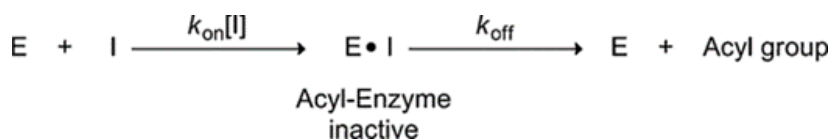
$$E \ + \ I \ \xrightarrow{k_{on}[I]} \ E \bullet I \ \xrightarrow{k_{off}} \ E \ + \ \text{Acyl group}$$

Acyl-Enzyme
inactive

Fig. 15: Interaction acyl-enzyme inhibitors-HNE

Introduction

N-benzoyl pyrazoles, identified by Prof. Quinn's group using high-throughput chemolibrary screening, represent a series of potent and specific HNE inhibitors and the most active terms show a K_i in the nanomolar range (**Fig. 16**).
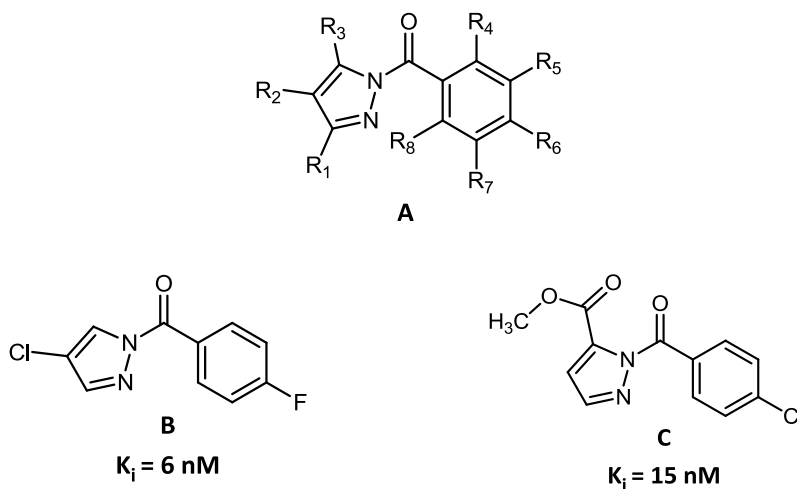

Fig: 16: *N*-benzoyl pyrazoles

They act as pseudo-irreversible HNE inhibitors and molecular modeling studies showed how the active derivatives effectively bind to the active site of HNE by blocking the enzyme (Schepetkin, I. A. et al. 2007). For this purpose, the substituted phenyl ring proved to be fundamental, but the ortho substitution is not favorable for the activity, since it prevents the free rotation of the phenyl rings locking the molecule in a position not suited for the interaction with the active site. (Khlebnikov, A. I. et al. 2008).

In 1982 Teshima et al. reported a series of 4H-3,1-benzoxazin-4-ones as serine protease inhibitors with a low selectivity for HNE. Ser195 attacks the carbonyl of the benzoxazinone leading to the ring opening to form a stable acyl-enzyme complex (Radhakrishnan, R. et al. 1987) (**Fig. 17**).
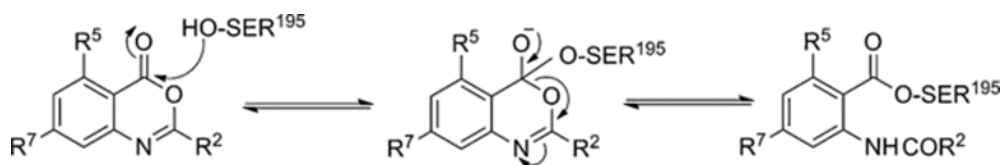
Fig. 17: benzoxazinones mechanism of action

Further studies were carried out to improve the inhibitory activity and selectivity of these compounds, till 2009 a class of 2-pyridine-benzoxazinone derivative having an IC_{50} = 61 nM (**Fig. 18**, compound **D**) was discovered (Shreder, K. R. et al. 2009). Structure activity relationship studies indicate that pyridine-3-yl at position 2 of benzoxazinone is preferred over a phenyl ring. Electron-donating groups at 7-position improves the chemical stability of benzoxazinones and the disubstitution at 5- and 7-position is particularly favorable for HNE inhibitory activity. Among the 5,7-disubstituted benzoxazinones examined, the 5-ethyl-7-methoxy derivatives, bearing a piperazine or a piperidine at pyridine ring (**Fig. 18**, compounds E and F), were found to have the best balance of chemical stability and potency (Lucas, S. D. et al. 2011).
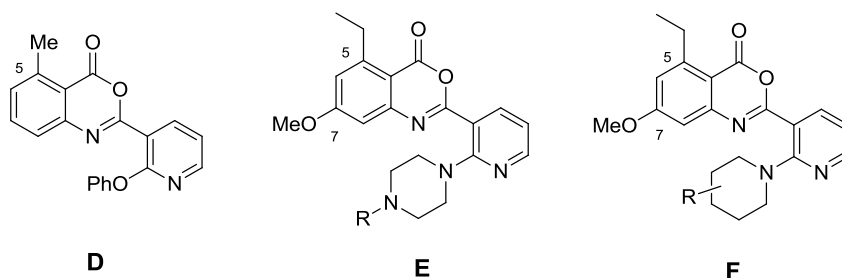

Fig. 18: 2-Pyridin benzoxazinone derivatives

β-lactam derivatives represent another important class of inhibitors. The first report of β-lactam-based HNE inhibitors by Merck back in 1986 led to major efforts to obtain β-lactams as promising candidates for further development as HNE inhibitors. Various modifications were performed on the β-lactam

29

nucleus and recently the group of Prof. Moreira came to the synthesis of 4-oxo-β-lactams, which are potent and selective HNE inhibitors. Some docking studies have also shown that the presence of two ethyl groups on C3 of the β-lactam allows a good anchoring of the molecule into the hydrophobic pocket S1. It is due to the correct orientation of Ser195 oxygen atom versus at least one of the carbon atoms of the carbonyl groups of the β-lactam ring (Mulchande, J. et al. 2010). An example is compound **G** (k_{on}= 3.24 x 10^6 M^{-1} s^{-1}).

G
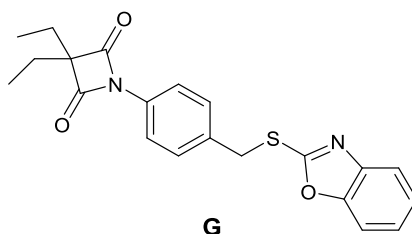
Transition state analogues

Compounds acting as transition-state analogues are attacked by Ser195, forming a stable tetrahedron intermediate which inhibits irreversibly HNE. The bond is also stabilized by the formation of hydrogen bridges between the functional groups of the molecule and NH groups of the amino acid residues present in the active site. The older inhibitors of this type were molecules showing a formyl group. However, due to pharmacokinetic problems, the research was subsequently focused on the replacement of aldehyde hydrogen atom with electron-withdrawing groups to improve the stability and the electrophilicity of the carbonyl carbon atom (Lucas, S. D. et al. 2011).

The first inhibitors of this class working with this mechanism of action were peptidyl trifluoromethyl ketone derivatives (TFMKs). These molecules, synthesized by AstraZeneca, initially appeared as promising compounds for the treatment of respiratory diseases. One of interesting compound **was ICI 200,880** which showed a good inhibitory potency (K_i = 0.2 nM), but a high metabolic instability due to the peptide backbone (Edwards, P. D. et al. 1996).
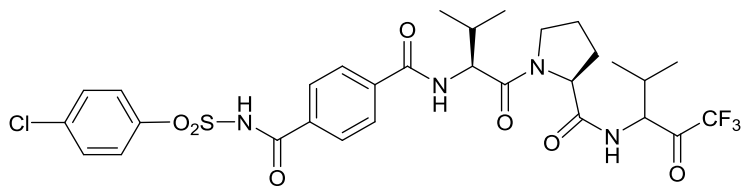
ICI 200,880

Another potent compound, identified during the course of a screening program carried out by Ono Pharmaceutical to find orally active inhibitors is **ONO-6818**. This compound is a potent HNE inhibitor (k_i = 12.6 nM) and exhibit a potent oral activity (ED_{50} = 1.4 mg/kg). For all these reasons, it was selected as a promising therapeutic agent for the treatment of HNE-related chronic inflammatory diseases, such as COPD, ALI and ARDS. It reached Phase II clinical trials in 2002, however, the development was discontinued when data from Japanese Phase IIa study in COPD patients revealed an abnormal elevation in liver functions related to the treatment (Ohbayashi, H. 2005).
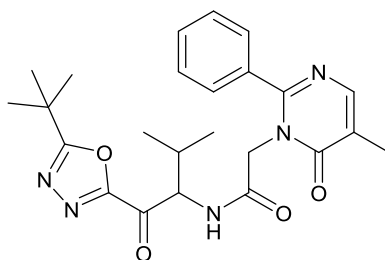
ONO-6818

1.6.3 *3rd and 4th generation*

Compounds with pyridone and dihydropyrimidone scaffold are the most representative terms of non-reactive, reversible inhibitors belonging to the 3rd and 4th generation of neutrophil elastase inhibitors. An unique binding mode in the active center of the enzyme (S1 pocket) triggers a conformational change in the protease creating a *de novo* formed deep S2 pocket enabling further unprecedented target interaction (Hansen, G. et al. 2011). This

interaction does not followed the linear topology of the substrate binding cleft as it is the case with 1st and 2nd generation inhibitors. On the contrary, the orientation of 3rd and 4th generation inhibitors is almost perpendicular to the natural substrate-binding cleft. Whereas 3rd generation inhibitors, binding S1 pocket are able only to create the de novo S2 pocket, while 4th generation inhibitors are also able to bind the new deepened S2 pocket (Fig. **19** e **20**) (Von Nussbaum, F. et al. 2015a).
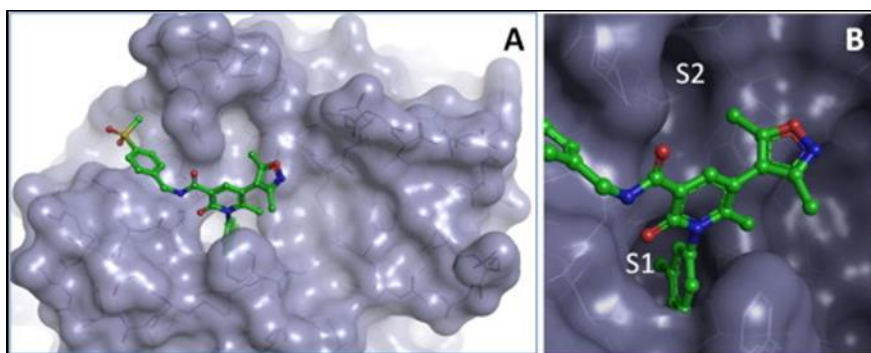

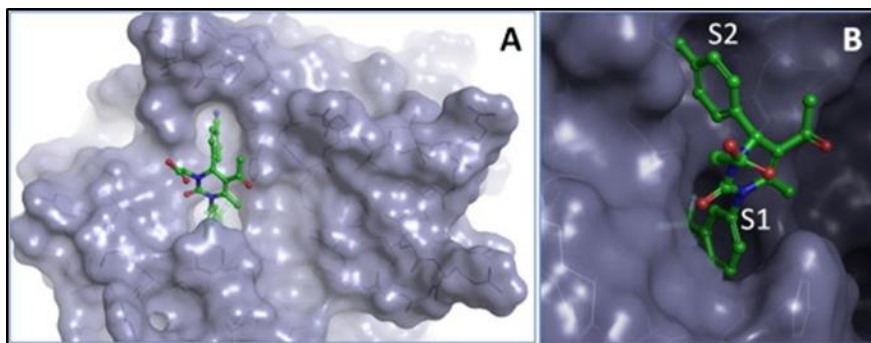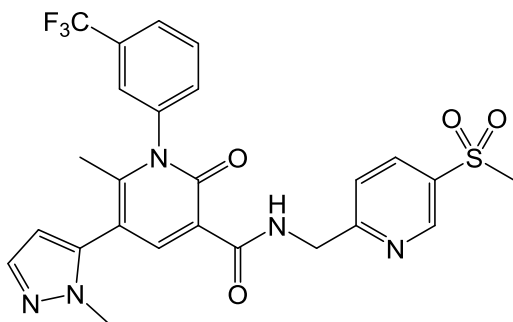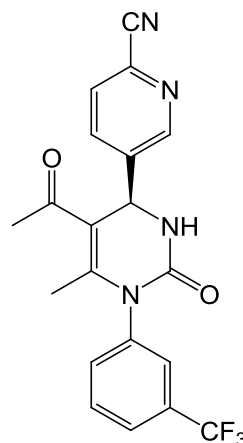**Fig. 19**: HNE-3rd generation inhibitor complex

Fig. 20: HNE-4th generation inhibitor complex

The drug-like properties of these compounds are very interesting and the two most significant candidates are **Alvelestat** (**AZD9668**) and **BAY-678**.

Alvelestat

BAY-678

Both clinical candidates, **Alvelestat** and **BAY-678** contain an identical S1 binding motif, *m*-(trifluoromethyl)-phenyl group. X-ray studies of the complex HNE-inhibitor have surprisingly revealed that S1 binding motif in conjunction with the central pyridone scaffold widens the remote S2 pocket significantly.

These modern inhibitors have displayed an outstanding selectivity versus similar serine proteases and a very high target specificity with no significant interactions with other pharmaceutically relevant targets, in contrast to the 2nd generation inhibitors.

AZD9668 and **BAY-678** have revealed significant efficacy in pre-clinical models of ALI and lung emphysema, demonstrating their anti-inflammatory and anti-remodeling activity. Additionally, **BAY-678** has shown significant beneficial pulmonary hemodynamic and vascular effects in models of PAH (Pulmonary Arterial Hypertension) in rats and mice. The safety and efficacy of both compounds have been initially assessed in clinical Phase I trials with healthy volunteers and with COPD patients (Stevens, T. et al. 2011) (Gunawardena, K. et al. 2010); all these trials have confirmed a very good safety and tolerability of these two 3rd and 4th generation elastase inhibitors.

But at the moment only **AZD9668** is in Phase II of clinical trials for the treatment of cystic fibrosis and bronchiectasis; for these pathologies it has proved to be particularly effective as it results in an increase in lung function

and a reduction in inflammatory biomarkers in the expectorate (Stockley, R. et al. 2013).

1.6.4 *5th generation*

The 5th generation of neutrophil elastase inhibitors are structurally closely related to that of 4th generation. However, in this case, an additional substituent results in an unprecedented improvement in potency though it does not directly interact with the target. In fact, the additional substituent raises the rotational barrier at the crucial pyrimidone-cyanophenyl axis and thereby freezes the structure in an ideal bioactive conformation thus pre-organizing the inhibitor for the forthcoming binding event. Among these compounds are significant BAY 85-8501, BAY-8040 produced by Bayer and a derivative developed by Chiesi Farmaceutici with triazole-pyrimidone (H) scaffold.

BAY 85-8501   **BAY-8040**   **H**
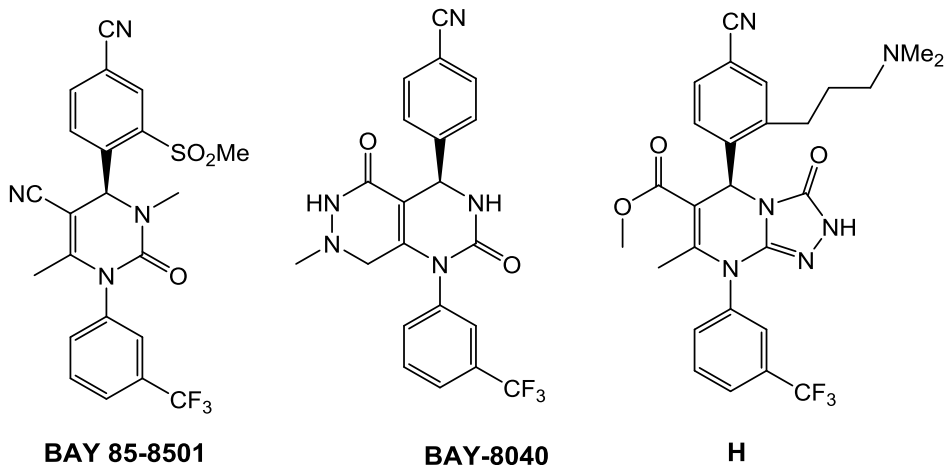
BAY 85-8501 displays an extraordinary potency (k_i = 0.08 nM) comparable to the endogenous anti-proteases and remarkably two orders of magnitude higher when compared with corresponding 4th generation inhibitors. It also has high selectivity, excellent metabolic stability which results in low clearance and

increased half-life without going to inhibit CYP isoforms. In the preclinical phase, this compound confirmed anti-inflammatory effect, when tested in emphysema and ALIanimal model. In all studies, this compound proved to be safe and well tolerated without evidence of acute side effects; currently the compound is in Phase II clinical trials (Von Nussbaum, F. et al. 2015b). Compound **BAY-8040**, with pyrimido-pyridazinic structure is a promising inhibitor with $IC_{50} = 28$ nM (Von Nussbaum, F. et al. 2016). The X-ray structure of the compound complexed with the protease showed a unique but highly stable hydrogen bond between carbonyl group of the pyrimidone and the amino-group of Val216 (**Fig. 21**).
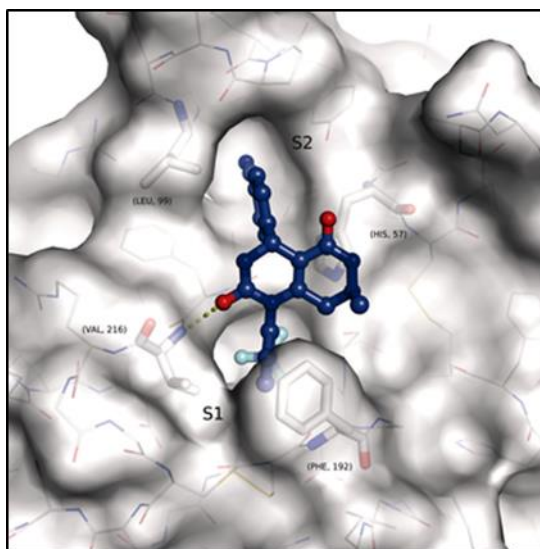

Fig. 21: HNE-BAY-8040 complex

Finally, another promising compound of this class is compound **H**, developed by Chiesi Farmaceutici, which exhibits an $IC_{50} < 20$ nM. The interest of this compound is due not only to the potency, but also to its possible administration via aerosol, therefore dismissing the side effects of the systemic route (Armani, E. et al. 2015).

1.7 PROLASTIN® AND SIVELESTAT®

Despite the large number of molecules previously described, at present only two drugs are commercially available for clinical use.

Prolastin® (purified α1-PI) is a peptide drug, analog to the natural α1-PI, which can be obtained by recombinant DNA techniques or it can be isolated from human serum by various methods of purification (Tebbutt, S. J. 2000). It is currently used for the treatment of α1-PI deficiency, a genetic disorder characterized by a low level of HNE endogenous inhibitor in the blood that may cause the development of a severe form of emphysema (Kohnlein, T. et al. 2008) (Fregonese, L. et al. 2008). This drug represents the most direct therapeutic approach for the α1-PI deficiency and it is administered by venous infusion in order to maintain plasma levels above 11 μM, the minimal concentration needed to protect the respiratory system from excessive HNE activities (American Thoracic Society, 2003). To maintain these levels, the drug should be administered weekly, with doses ranging from 60 to 120 mg/kg. After a few days of discontinuation of treatment, HNE activity again occurs on the surface of the respiratory epithelium (Wewers, M. D. et al. 1987). Some non-randomized observation studies also showed a slower decline in pulmonary function in subjects receiving Prolastin® compared to the patients who did not receive enhancement therapy. At present, the formulation of Prolastin for aerosol is undergoing clinical testing; it will be significantly more beneficial than the endovenous administration, as it would dramatically reduce the dosage and drive the drug directly to the site of action (Griese, M. et al. 2008). In 2003, the FDA also approved two new α1-PI intravenous formulations, **Aralast** (Baxter) and **Zemaira** (CSL Boehring), but they were introduced in therapy only in the USA. Additionally, in May 2007, the FDA announced the validation of **Aralast NP®** (Baxter Heathcare), with features similar to Aralast (Stoller, J. K. et al., 2002) (Alpha Therapeutic Corp. 2003). Some modifications to the drug production process also allowed **Prolastin®-**

C that have a higher purity compared to simple Prolastin (Stocks, J. M. et al. 2010).

Sivelestat by Ono Pharma (ONO-5046) is the second drug, approved in 2002, but only in Japan and Korea. In the same year, Eli Lilly started a clinical study of the same drug for the western market but the FDA stopped the project due to unsatisfactory results originating from the clinical trials (Bayer Healthcare, 2004). It is a selective HNE non-peptide and low molecular weight inhibitor (M.W. 528.51).
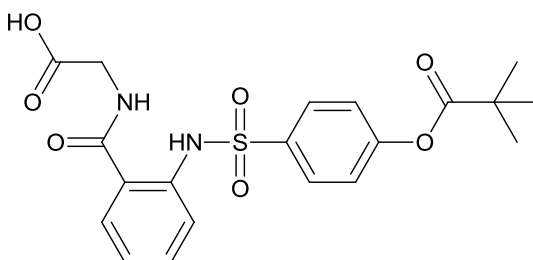
Sivelestat (**ONO-5046**)

Sivelestat works as an acyl-enzyme inhibitor and it shows an $IC_{50} = 44$ nM (Ohbayashi, H. 2005). Using electrospray ionization mass spectrometry, it was possible to identify the enzyme-inhibitor complex after 10 minutes of incubation with the enzyme, so its inhibition mechanism as reported in Fig. 22.
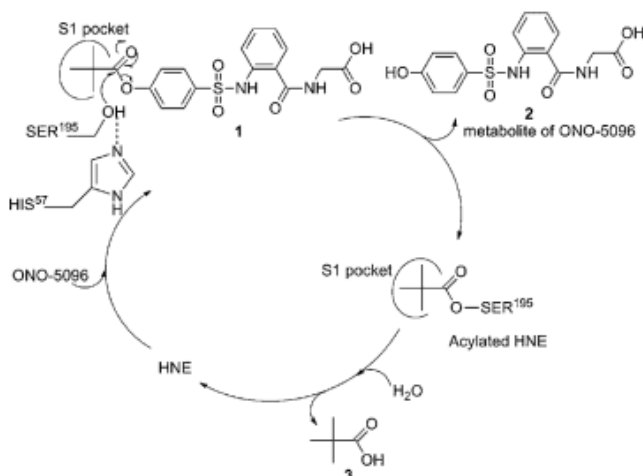
Fig. 22: Mechanism of action of Sivelestat

It is commercialized as an injectable formulation, **Elaspol® 100**, for the treatment of the respiratory diseases ARDS and ALI, associated with systemic inflammatory response syndrome (SIRS) (Fujii, M. et al. 2010). However, its clinical efficacy is still not entirely clear: some studies have shown that Sivelestat can reduce mechanical ventilation, shorten stay in intensive care, and prolong survival of the patient, while others have failed in the same direction (Tamakuma, S. et al. 2004) (Aikawa, N. et al. 2011). However, this discrepancy in results may also be due to the different characteristics of patients treated with the drug, such as age, baseline respiratory condition and compromised non-pulmonary tissue (Zeiher, B. G. et al. 2004) (Tamakuma, S. et al. 2004). Sivelestat is also able to mitigate the cardiopulmonary bypass inflammatory response in pediatric surgery. Cardiopulmonary bypass (CPB) causes the activation of a systemic inflammatory response resulting in release of pro-inflammatory cytokines and growth factors. Neutrophil activation occurs due to the contact between the tissues and the newly installed surgical device (Inoue, N. et al. 2013), causing endothelial adhesion, massive release of pro-inflammatory factors and acute tissue damage. Administration of Sivelestat sodium salt greatly attenuates systemic inflammatory response, decreasing levels of HNE and IL-8

2. BACKGROUND AND AIMS OF THE WORK

Our research group has been involved for many years in the design and synthesis of Human Neutrophil Elastase (HNE) inhibitors. Several nitrogen bicyclic scaffolds such as indazole (Crocetti, L. et al. 2011) (Crocetti, L. et al. 2013), indole (Crocetti, L. et al. 2016) and cinnoline (Giovannoni, M. P. et al. 2016) have been investigated.
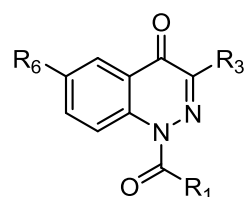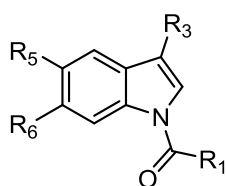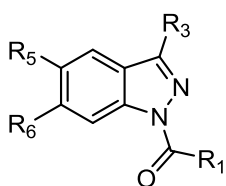

Among the various investigated nucleus, the N-benzoylindazole derivatives showed the best profile as for potency and selectivity. On the more active compounds, aqueous buffer stability studies were performed as well as inhibition test on other proteases to evaluate their selectivity and enzyme kinetic studies to define the mechanism of action. The results suggest that they work as pseudo-irreversible HNE inhibitors, which covalently attack the enzyme site but can be reversed by hydrolysis of the acyl-enzyme complex. In this class of compounds, we can highlight two fundamental requirements for the activity: the presence of the N-CO function at position 1, that undergoes the nucleophilic attack by Ser195, the amino acid of the catalytic triad responsible for the proteolytic action, and the presence of the N at position 2, that is involved in an important hydrogen bond with the enzyme pocket, thus favoring the correct anchorage of the molecules to the active site of the enzyme.

Compounds **L** and **EL17** are two representative terms and are very potent HNE inhibitors showing an IC_{50}= 7 and 20 nM respectively.

Background and aims of the work
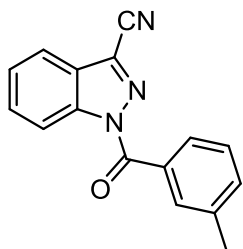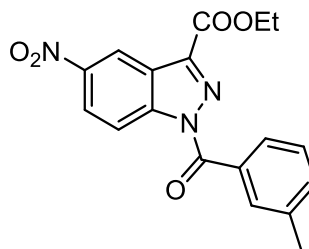
L (IC$_{50}$= 7 nM)   EL17 (IC$_{50}$= 20 nM)

Although compound **L** was the most potent compound of this series, **EL17** shows the best compromise among inhibitory activity, chemical stability and selectivity. For these reasons, it was also evaluated in vivo in the rat model of rheumatoid arthritis induced by Complete Freund's Adjuvant (CFA) (Di Cesare Mannelli, L. et al. 2016). The Paw Pressure Test and the Incapacitance Test indicate that a single administration of **EL17** significantly reduced CFA-dependent hypersensitivity to mechanical noxious stimuli and the postural unbalance related to spontaneous pain. Additionally, the histological evaluation of the tibio-tarsal joint evidenced a significant prevention of articular derangement after **EL17** treatment (30 mg/kg). The protective effects are directly correlated with a complete reversion of the plasmatic Neutrophil Elastase activity increase induced by CFA.

On these basis, the research performed in the period as PhD student consisted in the design and synthesis of new potential HNE inhibitors, with two different aims:

1- On one side, we focused on the synthesis of 7-azaindole derivatives, as isomers of the potent indazoles above described, where the nitrogen was formally shifted from position 2 to position 7.

    We have investigated the positions 1, 2 and 3, by introducing those substituents that in the series of indazoles gave the best results. Thus, at position 3, other than the carbethoxy and the carbonitrile, we inserted various groups with different chemical properties (halogens,

heterocycles etc.) in order to understand the importance of this position in the interaction with the enzyme. We studied the affect on activity by moving the substituent from position 3 to position 2 and in addition we also synthesized a 2,3-disubstituted compound. On the other hand, at position 1 we introduced various substituted benzoyl fragments and different acyl groups, so keeping the N-CO function, fundamental for activity in the reference indazoles.
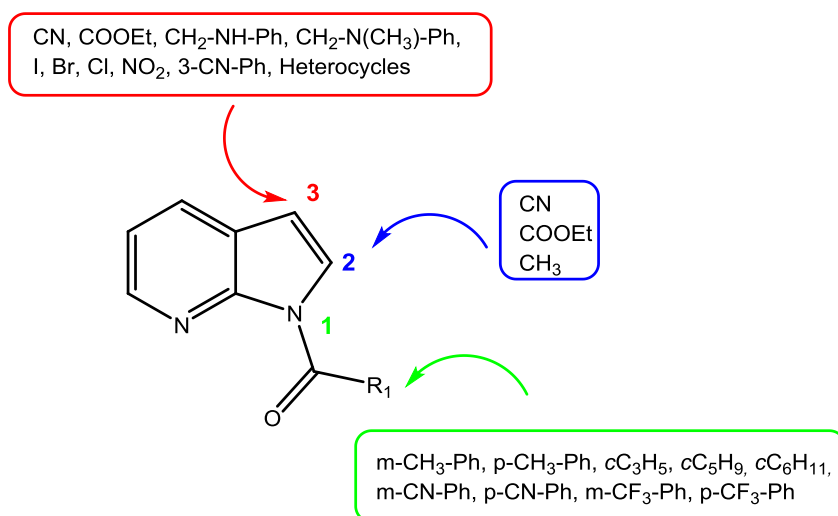
2- On the other side, we moved our attention on the isoxazol-5(2H)-one nucleus, a small and flexible monocyclic scaffold; additionally we started to synthesize benzo[c]isoxazol-3(1H)-ones as elaboration of the monocyclic derivatives.

Background and aims of the work
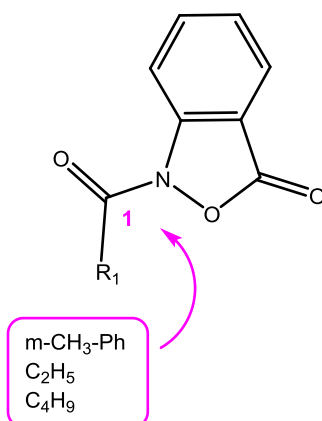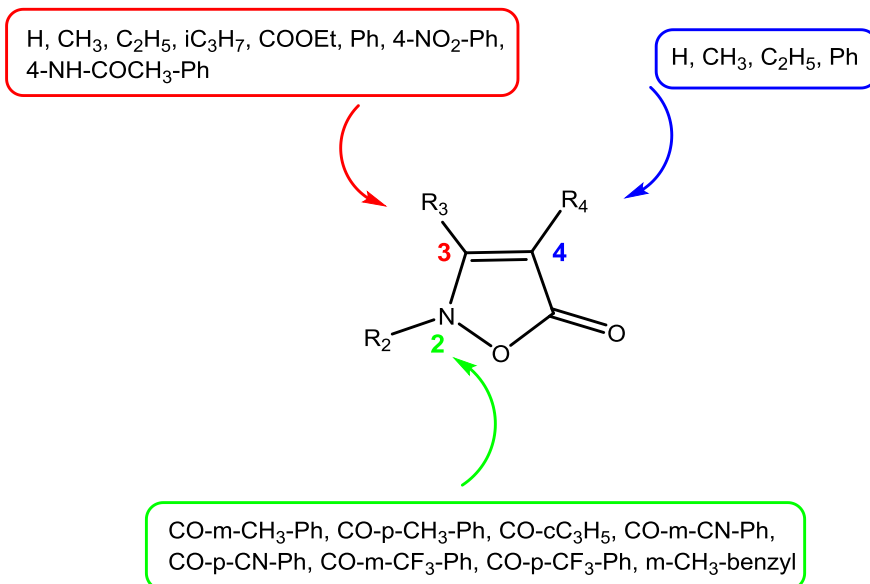
As regards the isoxazolone derivatives, the first approach was to synthesize various terms bearing the same groups and functions that in the other series of compounds previously investigated gave the best results. So we inserted at the nitrogen of position 2 benzoyl or acyl groups in order to reproduce the N-CO function, to understand if also for this series of compounds it is fundamental for the activity. For this purpose we also realized some terms lacking the N-CO group at position 2. The research has also provided the

introduction at positions 3 and 4 of a variety of substituents such as small alkyls and (substituted) phenyl rings.

The biological evaluation of all new compounds was performed by Professor Quinn, University of Montana and consisted of HNE inhibition assays, studies of chemical stability in aqueous buffer, evaluation of the reversibility of HNE-inhibitor complex over time and kinetic of HNE inhibition by a selected compound.

Moreover, some preliminary molecular modeling studies were conducted by Dr. Andrei Khleibnikov on isoxazolones derivatives in order to start to investigate the interactions of new compounds with the target enzyme.

3. CHEMISTRY

The synthetic routes affording all final 7-azaindoles are depicted in **Schemes 1-7**, while the procedure affording the compounds with isoxazolones scaffold are reported in the **Schemes 8-9**. Some of these compounds have recently been published by our research group (Vergelli, C. et al. 2017).

Scheme 1 shows the synthetic pathway followed to obtain the 7-azaindole derivatives bearing a carbonitrile or a carbethoxy group at position 3. On one side, the commercially available 7-azaindole-3-carboxylic acid **1** was transformed into the corresponding, not isolated, acid chloride which was subsequently reacted with an aqueous ammonia solution to give the amide **3** (Carbone, A. et al. 2015); this last one, by dehydration with $POCl_3$, was converted into the 7-azaindole-3-carbonitrile **4** (Bahekar, R. H. et al. 2007). On the other side, compound **1** was also transformed into the 3-carbethoxy derivative **6** (Jiang, J. H. et al. 2011) through a classic esterification reaction. On both compounds **4** and **6**, the acylation at position 1 was carried out with the appropriate acyl or benzoyl chloride and triethylamine in anhydrous dichloromethane to give the final products **5a-i** and **7a-e**.

In **Scheme 2** is showed the synthetic route to obtain the 7-azaindoles substituted at position 3 respectively with halogens or with a nitro group. The insertion of the iodine (**9a**) (Baltus, C. B. et al. 2016) was performed with N-iodosuccinimmide in anhydrous acetonitrile at high temperature. Instead, for the introduction of the bromine (**9b**) (Baltus, C. B. et al. 2016) or the chlorine (**9c**) (Minakata, S. et al. 1997), the halogenation reaction was carried out with N-bromosuccinimmide and N-chlorosuccinimmide at room temperature in anhydrous dichlorometane. The nitro group (**9d**) (Robinson, M. M. et al. 1959) was introduced with the classic nitration reaction in concentrate sulfuric acid and nitric acid at 0°C. Finally, the benzoylation to obtain the final compounds

10a-d was performed with m-toluoyl chloride and triethylamine in anhydrous dichlorometane.

Scheme 3 reports the procedure followed to obtain the final compounds **15a-e** bearing at position 3 various different heterocycles such as pyridine, furan and thiophene or a 3-CN-phenyl ring. Starting from the commercially available 7-azaindole **8**, we first protected the nitrogen at position 1 with benzensulfonyl chloride thus obtaining compound **11** (Sandham, D. A. et al. 2009). After the iodination of position 3 (**12**) (Zhang, J. et al. 2011), a coupling reaction was carried out using the appropriate boronic acid and Tetrakis in toluene at high temperature (**13a-e**). Then we deprotected N-1 with tetrabutylammonium fluoride (TBAF) in dry THF (**14a-e**) (Lind, K. E. et al. 2008) (Ibrahim, P. N. et al. 2007) and we performed the benzoylation, following the procedure previously described, to obtain the final products **15a-e**.

The synthesis of compounds **18** and **21**, substituted at position 3 with an oxadiazole ring as bioisoster of the carbethoxy group, is reported in **Schemes 4** and **5**. By the treatment of the amide **3** (**Scheme 4**) (Carbone, A. et al. 2015) with *N,N*-dimethylacetamide dimethyl acetal in toluene we obtained compound **16**, which in turn was treated with hydroxylamine hydrochloride to give the corresponding oxadiazole derivative **17**. The final compound **18** was obtained through the benzoylation of N-1 following the same procedure above reported.

Instead compound **21** (**Scheme 5**), even bearing an oxadiazole ring at position 3 but differently connected, was obtained starting from the 7-azaindole-3-carbonitrile **4** (Bahekar, R. H. et al. 2007) which was converted into the intermediate **19** (Lape, H. E. et al. 1968) with hydroxylamine hydrochloride and sodium carbonate. The cyclization of compound **19** with dicyclohexylcarbodiimide and acetic acid afforded the 5-methyl-3-(1H-pyrrolo[2,3-b]pyridine-3-yl)-1,2,4-oxadiazole **20**, which was benzoylated at

Chemistry

position 1 with *m*-toluoyl chloride and triethylamine in anhydrous dichloromethane to obtain the final product **21**.

Scheme 6 shows the synthetic pathway affording the final compounds **26** and **30**. After the formylation of the 7-azaindole (**8**) at position 3 with hexamethylentetramine and acetic acid (**22**) (Singla, P. et al. 2016), we protected the nitrogen at position 1 (**23**) (Chavan, N. L. et al. 2010) and then we performed a reductive amination using aniline or N-methylaniline and NaBH(OAc)$_3$ in dry dichloromethane, thus obtaining compounds **24a** and **24b**. Compound **24b** (R=CH$_3$) was directly deprotected at N1 and then subjected to the benzoylation obtaining the final compound **26**. On the other hand, compound **24a** (R=H) was further protected with allyl chloroformate furnishing compound **27**. This intermediate was treated with TBAF to give compound **28**, which was benzoylated (**29**), and finally, using Tetrakis and phenyl silane, the allhyl chloroformate was removed to obtain the final product **30**.

To obtain the 7-azaindole derivatives substituted at position 2 or disubstituted at position 2 and 3, we followed the procedure shown in **Scheme 7**. Starting from compound **11** (Sandham, D. A. et al. 2009), the introduction of the substituents at position 2 was carried out with lithium diisopropylamide (LDA) and the appropriate halogen derivative at -78°C (**31a,b**) (Sandham, D. A. et al. 2009) (Ahrendt, K. A. et al. 2009); then we removed the protection at position 1 following the same procedure described in the previous scheme and we obtain compounds **32a,b** (Sandham, D. A. et al. 2009) (Baltus, C. B. et al. 2016). On compound **32a** (R=CH$_3$) we performed a formylation (**33**) (Bahekar, R. H. et al. 2007), according to the procedure reported in **Scheme 6**, followed by the treatment with hydroxylamine hydrochloride and NaHCO$_3$ at high temperature which afforded the corresponding oxime **34** (Bahekar, R. H. et al. 2007). Dehydration with POCl$_3$ of **34** furnished the 7-azaindole-2-methyl-3-carbonitrile (**35**) (Bahekar, R. H. et al. 2007), which was finally benzoylated at position 1 with *m*-toluoyl chloride and triethylamine in

anhydrous dichloromethane (final compound **36**). Instead, the 2-carbethoxy derivative **32b** was as directly benzoylated at N-1 providing the final product **37** and converted into the amide intermediate **38** (Jia, H. et al. 2014). This last one was then transformed into the 2-carbonitrile (**39**) which in turn was benzoylated to give the final product **40**.

Before moving on the description of the **Scheme 8**, in which are reported the procedures followed to obtain the final products with the isoxazolone scaffold, it is essential to mention that the isoxazolone nucleus shows three different tautomeric forms, depending on the solvent and the substituent at position 3 and 4, as reported below (Laufer, S. A. et al. 2008).

NH-form   CH-form   OH-form
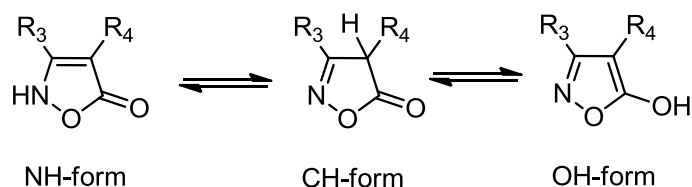
The NH-form is the most representative especially in polar solvents, but in the literature it is possible to find examples of alkylation and acylation reactions which afforded 2-N-CO-R and 5-O-CO-R derivatives, originating from the NH-form and OH-form respectively (Frolund, B. et al. 2005). Taken into account this aspect, we performed the synthesis of our final compounds as reported in **Scheme 8**.

The starting products to obtain the isoxalone scaffold are ketoesters **41a-m** which were synthetized following the procedure reported in the literature (Beccalli, E. M. et al. 1984) (Kalaitzakis, D. et al. 2007) (Shneider, P. et al. 2009) (Raeppel, F. et al. 2015) (Shu, Z. et al. 2011) if they are not commercially available. The isoxazolone nucleus, suitable substituted at position 3 and 4, was obtained or by treatment with hydroxylamine hydrochloride in ethanol and in the presence of piperidine (**42a-g**) (Krogsgaar-Laersen, P. et al. 1973) (Sato, K. et al. 1986) (Yamaguchi, M. et al. 2009)
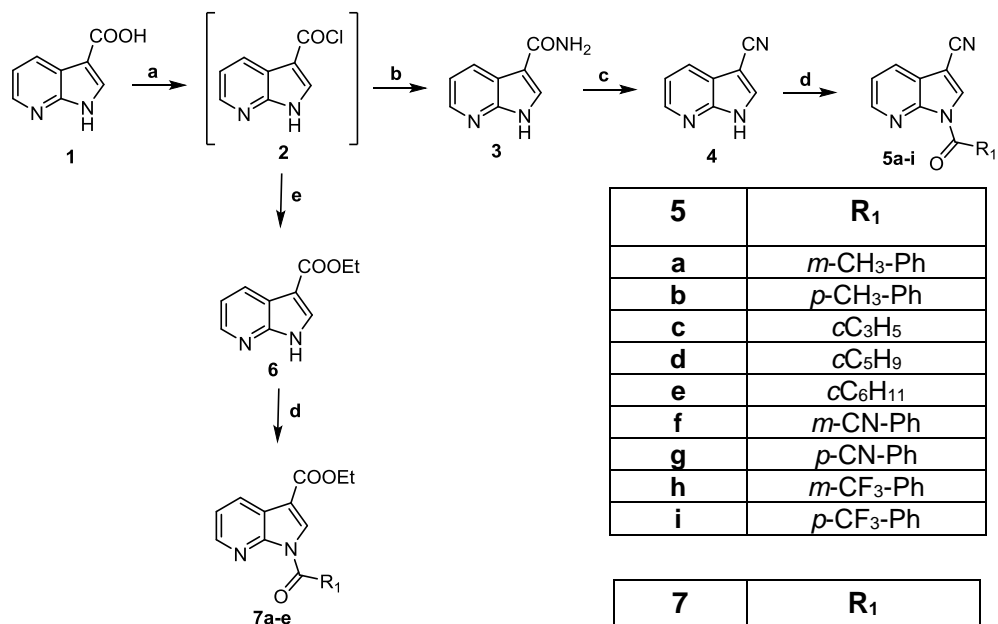
Chemistry

(Adembri, G. et al. 1965) (Jacobsen, N. et al. 1984), or by treatment with hydroxylamine hydrochloride in a mixture of methanol/water 1:1 at reflux (**42h-m**) (Boulton, A. J. et al. 1961) (Beccalli, E. M. et al. 1987) (Beccalli, E. M. et al. 1984) (Maquestiau, A. et al. 1974) (Belzecki, C. et al. 1958) (Breslow, T. et al. 1965). The final compounds originating from the acylation and/or benzoylation on the isoxazolones **42a-m** were grouped into two different series depending on the nature of the substituent at position 3 and 4: compounds of type **43** (R_3, R_4= H, alkyl) and compounds of type **45** (R_3, R_4 = H, alkyl, phenyl). This reaction was the limiting step of the synthesis and needed a lot of times and attempts to be optimized. At the beginning, the acylation was performed with the appropriate acyl chloride and potassium carbonate in *tert*-butanol at 80°C, but the yields were very low and the reaction mixture difficult to purify. Therefore, by varying the reaction conditions and investigating different solvents, bases and stoichiometric ratios, we found that the acylations carried out with the appropriate acyl or benzoyl chloride and natrium hydride in THF at room temperature gave the best yields. Thus, the final compounds of type **43** and **45** were obtained following these optimized conditions.

In compound **43l** and **43n**, the replacement of the carbonyl group with a thiocarbonyl group with Lawesson's reagent in toluene at high temperature afforded compounds **44a** and **44b**. Finally, reaction of **42a**, **42f** and **42g**, with 3-methylbenzyl chloride in anhydrous acetonitrile and potassium carbonate resulted in **46a-c**. All acylation and alkylation reactions reported in **Scheme 8** led to an only one compound probably originating from the NH-form of the isoxazolone nucleus, according with the data reported in the literature. Only in the case of the treatment of **42g** with *m*-toluoyl chloride, we observed the formation of a couple of compounds in very different ratio (95:5) but showing the same molecular weight, as demonstrated with mass spectrometry techniques. The main product has been completely characterized as compound **45b**, while the other one was probably the isomer originating from the OH-form, but the obtained amount was too small to further investigation.

In order to univocally assign the structure to the final compounds **43a-s** and **45a-o**, a crystallographic analysis was performed on products **43j** and **45a**. The results definitively confirm the structure reported in **Scheme 8**, thus originating from the acylation/benzoylation of the NH-form, in agreement with the literature (for Figures and Tables see Material and methods, Crystallographic Analysis).

In the last scheme (**Scheme 9**), we reported the synthesis of bicyclic compounds with benzo[*c*]isoxazol-3(*1H*)-one structure. On the commercially available 2-nitrobenzoyl chloride **47**, we performed an esterification with anhydrous methanol at room temperature obtaining the corresponding methyl ester **48** (Li, L. et al. 2014), which was cyclized with ammonium chloride and zinc in tetrahydrofuran and water to afford compound **49** (Wierenga, W. et al. 1984). The final products **50a-c** were obtained with the appropriate benzoyl or acyl chloride and potassium carbonate in *tert*-butanol.
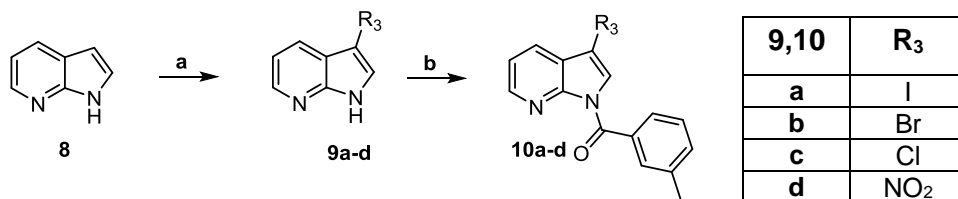
Chemistry

SCHEME 1

5	R$_1$
a	*m*-CH$_3$-Ph
b	*p*-CH$_3$-Ph
c	*c*C$_3$H$_5$
d	*c*C$_5$H$_9$
e	*c*C$_6$H$_{11}$
f	*m*-CN-Ph
g	*p*-CN-Ph
h	*m*-CF$_3$-Ph
i	*p*-CF$_3$-Ph

7	R$_1$
a	*m*-CH$_3$-Ph
b	*p*-CH$_3$-Ph
c	*c*C$_3$H$_5$
d	*m*-CN-Ph
e	*p*-CN-Ph

Reagents and conditions:

a) SOCl$_2$, Et$_3$N, 0°C; reflux, 1h.

b) NH$_4$OH 33%, 0°C, 1h.

c) POCl$_3$, reflux, 1h.

d) R$_1$-COCl, Et$_3$N, dry DCM, 0°C, 2h; r.t., 2h.

e) EtOH abs, r.t., 16h.

SCHEME 2

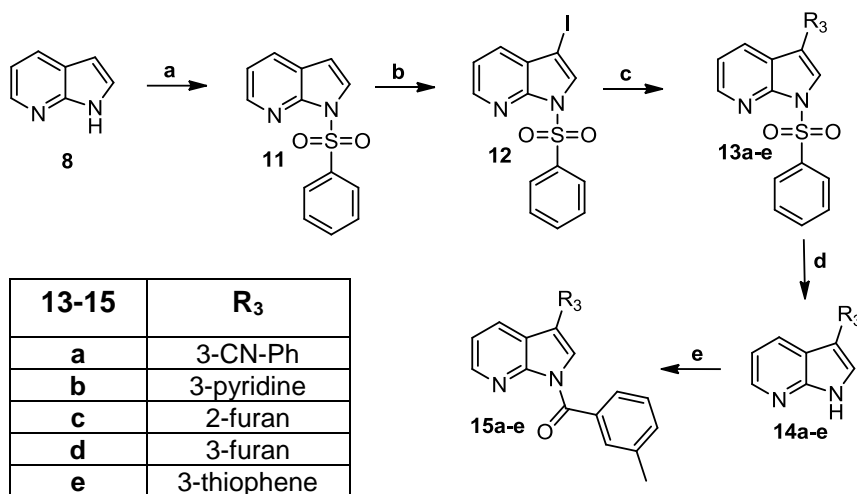| 9,10	R₃
a	I
b	Br
c	Cl
d	NO₂

Reagents and conditions:

a) (R₃= I) NIS, dry MeCN, reflux, 3h.

   (R₃= Br, Cl) NBS or NCS, dry DCM, 0°C, 15 min; r.t., overnight.

   (R₃= NO₂) H₂SO₄ conc., HNO₃ (1:1) 0°C, 30 min.

b) *m*-Toluoyl chloride, Et₃N, dry DCM, 0°C, 2h; r.t., 2h.

SCHEME 3

13-15	R₃
a	3-CN-Ph
b	3-pyridine
c	2-furan
d	3-furan
e	3-thiophene

Reagents and conditions

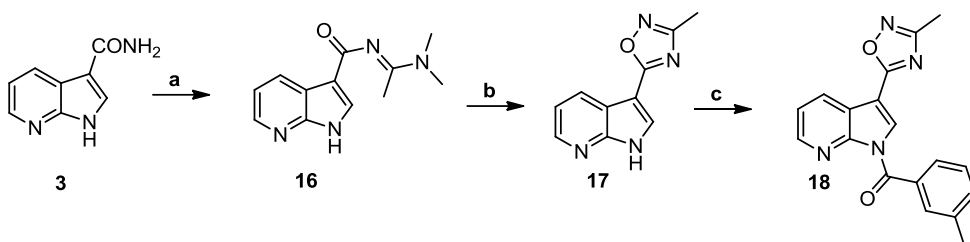a) Ph-SO₂Cl, Et₃N, dry DCM, 0°C, 2h; r.t., 2h.

b) NIS, dry MeCN, reflux, 3h.

c) R₃-B(OH)₂, Tetrakis, Na₂CO₃ 2M, H₂O, toluene, reflux, 4h.

d) TBAF, dry THF, reflux, 3h.

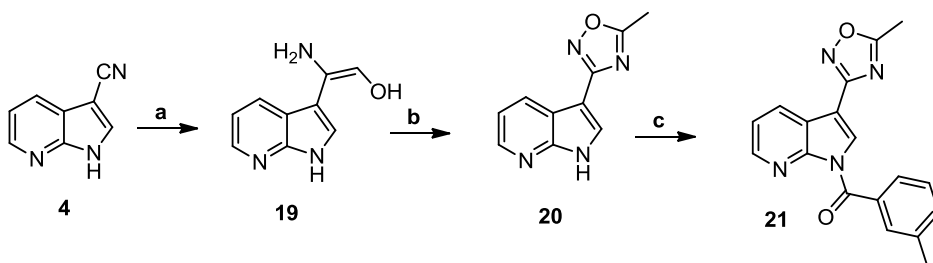e) *m*-Toluoyl chloride, Et₃N, dry DCM, 0°C, 2h; r.t., 2h.

Chemistry

SCHEME 4

Reagents and conditions:

a) *N,N*-DMA-DMA, dry DMF, reflux, 2h.

b) $NH_2OH \cdot HCl$, glacial CH_3COOH, NaOH 10%, dioxane, reflux, 5h.

c) *m*-Toluoyl chloride, Et_3N, dry DCM, 0°C, 2h; r.t., 2h.

SCHEME 5

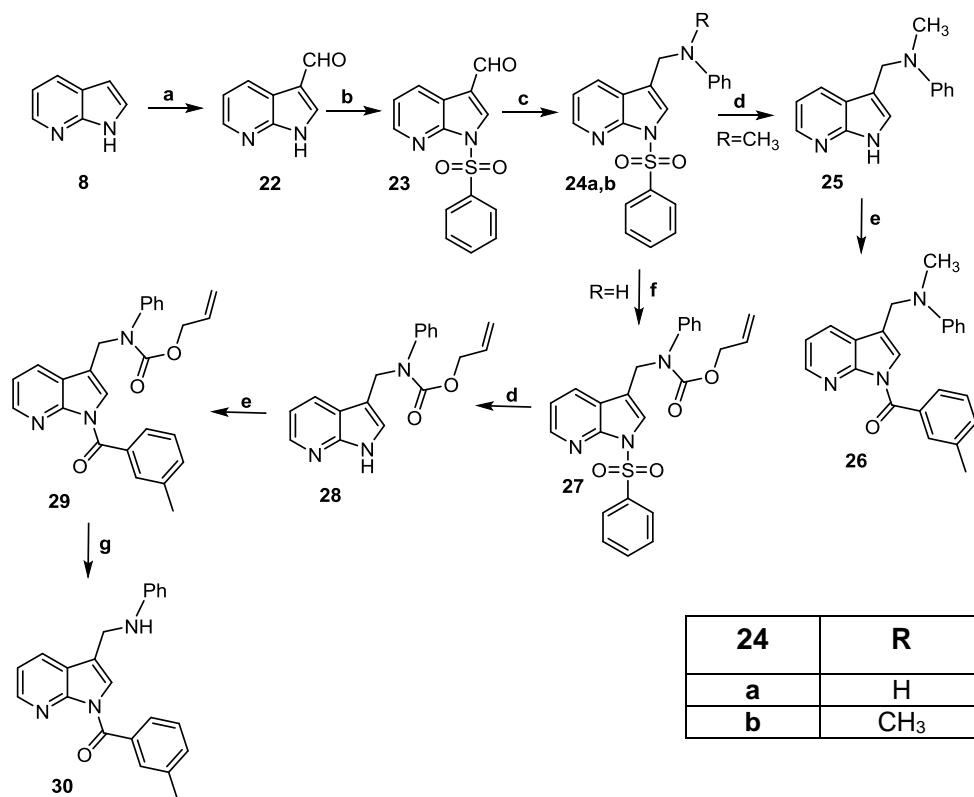**Reagents and conditions:**

a) $NH_2OH \cdot HCl$, EtOH, 0°C; Na_2CO_3, H_2O, reflux, 8h.

b) DCC, glacial CH_3COOH, dry DMF, 0°C, 2h; r.t., 2h.

c) *m*-Toluoyl chloride, Et_3N, dry DCM, 0°C, 2h; r.t., 2h.

SCHEME 6

24	R
a	H
b	CH₃

Reagents and conditions:

a) HMTA, CH₃COOH, reflux, 4h.

b) Ph-SO₂Cl, Et₃N, dry DCM, 0°C, 2h; r.t., 2h.

c) R-NH-Ph, glacial CH₃COOH, dry DCM, r.t., 30 min; NaBH(OAc)₃, r.t., overnight.

d) TBAF, dry THF, reflux, 3h.

e) *m*-Toluoyl chloride, Et₃N, dry DCM, 0°C, 2h; r.t., 2h.

f) Allyl chloroformate, NaN₃, dioxane, H₂O, r.t., 1h; Na₂CO₃ 1%, overnight.

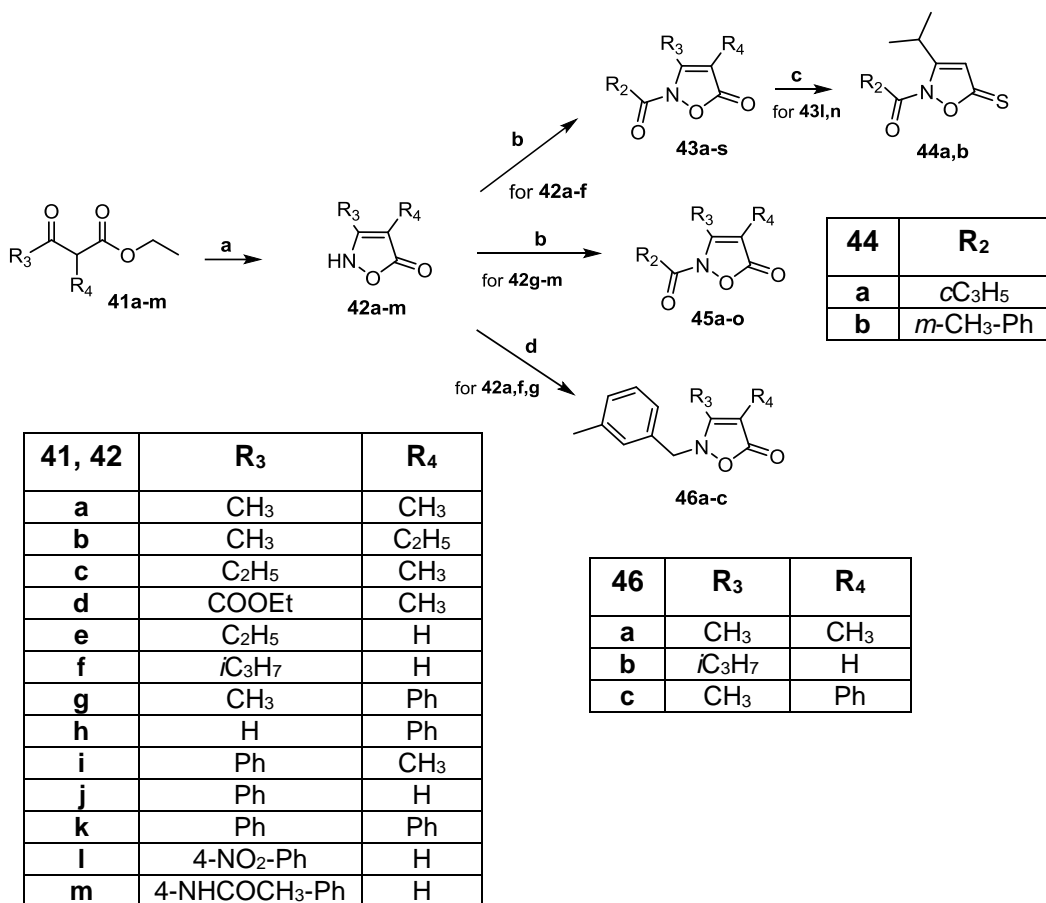g) Tetrakis, phenylsilane, dry DCM, r.t., 1h.

Chemistry

SCHEME 7

31, 32	R$_2$
a	CH$_3$
b	COOEt
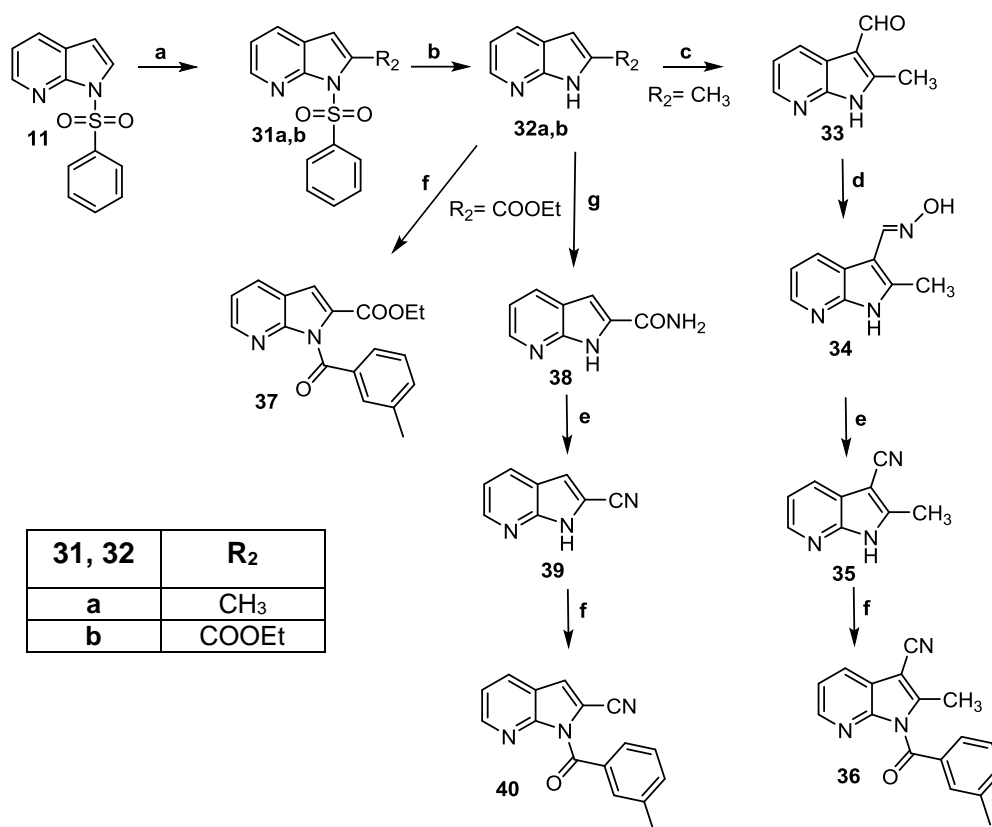
Reagents and conditions:

a) LDA, dry THF, -78°C, 30 min; CH$_3$-I (for **31a**) or ClCOOEt (for **31b**), r.t., 2h.

b) TBAF, dry THF, reflux, 2h.

c) HMTA, CH$_3$COOH, reflux, 3h.

d) NH$_2$OH·HCl, H$_2$O, 60°C, 30 min; NaHCO$_3$, reflux, 4h.

e) POCl$_3$, reflux, 1h.

f) *m*-Toluoyl chloride, Et$_3$N, dry DCM, 0°C, 2h; r.t., 2h.

g) NH$_4$OH 33%, EtOH, 100°C, 8h.

SCHEME 8

41, 42	R₃	R₄
a	CH₃	CH₃
b	CH₃	C₂H₅
c	C₂H₅	CH₃
d	COOEt	CH₃
e	C₂H₅	H
f	iC₃H₇	H
g	CH₃	Ph
h	H	Ph
i	Ph	CH₃
j	Ph	H
k	Ph	Ph
l	4-NO₂-Ph	H
m	4-NHCOCH₃-Ph	H

44	R₂
a	cC₃H₅
b	m-CH₃-Ph

46	R₃	R₄
a	CH₃	CH₃
b	iC₃H₇	H
c	CH₃	Ph

Reagents and conditions:

a) (for **42a-g**) NH₂OH·HCl, piperidine, EtOH, reflux, 4-5h.

   (for **42h-m**) NH₂OH·HCl, H₂O/MeOH 1:1, 80°C, 1-4h.

b) R₂-COCl, NaH, dry THF, r.t., overnight.

c) Lawesson's reagent, toluene, reflux, 5h.

d) 3-methylbenzyl chloride, K₂CO₃, dry MeCN, reflux, 2h.

Chemistry

43	R$_2$	R$_3$	R$_4$
a	cC$_3$H$_5$	CH$_3$	CH$_3$
b	m-CH$_3$-Ph	CH$_3$	CH$_3$
c	cC$_3$H$_5$	CH$_3$	C$_2$H$_5$
d	m-CH$_3$-Ph	CH$_3$	C$_2$H$_5$
e	cC$_3$H$_5$	C$_2$H$_5$	CH$_3$
f	m-CH$_3$-Ph	C$_2$H$_5$	CH$_3$
g	cC$_3$H$_5$	COOEt	CH$_3$
h	m-CH$_3$-Ph	COOEt	CH$_3$
i	cC$_3$H$_5$	C$_2$H$_5$	H
j	m-CH$_3$-Ph	C$_2$H$_5$	H
k	C$_2$H$_5$	iC$_3$H$_7$	H
l	cC$_3$H$_5$	iC$_3$H$_7$	H
m	cC$_5$H$_9$	iC$_3$H$_7$	H
n	m-CH$_3$-Ph	iC$_3$H$_7$	H
o	p-CH$_3$-Ph	iC$_3$H$_7$	H
p	m-CN-Ph	iC$_3$H$_7$	H
q	p-CN-Ph	iC$_3$H$_7$	H
r	m-CF$_3$-Ph	iC$_3$H$_7$	H
s	p-CF$_3$-Ph	iC$_3$H$_7$	H

45	R$_2$	R$_3$	R$_4$
a	cC$_3$H$_5$	CH$_3$	Ph
b	m-CH$_3$-Ph	CH$_3$	Ph
c	m-CN-Ph	CH$_3$	Ph
d	m-CF$_3$-Ph	CH$_3$	Ph
e	cC$_3$H$_5$	H	Ph
f	m-CH$_3$-Ph	H	Ph
g	cC$_3$H$_5$	Ph	CH$_3$
h	m-CH$_3$-Ph	Ph	CH$_3$
i	cC$_3$H$_5$	Ph	H
j	m-CH$_3$-Ph	Ph	H
k	cC$_3$H$_5$	Ph	Ph
l	m-CH$_3$-Ph	Ph	Ph
m	cC$_3$H$_5$	4-NO$_2$-Ph	H
n	m-CH$_3$-Ph	4-NO$_2$-Ph	H
o	m-CH$_3$-Ph	4-NHCOCH$_3$-Ph	H

SCHEME 9
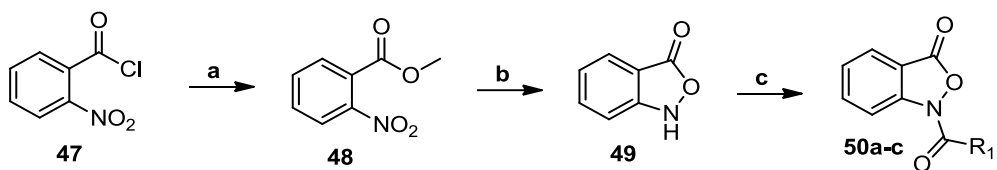
50	R$_1$
a	C$_2$H$_5$
b	C$_4$H$_9$
c	*m*-CH$_3$-Ph

Reagents and conditions:

a) dry MeOH, r.t., 2h.

b) NH$_4$Cl, Zn°, THF, H$_2$O, r.t., 2h.

c) R$_1$-COCl, K$_2$CO$_3$, t-BuOH, 80°C, 2h.

4. RESULTS AND DISCUSSION

4.1 *Biological evaluation and structure activity relationships (SARs)*

All new products were tested as HNE inhibitors in the laboratory of Prof. Quinn, University of Montana. Experiments were conducted in triplicate using *N*-methylsuccinyl-Ala-Ala-Pro-Val-7-amino-4-cumarin (Calbiochem) as substrate for HNE. The results are reported in the **Tables 1-6** and are compared with Sivelestat, the only HNE inhibitor commercially available and with compound **L**, a potent reference compound synthesized by us (see Aim of the work).

Tables 1, **2** and **3** show activity values for compounds with 7-azaindole structure, isomers of the potent indazoles previously described (see Aim of the work). A look at the results indicates that this nucleus may be an appropriate scaffold for HNE inhibitors since the most part of the new synthetized compounds show an inhibitory activity in the micromolar/submicromolar range and some terms even exhibit an IC_{50} at nanomolar levels.

Starting to analyze **Table 1**, the first observation is that both the 3-CN derivatives **5a** and **5b**, isomers of the powerful indazole **L**, are very potent inhibitors showing an IC_{50} = 15 and 14 nM respectively. This result indicates that the shift of the nitrogen from position 2 to position 7 doesn't affect the inhibitory activity. The replacement of the methyl on the benzoyl fragment with other groups such as cyano (**5f** and **5g**) or trifluoromethyl (**5h** and **5i**), that in the literature are present in potent HNE inhibitors is not favorable for the activity as in *meta* and in *para* position. On the other hand, the insertion at position 1 of acyl groups (compounds **5c-e**) gave good results only in the case of the cyclopropancarbonyl fragment resulting in compound **5c** which showed IC_{50} = 87 nM. Going to the series of the 3-carbethoxy derivatives, although compounds **7a-c** maintain good levels of inhibition (IC_{50} = 0.77 µM, 0.64 µM and 0.62 µM respectively), they are 10 fold less potent than the corresponding

3-CN derivatives **5a-c**. The introduction of the CN group on the benzoyl fragment as in compounds **7d** and **7e** leads to a decrease of activity, analogously to the previously discussed series.

Instead, analyzing the results shown in **Table 2,** it is possible to highlight that the shift of the carbonitrile or carbethoxy groups determines the total loss of activity (**37**) or a dramatic decrease of activity, as for compound **40** which shows an IC_{50} about two order of magnitude higher with respect to its 3-CN isomer. Also the introduction of a methyl group at position 2 of the potent **5a** (compound **36**) is detrimental for activity, affording a product with an $IC_{50} = 10.8$ µM.

From the above discussed data, it emerges that the methylbenzoyl group is the best substituent for position 1, as when the methyl is in *meta* and in *para* position. So, also taking into account our previous results for the indazole series, we selected the *m*-methylbenzoyl fragment and keeping this group at position N-1, we modified the position 3 of the 7-azaindole nucleus by inserting a variety of substituents with different characteristics. The data are reported in **Table 3**. As we can see, the performed modifications do not improve the HNE inhibitory activity since the most part of compounds work in the micromolar range. Only compounds **10d** and **18** are potent HNE inhibitors with $IC_{50} = 24$ and 80 nM respectively. Indeed, compound **10d**, substituted at position 3 with a NO_2 groups, is a reaction intermediate since the NO_2 group will be further processed (reduction and acetylation) to overcome the problems of toxicity linked to its metabolism. It was sent to the pharmacological experimentation, given the strong similarities between the NO_2 and CN group, and the potent activity of **10d** confirms that the presence of an electron-withdrawing group at position 3 is favorable for the activity. On the other hand, it is intriguing the different activity of the isomers **18** and **21**, bearing at position 3 the same oxadiazole ring but differently connected. In fact, compound **21** is about 45 fold less potent then compound **18**, suggesting a worse orientation and/or interaction at the level of the active site. This aspect is not easily understandable since the oxadiazole ring, isoster of the

carbethoxy group, appears to be able to freely rotate around the simple bond. The molecular modeling studies, provided for these compounds, will help us to clarify this apparent incongruity, as well as to understand the comparable activity of 7-azaindole derivatives with respect to the indazoles and hence the role of N-7 for the anchoring of this molecules to the enzyme pocket.

The graphical summary of the preliminary structure activity relationships (SARs) of this series of compounds is reported below.
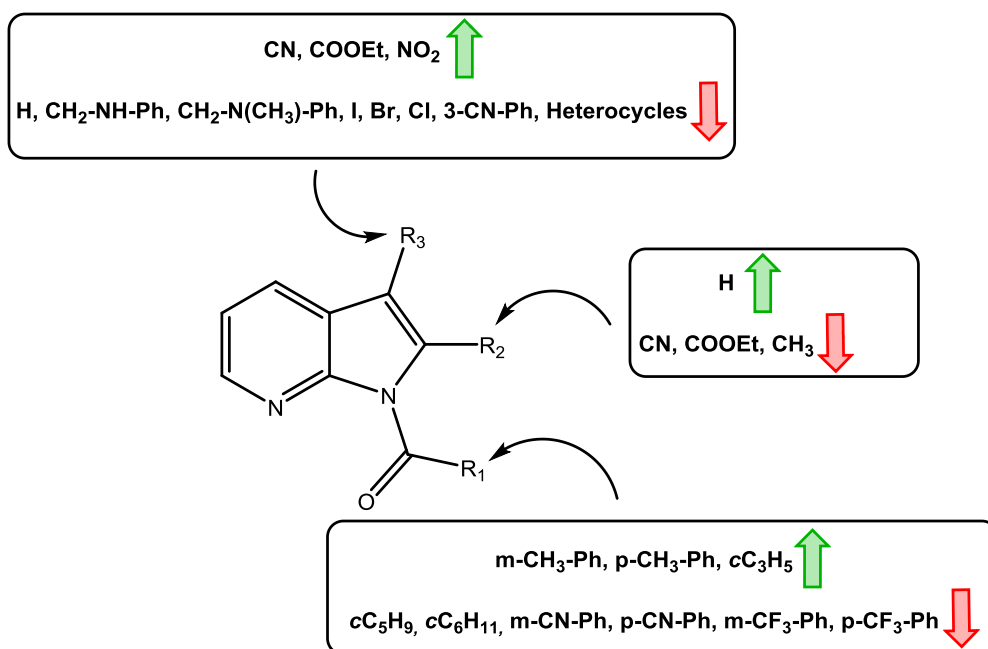
The HNE inhibitory activity of compounds with isoxazolone scaffold is reported in the **Tables 4** and **5**. Following the same organization reported in **Scheme 8,** the data of **Table 4** refer to the isoxazolones alternatively substituted in positions 3 and 4 with small alkyl groups (**43a-s**), while **Table 5** shows the results of compounds **45a-o**, substituted at position 3 and/or 4 with a (substituted)phenyl ring. All the results demonstrated that also the isoxazolone nucleus is an appropriate scaffold for the synthesis of HNE inhibitors.

Going to specifically analyze the results and starting from **Table 4**, we can observe that the contemporary presence of small alkyl groups at position 3 and 4 (**43a-f**) leads to compounds with an appreciable HNE inhibitory activity in the micromolar/submicromolar range; on the other hand the introduction at position 3 of a carbethoxy group (**43g,h**) give very different results, depending on the substituent at N-2 (**43g** IC_{50} = 440 nM, **43h** IC_{50} = 39.7 µM). Instead, the elimination of the methyl group at position 4 (**43i-s**) gives compounds endowed with excellent inhibitory activity, indicating the importance of the unsubstitution of this position. This aspect can be highlighted comparing compounds **43i** and **43j** (IC_{50} = 96 and 43 nM respectively) with the corresponding 4-methyl derivatives **43e** and **43f** (IC_{50} = 2.2 and 1.8 µM respectively). Some other products of the 4-unsubstituted series, like compounds **43l**, **43n**, **43o** and **43s** are very potent HNE inhibitors exhibiting IC_{50} values in the nanomolar range (20-42 nM). At this regard, it is interesting to observe that the replacement of the methyl group at *meta* and *para* position of compounds **43n** and **43o** with a trifluoromethyl group (**43r** and **43s**) does not modify the inhibitory activity when the substituent was in *para* position of the benzoyl group (i.e. compounds **43o** and **43s** with IC_{50} = 20 and 34 nM respectively), but results in a decrease of activity when the substituent was in *meta* position (**43r**, IC_{50} = 1.2 µM). These compounds display two carbonyl groups (2-N-CO and 5-CO) as possible point of attack for Ser195, the amino acid of the HNE catalytic site responsible for the nucleophilic attack and leading to the hydrolysis of the substrate. The evidence that all 2-N-acyl/benzoyl derivatives are good HNE inhibitors suggests that the carbonyl group involved in the catalysis was the N-CO at position 2. The importance of this function seems to be confirmed by the complete inactivity of the 2-N-benzyl derivatives **46a** and **46b**. Indeed this observation is consistent with our previous results for indazole derivatives (Crocetti, L. et al. 2011) (Crocetti, L. et al. 2013).

On the other hand, informations about the importance of the endocyclic carbonyl group at position 5, which does not seem involved in the catalysis,

come from compounds **44a** and **44b,** the thioanalogues of the two potent compounds **43l** and **43n**. However, the low activity (**44a**, IC$_{50}$ = 2.1 µM) or inactivity (**44b**) of these new products clearly suggest that the 5-CO group is important anyway for the interaction with the target. To assess if this low activity/inactivity was the result of increased bulkiness and/or decrease H-binding acceptor efficacy of sulfur with respect to oxygen in the carbonyl groups or if it was related to other reasons, we performed molecular modeling studies (see Molecular Modeling section).

The fundamental structure activity relationships of isoxazolones **43a-s** are summarized below.
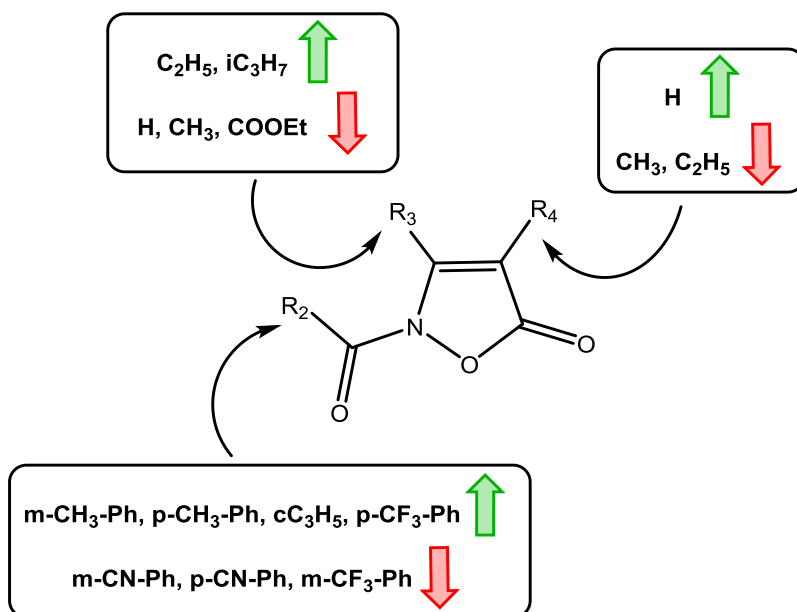
In **Table 5** are presented the results of isoxazolones bearing at positions 3 and 4 at least one phenyl ring. Beginning the analysis of the data from 3-methyl-4-phenylisoxazol-5(2H)-one derivatives (compounds **45a-d**), the biological results suggest that also in this case, as in the series previously described, the best substituents at position N-2 are the *m*-methylbenzoyl or the cyclopropanecarbonyl fragment, as in compounds **45a** and **45b** which
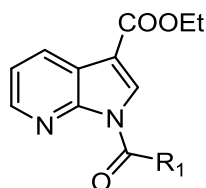
show activity values in the nanomolar range (IC_{50} = 59 and 77 nM respectively). The replacement of the methyl on the benzoyl fragment at position 2 with other groups such as cyano (**45c**) or trifluoromethyl (**45d**), in any case is not favorable for the activity (IC_{50} = 6.3 µM and 0.20 µM respectively). Thus, keeping the *m*-methylbenzoyl and ciclopropanecarbonyl at position N-2, we further modified the positions 3 and 4 of the isoxazolone. Compounds **45e** and **45f** which are the 3-norderivatives of compounds **45a** and **45b**, are very potent HNE inhibitors with IC_{50} = 16 and 46 nM respectively. Instead, moving the phenyl from position 4 to position 3 we observe a decrease or a total collapse of the activity, as we can see in compounds **45g-o**. In particular, the insertion in *para* position on the phenyl ring of those substituents that in the previous series gave good results (such as nitro or acetamide) leads to compounds completely avoid of activity (**45m-o**). Similar results were obtained by introducing two phenyl rings at positions 3 and 4 at the same time (**45k,l**). Based on these results, we can affirm that the position 4 of the isoxazolone scaffold bears bulky groups such a phenyl ring when position 3 is unsubstituted or substituted with a methyl group, while the same phenyl ring is never tolerate at position 3 independently from the substituent at position 4. Finally, as for compounds **46a,b** of the above discussed series, the replacement of the benzoyl group at position 2 of compound **45b** with a benzyl fragment (compound **46c**) afforded a completely inactive product, in according with our previous affirmation.
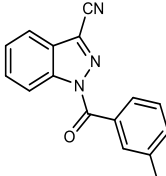
The graphical summary of SARs for compounds of type **45** is reported below.

Results and discussion
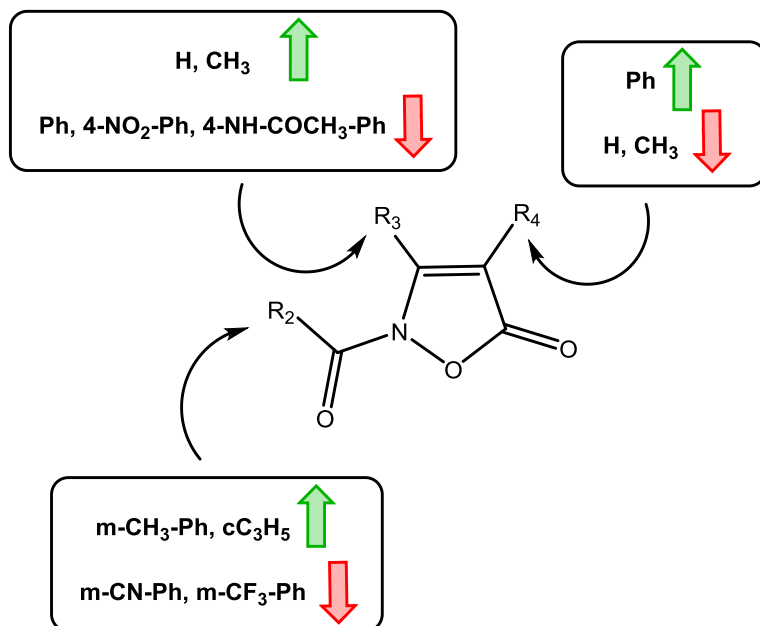
At the end, the **Table 6** shows the activity values of benzoisoxazolone derivatives **50a-c**, which were designed and synthetized as elaboration of the isoxazolone scaffold and until now obtained. Only the *m*-methylbenzoyl derivative **50c** has a remarkable activity with an IC_{50} of 638 nM, while the other compounds are less active (**50a**) or inactive (**50b**). This new series is under development.

Table 1: HNE inhibitory activity of 7-azaindole derivatives **5a-i** and **7a-e**
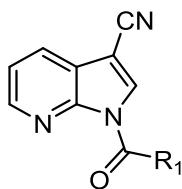
5a-i

7a-e

Compound	R_1	IC$_{50}$ (µM)[a]
5a	m-CH$_3$-Ph	0.015 ± 0.004
5b	p-CH$_3$-Ph	0.014 ± 0.004
5c	cC$_3$H$_5$	0.087 ± 0.021
5d	cC$_5$H$_9$	2.6 ± 0.21
5e	cC$_6$H$_{11}$	1.5 ± 0.32
5f	m-CN-Ph	19.1 ± 2.3
5g	p-CN-Ph	12.6 ± 2.5
5h	m-CF$_3$-Ph	1.8 ± 0.24
5i	p-CF$_3$-Ph	1.5 ± 0.23
7a	m-CH$_3$-Ph	0.77 ± 0.15
7b	p-CH$_3$-Ph	0.64 ± 0.12
7c	cC$_3$H$_5$	0.62 ± 0.14
7d	m-CN-Ph	11.5 ± 2.1
7e	p-CN-Ph	38.5 ± 4.8
Sivelestat	-	0.050 ± 0.020
	-	0.007 ± 0.0015

[a]IC$_{50}$ values are presented as the mean ± SD of three independent experiments.

Results and discussion

Table 2: HNE inhibitory activity of 7-azaindole derivatives **36**, **37** and **40**

36, 37, 40
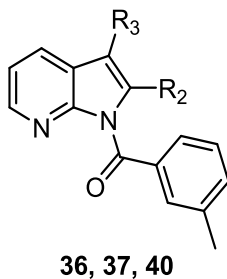
Compound	R_2	R_3	IC_{50} (µM)[a]
36	CH_3	CN	10.8 ± 2.2
37	COOEt	-	NA[b]
40	CN	-	3.5 ± 1.2
Sivelestat	-	-	0.050 ± 0.020

[a]IC_{50} values are presented as the mean ± SD of three independent experiments.
[b]NA: no inhibitory activity was found at the highest concentration of compound tested (50 µM).

Table 3: HNE inhibitory activity of 7-azaindole derivatives **10a-d**, **15a-e**, **18**, **21**, **26** and **30**.
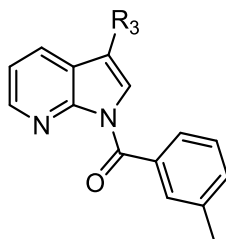
10a-d, 15a-e, 18, 21, 26, 30

Compound	R_3	IC$_{50}$ (µM)[a]
10a	I	7.3 ± 2.6
10b	Br	11.9 ± 3.2
10c	Cl	28.5 ± 1.2
10d	NO$_2$	0.024 ± 0.009
15a	3-CN-Ph	6.7 ± 2.1
15b	3-pyridine	6.0 ± 0.7
15c	2-furan	44.8 ± 3.8
15d	3-furan	42.6 ± 2.8
15e	3-thiophene	NA[b]
18	3-methyl-1,2,4-oxadiazole	0.080 ± 0.020
21	5-methyl-1,2,4-oxadiazole	3.6 ± 1.1
26	CH$_2$-N(CH$_3$)-Ph	2.4 ± 0.46
30	CH$_2$-NH-Ph	1.8 ± 0.2
Sivelestat	-	0.050 ± 0.020

[a]IC$_{50}$ values are presented as the mean ± SD of three independent experiments.
[b]NA: no inhibitory activity was found at the highest concentration of compound tested (50 µM).

Results and discussion

Table 4: HNE inhibitory activity of isoxazolone derivatives **43a-s**, **44a**,**b** and **46a**,**b**
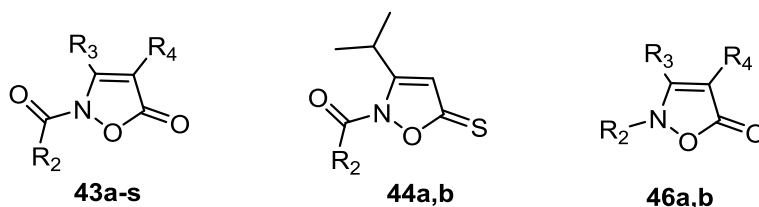
Compound	R_2	R_3	R_4	IC_{50} (µM)[a]
43a	cC_3H_5	CH_3	CH_3	0.12 ± 0.023
43b	m-CH$_3$-Ph	CH_3	CH_3	10.9 ±1.2
43c	cC_3H_5	CH_3	C_2H_5	0.13 ± 0.025
43d	m-CH$_3$-Ph	CH_3	C_2H_5	0.094 ± 0.023
43e	cC_3H_5	C_2H_5	CH_3	2.2 ± 0.28
43f	m-CH$_3$-Ph	C_2H_5	CH_3	1.8 ± 0.32
43g	cC_3H_5	COOEt	CH_3	0.44 ± 0.14
43h	m-CH$_3$-Ph	COOEt	CH_3	39.7 ± 5.1
43i	cC_3H_5	C_2H_5	H	0.096 ± 0.022
43j	m-CH$_3$-Ph	C_2H_5	H	0.043 ± 0.011
43k	C_2H_5	iC_3H_7	H	1.1 ± 0.14
43l	cC_3H_5	iC_3H_7	H	0.034 ± 0.009
43m	cC_5H_9	iC_3H_7	H	0.56 ± 0.15
43n	m-CH$_3$-Ph	iC_3H_7	H	0.042 ± 0.011
43o	p-CH$_3$-Ph	iC_3H_7	H	0.020 ± 0.007
43p	m-CN-Ph	iC_3H_7	H	6.5 ± 1.7
43q	p-CN-Ph	iC_3H_7	H	18.2 ± 2.5
43r	m-CF$_3$-Ph	iC_3H_7	H	1.2 ± 0.22
43s	p-CF$_3$-Ph	iC_3H_7	H	0.034 ± 0.012
44a	cC_3H_5	-	-	2.1 ± 0.31
44b	m-CH$_3$-Ph	-	-	NA[b]
46a	m-CH$_3$-benzyl	CH_3	CH_3	NA[b]
46b	m-CH$_3$-benzyl	iC_3H_7	H	NA[b]
Sivelestat	-	-	-	0.050 ± 0.020

[a]IC_{50} values are presented as the mean ± SD of three independent experiments.
[b]NA: no inhibitory activity was found at the highest concentration of compound tested (50 µM).

**Table 5:** HNE inhibitory activity of isoxazolone derivatives **45a-o** and **46c**.
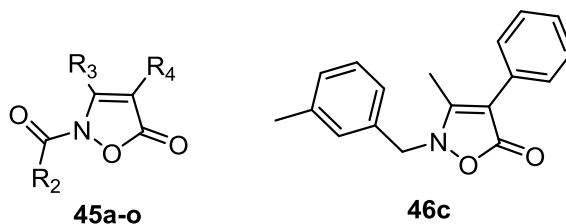
Compound	R_2	R_3	R_4	IC_{50} (µM)[a]
45a	cC_3H_5	CH_3	Ph	0.059 ± 0.018
45b	m-CH_3-Ph	CH_3	Ph	0.077 ± 0.027
45c	m-CN-Ph	CH_3	Ph	6.3 ± 1.4
45d	m-CF_3-Ph	CH_3	Ph	0.20 ± 0.027
45e	cC_3H_5	H	Ph	0.016 ± 0.005
45f	m-CH_3-Ph	H	Ph	0.046 ± 0.012
45g	cC_3H_5	Ph	CH_3	1.1 ± 0.14
45h	m-CH_3-Ph	Ph	CH_3	13.6 ± 2.4
45i	cC_3H_5	Ph	H	12.7 ± 2.7
45j	m-CH_3-Ph	Ph	H	48.7 ± 3.3
45k	cC_3H_5	Ph	Ph	17.2 ± 2.3
45l	m-CH_3-Ph	Ph	Ph	10.1 ± 1.3
45m	cC_3H_5	4-NO_2-Ph	H	NA[b]
45n	m-CH_3-Ph	4-NO_2-Ph	H	NA[b]
45o	m-CH_3-Ph	4-$NHCOCH_3$-Ph	H	28.6 ± 3.3
46c	-	-	-	NA[b]
Sivelestat	-	-	-	0.050 ± 0.020

[a]IC_{50} values are presented as the mean ± SD of three independent experiments.
[b]NA: no inhibitory activity was found at the highest concentration of compound tested (50 µM).

Results and discussion

Table 6: HNE inhibitory activity of benzoisoxazolone derivatives **50a-c**.
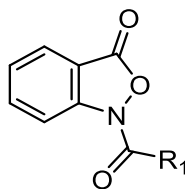
50a-c

Compound	R_1	IC$_{50}$ (µM)[a]
50a	C_2H_5	25.1 ± 3.6
50b	C_4H_9	NA[b]
50c	*m*-CH$_3$-Ph	0.638 ± 0.121
Sivelestat	-	0.050 ± 0.020

[a]IC$_{50}$ values are presented as the mean ± SD of three independent experiments.
[b]NA: no inhibitory activity was found at the highest concentration of compound tested (50 µM)

4.2 *Stability and kinetic features*

Some selected isoxazolones belonging to the first series (compounds of type **43**, substituted at position 3 and 4 with small alkyl group) were further evaluated for chemical stability in aqueous buffer using spectrophotometry to detect compounds hydrolysis. The compounds had $t_{1/2}$ values from 3.1 to 19.3 h for spontaneous hydrolysis (**Table 7**), indicating that these isoxazolones were more stable than our previously described HNE inhibitors with *N*-benzoylindazole scaffolds (Crocetti, L. et al. 2011) (Crocetti, L. et al. 2013).

Table 7: half-Life ($t_{1/2}$) for the hydrolysis of selected isoxazolone derivatives in aqueous buffer in absence and in the presence of HNE.

Compound	max (nm)[a]	t$_{1/2}$ (h)	
		spontaneous hydrolysis	in the presence HNE[b]
43d	290	7.7	3.5
43i	275	19.3	4.0
43j	285	5.3	2.1
43l	275	19.3	4.3
43n	285	6.2	2.6
43o	290	8.9	3.4
43s	285	3.1	0.9

[a]Absorption maximum of the compounds for monitoring hydrolysis. [b]Hydrolysis was monitored in the presence of 400 mU/ml HNE.

We also tested compound hydrolysis in the presence of HNE and found that the speed of hydrolysis gradually increased with increasing enzyme concentration. As an example, **Fig. 23** shows dose-dependent hydrolysis of compound **43i** over time. In the presence of 400 mU/ml HNE, the hydrolysis was 2.2-4.8-fold higher than for spontaneous hydrolysis (i.e., without HNE) (see **Table 7**).
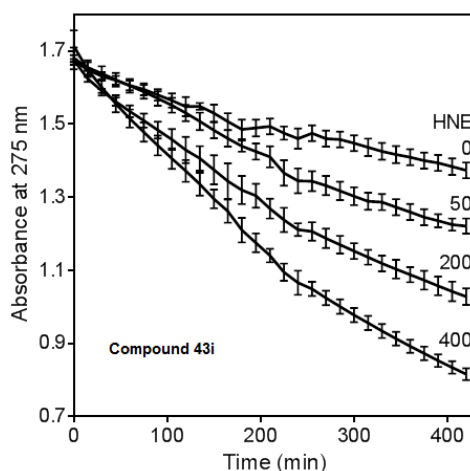
Fig. 23: analysis of compound **43i** spontaneous hydrolysis. Compound **43i** (80 µM) was incubated in 0.05 M phosphate buffer (pH 7.5, 25 °C)

supplemented with 0, 50, 200, and 400 µg/mL HNE, as indicated. Spontaneous hydrolysis was monitored by measuring changes in absorbance at 275 nm (absorption maximum of compound 43i) over time. The data are presented as the mean ± S.D. of triplicate samples from one experiment, which is representative of two independent experiments.

We also evaluated reversibility of the HNE-inhibitor complex over time for most potent compounds. As shown in **Fig. 24**, HNE inhibition was maximal during the first 30 min for compounds **43n**, **43d**, **43l**, **43i** and **43j**. However, inhibition by compound **43s** was reversed after 10 min. The most stable inhibition was found for **43o**, where inhibition of HNE activity was reversed only after 2h.
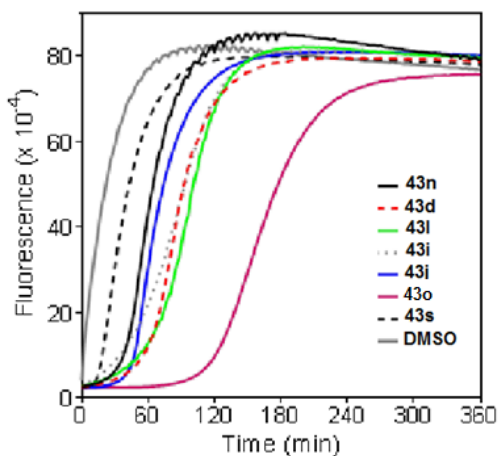
Fig. 24: evaluation of HNE inhibition by selected isoxazolone derivatives. HNE was incubated with the indicated compounds at 5 µM concentrations, and kinetic curves monitoring substrate cleavage catalyzed by HNE are shown. Representative curves are from three independent experiments.

Compound **43o** was the selected to perform additional kinetic experiments. As shown in **Fig. 25**, the representative double-reciprocal Lineweaver-Burk plot of fluorogenic substrate hydrolysis by HNE in the absence and presence of compound **43o** indicates that this compound is a competitive HNE inhibitor.
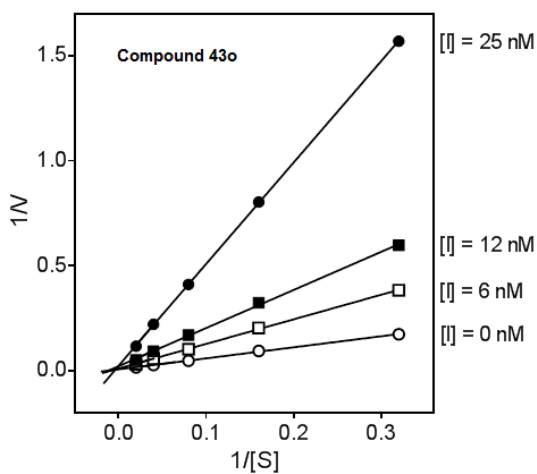
Fig. 25: kinetics of HNE inhibition by compound **43o**. Representative double-reciprocal Lineweaver-Burk plot from three independent experiments.

73

4.3 *Molecular Modeling*

For some compounds with the isoxazolone scaffold, molecular modeling studies were conducted by Dr. Andrei Khlebnikov of the research group of Prof. Quinn. Molecular docking of derivatives **43l**, **43n**, **43o**, **43q**, **44a** and **44b** into the HNE binding site (1HNE entry of Protein Data Bank) was performed and the side chains of selected residues in HNE binding site were considered flexible, as described in our previous studies (Crocetti, L. et al. 2013) (Crocetti, L. et al. 2016).

Table 8: biological activities, geometric parameters, and docking scores of the enzyme–inhibitor complexes predicted by molecular docking with MVD.

Compound	IC_{50} (μM)[a]	α	d_1	d_2	d_3	L[b]	Docking Score ΔE (kcal/mol)
43l[c]	0.034	85.2	2.903	2.763, 3.967	2.829	5.592	-58.9
44a	2.1	139.6	4.148	2.379, 3.611	2.560	4.939	-44.0
43n	0.042	81.6	3.861	2.399, 3.627	2.596	4.995	-34.2
44b	NA	148.3	4.659	2.750, 3.962	2.849	5.599	-21.1
43o[c]	0.020	104.1	3.134	2.760, 3.975	2.819	5.579	-67.6
43q[c]	18.2	89.4	4.500	3.130, 4.319	3.286	6.416	-58.4

[a]HNE inhibitory activity. [b]The length of the proton transfer channel was calculated as $L = d_3 + \min(d_2)$. [c]According to the docking results, a Michaelis complex with Ser195 is formed with participation of the ester carbonyl group.

According to the docking scores ΔE of the poses (**Table 8**), isoxazolones are effectively anchored within HNE binding site. However, it is well known that catalytic activity of serine protease is related to synchronous proton transfer from serine via histidine to aspartate residues (Vergely, I. et al. 1996). In HNE, this catalytic triad corresponds to Ser195, His57 and Asp102 respectively. The length of the proton transfer channel is characterized by the magnitude of L (see **Table 8**). Additionally, effectiveness of HNE binding to a ligand depends on its ability to form a Michaelis complex between a carbonyl group of the ligand and an oxyanione hole centered at the hydroxyl oxygen atom of Ser195. Geometry which favours Michaelis complex formation corresponds to ligand orientation with angle α values from 80° to 120° and with shortened distance d_1 (1.8-2.6 Å) (Vergely, I. et al. 1996) (**Table 8**). Although a low-energy docking pose of each ligand is not completely identical to the Michaelis complex, they must have certain similarity. Hence, it is reasonable to use the geometry of the low-energy pose to evaluate the possibility of complex formation. Compounds **43l**, **43n**, **43o**, **43q**, **44a** and **44b** occupy an area in the HNE binding site in the vicinity of the terminal part of the co-crystallized peptide. As presented in **Table 8**, the sulfur-containing compounds **44a** and **44b** had larger distances d_1 (4.148 Å and 4.659 Å, respectively) than their counterparts **43l** and **43n** and they were characterized by an angle α that was not suitable for easy formation of a Michaelis complex (139.6° and 148.3°, respectively). The different orientation within the binding site of sulfur compounds, with respect to compounds containing the 5-carbonyl group could also be caused by higher values of C=S bond length and radius of the sulfur atom (**Fig. 26**).
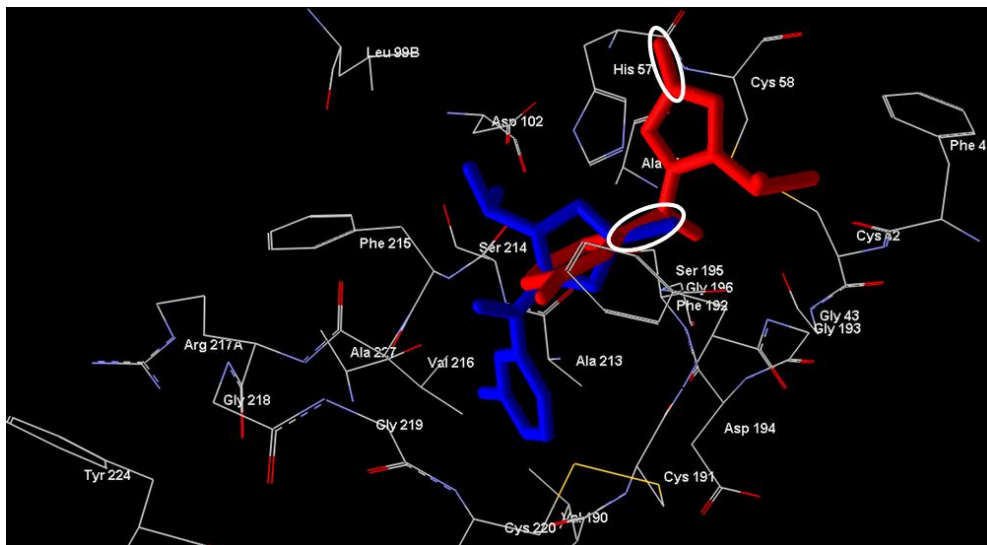
Fig. 26: Docking poses of compounds **43n** (blue) and **44b** (red). The ovals represent respectively the C=S and C=O fragment of the two compounds, respectively. Residues within 6 Å from the co-crystallized ligand are shown.

From the docking studies, it is interesting to note that these isoxazolone compounds show involvement of the endocyclic carbonyl group in formation of a Michaelis adduct, but also the amide carbonyl group is important for proper anchoring of the ligands to the enzyme pocket. For example, compounds **43o** and **43q** show values of angle α in the exact range (**Table 8**) and are located similarly in the HNE binding site to allow formation a Michaelis complex with the endocyclic carbonyl group. In particular, inhibitor **43o**, which has the best inhibitory activity (IC_{50} = 20 nM) forms a hydrogen bond between the oxygen of the 5-carbonyl group and the NH group of Ser195 that likely improves the enzyme-ligand orientation, in addition to the involvement of the 5-carbonyl carbon atom and the Ser195 hydroxyl group, for the formation of Michaelis complex (**Fig. 27**).
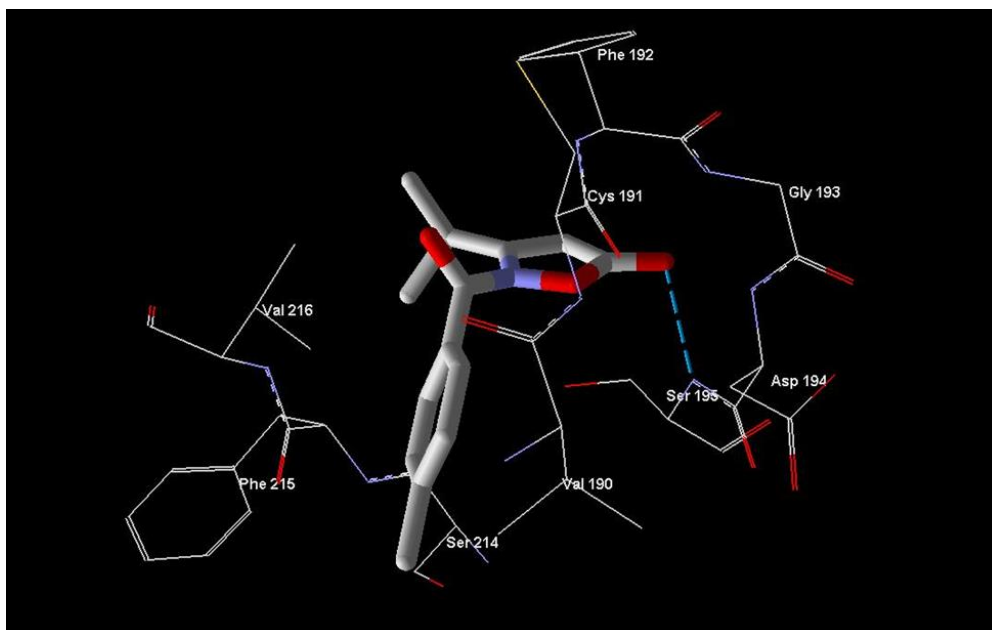
Fig. 27: docking pose of compound **43o**. Residues within 3Å of the pose are visible. The H-bond is shown by a light-blue dashed line.

In compound **43q**, the 5-carbonyl group (carbon atom) is located at a longer distance d1 from Ser195 than that of **43o** (see **Table 8**). This is due to the H-bond interaction of the oxygen atom of the 5-carbonyl group that involves the NH group of Gly193 instead of the NH group of Ser195. Moreover, for derivative **43q**, the imidazole ring of His57 is rotated unfavorably, thus enhancing the length *L* of the proton transfer channel (**Table 8**). Consequently, the conditions for formation of a Michaelis complex are not as suitable and lead to reduced inhibitory activity (IC_{50} = 18.2 μM). Differences between **43o** and **43q**, which are p-tolyl- and p-cyanophenyl derivatives, respectively, could also likely be related to variations in hydrophobicity, polarity of substituents, and different orientation of flexible side chains in the ligand-enzyme complex. Thus, our docking studies indicate that the 2-amido carbonyl group also plays an important role in positioning the ligand within the binding site, although the attack of the Ser195 is directed at the endocyclic C=O group (5-carbonyl group).

Results and discussion

The sum of non-bonding interaction energies between HNE and the two atoms of the amido carbonyl moiety of 43o equals -12.86 kcal/mol, which is even more negative than for the endocyclic carbonyl (-9.11 kcal/mol), indicating a strong interaction with the enzyme. Non-specific Van der Waals interaction by the tolyl ring and/or polar interactions by the 2-amido group are responsible for proper anchoring of **43o** to the sub-pocket of the binding site surrounded by Cys191, Phe192, Phe215, Val216, and Cys220. Although **43q** shows these non-specific interactions with the sub-pocket binding site, the different orientation in the enzyme pocket caused by the H-bond interaction of the oxygen atom of the 5-carbonyl group involving the NH Gly193 could explain the lower inhibitory activity compared to **43o**.

5. CONCLUSIONS

The work performed during this period as PhD student affords interesting results in the design and synthesis of two different classes of HNE inhibitors.

➤ The first one, characterized by the 7-azaindole scaffold, includes some potent HNE inhibitors all showing at position 3 an electron withdrawing group, such as CN or NO_2. This feature seems to be important for activity, as well as at position 1 the presence of the N-CO group that we believe to be the point of attack of Ser195. Furthermore, position 2 should not be replaced.

R_3 = CN, NO_2

R_1 = m-CH_3-Ph, p-CH_3-Ph
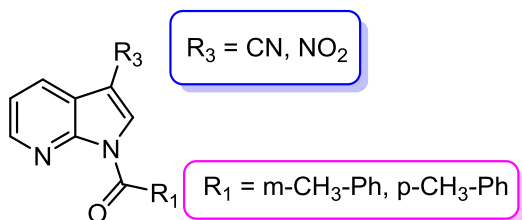
IC_{50} = 14-24 nM

For this first series of compounds, designed as isomers of the potent indazoles previously reported by us, the results of the underway molecular modeling studies will be particularly important to understand the role of the nitrogen at position 7 in the anchoring of the molecules to the enzyme, as well as the importance of the substituents in the different positions. These information will be useful for the continuation of this project.

➤ The second class consists of compounds with isoxazolone nucleus, another appropriate scaffold for the synthesis of HNE inhibitors. The most active compounds show IC_{50} = 20-80 nM. The best results were obtained when at position 3 is present an alkyl group (ethyl, isopropyl) and position 4 is unsubstituted (compound of type **43**); alternatively

Conclusions

potent compounds were obtained when position 3 is unsubstituted or bearing a methyl group and at position 4 a phenyl ring is present (compounds of type **45**).

$R_3 = C_2H_5, iC_3H_7$ | $R_4 = H$ | $R_3 = H, CH_3$ | $R_4 = Ph$

43 $R_2 = cC_3H_5, m\text{-}CH_3\text{-}Ph$ **45**
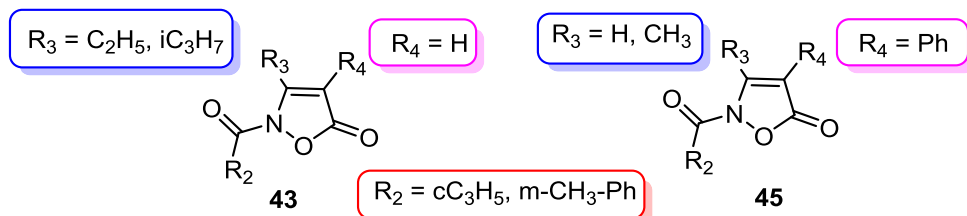
IC_{50} = 20-80 nM

Since these compounds show two carbonyl groups as possible points of attack of the Ser195, molecular modeling studies were performed on products of type **43** (R_3, R_4 =H, alkyl) with the aim to clarify the interaction with the target. Docking studies show that the attack of the Ser195 is directed at the endocyclic C=O at position 5, but that also the 2-N-CO-R group is important for the anchoring to sub-pocket of the binding site surrounded by Cys191, Phe192, Phe215, Val216 and Cys220 through nonspecific van der Walls and polar interactions. These observations are in agreement with the inactivity of the 2-N-alkyl/aryl derivatives and of the thioanalogues. We are waiting for the results of docking studies on compounds of type **45** (bearing at position 4 a phenyl ring) whose activity seems in contrast with the results of the 4-unsubstituted isoxazolones of type **43**. This apparent incongruity could be explained hypothesizing a π-π interaction of the phenyl ring with the enzyme. Studies of chemical stability in aqueous buffer indicate that the new isoxazolones are very stable with $t_{1/2}$ values from 3.1 to 19.3 h. Experiments of reversibility of the HNE-inhibition complex over time for the most potent compounds, together with additional kinetic experiments indicate that this class of compounds work as competitive HNE inhibitors.

6. MATERIAL AND METHODS

6.1 *CHEMISTRY*

All melting points were determined on a Büchi apparatus (New Castle, DE) and are uncorrected. Extracts were dried over Na_2SO_4, and the solvents were removed under reduced pressure. Merck F-254 commercial plates (Merck, Durham, NC) were used for analytical TLC to follow the course of reactions. Silica gel 60 (Merck 70–230 mesh, Merck, Durham, NC) was used for column chromatography. ^{1}H-NMR, ^{13}C-NMR, HMBC and HSQC spectra were recorded on an Avance 400 instrument (Bruker Biospin Version 002 with SGU, Bruker Inc., Billerica, MA). Chemical shifts (δ) are reported in ppm to the nearest 0.01 ppm using the solvent as an internal standard. Coupling constants (J values) are given in Hz and were calculated using TopSpin 1.3 software (Nicolet Instrument Corp., Madison, WI) and are rounded to the nearest 0.1 vHz. Mass spectra (m/z) were recorded on an ESI-TOF mass spectrometer (Brucker Micro TOF, Bruker Inc., Billerica, MA), and reported mass values are within the error limits of ±5 ppm mass units. Microanalyses indicated by the symbols of the elements or functions were performed with a Perkin–Elmer 260 elemental analyzer (PerkinElmer, Inc., Waltham, MA) for C, H, and N, and the results were within ±0.4% of the theoretical values, unless otherwise stated. Reagents and starting material were commercially available.

General procedure for acylation or benzoylation at N-1 of the 7-azaindole derivatives. To a cooled (0°C) suspension of the appropriate substrate (0.56 mmol) in anhydrous CH_2Cl_2 (2 mL), 0.72 mmol of Et_3N and 1.67 mmol of the appropriate acyl or benzoyl chloride were added. The mixture was stirred at 0°C for 2h and then at room temperature for an additional 2h. The solvent was evaporated, cold water was added, and the mixture was neutralized with 0.5 N NaOH. The reaction mixture was extracted with CH_2Cl_2 (3 x 15 mL), the solvent was dried over sodium sulfate and evaporated in vacuum. The final compounds were purified by crystallization from ethanol or by column

chromatography using cyclohexane/ethyl acetate or hexane/ethyl acetate as eluents in different ratio.
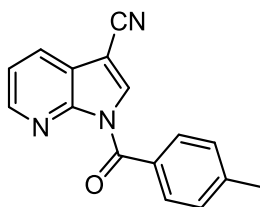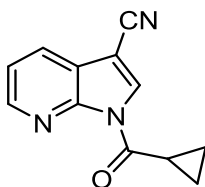
1-(3-Methylbenzoyl)-1H-pyrrolo[2,3-b]pyridine-3-carbonitrile (5a)
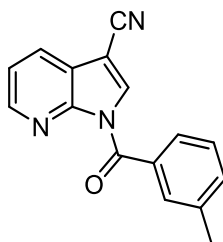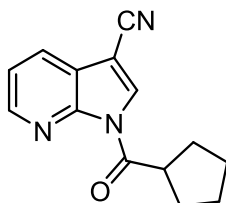

Obtained from compound **4** (Bahekar, R. H. et al. 2007) following the general procedure reported at **pag. 81**. Compound **5a** was purified by crystallization (EtOH).

Yield = 48%; mp = 127-129°C (EtOH). $\underline{^1\text{H-NMR}}$ (DMSO-d_6) δ 2.36 (s, 3H, CH$_3$), 7.40-7.46 (m, 2H, Ar), 7.53-7.58 (m, 2H, Ar), 7.63 (s, 1H, Ar), 8.24 (d, 1H, Ar, J = 8.0 Hz), 8.36 (d, 1H, Ar, J = 4.8 Hz), 8.82 (s, 1H, Ar). $\underline{^{13}\text{C-NMR}}$ (DMSO-d_6) δ 21.21 (CH$_3$), 101.00 (C), 114.37 (C), 116.00 (CH), 120.89 (CH), 128.31 (CH), 128.86 (CH), 129.03 (CH), 131.19 (CH), 132.76 (C), 135.04 (CH), 138.53 (C), 146.55 (CH), 147.08 (C), 149.00 (C), 167.10 (C). IR = 1693 cm^{-1} (C=O), 2229 cm^{-1} (CN). ESI-MS calcd. for C$_{16}$H$_{11}$N$_3$O, 261.28; found: m/z 262.09 [M+H]$^+$. Anal. C$_{16}$H$_{11}$N$_3$O (C, H, N).
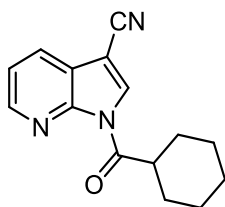
1-(4-Methylbenzoyl)-1H-pyrrolo[2,3-b]pyridine-3-carbonitrile (5b)

Obtained from compound **4** (Bahekar, R. H. et al. 2007) following the general procedure reported at **pag. 81**. Compound **5b** was purified by crystallization (EtOH).

Yield = 55%; mp = 146-149°C (EtOH). $\underline{^1\text{H-NMR}}$ (DMSO-d_6) δ 2.41 (s, 3H, CH$_3$), 7.35 (d, 2H, Ar, J = 8.0 Hz), 7.41-7.46 (m, 1H, Ar), 7.70 (d, 2H, Ar, J = 8.0 Hz), 8.23 (dd, 1H, Ar, J = 1.4 Hz and J = 7.8 Hz), 8.31-8.36 (m, 1H, Ar), 8.84 (s, 1H, Ar). $\underline{^{13}\text{C-NMR}}$ (DMSO-d_6) δ 21.80 (CH$_3$), 101.00 (C), 115.05 (C), 115.62 (CH), 121.21 (C), 123.85 (CH), 128.33 (CH), 129.52 (CH), 129.59 (CH), 129.81 (CH), 129.86 (CH), 130.00 (C), 142.40 (CH), 144.25 (C), 146.66 (C), 167.70 (C). $\underline{\text{IR}}$ = 1697 cm^{-1} (C=O), 2267 cm^{-1} (CN). ESI-MS calcd. for C$_{16}$H$_{11}$N$_3$O, 261.28; found: m/z 262.09 [M+H]$^+$. Anal. C$_{16}$H$_{11}$N$_3$O (C, H, N).

1-(Cyclopropanecarbonyl)-1H-pyrrolo[2,3-b]pyridine-3-carbonitrile (5c)
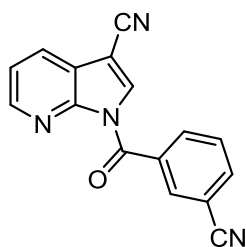

Obtained from compound **4** (Bahekar, R. H. et al. 2007) following the general procedure reported at **pag. 81**. Compound **5c** was purified by crystallization (EtOH).

Material and methods

Yield = 84%; mp = 142-145°C (EtOH). ^{1}H-NMR (DMSO-d$_6$) δ 1.23-1.29 (m, 4H, 2 x CH$_2$), 4.00-4.05 (m, 1H, CH), 7.49-7.54 (m, 1H, Ar), 8.24 (d, 1H, Ar, J = 7.6 Hz), 8.55 (d, 1H, Ar, J = 4.0 Hz), 8.89 (s, 1H, Ar). ^{13}C-NMR (DMSO-d$_6$) δ 12.60 (CH$_2$), 15.24 (CH), 89.79 (C), 114.25 (C), 120.94 (CH), 121.67 (C), 129.50 (CH), 135.26 (CH), 146.50 (CH), 146.64 (C), 172.69 (C). IR = 1711 cm^{-1} (C=O), 2226 cm^{-1} (CN). ESI-MS calcd. for C$_{12}$H$_9$N$_3$O, 211.22; found: *m/z* 212.08 [M+H]$^+$. Anal. C$_{12}$H$_9$N$_3$O (C, H, N).

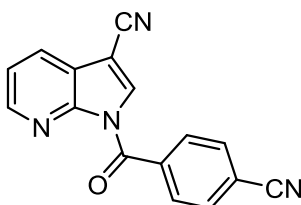**1-(Cyclopentanecarbonyl)-1H-pyrrolo[2,3-b]pyridine-3-carbonitrile (5d)**

Obtained from compound **4** (Bahekar, R. H. et al. 2007) following the general procedure reported at **pag. 81**. Compound **5d** was purified by crystallization (EtOH).

Yield = 39%; mp = 97-100°C (EtOH). ^{1}H-NMR (DMSO-d$_6$) δ 1.63-1.68 (m, 4H, 2 x CH$_2$), 1.81-1.86 (m, 2H, CH$_2$), 1.99-2.04 (m, 2H, CH$_2$), 4.61-4.66 (m, 1H, CH), 7.46-7.51 (m, 1H, Ar), 8.22 (d, 1H, Ar, J = 7.6 Hz), 8.56 (d, 1H, Ar, J = 3.6 Hz), 8.92 (s, 1H, Ar). ^{13}C-NMR (DMSO-d$_6$) δ 26.28 (CH$_2$), 29.98 (CH$_2$), 45.19 (CH), 89.95 (C), 114.26 (C), 120.80 (CH), 121.61 (C), 129.33 (CH), 135.69 (CH), 146.64 (C), 146.70 (CH), 174.41 (C). IR = 1710 cm^{-1} (C=O), 2230 cm^{-1} (CN). ESI-MS calcd. for C$_{14}$H$_{13}$N$_3$O, 239.27; found: *m/z* 240.11 [M+H]$^+$. Anal. C$_{14}$H$_{13}$N$_3$O (C, H, N).

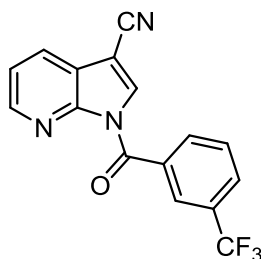**1-(Cyclohexanecarbonyl)-1H-pyrrolo[2,3-b]pyridine-3-carbonitrile (5e)**

Obtained from compound **4** (Bahekar, R. H. et al. 2007) following the general procedure reported at **pag. 81**. Compound **5e** was purified by crystallization (EtOH).

Yield = 39%; mp = 172-175°C (EtOH). <u>^{1}H-NMR</u> (DMSO-d_6) δ 1.22-1.28 (m, 1H, CH), 1.34-1.50 (m, 4H, 2 x CH$_2$), 1.65-1.70 (m, 1H, CH), 1.77-1.82 (m, 2H, CH$_2$), 1.95-2.00 (m, 2H, CH$_2$), 4.23-4.28 (m, 1H, CH), 7.48 (dd, 1H, Ar, J = 4.8 Hz and J = 7.6 Hz), 8.22 (d, 1H, Ar, J = 8.0 Hz), 8.57 (d, 1H, Ar, J = 4.4 Hz), 8.90 (s, 1H, Ar). <u>^{13}C-NMR</u> (DMSO-d_6) δ 25.49 (CH$_2$), 25.79 (CH$_2$), 28.96 (CH$_2$), 43.95 (CH), 90.05 (C), 114.24 (C), 120.79 (CH), 121.55 (C), 129.34 (CH), 135.53 (CH), 140.00 (C), 146.83 (CH), 174.26 (C). <u>IR</u> = 1711 cm^{-1} (C=O), 2220 cm^{-1} (CN). ESI-MS calcd. for C$_{15}$H$_{15}$N$_3$O, 253.30; found: *m/z* 254.12 [M+H]$^+$. Anal. C$_{15}$H$_{15}$N$_3$O (C, H, N).

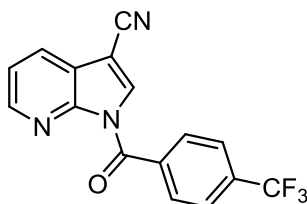**1-(3-Cyanobenzoyl)-1H-pyrrolo[2,3-b]pyridine-3-carbonitrile (5f)**

Obtained from compound **4** (Bahekar, R. H. et al. 2007) following the general procedure reported at **pag. 81**. Compound **5f** was purified by column chromatography using cyclohexane/ethyl acetate 2:1 as eluent.

Yield = 10%; oil. <u>^{1}H-NMR</u> (CDCl$_3$-d$_1$) δ 7.35-7.40 (m, 1H, Ar), 7.66 (t, 1H, Ar, $J = 7.6$ Hz), 7.95 (d, 1H, Ar, $J = 8.0$ Hz), 8.03 (d, 1H, Ar, $J = 8.0$ Hz), 8.12 (s, 1H, Ar), 8.13 (dd, 1H, Ar, $J = 1.2$ Hz and $J = 8.0$ Hz), 8.30 (d, 1H, Ar, $J = 4.4$ Hz), 8.40 (s, 1H, Ar). <u>^{13}C-NMR</u> (CDCl$_3$-d$_1$) δ 101.02 (C), 113.15 (C), 115.54 (C), 115.68 (CH), 118.61 (C), 121.20 (C), 123.86 (CH), 128.33 (CH), 129.97 (CH), 131.22 (C), 133.10 (CH), 135.43 (CH), 138.05 (CH), 142.46 (CH), 146.66 (C), 167.75 (C). ESI-MS calcd. for C$_{16}$H$_8$N$_4$O, 272.26; found: *m/z* 273.07 [M+H]$^+$. Anal. C$_{16}$H$_8$N$_4$O (C, H, N).

**1-(4-Cyanobenzoyl)-1H-pyrrolo[2,3-b]pyridine-3-carbonitrile (5g)**

Obtained from compound **4** (Bahekar, R. H. et al. 2007) following the general procedure reported at **pag. 81**. Compound **5g** was purified by column chromatography using cyclohexane/ethyl acetate 2:1 as eluent.

Yield = 39%; oil. $\underline{^1\text{H-NMR}}$ (CDCl$_3$-d$_1$) δ 7.35-7.40 (m, 1H, Ar), 7.81 (d, 2H, Ar, J = 8.0 Hz), 7.89 (d, 2H, Ar, J = 8.0 Hz), 8.12 (dd, 1H, Ar, J = 1.2 Hz and J = 7.6 Hz), 8.29 (d, 1H, Ar, J = 4.4 Hz), 8.39 (s, 1H, Ar). $\underline{^{13}\text{C-NMR}}$ (CDCl$_3$-d$_1$) δ 92.41 (C), 112.95 (C), 116.95 (C), 117.68 (C), 117.75 (C), 120.74 (CH), 121.13 (C), 129.03 (CH), 130.79 (CH), 132.01 (CH), 133.95 (CH), 136.34 (CH), 146.55 (C), 165.36 (C). ESI-MS calcd. for C$_{16}$H$_8$N$_4$O, 272.26; found: *m/z* 273.07 [M+H]$^+$. Anal. C$_{16}$H$_8$N$_4$O (C, H, N).

1-(3-(Trifluoromethyl)benzoyl)-1H-pyrrolo[2,3-b]pyridine-3-carbonitrile (5h)

Obtained from compound **4** (Bahekar, R. H. et al. 2007) following the general procedure reported at **pag. 81**. Compound **5h** was purified by crystallization (EtOH).

Yield = 45%; mp = 155-157°C (EtOH). $\underline{^1\text{H-NMR}}$ (CDCl$_3$-d$_1$) δ 7.33-7.38 (m, 1H, Ar), 7.67 (t, 1H, Ar, J = 8.0 Hz), 7.94 (d, 1H, Ar, J = 8.4 Hz), 8.00 (d, 1H, Ar, J = 7.6 Hz), 8.08 (s, 1H, Ar), 8.13 (dd, 1H, Ar, J = 1.6 Hz and J = 8.0 Hz), 8.33 (dd, 1H, Ar, J = 1.6 Hz and J = 4.8 Hz), 8.38 (s, 1H, Ar). $\underline{^{13}\text{C-NMR}}$ (CDCl$_3$-d$_1$) δ 92.54 (C), 113.69 (C), 121.23 (CH), 121.71 (CH), 125.40 (C), 128.33 (C, q, J = 31.4 Hz), 128.37 (CH), 130.82 (C, q, J = 28.8 Hz), 131.32 (CH), 131.67 (C), 133.67 (CH), 134.32 (CH), 134.86 (CH), 147.09 (CH), 147.19 (C), 166.10 (C). ESI-MS calcd. for C$_{16}$H$_8$F$_3$N$_3$O, 315.25; found: *m/z* 316.07 [M+H]$^+$. Anal. C$_{16}$H$_8$F$_3$N$_3$O (C, H, N).

1-(4-(Trifluoromethyl)benzoyl)-1H-pyrrolo[2,3-b]pyridine-3-carbonitrile (5i)

Obtained from compound **4** (Bahekar, R. H. et al. 2007) following the general procedure reported at **pag. 81**. Compound **5i** was purified by crystallization (EtOH).

Yield = 14%; mp = 120-123°C (EtOH). ^{1}H-NMR (CDCl$_3$-d$_1$) δ 7.33-7.38 (m, 1H, Ar), 7.78 (d, 2H, Ar, J = 8.4 Hz), 7.91 (d, 2H, Ar, J = 8.0 Hz), 8.12 (d, 2H, Ar, J = 7.6 Hz), 8.35 (s, 1H, Ar). ^{13}C-NMR (CDCl$_3$-d$_1$) δ 101.15 (C), 115.65 (C), 121.23 (C), 121.71 (CH), 125.67 (CH), 124.13 (C, q, J = 31.6 Hz), 128.37 (CH), 130.82 (C, q, J = 28.8 Hz), 131.32 (CH), 133.67 (CH), 136.32 (C), 142.10 (CH), 146.19 (C), 167.70 (C). ESI-MS calcd. for C$_{16}$H$_8$F$_3$N$_3$O, 315.25; found: m/z 316.07 [M+H]$^+$. Anal. C$_{16}$H$_8$F$_3$N$_3$O (C, H, N).

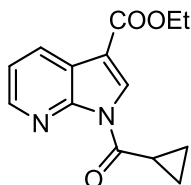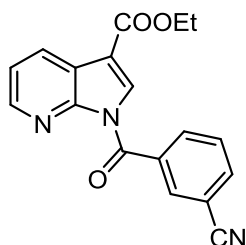## Ethyl 1-(3-methylbenzoyl)-1H-pyrrolo[2,3-b]pyridine-3-carboxylate (7a)
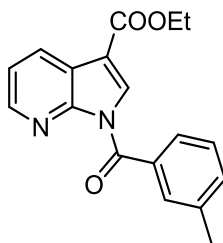
Obtained from compound **6** (Jiang, J. H. et al. 2011) following the general procedure reported at **pag. 81**. Compound **7a** was purified by crystallization (EtOH).

Yield = 25%; mp = 92-95°C (EtOH). ^{1}H-NMR (CDCl$_3$-d$_1$) δ 1.42 (t, 3H, OCH$_2$*CH$_3$*, J = 7.0 Hz), 2.43 (s, 3H, CH$_3$), 4.41 (q, 2H, O*CH$_2$*CH$_3$, J = 7.0 Hz), 7.31 (t, 1H, Ar, J = 6.0 Hz), 7.39 (t, 1H, Ar, J = 7.2 Hz), 7.47 (d, 1H, Ar, J = 6.8 Hz), 7.56 (d, 1H, Ar, J = 7.2 Hz), 7.66 (s, 1H, Ar), 8.30 (s,1H, Ar), 8.41 (s, 1H, Ar), 8.48 (d, 1H, Ar, J = 7.6 Hz). ^{13}C-NMR (CDCl$_3$-d$_1$) δ 14.45 (CH$_3$), 21.37 (CH$_3$), 60.69 (CH$_2$), 110.81 (C), 120.13 (CH), 120.74 (C), 127.70 (CH), 128.31 (CH), 130.60 (CH), 130.90 (CH), 132.80 (C), 133.20 (CH), 134.30 (CH), 138.60 (C), 145.60 (CH), 148.40 (C), 163.70 (C), 167.60 (C). ESI-MS calcd. for C$_{18}$H$_{16}$N$_2$O$_3$, 308.33; found: *m/z* 309.12 [M+H]$^+$. Anal. C$_{18}$H$_{16}$N$_2$O$_3$ (C, H, N).

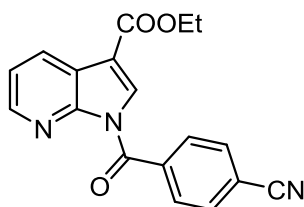**Ethyl 1-(4-methylbenzoyl)-1H-pyrrolo[2,3-b]pyridine-3-carboxylate (7b)**
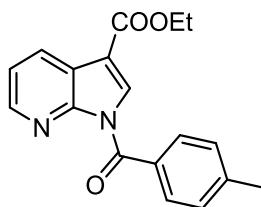
Obtained from compound **6** (Jiang, J. H. et al. 2011) following the general procedure reported at **pag. 81**. Compound **7b** was purified by crystallization (EtOH).

Yield = 30%; mp = 100-103°C (EtOH). ^{1}H-NMR (CDCl$_3$-d$_1$) δ 1.42 (t, 3H, OCH$_2$*CH$_3$*, J = 7.2 Hz), 2.47 (s, 3H, CH$_3$), 4.41 (q, 2H, O*CH$_2$*CH$_3$, J = 7.2 Hz), 7.30-7.35 (m, 3H, Ar), 7.73 (d, 2H, Ar, J = 8.4 Hz), 8.32 (s, 1H, Ar), 8.40 (dd, 1H, Ar, J = 1.6 Hz and J = 4.8 Hz), 8.48 (dd, 1H, Ar, J = 1.6 Hz and J = 7.6 Hz). ^{13}C-NMR (CDCl$_3$-d$_1$) δ 14.40 (CH$_3$), 24.30 (CH$_3$), 60.90 (CH$_2$), 101.00 (C), 120.13 (CH), 120.74 (C), 126.00 (CH), 128.31 (CH), 130.62 (CH), 130.97 (CH), 132.86 (C), 133.20 (CH), 134.38 (CH), 138.60 (C), 145.60 (CH), 148.49 (C), 162.50 (C), 167.70 (C). ESI-MS calcd. for C$_{18}$H$_{16}$N$_2$O$_3$, 308.33; found: *m/z* 309.12 [M+H]$^+$. Anal. C$_{18}$H$_{16}$N$_2$O$_3$ (C, H, N).

Ethyl 1-(cyclopropanecarbonyl)-1H-pyrrolo[2,3-b]pyridine-3-carboxylate (7c)

Obtained from compound **6** (Jiang, J. H. et al. 2011) following the general procedure reported at **pag. 81**. Compound **7c** was purified by crystallization (EtOH).

Yield = 73%; mp = 77-80°C (EtOH). $\underline{^1\text{H-NMR}}$ (CDCl$_3$-d$_1$) δ 1.23-1.28 (m, 2H, CH$_2$), 1.39-1.44 (m, 5H, 3H OCH$_2$*CH$_3$* + 2H CH$_2$), 4.21-4.26 (m, 1H, CH), 4.40 (q, 2H, O*CH$_2$*CH$_3$, $J = 7.2$ Hz), 7.29-7.34 (m, 1H, Ar), 8.42 (dd, 1H, Ar, $J = 1.6$ Hz and $J = 4.6$ Hz), 8.48 (dd, 1H, Ar, $J = 1.6$ Hz and $J = 7.6$ Hz), 8.63 (s, 1H, Ar). $\underline{^{13}\text{C NMR}}$ (CDCl$_3$-d$_1$) δ 12.42 (CH$_2$), 14.42 (CH$_3$), 14.94 (CH), 60.61 (CH$_2$), 110.42 (C), 119.86 (CH), 121.59 (C), 130.69 (CH), 131.20 (CH), 144.64 (CH), 149.00 (C), 164.00 (C), 173.69 (C). $\underline{\text{IR}}$ = 1701 cm^{-1} (C=O amide), 1718 cm^{-1} (C=O ester). ESI-MS calcd. for C$_{14}$H$_{14}$N$_2$O$_3$, 258.27; found: *m/z* 259.10 [M+H]$^+$. Anal. C$_{14}$H$_{14}$N$_2$O$_3$ (C, H, N).

Ethyl 1-(3-cyanobenzoyl)-1H-pyrrolo[2,3-b]pyridine-3-carboxylate (7d)

Obtained from compound **6** (Jiang, J. H. et al. 2011) following the general procedure reported at **pag. 81**. Compound **7d** was purified by column chromatography using cyclohexane/ethyl acetate 2:1 as eluent.

Yield = 15%; oil. $\underline{^1\text{H-NMR}}$ (CDCl$_3$-d$_1$) δ 1.44 (t, 3H, OCH$_2$*CH$_3$*, J = 7.0 Hz), 4.44 (q, 2H, O*CH$_2$*CH$_3$, J = 7.0 Hz), 7.28-7.33 (m, 1H, Ar), 7.64 (t, 1H, Ar, J = 8.0 Hz), 7.93 (d, 1H, Ar, J = 7.6 Hz), 8.03 (d, 1H, Ar, J = 8.0 Hz), 8.09 (s, 1H, Ar), 8.24 (dd, 1H, Ar, J = 1.2 Hz and J = 4.4 Hz), 8.48-8.53 (m, 2H, Ar). $\underline{^{13}\text{C-NMR}}$ (CDCl$_3$-d$_1$) δ 14.42 (CH$_3$), 60.87 (CH$_2$), 112.37 (C), 112.73 (C), 117.73 (C), 120.48 (CH), 120.88 (C), 129.15 (CH), 130.87 (CH), 132.09 (CH), 134.04 (CH), 134.32 (CH), 134.42 (C), 136.14 (CH), 145.26 (CH), 147.75 (C), 163.29 (C), 165.62 (C). ESI-MS calcd. for C$_{18}$H$_{13}$N$_3$O$_3$, 319.31; found: *m/z* 320.10 [M+H]$^+$. Anal. C$_{18}$H$_{13}$N$_3$O$_3$ (C, H, N).

Ethyl 1-(4-cyanobenzoyl)-1H-pyrrolo[2,3-b]pyridine-3-carboxylate (7e)

Obtained from compound **6** (Jiang, J. H. et al. 2011) following the general procedure reported at **pag. 81**. Compound **7e** was purified by column chromatography using cyclohexane/ethyl acetate 1:1 as eluent.

Yield = 30%; oil. ^{1}H-NMR (CDCl$_3$-d$_1$) δ 1.43 (t, 3H, OCH$_2$CH$_3$, J = 7.2 Hz), 4.43 (q, 2H, OCH$_2$CH$_3$, J = 7.2 Hz), 7.27-7.32 (m, 1H, Ar), 7.79 (d, 2H, Ar, J = 8.4 Hz), 7.88 (d, 2H, Ar, J = 8.0 Hz), 8.23 (d, 1H, Ar, J = 4.4 Hz), 8.44-8.49 (m, 2H, Ar). ^{13}C-NMR (CDCl$_3$-d$_1$) δ14.41 (CH$_3$), 60.87 (CH$_2$), 112.38 (C), 116.46 (C), 117.87 (C), 120.42 (CH), 120.84 (C), 130.62 (CH), 130.84 (CH), 131.98 (CH), 137.12 (C), 142.28 (CH), 147.82 (C), 163.29 (C), 166.08 (C). ESI-MS calcd. for C$_{18}$H$_{13}$N$_3$O$_3$, 319.31; found: *m/z* 320.10 [M+H]$^+$. Anal. C$_{18}$H$_{13}$N$_3$O$_3$ (C, H, N).

**(3-Iodo-1H-pyrrolo[2,3-b]pyridin-1-yl)(m-tolyl)methanone (10a)**
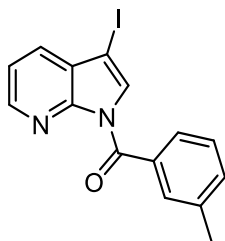
Obtained from compound **9a** (Baltus, C. B. et al. 2016) following the general procedure reported at **pag. 81**. Compound **10a** was purified by column chromatography using cyclohexane/ethyl acetate 6:1 as eluent.

Yield = 47%; oil. <u>^{1}H-NMR</u> (CDCl$_3$-d$_1$) δ 2.42 (s, 3H, CH$_3$), 7.26-7.31 (m, 1H, Ar), 7.37 (t, 1H, Ar, J = 7.6 Hz), 7.44 (d, 1H, Ar, J = 7.2 Hz), 7.55 (d, 1H, Ar, J = 7.6 Hz), 7.63 (s, 1H, Ar), 7.76 (dd, 1H, Ar, J = 1.6 Hz and J = 8.0 Hz), 7.82 (s, 1H, Ar), 8.36 (d, 1H, Ar, J = 4.8 Hz). <u>^{13}C-NMR</u> (CDCl$_3$-d$_1$) δ 21.70 (CH$_3$), 95.64 (C), 119.46 (CH), 123.68 (C), 126.78 (CH), 127.46 (CH), 128.05 (CH), 129.11 (CH), 131.72 (CH), 133.42 (C), 133.82 (CH), 138.36 (C), 143.70 (CH), 146.31 (C), 167.55 (C). ESI-MS calcd. for C$_{15}$H$_{11}$IN$_2$O, 362.17; found: *m/z* 362.99 [M+H]$^+$. Anal. C$_{15}$H$_{11}$IN$_2$O (C, H, N).

(3-Bromo-1H-pyrrolo[2,3-b]pyridin-1-yl)(m-tolyl)methanone (10b)
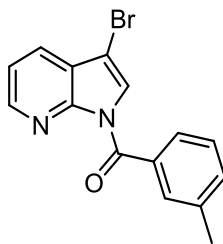
Obtained from compound **9b** (Baltus, C. B. et al. 2016) following the general procedure reported at **pag. 81**. Compound **10b** was purified by column chromatography using cyclohexane/ethyl acetate 5:1 as eluent.

Yield = 25%; oil. <u>^{1}H-NMR</u> (CDCl$_3$-d$_1$) δ 2.42 (s, 3H, CH$_3$), 7.24-7.29 (m, 1H, Ar), 7.37 (t, 1H, Ar, J = 7.6 Hz), 7.44 (d, 1H, Ar, J = 7.6 Hz), 7.55 (d, 1H, Ar, J = 7.6 Hz), 7.63 (s, 1H, Ar), 7.76 (s, 1H, Ar), 7.89 (dd, 1H, Ar, J = 1.6 Hz and J = 7.6 Hz), 8.38 (dd, 1H, Ar, J = 1.6 Hz and J = 4.8 Hz). <u>^{13}C-NMR</u> (CDCl$_3$-d$_1$) δ 21.77 (CH$_3$), 96.58 (C), 119.46 (CH), 122.68 (C), 126.78 (CH), 127.46 (CH), 128.05 (CH), 129.11 (CH), 130.59 (CH), 133.42 (C), 133.82 (CH), 138.36 (C), 145.77 (CH), 147.03 (C), 167.08 (C). ESI-MS calcd. for C$_{15}$H$_{11}$BrN$_2$O, 315.16; found: *m/z* 317.01 [M+H]$^+$. Anal. C$_{15}$H$_{11}$BrN$_2$O (C, H, N).

(3-Chloro-1H-pyrrolo[2,3-b]pyridin-1-yl)(m-tolyl)methanone (10c)
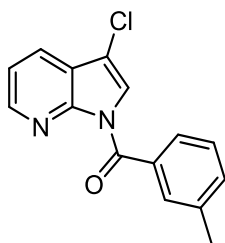
Obtained from compound **9c** (Minakata, S. et al. 1997) following the general procedure reported at **pag. 81**. Compound **10c** was purified by column chromatography using cyclohexane/ethyl acetate 6:1 as eluent.

Yield = 25%; oil. $\underline{^1H\text{-NMR}}$ (CDCl$_3$-d$_1$) δ 2.42 (s, 3H, CH$_3$), 7.24-7.29 (m, 1H, Ar), 7.37 (t, 1H, Ar, J = 7.6 Hz), 7.44 (d, 1H, Ar, J = 7.2 Hz), 7.55 (d, 1H, Ar, J = 7.6 Hz), 7.62 (s, 1H, Ar), 7.69 (s, 1H, Ar), 7.94 (dd, 1H, Ar, J = 1.2 Hz and J = 6.4 Hz), 8.39 (d, 1H, Ar, J = 4.8 Hz). $\underline{^{13}C\text{-NMR}}$ (CDCl$_3$-d$_1$) δ 20.96 (CH$_3$), 101.05 (C), 115.68 (CH), 121.24 (C), 123.81 (CH), 128.10 (CH), 128.36 (CH), 129.11 (CH), 130.17 (CH), 130.42 (C), 134.81 (CH), 138.95 (C), 142.46 (CH), 146.63 (C), 167.76 (C). ESI-MS calcd. for C$_{15}$H$_{11}$ClN$_2$O, 270.72; found: *m/z* 272.05 [M+H]$^+$. Anal. C$_{15}$H$_{11}$ClN$_2$O (C, H, N).

(3-Nitro-1H-pyrrolo[2,3-b]pyridin-1-yl)(m-tolyl)methanone (10d)
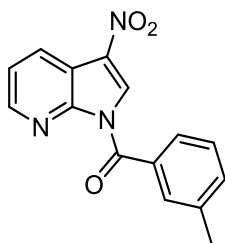
Obtained from compound **9d** (Robinson, M. M. et al. 1959) following the general procedure reported at **pag. 81**. Compound **10d** was purified by column chromatography using cyclohexane/ethyl acetate 3:1 as eluent.

Yield = 35%; oil. ^{1}H-NMR (CDCl$_3$-d$_1$) δ 2.44 (s, 3H, CH$_3$), 7.39-7.46 (m, 2H, Ar), 7.52 (d, 1H, Ar, J = 7.6 Hz), 7.59 (d, 1H, Ar, J = 8.0 Hz), 7.68 (s, 1H, Ar), 8.47 (dd, 1H, Ar, J = 1.6 Hz and J = 4.8 Hz), 8.59-8.64 (m, 2H, Ar). ^{13}C-NMR (CDCl$_3$-d$_1$) δ 21.62 (CH$_3$), 113.61 (C), 115.68 (CH), 126.15 (CH), 128.05 (C), 128.16 (CH), 128.30 (CH), 129.18 (CH), 130.16 (CH), 130.45 (C), 134.89 (CH), 138.91 (C), 142.42 (CH), 148.76 (C), 167.73 (C). ESI-MS calcd. for C$_{15}$H$_{11}$N$_3$O$_3$, 281.27; found: *m/z* 282.08 [M+H]$^+$. Anal. C$_{15}$H$_{11}$N$_3$O$_3$ (C, H, N).

General procedure for compounds (13a-e). To a suspension of intermediate **12** (0.34 mmol) (Zhang, J. et al. 2011) in 3 mL of toluene, 0.051 mmol of Tetrakis (catalytic amount), 3 mL of Na$_2$CO$_3$ 2M solution and 0.68 mmol of appropriate hetero(phenyl)-boronic acid were added. The mixture was stirred at reflux for 4h. After cooling, ice-cold water (20 mL) was added, the suspension was extracted with CH$_2$Cl$_2$ (3 x 15 mL), dried over sodium sulfate and the solvent was evaporated *under vacuum* to afford the compounds, which were purified by column chromatography using cyclohexane/ethyl acetate 3:1 (for **13a-d**) or hexane/acetone 4:1 (for **13e**) as eluent.

3-(1-(Phenylsulfonyl)-1H-pyrrolo[2,3-b]pyridin-3-yl)benzonitrile (13a)
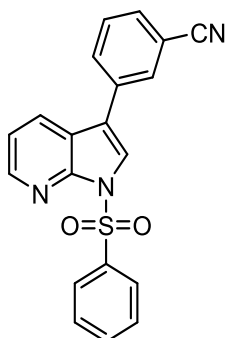
Yield = 74%; oil. ^{1}H-NMR (CDCl$_3$-d$_1$) δ 7.25-7.30 (m, 1H, Ar), 7.51 (t, 2H, Ar, $J = 8.0$ Hz), 7.56-7.62 (m, 2H, Ar), 7.65 (d, 1H, Ar, $J = 7.6$ Hz), 7.82 (dd, 1H, Ar, $J = 1.2$ Hz and $J = 6.4$ Hz), 7.86 (s, 1H, Ar), 7.94 (s, 1H, Ar), 8.06 (dd, 1H, Ar, $J = 1.2$ Hz and $J = 8.0$ Hz), 8.26 (d, 2H, Ar, $J = 7.2$ Hz), 8.51 (dd, 1H, Ar, $J = 1.2$ Hz and $J = 4.8$ Hz). ESI-MS calcd. for C$_{20}$H$_{13}$N$_3$O$_2$S, 359.40; found: m/z 360.08 [M+H]$^+$. Anal. C$_{20}$H$_{13}$N$_3$O$_2$S (C, H, N).

1-(Phenylsulfonyl)-3-(pyridin-3-yl)-1H-pyrrolo[2,3-b]pyridine (13b)
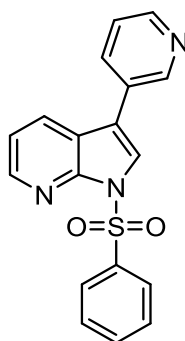
Yield = 88%; oil. ^{1}H-NMR (CDCl$_3$-d$_1$) δ 7.25-7.30 (m, 1H, Ar), 7.40-7.46 (m, 1H, Ar), 7.48-7.59 (m, 2H, Ar), 7.63-7.74 (m, 1H, Ar), 7.90 (dd, 1H, Ar, $J = 1.6$ Hz and $J = 8.0$ Hz), 7.94 (s, 1H, Ar), 8.06 (d, 1H, Ar, $J = 8.0$ Hz), 8.19 (d, 2H, Ar, $J = 8.4$ Hz), 8.50 (d, 1H, Ar, $J = 4.8$ Hz), 8.61 (d, 1H, Ar, $J = 4.8$ Hz), 8.87

(s, 1H, Ar). ESI-MS calcd. for $C_{18}H_{13}N_3O_2S$, 335.38; found: *m/z* 336.08 [M+H]⁺. Anal. $C_{18}H_{13}N_3O_2S$ (C, H, N).

**3-(Furan-2-yl)-1-(phenylsulfonyl)-1H-pyrrolo[2,3-b]pyridine (13c)**
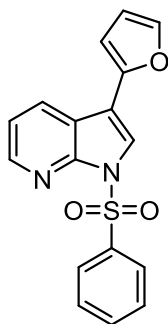
Yield = 90%; oil. ¹H-NMR (CDCl₃-d₁) δ 6.48-6.53 (m, 1H, Ar), 6.61 (d, 1H, Ar, *J* = 3.2 Hz), 7.22-7.27 (m, 1H, Ar), 7.43-7.49 (m, 3H, Ar), 7.55 (t, 1H, Ar, *J* = 7.2 Hz), 7.99 (s, 1H, Ar), 8.16-8.21 (m, 3H, Ar), 8.46 (dd, 1H, Ar, *J* = 1.2 Hz and *J* = 4.8 Hz). ESI-MS calcd. for $C_{17}H_{12}N_2O_3S$, 324.35; found: *m/z* 325.06 [M+H]⁺. Anal. $C_{17}H_{12}N_2O_3S$ (C, H, N).

3-(Furan-3-yl)-1-(phenylsulfonyl)-1H-pyrrolo[2,3-b]pyridine (13d)
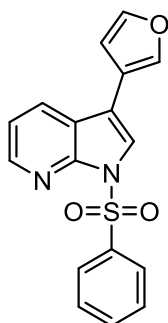
Yield = 94%; mp = 137-140°C (EtOH). ¹H-NMR (CDCl₃-d₁) δ 6.68 (s, 1H, Ar), 7.21-7.26 (m, 1H, Ar), 7.47 (t, 2H, Ar, *J* = 7.6 Hz), 7.52-7.58 (m, 2H, Ar), 7.77

Material and methods

(s, 1H, Ar), 7.82 (s, 1H, Ar), 7.96 (dd, 1H, Ar, J = 1.2 Hz and J = 8.4 Hz), 8.21 (d, 2H, Ar, J = 7.6 Hz), 8.46 (dd, 1H, Ar, J = 1.2 Hz and J = 4.8 Hz). ESI-MS calcd. for $C_{17}H_{12}N_2O_3S$, 324.35; found: *m/z* 325.06 [M+H]$^+$. Anal. $C_{17}H_{12}N_2O_3S$ (C, H, N).

1-(Phenylsulfonyl)-3-(thiophen-3-yl)-1H-pyrrolo[2,3-b]pyridine (13e)
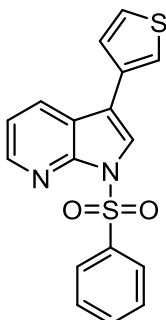
Yield = 68%; mp = 164-167°C (EtOH). ^{1}H-NMR (CDCl$_3$-d$_1$) δ 7.21-7.26 (m, 1H, Ar), 7.35 (dd, 1H, Ar, J = 1.2 Hz and J = 7.6 Hz), 7.43-7.49 (m, 4H, Ar), 7.57 (t, 1H, Ar, J = 7.6 Hz), 7.89 (s, 1H, Ar), 8.09 (dd, 1H, Ar, J = 1.2 Hz and J = 7.6 Hz), 8.22 (d, 2H, Ar, J = 7.6 Hz), 8.47 (dd, 1H, Ar, J = 1.2 Hz and J = 4.8 Hz). ESI-MS calcd. for $C_{17}H_{12}N_2O_2S_2$, 340.42; found: *m/z* 341.04 [M+H]$^+$. Anal. $C_{17}H_{12}N_2O_2S_2$ (C, H, N).

3-(1-(3-Methylbenzoyl)-1H-pyrrolo[2,3-b]pyridin-3-yl)benzonitrile (15a)
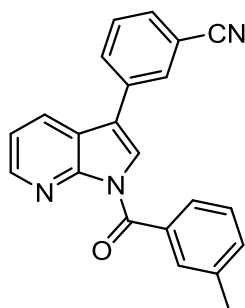
Obtained from compound **14a** (Lind, K. E. et al. 2008) following the general procedure reported at **pag. 81**. Compound **15a** was purified by column chromatography using cyclohexane/ethyl acetate 4:1 as eluent.

Yield = 42%; oil. $\underline{^1\text{H-NMR}}$ (CDCl$_3$-d$_1$) δ 2.44 (s, 3H, CH$_3$), 7.26-7.31 (m, 1H, Ar), 7.39 (t, 1H, Ar, J = 7.6 Hz), 7.46 (d, 1H, Ar, J = 7.6 Hz), 7.56-7.61 (m, 2H, Ar), 7.63-7.68 (m, 2H, Ar), 7.87 (d, 1H, Ar, J = 8.0 Hz), 7.90 (d, 2H, Ar, J = 5.6 Hz), 8.14 (d, 1H, Ar, J = 7.6 Hz), 8.41 (d, 1H, Ar, J = 3.2 Hz). $\underline{^{13}\text{C-NMR}}$ (CDCl$_3$-d$_1$) δ 21.40 (CH$_3$), 113.36 (C), 118.09 (C), 118.52 (C), 119.40 (CH), 121.14 (C), 125.07 (CH), 127.47 (CH), 128.12 (CH), 129.94 (CH), 130.67 (CH), 130.82 (CH), 130.98 (CH), 131.76 (CH), 133.53 (C), 133.90 (CH), 134.52 (C), 138.46 (C), 145.46 (CH), 148.76 (C), 167.77 (C). ESI-MS calcd. for C$_{22}$H$_{15}$N$_3$O, 337.37; found: m/z 338.12 [M+H]$^+$. Anal. C$_{22}$H$_{15}$N$_3$O (C, H, N).
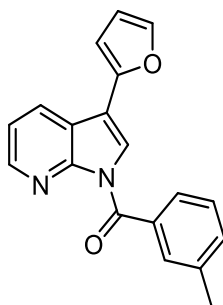
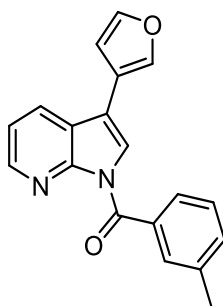**(3-(Pyridin-3-yl)-1H-pyrrolo[2,3-b]pyridin-1-yl)(m-tolyl)methanone (15b)**
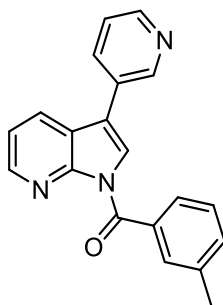
Obtained from compound **14b** (Ibrahim, P. N. et al. 2007) following the general procedure reported at **pag. 81**. Compound **15b** was purified by column chromatography using cyclohexane/ethyl acetate 1:1 as eluent.

Yield = 43%; oil. ^{1}H-NMR (CDCl$_3$-d$_1$) δ 2.44 (s, 3H, CH$_3$), 7.25-7.32 (m, 1H, Ar), 7.39 (t, 1H, Ar, J = 7.6 Hz), 7.44 (t, 2H, Ar, J = 7.6 Hz), 7.61 (d, 1H, Ar, J = 7.6 Hz), 7.69 (s, 1H, Ar), 7.91 (s, 1H, Ar), 7.97 (d, 1H, Ar, J = 8.0 Hz), 8.15 (dd, 1H, Ar, J = 1.2 Hz and J = 8.0 Hz), 8.40 (d, 1H, Ar, J = 4.4 Hz), 8.63 (d, 1H, Ar, J = 4.0 Hz), 8.87 (s, 1H, Ar). ^{13}C-NMR (CDCl$_3$-d$_1$) δ 21.54 (CH$_3$), 116.71 (C), 119.51 (CH), 121.37 (C), 124.10 (CH), 124.96 (CH), 127.47 (CH), 128.19 (CH), 128.33 (CH), 129.34 (C), 130.77 (CH), 132.90 (CH), 133.57 (C), 133.86 (CH), 135.00 (CH), 138.30 (C), 145.48 (CH), 148.13 (CH), 148.92 (C), 167.99 (C). ESI-MS calcd. for C$_{20}$H$_{15}$N$_3$O, 313.35; found: *m/z* 314.12 [M+H]$^+$. Anal. C$_{20}$H$_{15}$N$_3$O (C, H, N).
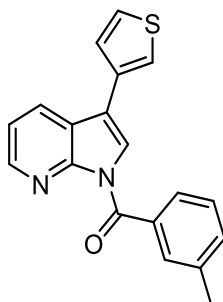
(3-(Furan-2-yl)-1H-pyrrolo[2,3-b]pyridin-1-yl)(m-tolyl)methanone (15c)

Obtained from compound **14c** (Ibrahim, P. N. et al. 2007) following the general procedure reported at **pag. 81**. Compound **15c** was purified by column chromatography using cyclohexane/ethyl acetate 3:1 as eluent.

Yield = 61%; oil. ^{1}H-NMR (CDCl$_3$-d$_1$) δ 2.42 (s, 3H, CH$_3$), 6.51 (s, 1H, Ar), 6.64 (d, 1H, Ar, J = 3.2 Hz), 7.24-7.29 (m, 1H, Ar), 7.36 (t, 1H, Ar, J = 7.6 Hz), 7.42 (d, 1H, Ar, J = 7.6 Hz), 7.48 (s, 1H, Ar), 7.57 (d, 1H, Ar, J = 7.6 Hz), 7.65 (s, 1H, Ar), 7.93 (s, 1H, Ar), 8.26 (d, 1H, Ar, J = 8.0 Hz), 8.39 (d, 1H, Ar, J = 4.8 Hz). ^{13}C-NMR (CDCl$_3$-d$_1$) δ 21.60 (CH$_3$), 106.15 (CH), 111.01 (C), 111.47 (CH), 119.37 (CH), 120.29 (C), 122.90 (CH), 127.36 (CH), 127.05 (CH), 129.10 (CH), 130.66 (CH), 133.60 (CH), 133.83 (C), 138.29 (C), 141.83 (CH), 145.31 (CH), 148.17 (C), 148.65 (C), 167.73 (C). ESI-MS calcd. for C$_{19}$H$_{14}$N$_2$O$_2$, 302.33; found: *m/z* 303.11 [M+H]$^+$. Anal. C$_{19}$H$_{14}$N$_2$O$_2$ (C, H, N).

**(3-(Furan-3-yl)-1H-pyrrolo[2,3-b]pyridin-1-yl)(m-tolyl)methanone (15d)**

Obtained from compound **14d** (Ibrahim, P. N. et al. 2007) following the general procedure reported at **pag. 81**. Compound **15d** was purified by column chromatography using hexane/acetone 4:1 as eluent.

Yield = 31%; oil. $\underline{^{1}\text{H-NMR}}$ (CDCl$_3$-d$_1$) δ 2.42 (s, 3H, CH$_3$), 6.69 (s, 1H, Ar), 7.21-7.26 (m, 1H, Ar), 7.37 (t, 1H, Ar, $J = 7.2$ Hz), 7.43 (d, 1H, Ar, $J = 7.6$ Hz), 7.53 (s, 1H, Ar), 7.57 (d, 1H, Ar, $J = 7.6$ Hz), 7.66 (s, 1H, Ar), 7.80 (s, 1H, Ar), 7.83 (s, 1H, Ar), 8.04 (dd, 1H, Ar, $J = 1.2$ Hz and $J = 8.0$ Hz), 8.36 (d, 1H, Ar, $J = 4.8$ Hz). $\underline{^{13}\text{C-NMR}}$ (CDCl$_3$-d$_1$) δ 21.39 (CH$_3$), 109.39 (CH), 111.72 (C), 117.78 (C), 119.18 (CH), 121.79 (C), 123.75 (CH), 127.39 (CH), 127.94 (CH), 128.41 (CH), 130.65 (CH), 133.63 (CH), 134.05 (C), 138.20 (C), 138.95 (CH), 143.70 (CH), 145.10 (CH), 148.83 (C), 167.95 (C). ESI-MS calcd. for C$_{19}$H$_{14}$N$_2$O$_2$, 302.33; found: *m/z* 303.11 [M+H]$^+$. Anal. C$_{19}$H$_{14}$N$_2$O$_2$ (C, H, N).

(3-(Thiophen-3-yl)-1H-pyrrolo[2,3-b]pyridin-1-yl)(m-tolyl)methanone (15e)

Obtained from compound **14e** (Ibrahim, P. N. et al. 2007) following the general procedure reported at **pag. 81**. Compound **15e** was purified by column chromatography using hexane/acetone 4:1 a eluent.

Yield = 55%; oil. ^{1}H-NMR (CDCl$_3$-d$_1$) δ 2.42 (s, 3H, CH$_3$), 7.22-7.28 (m, 1H, Ar), 7.34-7.39 (m, 2H, Ar), 7.41-7.46 (m, 2H, Ar), 7.52 (s, 1H, Ar), 7.58 (d, 1H, Ar, J = 7.2 Hz), 7.67 (s, 1H, Ar), 7.84 (s, 1H, Ar), 8.17 (dd, 1H, Ar, J = 1.6 Hz and J = 8.0 Hz), 8.38 (dd, 1H, Ar, J = 1.6 Hz and J = 4.8 Hz). ^{13}C-NMR (CDCl$_3$-d$_1$) δ 21.54 (CH$_3$), 115.54 (C), 119.29 (CH), 121.09 (CH), 121.88 (C), 124.05 (CH), 126.53 (CH), 126.74 (CH), 127.48 (CH), 128.06 (CH), 128.59 (CH), 130.70 (CH), 133.34 (C), 133.61 (CH), 133.98 (C), 138.26 (C), 145.02 (CH), 148.77 (C), 167.94 (C). ESI-MS calcd. for C$_{19}$H$_{14}$N$_2$OS, 318.39; found: *m/z* 319.19 [M+H]$^+$. Anal. C$_{19}$H$_{14}$N$_2$OS (C, H, N).

(E)-N-(1-(dimethylamino)ethylidene)-1H-pyrrolo[2,3-b]pyridine-3-carboxamide (16)
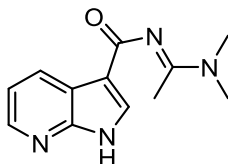
To a suspension of 0.68 mmol of intermediate **3** (Carbone, A. et al. 2015) in anhydrous toluene (2 mL), 0.30 mL of dry DMF (catalytic amount) and 2.38 mmol of *N,N*-dimethylacetamide dimethyl acetal were added. The mixture was stirred at reflux for 2h. After cooling, ice-cold water (20 mL) was added and the suspension was extracted with ethyl acetate (3 x 15 mL). Evaporation of solvent afforded the desired compound, which was purified by column chromatography using CH_2Cl_2/MeOH 95:5 as eluent.

Yield = 38%; oil. <u>^{1}H-NMR</u> (CDCl$_3$-d$_1$) δ 2.34 (s, 3H, N=C-CH$_3$), 3.10 (s, 3H, NCH$_3$), 3.19 (s, 3H, NCH$_3$), 7.16-7.21 (m, 1H, Ar), 8.10 (s, 1H, Ar), 8.33 (dd, 1H, Ar, $J = 1.2$ Hz and $J = 4.4$ Hz), 8.65 (dd, 1H, Ar, $J = 1.6$ Hz and $J = 8.0$ Hz), 12.04 (exch br s, 1H, NH). ESI-MS calcd. for $C_{12}H_{14}N_4O$, 230.27; found: *m/z* 231.12 [M+H]$^+$. Anal. $C_{12}H_{14}N_4O$ (C, H, N).

3-Methyl-5-(1H-pyrrolo[2,3-b]pyridin-3-yl)-1,2,4-oxadiazole (17)
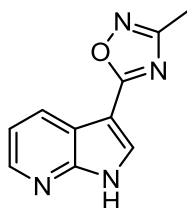

A mixture of 0.26 mmol of **16**, 0.39 mmol of hydroxylamine hydrochloride, 1.2 mL of glacial acetic acid, 0.25 mL of NaOH 10% in 1.5 mL of dioxane was heated at reflux under stirring for 5h. After cooling, ice-cold water (20 mL) was

added and the precipitate was recovered by vacuum filtration to obtain the pure compound.

Yield = 57%; mp = 206-209°C (EtOH). $\underline{^1\text{H-NMR}}$ (DMSO-d_6) δ 2.38 (s, 3H, CH_3), 7.27-7.32 (m, 1H, Ar), 8.36-8.41 (m, 2H, Ar), 8.47 (s, 1H, Ar), 12.75 (exch br s, 1H, NH). ESI-MS calcd. for $C_{10}H_8N_4O$, 200.20; found: *m/z* 201.07 [M+H]$^+$. Anal. $C_{10}H_8N_4O$ (C, H, N).

## (3-(3-methyl-1,2,4-oxadiazol-5-yl)-1H-pyrrolo[2,3-b]pyridin-1-yl)(m-tolyl)methanone (18)
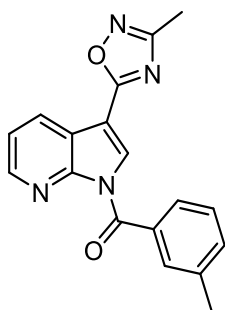
Obtained from compound **17** following the general procedure reported at **pag. 81**. Compound **18** was purified by column chromatography using cyclohexane/ethyl acetate 4:1 as eluent.

Yield = 42%; mp = 151-153°C (EtOH). $\underline{^1\text{H-NMR}}$ (CDCl$_3$-d_1) δ 2.44 (s, 3H, m-*CH$_3$*-Ph), 2.49 (s, 3H, CH_3), 7.36-7.42 (m, 2H, Ar), 7.49 (d, 1H, Ar, *J* = 7.6 Hz), 7.60 (d, 1H, Ar, *J* = 7.6 Hz), 7.68 (s, 1H, Ar), 8.44 (s, 1H, Ar), 8.48 (dd, 1H, Ar, *J* = 1.6 Hz and *J* = 4.8 Hz), 8.61 (dd, 1H, Ar, *J* = 1.6 Hz and *J* = 7.6 Hz). $\underline{^{13}\text{C-}}$ $\underline{\text{NMR}}$ (CDCl$_3$-d_1) δ 11.68 (CH$_3$), 21.36 (CH$_3$), 104.38 (C), 119.59 (C), 120.34 (CH), 127.68 (CH), 128.39 (CH), 130.31 (CH), 130.53 (CH), 130.90 (CH), 132.66 (C), 134.48 (CH), 138.67 (C), 146.26 (CH), 148.37 (C), 167.31 (C), 167.57 (C), 171.04 (C). ESI-MS calcd. for $C_{18}H_{14}N_4O_2$, 318.33; found: *m/z* 319.12 [M+H]$^+$. Anal. $C_{18}H_{14}N_4O_2$ (C, H, N)

5-Methyl-3-(1H-pyrrolo[2,3-b]pyridin-3-yl)-1,2,4-oxadiazole (20)
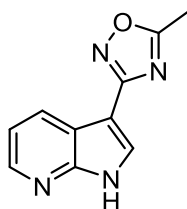
To a cooled (0°C) solution of 0.39 mmol of glacial acetic acid in dry DMF (1 mL), 0.58 mmol of *N,N'*-dicyclohexylcarbodiimide (DCC) was added. The mixture was stirred at 0°C for 1h, then 0.39 mmol of **19** (Lape, H. E. et al. 1968) was added and the reaction was still kept under stirring at 0°C another hour and then at reflux for 6h. After cooling, ice-cold water (20 mL) was added, the precipitate was recovered by vacuum filtration and it was purified by column chromatography using CH_2Cl_2/MeOH 9:1 as eluent.

Yield = 51%; mp = 194-197°C (EtOH). ^{1}H-NMR (DMSO-d_6) δ 2.62 (s, 3H, CH_3), 7.21-7.26 (m, 1H, Ar), 8.15 (s, 1H, Ar), 8.30-8.35 (m, 2H, Ar), 12.38 (exch br s, 1H, NH). ESI-MS calcd. for $C_{10}H_8N_4O$, 200.20; found: *m/z* 201.07 [M+H]$^+$. Anal. $C_{10}H_8N_4O$ (C, H, N).

(3-(5-Methyl-1,2,4-oxadiazol-3-yl)-1H-pyrrolo[2,3-b]pyridin-1-yl)(m-tolyl)methanone (21)
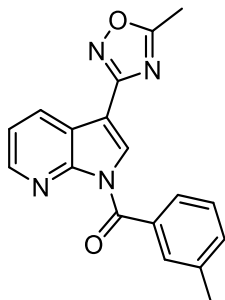
Obtained from compound **20** following the general procedure reported at **pag. 81**. Compound **21** was purified by column chromatography using cyclohexane/ethyl acetate 4:1 as eluent.

Yield = 47%; mp = 139-142°C (EtOH). $\underline{^{1}\text{H-NMR}}$ (CDCl$_3$-d$_1$) δ 2.43 (s, 3H, m-*CH$_3$*-Ph), 2.66 (s, 3H, CH$_3$), 7.33-7.41 (m, 2H, Ar), 7.46 (d, 1H, Ar, J = 7.2 Hz), 7.59 (d, 1H, Ar, J = 7.6 Hz), 7.67 (s, 1H, Ar), 8.32 (s, 1H, Ar), 8.47 (d, 1H, Ar, J = 4.4 Hz), 8.57 (d, 1H, Ar, J = 8.0 Hz). $\underline{^{13}\text{C-NMR}}$ (CDCl$_3$-d$_1$) δ 12.22 (CH$_3$), 21.34 (CH$_3$), 107.01 (C), 119.99 (CH), 120.23 (C), 127.50 (CH), 128.33 (CH), 129.28 (CH), 130.77 (CH), 131.07 (CH), 133.10 (C), 134.09 (CH), 138.56 (C), 145.69 (CH), 148.47 (C), 163.87 (C), 167.51 (C), 176.09 (C). ESI-MS calcd. for C$_{18}$H$_{14}$N$_4$O$_2$, 318.33; found: *m/z* 319.12 [M+H]$^+$. Anal. C$_{18}$H$_{14}$N$_4$O$_2$ (C, H, N).

General procedure for compounds (24a,b). To a solution of the intermediate **23** (0.98 mmol) (Chavan, N. L. et al. 2010) in anhydrous CH$_2$Cl$_2$ (5 mL), 3.92 mmol of aniline or *N*-methylaniline, commercially available, and 3.92 mmol of glacial acetic acid were added. The mixture was stirred at room temperature for 30 min, then 1.47 mmol of sodium triacetoxyborohydride was added and stirred at room temperature for 24h. Cyclohexane (20 mL) was added and the mixture was kept under stirring for 15-30 min. After evaporation

of solvent, the compounds **24a,b** were purified by column chromatography using toluene/ethyl acetate 9:1 (for **24a**) or cyclohexane/ethyl acetate 3:1 (for **24b**) as eluent.

**N-((1-(Phenylsulfonyl)-1H-pyrrolo[2,3-b]pyridin-3-yl)methyl)aniline (24a)**
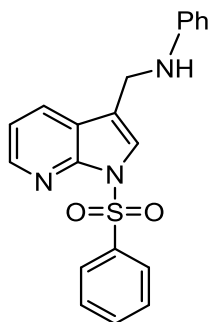
Yield = 70%; oil. ^{1}H-NMR (CDCl$_3$-d$_1$) δ 4.41 (s, 2H, *CH$_2$*NH), 6.67 (d, 2H, Ar, J = 8.0 Hz), 6.77 (d, 1H, Ar, J = 7.2 Hz), 7.15-7.21 (m, 3H, Ar), 7.45 (t, 2H, Ar, J = 8.0 Hz), 7.55 (t, 1H, Ar, J = 7.2 Hz), 7.68 (s, 1H, Ar), 7.88 (d, 1H, Ar, J = 7.6 Hz), 8.14 (d, 2H, Ar, J = 7.6 Hz), 8.43 (d, 1H, Ar, J = 4.4 Hz). ESI-MS calcd. for C$_{20}$H$_{17}$N$_3$O$_2$S, 363.44; found: *m/z* 364.11 [M+H]$^+$. Anal. C$_{20}$H$_{17}$N$_3$O$_2$S (C, H, N).

N-methyl-N-((1-(phenylsulfonyl)-1H-pyrrolo[2,3-b]pyridin-3-yl)methyl)aniline (24b)
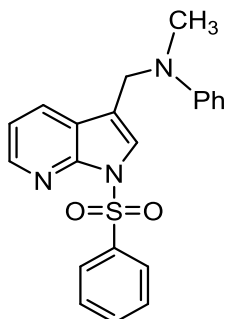
Yield = 65%; oil. ^{1}H-NMR (CDCl$_3$-d$_1$) δ 2.93 (s, 3H, CH$_3$N), 4.54 (s, 2H, CH$_2$N), 6.76-6.83 (m, 3H, Ar), 7.10-7.15 (m, 1H, Ar), 7.25 (t, 2H, Ar, J = 7.2 Hz), 7.45 (t, 2H, Ar, J = 8.0 Hz), 7.51-7.57 (m, 2H, Ar), 7.73 (d, 1H, Ar, J = 7.6 Hz), 8.12 (d, 2H, Ar, J = 8.0 Hz), 8.41 (dd, 1H, Ar, J = 1.2 Hz and J = 4.8 Hz). ESI-MS calcd. for C$_{21}$H$_{19}$N$_3$O$_2$S, 377.46; found: m/z 378.12 [M+H]$^+$. Anal. C$_{21}$H$_{19}$N$_3$O$_2$S (C, H, N).

N-((1H-pyrrolo[2,3-b]pyridin-3-yl)methyl)-N-methylaniline (25)
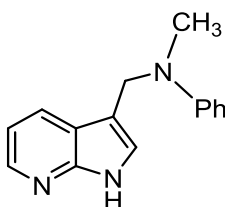
To a solution of intermediate **24b** (0.29 mmol) in anhydrous THF (3 mL), 0.87 mmol of TBAF was added and the mixture was stirred at reflux for 4h. After cooling, the solvent was evaporated and cold-ice water (20 mL) was added. The product was recovered by extraction with CH$_2$Cl$_2$ (3 x 15 mL). The solvent

was evaporated *under vacuum* to afford compound **25**, which was purified by column chromatography using cyclohexane/ethyl acetate 1:3 as eluent.

Yield = 44%; oil. $\underline{^1\text{H-NMR}}$ (CDCl$_3$-d$_1$) δ 2.94 (s, 3H, CH$_3$N), 4.64 (s, 2H, CH$_2$N), 6.76 (t, 1H, Ar, $J = 7.2$ Hz), 6.88 (d, 2H, Ar, $J = 8.4$ Hz), 7.02-7.07 (m, 1H, Ar), 7.19 (s, 1H, Ar), 7.25 (t, 2H, Ar, $J = 7.6$ Hz), 7.86 (d, 1H, Ar, $J = 8.0$ Hz), 8.28 (d, 1H, Ar, $J = 4.8$ Hz), 9.93 (exch br s, 1H, NH). ESI-MS calcd. for C$_{15}$H$_{15}$N$_3$, 237.30; found: *m/z* 238.13 [M+H]$^+$. Anal. C$_{15}$H$_{15}$N$_3$ (C, H, N).

(3-((Methyl(phenyl)amino)methyl)-1H-pyrrolo[2,3-b]pyridin-1-yl)(m-tolyl)methanone (26)
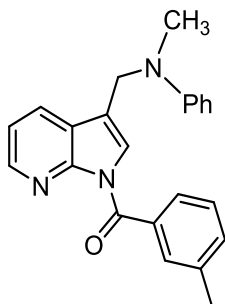
Obtained from compound **25** following the general procedure reported at **pag. 81**. Compound **26** was purified by column chromatography using cyclohexane/ethyl acetate 3:1 as eluent.

Yield = 65%; oil. $\underline{^1\text{H-NMR}}$ (CDCl$_3$-d$_1$) δ 2.39 (s, 3H, m-*CH$_3$*-Ph), 2.96 (s, 3H, *CH$_3$*N), 4.60 (s, 2H, CH$_2$N), 6.79 (t, 1H, Ar, $J = 6.8$ Hz), 6.88 (d, 2H, Ar, $J = 8.0$ Hz), 7.11-7.16 (m, 1H, Ar), 7.23-7.28 (m, 2H, Ar), 7.33 (t, 1H, Ar, $J = 7.6$ Hz), 7.40 (d, 1H, Ar, $J = 7.6$ Hz), 7.48-7.53 (m, 2H, Ar), 7.59 (s, 1H, Ar), 7.82 (d, 1H, Ar, $J = 7.6$ Hz), 8.34 (dd, 1H, Ar, $J = 1.2$ Hz and $J = 4.4$ Hz). $\underline{^{13}\text{C-NMR}}$ (CDCl$_3$-d$_1$) δ 21.35 (CH$_3$), 38.28 (CH$_3$), 49.14 (CH$_2$), 113.68 (CH), 118.86 (CH), 122.55 (C), 125.61 (CH), 127.07 (CH), 127.37 (CH), 127.97 (CH), 128.02 (CH), 129.31 (CH), 130.64 (CH), 133.42 (CH), 133.92 (C), 138.12 (C),

144.89 (CH), 149.89 (C), 167.63 (C). ESI-MS calcd. for $C_{23}H_{21}N_3O$, 355.43; found: *m/z* 356.17 [M+H]$^+$. Anal. $C_{23}H_{21}N_3O$ (C, H, N).

Allyl phenyl((1-(phenylsulfonyl)-1H-pyrrolo[2,3-b]pyridin-3-yl)methyl)carbamate (27)
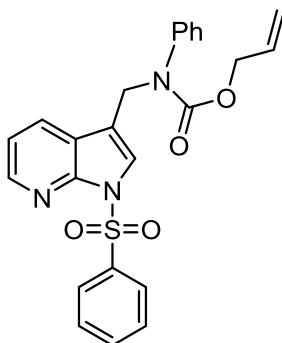

To a suspension of 0.30 mmol of allyl chloroformate in 0.30 mL of dioxane, 0.45 mmol of sodium azide in 0.30 mL of water was added and stirred at room temperature for 1h. Then, a solution of **24a** (0.36 mmol) in 0.70 mL of Na_2CO_3 1% and 0.70 mL of dioxane was added and the mixture was stirred at room temperature overnight. After addition of a little bit of water, the precipitate was recovered by vacuum filtration and crystallized from ethanol to obtain the desired compound.

Yield = 83%; mp = 119-122°C (EtOH). ^{1}H-NMR (DMSO-d$_6$) δ 4.57 (d, 2H, *CH$_2$*=CH, *J* = 4.8 Hz), 4.99 (s, 2H, CH$_2$N), 5.06-5.11 (m, 2H, O*CH$_2$*CH), 5.80-5.88 (m, 1H, CH$_2$=*CH*), 7.04 (d, 2H, Ar, *J* = 7.6 Hz), 7.20-7.28 (m, 4H, Ar), 7.53-7.59 (m, 3H, Ar), 7.67 (t, 1H, Ar, *J* = 7.2 Hz), 7.86 (d, 3H, Ar, *J* = 7.6 Hz), 8.32 (d, 1H, Ar, *J* = 3.6 Hz). ESI-MS calcd. for $C_{24}H_{21}N_3O_4S$, 447.51; found: *m/z* 448.13 [M+H]$^+$. Anal. $C_{24}H_{21}N_3O_4S$ (C, H, N).

Allyl ((1H-pyrrolo[2,3-b]pyridin-3-yl)methyl)(phenyl)carbamate (28)
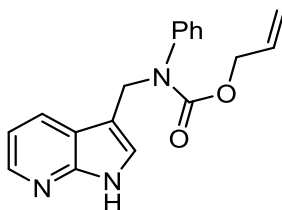
To a solution of intermediate **27** (0.30 mmol) in anhydrous THF (3 mL), 0.90 mmol of TBAF was added and the mixture was stirred at reflux for 3h. After cooling, the solvent was evaporated and cold-ice water (20 mL) was added. The product was recovered by extraction with DCM (3 x 15 mL). The solvent was evaporated *under vacuum* to afford compound **28**, which was purified by column chromatography using cyclohexane/ethyl acetate 1: 3 as eluent.

Yield = 44%; oil. <u>^{1}H-NMR</u> (CDCl$_3$-d$_1$) δ 4.63 (d, 2H, *CH$_2$*=CH, *J* = 4.8 Hz), 5.01 (s, 2H, CH$_2$N), 5.09-5.14 (m, 2H, O*CH$_2$*CH), 5.85-5.90 (m, 1H, CH$_2$=*CH*), 6.70-6.76 (m, 1H, Ar), 7.01-7.10 (m, 3H, Ar), 7.15 (s, 1H, Ar), 7.18-7.28 (m, 3H, Ar), 8.28-8.33 (m, 1H, Ar), 11.30 (exch br s, 1H, NH). ESI-MS calcd. for C$_{18}$H$_{17}$N$_3$O$_2$, 307.35; found: *m/z* 308.14 [M+H]$^+$. Anal. C$_{18}$H$_{17}$N$_3$O$_2$ (C, H, N).

## Allyl ((1-(3-methylbenzoyl)-1H-pyrrolo[2,3-b]pyridin-3-yl)methyl)(phenyl)carbamate (29)
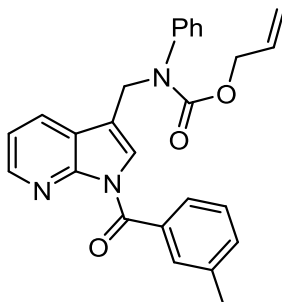
Obtained from compound **28** following the general procedure reported at **pag. 81**. Compound **29** was purified by column chromatography using hexane/acetone 4:1 as eluent.

Yield = 33%; oil. ^{1}H-NMR (CDCl$_3$-d$_1$) δ 2.39 (s, 3H, *m*-CH$_3$-Ph), 4.62 (d, 2H, *CH$_2$*=CH, *J* = 4.4 Hz), 4.97 (s, 2H, CH$_2$N), 5.10-5.15 (m, 2H, O-*CH$_2$*-CH), 5.79-5.84 (m, 1H, CH$_2$=*CH*), 7.02 (d, 2H, Ar, *J* = 6.4 Hz), 7.14-7.19 (m, 1H, Ar), 7.25-7.33 (m, 5H, Ar), 7.39 (t, 2H, Ar, *J* = 7.2 Hz), 7.52 (s, 1H, Ar), 7.90 (s, 1H, Ar), 8.39 (dd, 1H, Ar, *J* = 1.2 Hz and *J* = 4.8 Hz). ESI-MS calcd. for C$_{26}$H$_{23}$N$_3$O$_3$, 425.48; found: *m/z* 426.18 [M+H]$^+$. Anal. C$_{26}$H$_{23}$N$_3$O$_3$ (C, H, N).

(3-((Phenylamino)methyl)-1H-pyrrolo[2,3-b]pyridin-1-yl)(m-tolyl)methanone (30)
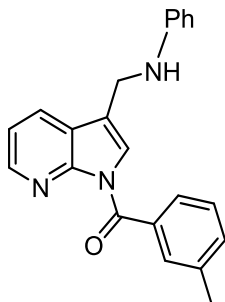
A mixture of **29** (0.05 mmol), phenylsilane (0.50 mmol) and Tetrakis (0.005 mmol) in CH_2Cl_2 (3 mL) was stirred at room temperature for 1h. After dilution with ice-cold water (20 mL), the suspension was extracted with CH_2Cl_2 (3 x 15 mL), dried over sodium sulfate, and the solvent was evaporated *under vacuum* to afford the final compound **30**, which was purified by column chromatography using toluene/ethyl acetate 9:1 as eluent.

Yield = 35%; oil. <u>^{1}H-NMR</u> ($CDCl_3$-d_1) δ 2.40 (s, 3H, *m*-CH$_3$-Ph), 4.47 (s, 2H, *CH$_2$*NH), 6.76 (d, 2H, Ar, $J = 8.0$ Hz), 6.81 (t, 1H, Ar, $J = 7.6$ Hz), 7.17-7.23 (m, 2H, Ar), 7.34 (t, 2H, Ar, $J = 7.6$ Hz), 7.41 (d, 1H, Ar, $J = 7.2$ Hz), 7.52 (d, 1H, Ar, $J = 7.6$ Hz), 7.59-7.64 (m, 2H, Ar), 7.97 (d, 1H, Ar, $J = 7.6$ Hz), 8.37 (d, 1H, Ar, $J = 4.0$ Hz). <u>^{13}C-NMR</u> ($CDCl_3$-d_1) δ 21.03 (CH$_3$), 39.47 (CH$_2$), 112.65 (C), 113.52 (CH), 113.59 (CH), 115.61 (CH), 120.22 (C), 120.87 (CH), 122.53 (CH), 128.10 (CH), 128.34 (CH), 129.19 (CH), 129.56 (CH), 130.13 (CH), 130.45 (C), 134.82 (CH), 138.90 (C), 142.44 (CH), 147.68 (C), 149.34 (C), 167.72 (C). ESI-MS calcd. for $C_{22}H_{19}N_3O$, 341.41; found: *m/z* 342.16 [M+H]$^+$. Anal. $C_{22}H_{19}N_3O$ (C, H, N).

**Ethyl 1-(phenylsulfonyl)-1H-pyrrolo[2,3-b]pyridine-2-carboxylate (31b)**
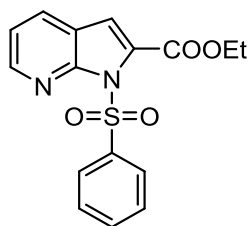
To a cooled solution (-78°C) of lithium diisopropylamide (LDA 2.0 M in THF/epthane/ethyl benzene) (0.78 mmol) in 10 mL of THF, 0.39 mmol of intermediate **11** (Sandham, D. A. et al. 2009) was added. The mixture was stirred at -78°C for 30 minutes, then 0.78 mmol of ethyl chloroformate was added and the reaction is still kept under stirring at -78°C another hour, and then at room temperature for 2h. After diluition with ice-cold water (20 mL), the reaction mixture was extracted with CH_2Cl_2 (3 x 15 mL), washed with Brine, dried over sodium sulfate and evaporated *under vacuum* to afford compound **31b**.

Yield = 78%; oil. <u>^{1}H-NMR</u> (CDCl$_3$-d$_1$) δ 1.42 (t, 3H, OCH$_2$*CH$_3$*, *J* = 7.2 Hz), 4.44 (q, 2H, O*CH$_2$*CH$_3$, *J* = 7.2 Hz), 7.02 (s, 1H, Ar), 7.20-7.25 (m, 1H, Ar), 7.53 (t, 2H, Ar, *J* = 7.6 Hz), 7.60 (t, 1H, Ar, *J* = 7.6 Hz), 7.86 (dd, 1H, Ar, *J* = 8.0 Hz and *J* = 1.2 Hz), 8.41 (d, 2H, Ar, *J* = 7.6 Hz), 8.53-8.58 (m, 1H, Ar). ESI-MS calcd. for C$_{16}$H$_{14}$N$_2$O$_4$S, 330.36; found: *m/z* 331.07 [M+H]$^+$. Anal. C$_{16}$H$_{14}$N$_2$O$_4$S (C, H, N).

Material and methods

**2-Methyl-1-(3-methylbenzoyl)-1H-pyrrolo[2,3-b]pyridine-3-carbonitrile (36)**
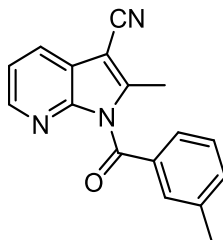
Obtained from compound **35** (Bahekar, R. H. et al. 2007) following the general procedure reported at **pag. 81**. Compound **36** was purified by column chromatography using cyclohexane/ethyl acetate 5:1 as eluent.

Yield = 10%; oil. ^{1}H-NMR (CDCl$_3$-d$_1$) δ 2.40 (s, 3H, *m*-CH$_3$-Ph), 2.74 (s, 3H, CH$_3$), 7.21-7.26 (m, 1H, Ar), 7.30-7.35 (m, 1H, Ar), 7.48 (d, 2H, Ar, *J* = 7.6 Hz), 7.64 (s, 1H, Ar), 7.98 (d, 1H, Ar, *J* = 7.2 Hz), 8.19 (d, 1H, Ar, *J* = 4.0 Hz). ^{13}C-NMR (CDCl$_3$-d$_1$) δ 9.43 (CH$_3$), 20.91 (CH$_3$), 101.37 (C), 115.65 (CH), 115.92 (C), 121.15 (CH), 128.10 (CH), 128.36 (CH), 129.14 (CH), 130.17 (CH), 130.49 (CH), 134.86 (CH), 137.33 (C), 138.91 (C), 142.4 (CH), 146.36 (C), 167.70 (C). ESI-MS calcd. for C$_{17}$H$_{13}$N$_3$O, 275.30; found: *m/z* 276.11 [M+H]$^+$. Anal. C$_{17}$H$_{13}$N$_3$O (C, H, N).

Ethyl 1-(3-methylbenzoyl)-1H-pyrrolo[2,3-b]pyridine-2-carboxylate (37)
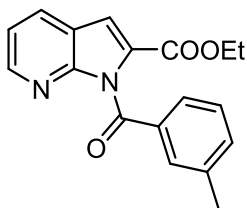
Obtained from compound **32b** (Baltus, C. B. et al. 2016) following the general procedure reported at **pag. 81**. Compound **37** was purified by column chromatography using cyclohexane/ethyl acetate 2:1 as eluent.

Yield = 34%; oil. <u>^{1}H-NMR</u> (CDCl$_3$-d$_1$) δ 1.45 (t, 3H, OCH$_2$*CH$_3$*, *J* = 7.2 Hz), 2.38 (s, 3H, CH$_3$-Ph), 4.21 (q, 2H, O*CH$_2$*CH$_3$, *J* = 7.2 Hz), 7.16-7.21 (m, 1H, Ar), 7.29-7.34 (m, 1H, Ar), 7.42 (d, 1H, Ar, *J* = 7.6 Hz), 7.56 (d, 1H, Ar, *J* = 7.6 Hz), 7.71 (s, 1H, Ar), 8.04 (d, 1H, Ar, *J* = 8.0 Hz), 8.41 (d, 1H, Ar, *J* = 4.4 Hz). <u>^{13}C-NMR</u> (CDCl$_3$-d$_1$) δ 13.94 (CH$_3$), 21.29 (CH$_3$), 61.59 (CH$_2$), 111.04 (CH), 118.64 (CH), 119.46 (C), 127.93 (CH), 128.56 (CH), 130.65 (C), 131.02 (CH), 131.18 (CH), 134.03 (C), 135.01 (CH), 138.61 (C), 147.70 (CH), 150.05 (C), 160.65 (C), 169.00 (C). ESI-MS calcd. for C$_{18}$H$_{16}$N$_2$O$_3$, 308.34; found: *m/z* 309.12 [M+H]$^+$. Anal. C$_{18}$H$_{16}$N$_2$O$_3$ (C, H, N).

## 1H-Pyrrolo[2,3-b]pyridine-2-carbonitrile (39)
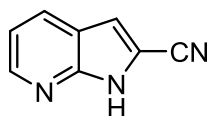
A mixture of intermediate **38** (0.68 mmol) (Jia, H. et al. 2014) and 4 mL of POCl$_3$ was stirred at reflux for 1h. After cooling, ice-cold water (20 mL) was added, then the suspension was extracted with CH$_2$Cl$_2$ (3 X 15 mL), dried over sodium sulfate and the solvent was evaporated *under vacuum* to afford compound **39**.

Yield = 41%; oil. <u>^{1}H-NMR</u> (CDCl$_3$-d$_1$) δ 7.22-7.27 (m, 1H, Ar), 7.41 (s, 1H, Ar), 8.18 (d, 1H, Ar, *J* = 7.2 Hz), 8.46 (d, 1H, Ar, *J* = 3.6 Hz), 8.70 (exch br s, 1H, NH). ESI-MS calcd. for C$_8$H$_5$N$_3$, 143.15; found: *m/z* 144.05 [M+H]$^+$. Anal. C$_8$H$_5$N$_3$ (C, H, N).

**1-(3-Methylbenzoyl)-1H-pyrrolo[2,3-b]pyridine-2-carbonitrile (40)**
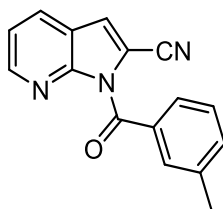
Obtained from compound **39** following the general procedure reported at **pag. 81**. Compound **40** was purified by column chromatography using cyclohexane/ethyl acetate 2:1 as eluent.

Yield = 41%; oil. $\underline{^1\text{H-NMR}}$ (CDCl$_3$-d$_1$) δ 2.41 (s, 3H, CH$_3$-Ph), 7.25-7.33 (m, 1H, Ar), 7.34-7.40 (m, 2H, Ar), 7.48 (d, 1H, Ar, J = 7.6 Hz), 7.58 (d, 1H, Ar, J = 7.6 Hz) 7.69 (s, 1H, Ar), 8.03 (dd, 1H, Ar, J = 8.0 Hz and J = 1.2 Hz), 8.38 (d, 1H, Ar, J = 3.6 Hz). $\underline{^{13}\text{C-NMR}}$ (CDCl$_3$-d$_1$) δ 21.53 (CH$_3$), 110.31 (C), 112.22 (C), 118.23 (CH), 119.60 (C), 120.03 (CH), 128.32 (CH), 128.59 (CH), 131.13 (CH), 131.61 (CH), 132.56 (C), 135.23 (CH), 138.52 (C), 148.37 (CH), 166.85 (C). ESI-MS calcd. for C$_{16}$H$_{11}$N$_3$O, 261.28; found: *m/z* 262.09 [M+H]$^+$. Anal. C$_{16}$H$_{11}$N$_3$O (C, H, N).

General procedure for acylation or benzoylation at N-2 of isoxazol-5(2H)-one. To a suspension of the appropriate substrate of type **42** (0.86 mmol) in 10 mL of anhydrous THF, 1.72 mmol of sodium hydride (60% dispersion in mineral oil) and 1.03 mmol of the appropriate acyl/aroyl chloride were added. The mixture was stirred at room temperature overnight. The solvent was concentrated *under vacuum* to obtain the final compounds **43a-s** and **45a-o**, which were purified by column chromatography using cyclohexane/ethyl acetate or toluene/ethyl acetate in different ratio as eluents.

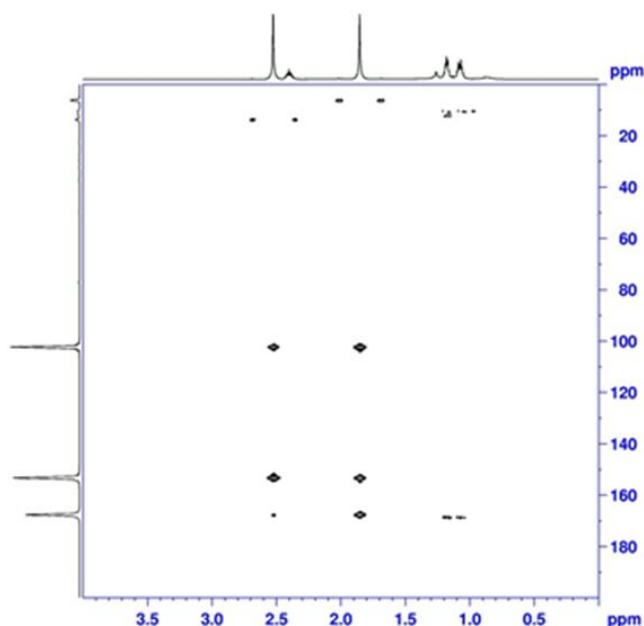**2-(Cyclopropanecarbonyl)-3,4-dimethylisoxazol-5(2H)-one (43a)**
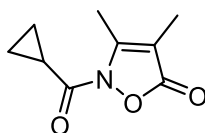
Obtained from compound **42a** (Krogsgaar-Laersen, P. et al. 1973) following the general procedure reported at **pag. 118**. Compound **43a** was purified by column chromatography using cyclohexane/ethyl acetate 2:1 as eluent.

Yield = 32%; oil. ^{1}H-NMR (CDCl$_3$-d$_1$) δ 1.02-1.07 (m, 2H, CH$_2$ cC$_3$H$_5$), 1.12-1.17 (m, 2H, CH$_2$ cC$_3$H$_5$), 1.82 (s, 3H, C$_4$-CH$_3$), 2.34-2.40 (m, 1H, CH cC$_3$H$_5$), 2.49 (s, 3H, C$_3$-CH$_3$). ^{13}C-NMR (CDCl$_3$-d$_1$) δ 6.26 (CH$_3$), 10.44 (CH$_2$), 12.50 (CH), 13.77 (CH$_3$), 102.41 (C), 153.33 (C), 167.77 (C), 168.74 (C). ESI-MS calcd. for C$_9$H$_{11}$NO$_3$, 181.19; found: _m/z_ 182.08 [M+H]$^+$. Anal. C$_9$H$_{11}$NO$_3$ (C, H, N).
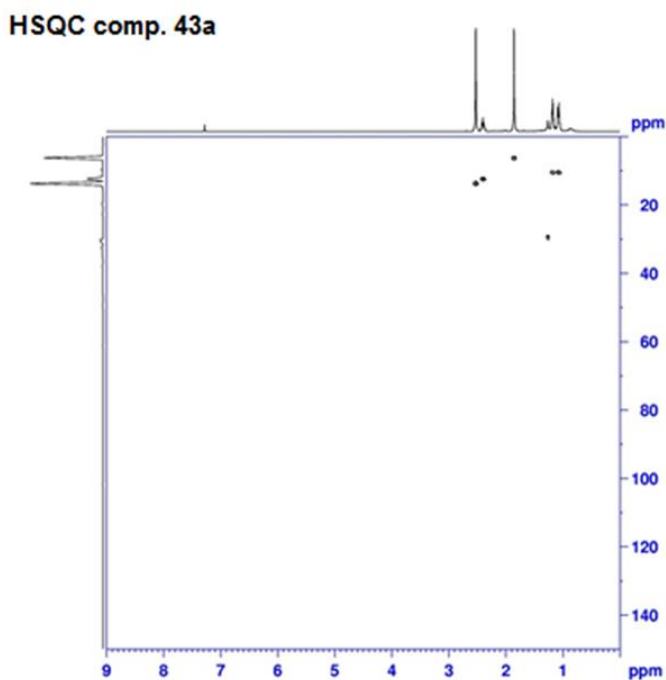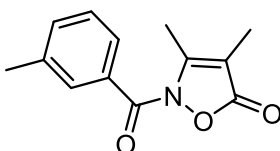

HSQC comp. 43a

HMBC comp. 43a

**3,4-Dimethyl-2-(3-methylbenzoyl)isoxazol-5(2H)-one (43b)**

Obtained from compound **42a** (Krogsgaar-Laersen, P. et al. 1973) following the general procedure reported at **pag. 118**. Compound **43b** was purified by column chromatography using toluene/ethyl acetate 95:5 as eluent.

Yield = 30%; oil. $\underline{^1\text{H-NMR}}$ (CDCl$_3$-d$_1$) δ 1.75 (s, 3H, C$_4$-CH$_3$), 2.05 (s, 3H, C$_3$-CH$_3$), 2.41 (s, 3H, *m-CH$_3$*-Ph), 7.35 (t, 1H, Ar, J = 8.0 Hz), 7.44 (d, 1H, Ar, J = 7.6 Hz), 7.80-7.85 (m, 2H, Ar). $\underline{^{13}\text{C-NMR}}$ (CDCl$_3$-d$_1$) δ 10.99 (CH$_3$), 20.12 (CH$_3$), 21.23 (CH$_3$), 29.70 (C), 127.38 (CH), 128.65 (CH), 130.68 (CH), 135.28 (CH), 134.10 (C), 138.70 (C), 143.10 (C), 157.61 (C), 169.57 (C). ESI-MS

calcd. for $C_{13}H_{13}NO_3$, 231.25; found: *m/z* 232.09 [M+H]$^+$. Anal. $C_{13}H_{13}NO_3$ (C, H, N).
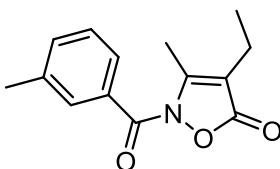
2-(Cyclopropanecarbonyl)-4-ethyl-3-methylisoxazol-5(2H)-one (43c)
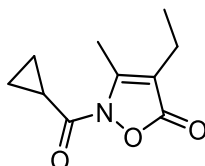
Obtained from compound **42b** (Sato, K. et al. 1986) following the general procedure reported at **pag. 118**. Compound **43c** was purified by column chromatography using cyclohexane/ethyl acetate 4:1 as eluent.

Yield = 26%; oil. ^{1}H-NMR (CDCl$_3$-d$_1$) δ 0.98-1.05 (m, 2H, CH$_2$ cC$_3$H$_5$), 1.10 (t, 3H, CH$_2$*CH$_3$*, *J* = 7.6 Hz), 1.13-1.18 (m, 2H, CH$_2$ cC$_3$H$_5$), 2.26 (q, 2H, *CH$_2$*CH$_3$, *J* = 7.6 Hz), 2.34-2.40 (m, 1H, CH cC$_3$H$_5$), 2.50 (s, 3H, C$_3$-CH$_3$). ^{13}C-NMR (CDCl$_3$-d$_1$) δ 10.96 (CH$_2$), 13.09 (CH$_3$), 13.58 (CH$_3$), 14.06 (CH), 15.53 (CH$_2$), 108.58 (C), 153.56 (C), 167.87 (C), 169.34 (C). ESI-MS calcd. for $C_{10}H_{13}NO_3$, 195.22; found: *m/z* 196.09 [M+H]$^+$. Anal. $C_{10}H_{13}NO_3$ (C, H, N).
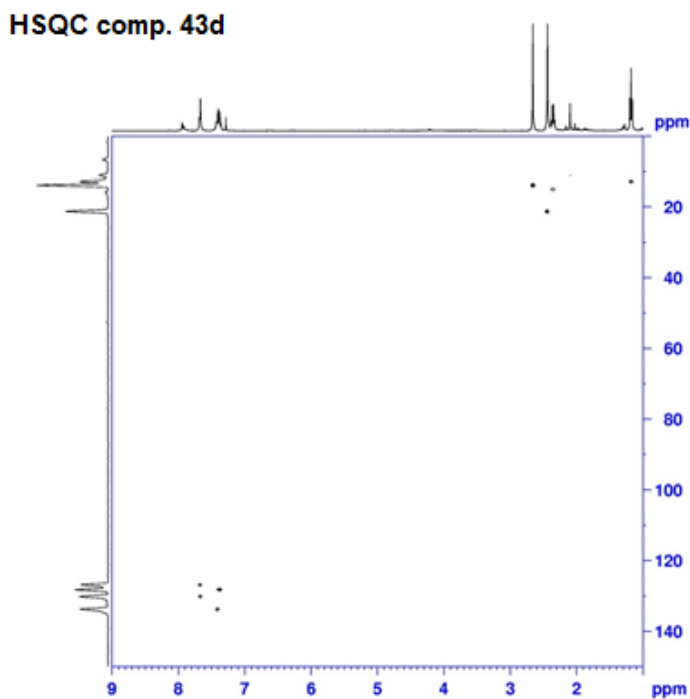
4-Ethyl-3-methyl-2-(3-methylbenzoyl)isoxazol-5(2H)-one (43d)
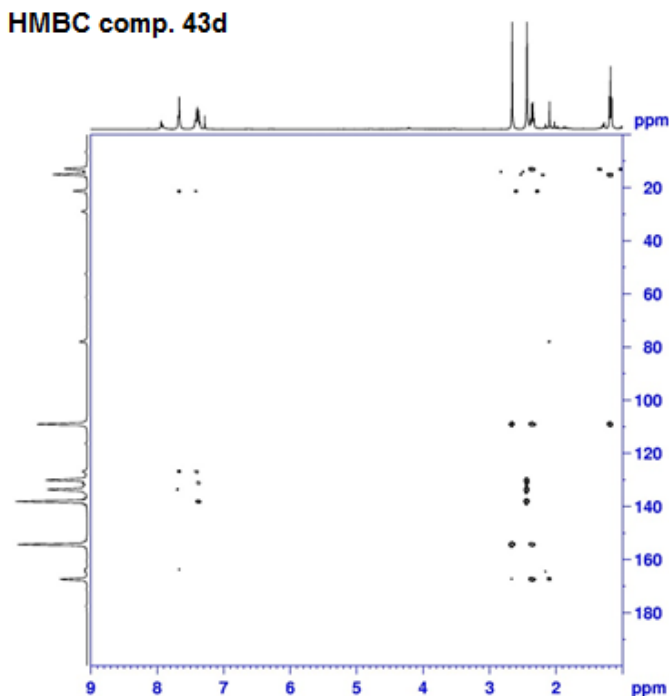

Obtained from compound **42b** (Sato, K. et al. 1986) following the general procedure reported at **pag. 118**. Compound **43d** was purified by column chromatography using cyclohexane/ethyl acetate 5:1 as eluent.

Material and methods

Yield = 34%; oil. ^{1}H-NMR (CDCl$_3$-d$_1$) δ 1.13 (t, 3H, CH$_2$*CH$_3$*, J = 7.6 Hz), 2.31 (q, 2H, *CH$_2$*CH$_3$, J = 7.6 Hz), 2.39 (s, 3H, *m*-*CH$_3$*-Ph), 2.61 (s, 3H, C$_3$-CH$_3$), 7.30-7.37 (m, 2H, Ar), 7.61-7.66 (m, 2H, Ar). ^{13}C-NMR (CDCl$_3$-d$_1$) δ 12.99 (CH$_3$), 13.90 (CH$_3$), 15.13 (CH$_2$), 21.34 (CH$_3$), 109.02 (C), 126.61 (CH), 127.70 (CH), 129.75 (CH), 131.41 (C), 133.78 (CH), 138.18 (C), 154.31 (C), 163.72 (C), 167.41 (C). ESI-MS calcd. for C$_{14}$H$_{15}$NO$_3$, 245.27; found: *m/z* 246.11 [M+H]$^+$. Anal. C$_{14}$H$_{15}$NO$_3$ (C, H, N).

HSQC comp. 43d

HMBC comp. 43d

2-(Cyclopropanecarbonyl)-3-ethyl-4-methylisoxazol-5(2H)-one (43e)

Obtained from compound **42c**, commercially available, following the general procedure reported at **pag. 118**. Compound **43e** was purified by column chromatography using cyclohexane/ethyl acetate 3:1 as eluent.
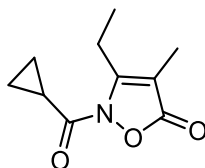
Yield = 54%; oil. <u>^{1}H-NMR</u> (CDCl$_3$-d$_1$) δ 0.97-1.05 (m, 2H, CH$_2$ cC$_3$H$_5$), 1.13-1.18 (m, 2H, CH$_2$ cC$_3$H$_5$), 1.20 (t, 3H, CH$_2$*CH$_3$*, *J* = 7.2 Hz), 1.82 (s, 3H, CH$_3$), 2.34-2.40 (m, 1H, CH cC$_3$H$_5$), 2.90 (q, 2H, *CH$_2$*CH$_3$, *J* = 7.2 Hz). <u>^{13}C-NMR</u> (CDCl$_3$-d$_1$) δ 6.03 (CH$_3$), 10.37 (CH$_2$), 12.06 (CH$_3$), 12.66 (CH), 20.74 (CH$_2$), 102.22 (C), 158.53 (C), 167.89 (C), 168.23 (C). ESI-MS calcd. for C$_{10}$H$_{13}$NO$_3$, 195.22; found: *m/z* 196.09 [M+H]$^+$. Anal. C$_{10}$H$_{13}$NO$_3$ (C, H, N).

Material and methods

HSQC comp. 43e

HMBC comp. 43e
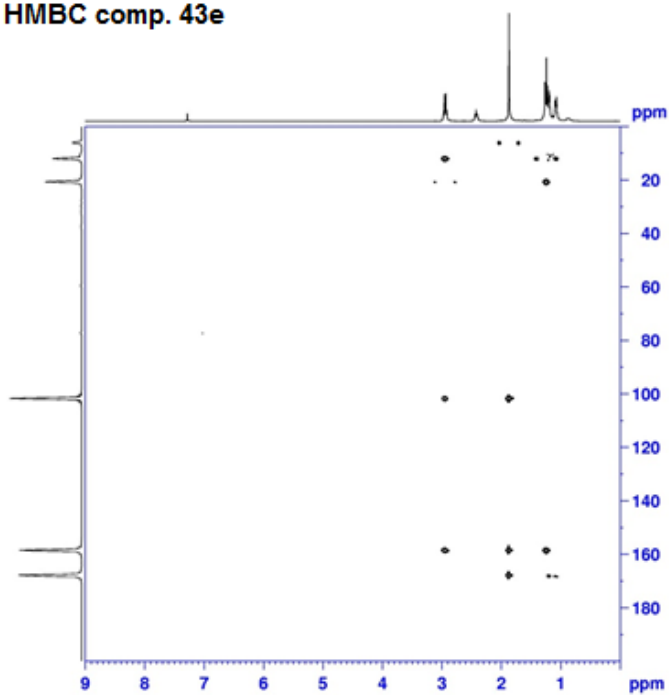
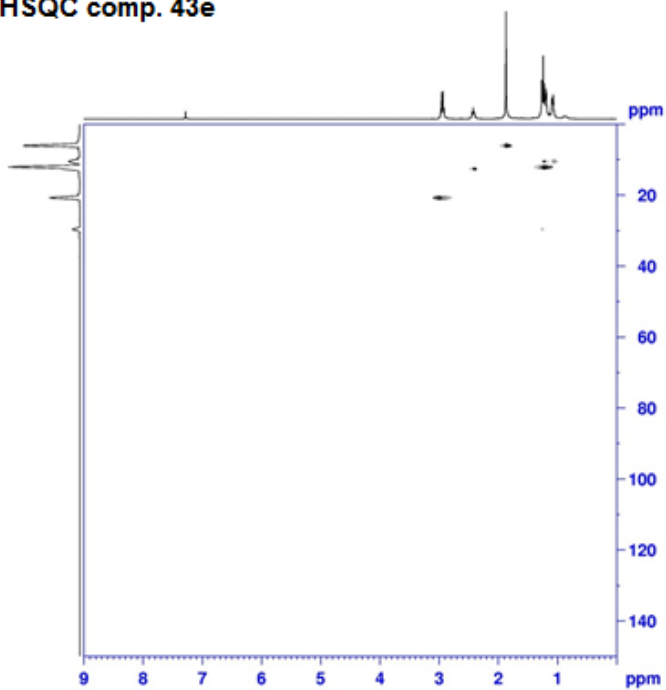**3-Ethyl-4-methyl-2-(3-methylbenzoyl)isoxazol-5(2H)-one (43f)**
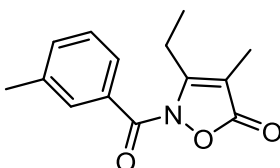
Obtained from compound **42c**, commercially available, following the general procedure reported at **pag. 118**. Compound **43f** was purified by column chromatography using toluene/ethyl acetate 95:5 as eluent.

Yield = 10%; oil. $\underline{^1\text{H-NMR}}$ (CDCl$_3$-d$_1$) δ 1.30 (t, 3H, CH$_2$*CH$_3$*, *J* = 7.6 Hz), 1.85 (s, 3H, CH$_3$), 2.44 (s, 3H, CH$_3$-Ph), 2.64 (q, 2H, *CH$_2$*CH$_3$, *J* = 7.6 Hz), 7.41 (t, 1H, Ar, *J* = 7.6 Hz), 7.49 (d, 1H, Ar, *J* = 7.6 Hz), 7.96 (d, 2H, Ar, *J* = 7.6 Hz). $\underline{^{13}\text{C-NMR}}$ (CDCl$_3$-d$_1$) δ 5.92 (CH$_3$), 11.36 (CH$_3$), 19.55 (CH$_2$), 21.41 (CH$_3$), 97.56 (C), 127.03 (C), 127.96 (CH), 128.76 (CH), 131.21 (CH), 135.47 (CH), 138.45 (C), 161.76 (C), 161.96 (C), 167.00 (C). ESI-MS calcd. for C$_{14}$H$_{15}$NO$_3$, 245.27; found: *m/z* 246.11 [M + H]$^+$. Anal. C$_{14}$H$_{15}$NO$_3$ (C, H, N).

Ethyl 2-(cyclopropanecarbonyl)-4-methyl-5-oxo-2,5-dihydroisoxazole-3-carboxylate (43g)

Obtained from compound **42d** (Adembri, G. et al. 1965) following the general procedure reported at **pag. 118**. Compound **43g** was purified by column chromatography using cyclohexane/ethyl acetate 3:1 as eluent.
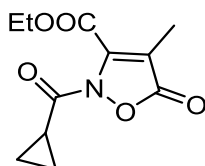
Yield = 38%; oil. $\underline{^1\text{H-NMR}}$ (CDCl$_3$-d$_1$) δ 1.11-1.16 (m, 2H, CH$_2$ cC$_3$H$_5$), 1.17-1.23 (m, 2H, CH$_2$ cC$_3$H$_5$), 1.35 (t, 3H, OCH$_2$*CH$_3$*, *J* = 7.2 Hz), 1.95 (s, 3H, CH$_3$),

2.25-2.31 (m, 1H, CH cC$_3$H$_5$), 4.41 (q, 2H, OCH$_2$CH$_3$, J = 7.2 Hz). ^{13}C-NMR (CDCl$_3$-d$_1$) δ 6.89 (CH), 10.91 (CH$_2$), 12.40 (CH$_3$), 13.88 (CH$_3$), 63.22 (CH$_2$), 107.85 (C), 145.28 (C), 158.92 (C), 167.45 (C), 168.67 (C). ESI-MS calcd. for C$_{11}$H$_{13}$NO$_5$, 239.22; found: *m/z* 240.08 [M+H]$^+$. Anal. C$_{11}$H$_{13}$NO$_5$ (C, H, N).

Ethyl 4-methyl-2-(3-methylbenzoyl)-5-oxo-2,5-dihydroisoxazole-3-carboxylate (43h)
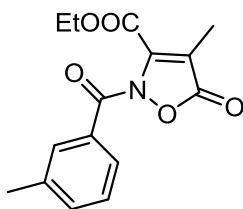

Obtained from compound **42d** (Adembri, G. et al. 1965) following the general procedure reported at **pag. 118**. Compound **43h** was purified by column chromatography using cyclohexane/ethyl acetate 3:1 as eluent.

Yield = 21%; oil. ^{1}H-NMR (CDCl$_3$-d$_1$) δ 1.42 (t, 3H, OCH$_2$CH$_3$, J = 7.2 Hz), 2.08 (s, 3H, CH$_3$), 2.44 (s, 3H, *CH$_3$*-Ph), 4.45 (q, 2H, OCH$_2$CH$_3$, J = 7.2 Hz), 7.42 (t, 1H, Ar, J = 7.6 Hz), 7.51 (d, 1H, Ar, J = 7.6 Hz), 7.97 (d, 2H, Ar, J = 7.6 Hz) . ^{13}C-NMR (CDCl$_3$-d$_1$) δ 6.68 (CH$_3$), 14.16 (CH$_3$), 21.26 (CH$_3$), 62.03 (CH$_2$), 101.14 (C), 126.42 (C), 128.07 (CH), 128.90 (CH), 131.34 (CH), 135.89 (CH), 138.81 (C), 156.61 (C), 160.17 (C), 161.66 (C), 163.86 (C). ESI-MS calcd. for C$_{15}$H$_{15}$NO$_5$, 289.28; found: *m/z* 290.10 [M+H]$^+$. Anal. C$_{15}$H$_{15}$NO$_5$ (C, H, N).

2-(Cyclopropanecarbonyl)-3-ethylisoxazol-5(2H)-one (43i)
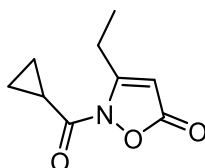
Obtained from compound **42e** (Yamaguchi, M. et al. 2009) following the general procedure reported at **pag. 118**. Compound **43i** was purified by column chromatography using cyclohexane/ethyl acetate 2:1 as eluent.

Yield = 47%; mp = 92-95°C (EtOH). $\underline{^1\text{H-NMR}}$ (CDCl$_3$-d$_1$) δ 1.05-1.10 (m, 2H, CH$_2$ cC$_3$H$_5$), 1.14-1.19 (m, 2H, CH$_2$ cC$_3$H$_5$), 1.25 (t, 3H, CH$_2$*CH$_3$*, *J* = 7.4 Hz), 2.36-2.42 (m, 1H, CH cC$_3$H$_5$), 2.95 (q, 2H, *CH$_2$*CH$_3$, *J* = 7.4 Hz), 5.32 (s, 1H, CH). ^{13}C-NMR (CDCl$_3$-d$_1$) δ 10.83 (CH$_2$), 11.33 (CH$_3$), 12.69 (CH), 22.69 (CH$_2$), 92.92 (CH), 164.65 (C), 166.69 (C), 168.69 (C). ESI-MS calcd. for C$_9$H$_{11}$NO$_3$, 181.19; found: *m/z* 182.08 [M + H]$^+$. Anal. C$_9$H$_{11}$NO$_3$ (C, H, N).
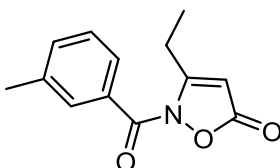
3-Ethyl-2-(3-methylbenzoyl)isoxazol-5(2H)-one (43j)

Obtained from compound **42e** (Yamaguchi, M. et al. 2009) following the general procedure reported at **pag. 118**. Compound **43j** was purified by column chromatography using cyclohexane/ethyl acetate 3:1 as eluent.

Yield = 48%; mp = 81-84°C (EtOH). $\underline{^1\text{H-NMR}}$ (CDCl$_3$-d$_1$) δ 1.32 (t, 3H, CH$_2$*CH$_3$*, *J* = 7.4 Hz), 2.40 (s, 3H, *CH$_3$*-Ph), 3.09 (q, 2H, *CH$_2$*CH$_3$, *J* = 7.4 Hz), 5.41 (s, 1H, CH), 7.33-7.40 (m, 2H, Ar), 7.64-7.69 (m, 2H, Ar). ^{13}C-NMR (CDCl$_3$-d$_1$) δ 11.49 (CH$_3$), 21.36 (CH$_3$), 23.07 (CH$_2$), 93.81 (CH), 127.02 (CH), 128.28 (CH),

130.23 (CH), 131.04 (C), 134.05 (CH), 138.28 (C), 163.38 (C), 166.20 (C), 166.66 (C). ESI-MS calcd. for $C_{13}H_{13}NO_3$, 231.25; found: *m/z* 232.09 [M+H]+. Anal. $C_{13}H_{13}NO_3$ (C, H, N).

3-Isopropyl-2-propionylisoxazol-5(2H)-one (43k)

Obtained from compound **42f** (Jacobsen, N. et al. 1984) following the general procedure reported at **pag. 118**. Compound **43k** was purified by column chromatography using cyclohexane/ethyl acetate 3:1 as eluent.

Yield = 47%; mp = 93-95°C (EtOH). <u>1H-NMR</u> (CDCl₃-d₁) δ 1.15 (t, 3H, CH₂*CH₃*, *J* = 7.4 Hz), 1.23 (d, 6H, CH*(CH₃)₂*, *J* = 6.8 Hz), 2.72 (q, 2H, *CH₂*CH₃, *J* = 7.4 Hz), 3.50-3.57 (m 1H, *CH*(CH₃)₂), 5.27 (s, 1H, CH). <u>13C-NMR</u> (CDCl₃-d₁) δ 7.73 (CH₃), 21.08 (CH₃), 28.10 (CH), 28.54 (CH₂), 91.70 (CH), 166.50 (C), 168.45 (C), 169.51 (C). ESI-MS calcd. for $C_9H_{13}NO_3$, 183.20; found: *m/z* 184.09 [M+H]+. Anal. $C_9H_{13}NO_3$ (C, H, N).

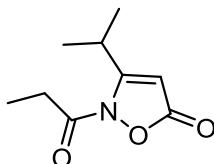**2-(Cyclopropanecarbonyl)-3-isopropylisoxazol-5(2H)-one (43l)**

Obtained from compound **42f** (Jacobsen, N. et al. 1984) following the general procedure reported at **pag. 118**. Compound **43l** was purified by column chromatography using cyclohexane/ethyl acetate 4:1 as eluent.

Yield = 27%; mp = 55-57°C (EtOH). ^{1}H-NMR (CDCl$_3$-d$_1$) δ 1.07-1.12 (m, 2H, CH$_2$ cC$_3$H$_5$), 1.16-1.21 (m, 2H, CH$_2$ cC$_3$H$_5$), 1.26 (d, 6H, CH*(CH$_3$)$_2$*, J = 6.8 Hz), 2.38-2.45 (m, 1H, CH cC$_3$H$_5$), 3.54-3.61 (m 1H, *CH*(CH$_3$)$_2$), 5.33 (s, 1H, CH). ^{13}C-NMR (CDCl$_3$-d$_1$) δ 10.88 (CH$_2$), 12.94 (CH), 21.17 (CH$_3$), 28.18 (CH), 91.72 (CH), 166.50 (C), 168.45 (C), 169.51 (C). ESI-MS calcd. for C$_{10}$H$_{13}$NO$_3$, 195.22; found: *m/z* 196.09 [M+H]$^+$. Anal. C$_{10}$H$_{13}$NO$_3$ (C, H, N).

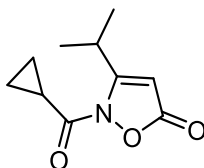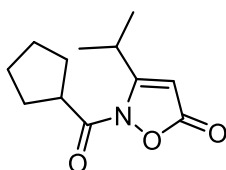**2-(Cyclopentanecarbonyl)-3-isopropylisoxazol-5(2H)-one (43m)**

Obtained from compound **42f** (Jacobsen, N. et al. 1984) following the general procedure reported at **pag. 118**. Compound **43m** was purified by column chromatography using cyclohexane/ethyl acetate 4:1 as eluent.

Yield = 23%; oil. ^{1}H-NMR (CDCl$_3$-d$_1$) δ 1.26 (d, 6H, CH*(CH$_3$)$_2$*, J = 6.8 Hz), 1.63-1.74 (m, 4H, 2 x CH$_2$ cC$_5$H$_9$), 1.82-1.87 (m, 2H, CH$_2$ cC$_5$H$_9$), 1.97-2.02 (m, 2H, CH$_2$ cC$_5$H$_9$), 3.32-3.37 (m, 1H, CH cC$_5$H$_9$), 3.57-3.62 (m 1H, *CH*(CH$_3$)$_2$), 5.30 (s, 1H, CH). ^{13}C-NMR (CDCl$_3$-d$_1$) δ 21.12 (CH$_3$), 25.95 (CH$_2$), 28.17 (CH), 29.56 (CH$_2$), 43.61 (CH), 91.66 (CH), 166.68 (C), 169.74 (C), 170.93 (C). ESI-MS calcd. for C$_{12}$H$_{17}$NO$_3$, 223.27; found: *m/z* 224.12 [M+H]$^+$. Anal. C$_{12}$H$_{17}$NO$_3$ (C, H, N).

3-Isopropyl-2-(3-methylbenzoyl)isoxazol-5(2H)-one (43n)

Obtained from compound **42f** (Jacobsen, N. et al. 1984) following the general procedure reported at **pag. 118**. Compound **43n** was purified by column chromatography using toluene/ethyl acetate 95:5 as eluent.

Yield = 17%; oil. ^{1}H-NMR (CDCl$_3$-d$_1$) δ 1.34 (d, 6H, CH*(CH$_3$)$_2$*, *J* = 6.8 Hz), 2.41 (s, 3H, *CH$_3$*-Ph), 3.70-3.78 (m 1H, *CH*(CH$_3$)$_2$), 5.42 (s, 1H, CH), 7.33-7.41 (m, 2H, Ar), 7.62-7.67 (m, 2H, Ar). ^{13}C-NMR (CDCl$_3$-d$_1$) δ 21.44 (CH$_3$), 21.96 (CH$_3$), 28.50 (CH), 92.85 (CH), 127.15 (CH), 128.30 (CH), 130.23 (CH), 131.38 (C), 134.08 (CH), 138.32 (C), 163.56 (C), 166.83 (C), 171.07 (C). ESI-MS calcd. for C$_{14}$H$_{15}$NO$_3$, 245.27; found: *m/z* 246.11 [M+H]$^+$. Anal. C$_{14}$H$_{15}$NO$_3$ (C, H, N).

HSQC comp. 43n

HMBC comp. 43n
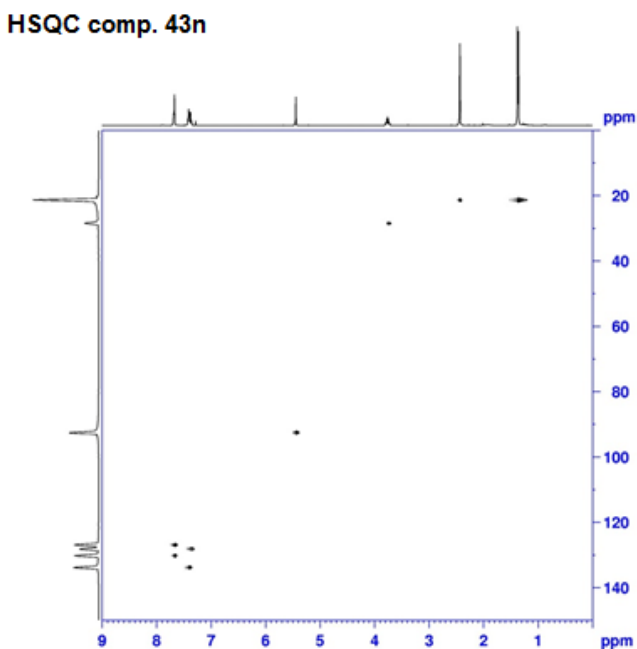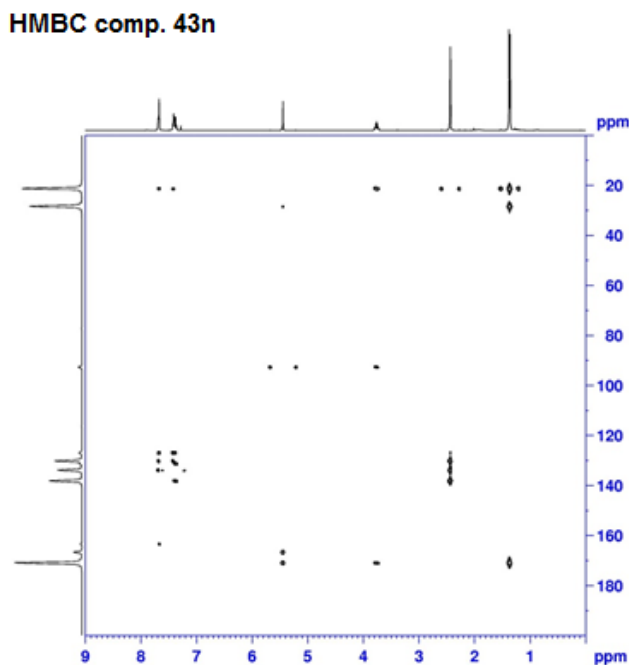
3-Isopropyl-2-(4-methylbenzoyl)isoxazol-5(2H)-one (43o)
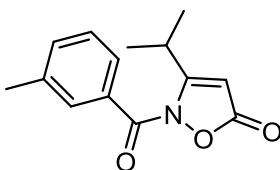

Obtained from compound **42f** (Jacobsen, N. et al. 1984) following the general procedure reported at **pag. 118**. Compound **43o** was purified by column chromatography using toluene/ethyl acetate 95:5 as eluent.

Yield = 45%; mp = 77-79°C (EtOH). ^{1}H-NMR (CDCl$_3$-d$_1$) δ 1.33 (d, 6H, CH*(CH$_3$)$_2$*, J = 7.0 Hz), 2.41 (s, 3H, *CH$_3$*-Ph), 3.66-3.79 (m 1H, *CH*(CH$_3$)$_2$), 5.40 (s, 1H, CH), 7.26 (d, 2H, Ar, J = 8.0 Hz), 7.78 (d, 2H, Ar, J = 8.0 Hz). ^{13}C-NMR (CDCl$_3$-d$_1$) δ 21.91 (CH$_3$), 22.30 (CH$_3$), 29.05 (CH), 93.10 (CH), 129.04 (C), 129.66 (CH), 130.69 (CH), 144.82 (C), 163.72 (C), 167.36 (C), 171.67 (C). ESI-MS calcd. for C$_{14}$H$_{15}$NO$_3$, 245.27; found: *m/z* 246.11 [M + H]$^{+}$. Anal. C$_{14}$H$_{15}$NO$_3$ (C, H, N).

Material and methods

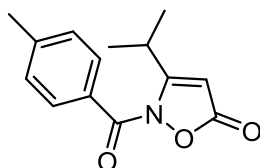**3-(3-Isopropyl-5-oxo-2,5-dihydroisoxazole-2-carbonyl)benzonitrile (43p)**

Obtained from compound **42f** (Jacobsen, N. et al. 1984) following the general procedure reported at **pag. 118**. Compound **43p** was purified by column chromatography using cyclohexane/ethyl acetate 3:1 as eluent.

Yield = 14%; oil. <u>^{1}H-NMR</u> (CDCl$_3$-d$_1$) δ 1.31 (d, 6H, CH$(CH_3)_2$, J = 6.8 Hz), 3.00-3.09 (m 1H, CH(CH$_3$)$_2$), 6.09 (s, 1H, CH), 7.70 (t, 1H, Ar, J = 8.0 Hz), 7.96 (d, 1H, Ar, J = 8.0 Hz), 8.41 (d, 1H, Ar, J = 8.0 Hz), 8.46 (s, 1H, Ar). <u>^{13}C-NMR</u> (CDCl$_3$-d$_1$) δ 21.92 (CH$_3$), 28.09 (CH), 86.78 (CH), 114.41 (C), 117.84 (C), 129.29 (C), 130.69 (CH), 134.65 (CH), 134.98 (CH), 138.19 (CH), 159.16 (C), 164.82 (C), 172.17 (C). <u>IR</u> = 1600 cm^{-1} (C=O amide), 1777 cm^{-1} (C=O ester), 2235 cm^{-1} (CN). ESI-MS calcd. for C$_{14}$H$_{12}$N$_2$O$_3$, 256.26; found: *m/z* 257.09 [M+H]$^+$. Anal. C$_{14}$H$_{12}$N$_2$O$_3$ (C, H, N).

4-(3-Isopropyl-5-oxo-2,5-dihydroisoxazole-2-carbonyl)benzonitrile (43q)
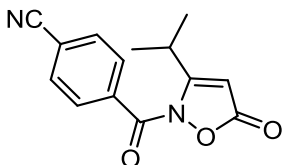
Obtained from compound **42f** (Jacobsen, N. et al. 1984) following the general procedure reported at **pag. 118**. Compound **43q** was purified by column chromatography using cyclohexane/ethyl acetate 3:1 as eluent.

Yield = 38%; mp = 113-115°C (EtOH). <u>^{1}H-NMR</u> (CDCl$_3$-d$_1$) δ 1.30 (d, 6H, CH$(CH_3)_2$, J = 7.2 Hz), 3.00-3.09 (m 1H, CH(CH$_3$)$_2$), 6.10 (s, 1H, CH), 7.84 (d,

2H, Ar, $J = 8.4$ Hz), 8.29 (d, 2H, Ar, $J = 8.0$ Hz). ^{13}C-NMR (CDCl$_3$-d$_1$) δ 21.29 (CH$_3$), 27.48 (CH), 86.16 (CH), 117.46 (C), 118.11 (C), 131.03 (CH), 132.72 (CH), 158.88 (C), 164.28 (C), 171.60 (C). ESI-MS calcd. for C$_{14}$H$_{12}$N$_2$O$_3$, 256.26; found: *m/z* 257.09 [M+H]$^+$. Anal. C$_{14}$H$_{12}$N$_2$O$_3$ (C, H, N).

3-Isopropyl-2-(3-(trifluoromethyl)benzoyl)isoxazol-5(2H)-one (43r)
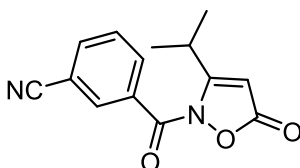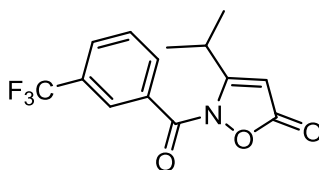

Obtained from compound **42f** (Jacobsen, N. et al. 1984) following the general procedure reported at **pag. 118**. Compound **43r** was purified by column chromatography using cyclohexane/ethyl acetate 5:1 as eluent.

Yield = 21%; oil. ^{1}H-NMR (CDCl$_3$-d$_1$) δ 1.39 (d, 6H, CH*(CH$_3$)$_2$*, $J = 6.8$ Hz), 3.73-3.78 (m 1H, *CH*(CH$_3$)$_2$), 5.51 (s, 1H, CH), 7.66 (t, 1H, Ar, $J = 7.6$ Hz), 7.87 (d, 1H, Ar, $J = 8.0$ Hz), 8.09 (d, 1H, Ar, $J = 8.0$ Hz), 8.14 (s, 1H, Ar). ^{13}C-NMR (CDCl$_3$-d$_1$) δ 21.83 (CH$_3$), 29.12 (CH), 94.07 (CH), 127.33 (C), 129.64 (CH), 130.20 (C), 131.93 (C), 132.87 (CH), 133.45 (CH), 162.29 (C), 166.72 (C), 171.54 (C). ESI-MS calcd. for C$_{14}$H$_{12}$F$_3$NO$_3$, 299.25; found: *m/z* 300.08 [M+H]$^+$. Anal. C$_{14}$H$_{12}$F$_3$NO$_3$ (C, H, N).

3-Isopropyl-2-(4-(trifluoromethyl)benzoyl)isoxazol-5(2H)-one (43s)

Obtained from compound **42f** (Jacobsen, N. et al. 1984) following the general procedure reported at **pag. 118**. Compound **43s** was purified by column chromatography using cyclohexane/ethyl acetate 2:1 as eluent.

Yield = 16%; oil. ^{1}H-NMR (CDCl$_3$-d$_1$) δ 1.36 (d, 6H, CH$(CH_3)_2$, J = 6.8 Hz), 3.69-3.77 (m 1H, CH(CH$_3$)$_2$), 5.47 (s, 1H, CH), 7.75 (d, 2H, Ar, J = 8.0 Hz), 7.97 (d, 2H, Ar, J = 8.0 Hz). ^{13}C-NMR (CDCl$_3$-d$_1$) δ 21.24 (CH$_3$), 28.51 (CH), 93.46 (CH), 125.40 (CH), 127.30 (C), 130.09 (CH), 130.20 (C), 134.72 (C), 161.81 (C), 166.10 (C), 170.86 (C). ESI-MS calcd. for C$_{14}$H$_{12}$F$_3$NO$_3$, 299.25; found: m/z 300.08 [M+H]$^+$. Anal. C$_{14}$H$_{12}$F$_3$NO$_3$ (C, H, N).

HSQC comp. 43s

HMBC comp. 43s
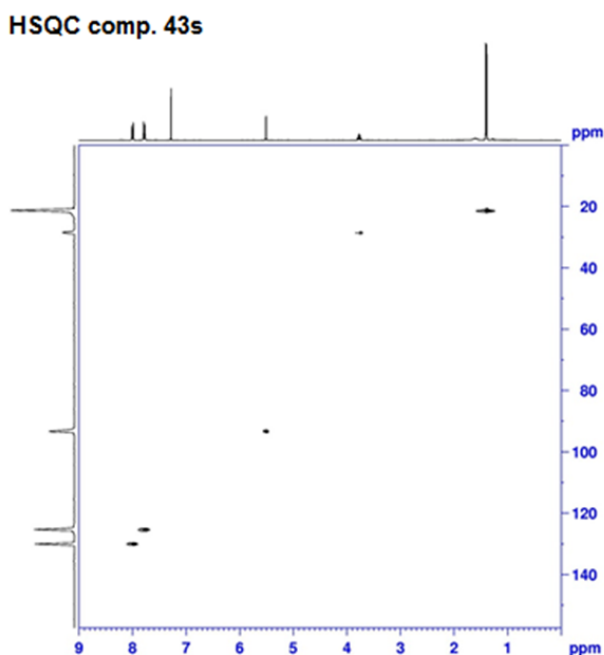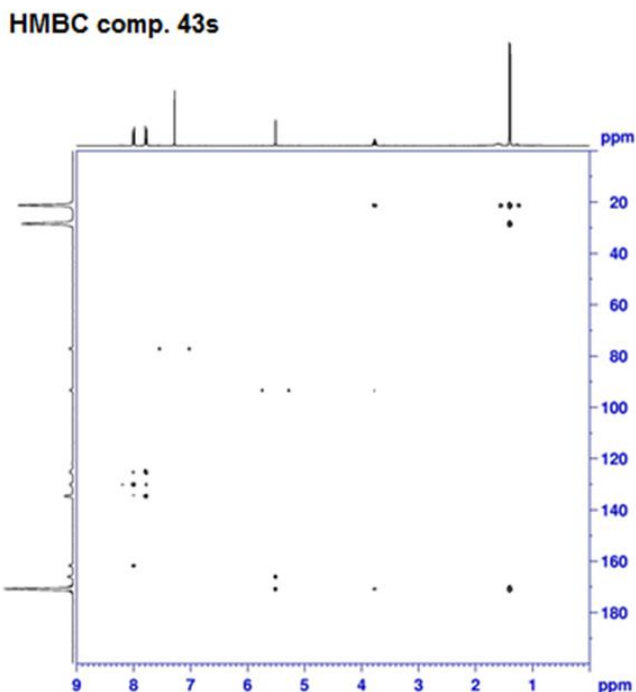
General procedure for compounds (44a,b). To a suspension of the appropriate substrate **43l** or **43n** (0.36 mmol) in 5 mL of anhydrous toluene, 0.72 mmol of Lawesson's reagent was added. The mixture was stirred at reflux for 6h. After cooling, the suspension was concentrated *in vacuum*, diluted with ice-cold water (10 mL) and extracted with ethyl acetate (3 x 15 mL). The organic phase was dried over sodium sulfate and the solvent was evaporated to obtain the final compounds **44a,b**, which were purified by column chromatography using cyclohexane/ethyl acetate in different ratio as eluent (5:1 for **44a** and 3:1 for **44b**).

Cyclopropyl-(3-isopropyl-5-thioxoisoxazol-2(5H)-yl)methanone (44a)
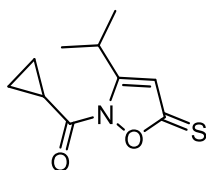
Yield = 26%; oil. ^{1}H-NMR (CDCl$_3$-d$_1$) δ 1.17-1.24 (m, 4H, 2 x CH$_2$ cC$_3$H$_5$), 1.27 (d, 6H, CH*(CH$_3$)$_2$*, *J* = 6.8 Hz), 2.55-2.61 (m, 1H, CH cC$_3$H$_5$), 3.54-3.61 (m 1H, *CH*(CH$_3$)$_2$), 6.12 (s, 1H, CH). ^{13}C-NMR (CDCl$_3$-d$_1$) δ 10.88 (CH$_2$), 14.76 (CH), 21.15 (CH$_3$), 35.40 (CH), 106.37 (CH), 166.84 (C), 169.52 (C), 171.69 (C). ESI-MS calcd. for C$_{10}$H$_{13}$NO$_2$S, 211.28; found: *m/z* 212.07 [M+H]$^+$. Anal. C$_{10}$H$_{13}$NO$_2$S (C, H, N).

(3-Isopropyl-5-thioxoisoxazol-2(5H)-yl)-(m-tolyl)methanone (44b)
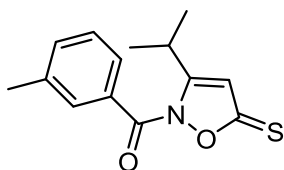
Yield = 40%; oil. ^{1}H-NMR (CDCl$_3$-d$_1$) δ 1.32 (d, 6H, CH*(CH$_3$)$_2$*, *J* = 6.4 Hz), 2.44 (s, 3H, *CH$_3$*-Ph), 2.83-2.92 (m 1H, *CH*(CH$_3$)$_2$), 7.05 (s, 1H, CH), 7.36-7.41 (m, 2H, Ar), 7.81-7.86 (m, 2H, Ar). ^{13}C-NMR (CDCl$_3$-d$_1$) δ 21.09 (CH$_3$), 37.59 (CH$_3$), 108.44 (CH), 122.51 (CH), 124.40 (CH), 127.37 (CH), 129.54 (CH), 131.38 (C), 134.14 (CH), 138.32 (C), 163.56 (C), 169.76 (C), 175.11 (C). ESI-MS calcd. for C$_{14}$H$_{15}$NO$_2$S, 261.34; found: *m/z* 262.09 [M+H]$^+$. Anal. C$_{14}$H$_{15}$NO$_2$S (C, H, N).

2-(Cyclopropanecarbonyl)-3-methyl-4-phenylisoxazol-5(*2H*)-one (45a)
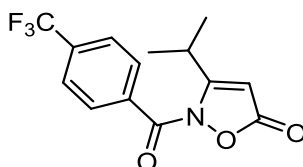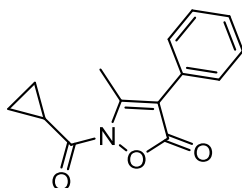

Obtained from compound **42g** (Beccalli, E. M. et al. 1987) following the general procedure reported at **pag. 118**. Compound **45a** was purified by column chromatography using toluene/ethyl acetate 95:5 as eluent.

Yield = 63%; mp = 83-86°C (EtOH). $\underline{{}^1\text{H-NMR}}$ (DMSO-d_6) δ 1.02-1.07 (m, 2H, CH_2 cC_3H_5), 1.09-1.15 (m, 2H, CH_2 cC_3H_5), 2.36-2.41 (m, 1H, CH cC_3H_5), 2.58 (s, 3H, C_3-CH_3), 7.35-7.41 (m, 1H, Ar), 7.43-7.48 (m, 4H, Ar). $\underline{{}^{13}\text{C-NMR}}$ (DMSO-d_6) δ 10.82 (CH_2), 13.25 (CH_3), 15.14 (CH), 106.28 (C), 128.25 (C), 128.58 (CH), 129.10 (CH), 129.35 (CH), 154.69 (C), 166.05 (C), 169.02 (C). $\underline{\text{IR}}$ = 1695 cm^{-1} (CO amide), 1755 cm^{-1} (CO ester). ESI-MS calcd. for $C_{14}H_{13}NO_3$, 243.26; found: *m/z* 244.09 [M+H]$^+$. Anal. $C_{14}H_{13}NO_3$ (C, H, N).

3-Methyl-2-(3-methylbenzoyl)-4-phenylisoxazol-5(*2H*)-one (45b)

Obtained from compound **42g** (Beccalli, E. M. et al. 1987) following the general procedure reported at **pag. 118**. Compound **45b** was purified by column chromatography using hexane/ethyl acetate 5:1 as eluent.

Yield = 52%; mp = 85-88°C (EtOH). $\underline{{}^1\text{H-NMR}}$ (CDCl$_3$-d_1) δ 2.43 (s, 3H, m-CH_3-Ph), 2.79 (s, 3H, C_3-CH_3), 7.35-7.40 (m, 3H, Ar), 7.43-7.51 (m, 4H, Ar), 7.70-7.75 (m, 2H, Ar). $\underline{{}^{13}\text{C-NMR}}$ (CDCl$_3$-d_1) δ 15.09 (CH_3), 21.58 (CH_3), 108.39 (C),

127.08 (CH), 127.62 (C), 128.28 (CH), 128.50 (CH), 128.81 (CH), 129.08 (CH), 130.28 (CH), 131.14 (C), 134.07 (CH), 138.32 (C), 154.62 (C), 163.79 (C), 165.90 (C). <u>IR</u> = 1690 cm^{-1} (CO amide), 1750 cm^{-1} (CO ester). ESI-MS calcd. for $C_{18}H_{15}NO_3$, 293.32; found: *m/z* 294.11 [M+H]$^+$. Anal. $C_{18}H_{15}NO_3$ (C, H, N).

HSQC comp. 45b

HMBC comp. 45b
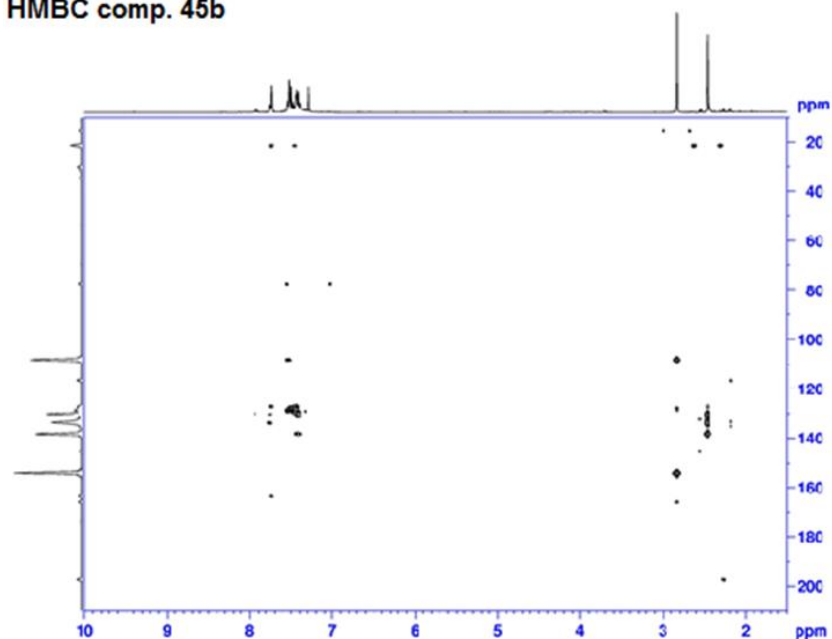
3-(3-Methyl-5-oxo-4-phenyl-2,5-dihydroisoxazole-2-carbonyl)benzonitrile (45c)
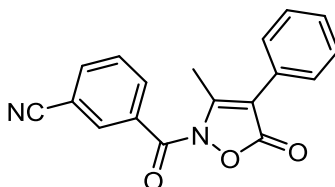
Obtained from compound **42g** (Beccalli, E. M. et al. 1987) following the general procedure reported at **pag. 118**. Compound **45c** was purified by column chromatography using hexane/ethyl acetate 5:2 as eluent.

Yield = 10%; mp = 118-119°C (EtOH). $\underline{^1H\text{-NMR}}$ (CDCl$_3$-d$_1$) δ 2.83 (s, 3H, C$_3$-CH$_3$), 7.45-7.55 (m, 5H, Ar), 7.67 (t, 1H, Ar, J = 7.2 Hz), 7.89 (d, 1H, Ar, J = 6.4 Hz), 8.16 (d, 1H, Ar, J = 7.6 Hz), 8.20 (s, 1H, Ar). $\underline{^{13}C\text{-NMR}}$ (CDCl$_3$-d$_1$) δ 14.94 (CH$_3$), 107.22 (C), 112.76 (C), 118.63 (C), 127.98 (CH), 128.67 (CH), 128.91 (CH), 129.54 (CH), 130.71 (CH), 131.86 (CH), 134.54 (C), 134.95 (C), 135.62 (CH), 139.52 (C), 157.64 (C), 165.87 (C). ESI-MS calcd. for C$_{18}$H$_{12}$N$_2$O$_3$, 304.30; found: *m/z* 305.09 [M+H]$^+$. Anal. C$_{18}$H$_{12}$N$_2$O$_3$ (C, H, N).

3-Methyl-4-phenyl-2-(3-(trifluoromethyl)benzoyl)isoxazol-5(*2H*)-one (45d)
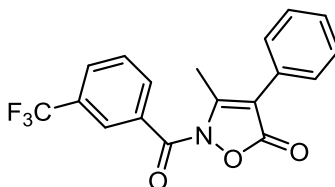
Obtained from compound **42g** (Beccalli, E. M. et al. 1987) following the general procedure reported at **pag. 118**. Compound **45d** was purified by column chromatography using hexane/ethyl acetate 5:2 as eluent.

Yield = 42%; mp = 96-97°C (EtOH). ^{1}H-NMR (CDCl$_3$-d$_1$) δ 2.85 (s, 3H, C$_3$-CH$_3$), 7.40-7.45 (m, 1H, Ar), 7.48-7.54 (m, 4H, Ar), 7.69 (t, 1H, Ar, J = 8.0 Hz), 7.90 (d, 1H, Ar, J = 7.8 Hz), 8.15 (d, 1H, Ar, J = 8.0 Hz), 8.20 (s, 1H, Ar). ^{13}C-NMR (CDCl$_3$-d$_1$) δ 15.61 (CH$_3$), 109.53 (C), 125.39 (C), 127.34 (CH), 127.38 (C), 127.84 (CH), 129.33 (CH), 129.49 (CH), 129.63 (CH), 129.71 (CH), 130.28 (C), 131.69 (C), 132.75 (CH), 133.47 (CH), 154.88 (C), 162.74 (C), 166.07 (C). ^{19}F-NMR (CDCl$_3$-d$_1$) δ -62.82. IR = 1689 cm^{-1} (CO amide), 1738 cm^{-1} (CO ester). ESI-MS calcd. for C$_{18}$H$_{12}$F$_3$NO$_3$, 347.29; found: *m/z* 348.08 [M+H]$^+$. Anal. C$_{18}$H$_{12}$F$_3$NO$_3$ (C, H, N).

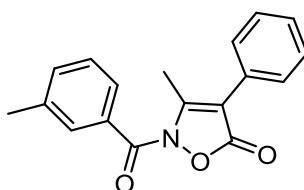## 2-(Cyclopropanecarbonyl)-4-phenylisoxazol-5(2H)-one (45e)

Obtained from compound **42h** (Beccalli, E. M. et al. 1984) following the general procedure reported at **pag. 118**. Compound **45e** was purified by column chromatography using cyclohexane/ethyl acetate 6:1 as eluent.

Yield = 28%; mp = 171-172°C (EtOH). ^{1}H-NMR (CDCl$_3$-d$_1$) δ 1.15-1.20 (m, 2H, CH$_2$ cC$_3$H$_5$), 1.26-1.31 (m, 2H, CH$_2$ cC$_3$H$_5$), 2.35-2.45 (m, 1H, CH cC$_3$H$_5$), 7.36 (d, 2H, Ar, J = 6.0 Hz), 7.42 (t, 1H, Ar, J = 7.2 Hz), 7.78 (d, 2H, Ar, J = 7.2 Hz), 8.72 (s, 1H, CH). ^{13}C-NMR (CDCl$_3$-d$_1$) δ 11.21 (CH$_2$), 11.82 (CH), 108.14 (C), 125.82 (CH), 127.46 (C), 128.64 (CH), 128.95 (CH), 136.06 (CH), 165.97 (C), 166.76 (C). ESI-MS calcd. for C$_{13}$H$_{11}$NO$_3$, 229.24; found: *m/z* 230.08 [M+H]$^+$. Anal. C$_{13}$H$_{11}$NO$_3$ (C, H, N).

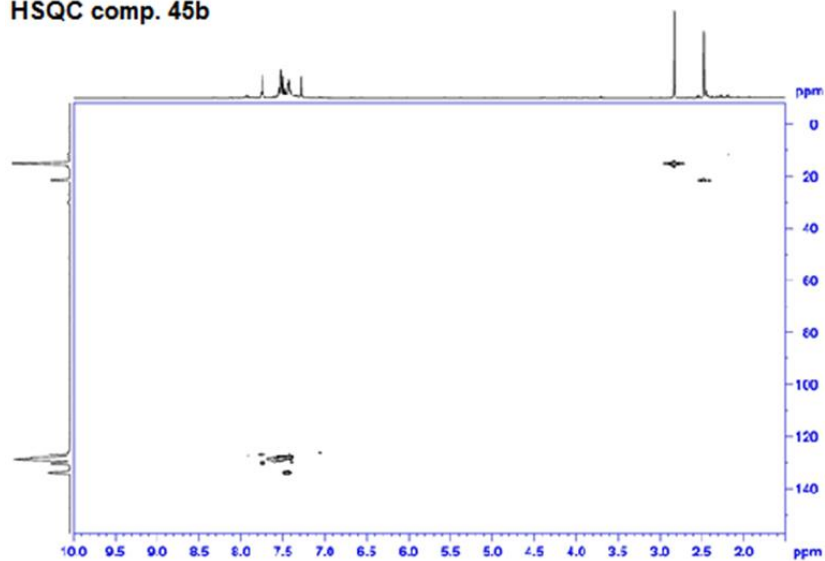**2-(3-Methylbenzoyl)-4-phenylisoxazol-5(2H)-one (45f)**
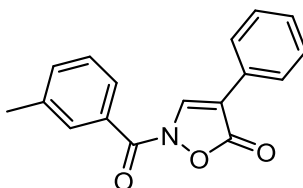
Obtained from compound **42h** (Beccalli, E. M. et al. 1984) following the general procedure reported at **pag. 118**. Compound **45f** was purified by column chromatography using hexane/acetone 4:1 as eluent.

Yield = 27%; mp = 119-120°C (EtOH). $\underline{^1\text{H-NMR}}$ (CDCl$_3$-d$_1$) δ 2.45 (s, 3H, CH$_3$), 7.37-7.46 (m, 5H, Ar), 7.80-7.85 (m, 4H, Ar), 8.89 (s, 1H, CH). $\underline{^{13}\text{C-NMR}}$ (CDCl$_3$-d$_1$) δ 21.39 (CH$_3$), 108.72 (C), 124.23 (C), 125.99 (CH), 126.92 (CH), 127.31 (CH), 128.60 (CH), 128.83 (CH), 129.01 (CH), 129.27 (CH), 129.66 (C), 130.55 (CH), 134.65 (CH), 138.09 (CH), 138.72 (C), 160.74 (C), 166.14 (C). ESI-MS calcd. for C$_{17}$H$_{13}$NO$_3$, 279.30; found: *m/z* 280.09 [M+H]$^+$. Anal. C$_{17}$H$_{13}$NO$_3$ (C, H, N).

2-(Cyclopropanecarbonyl)-4-methyl-3-phenylisoxazol-5(*2H*)-one (45g)
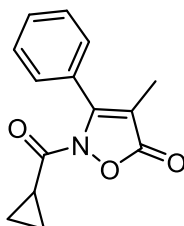
Obtained from compound **42i** (Beccalli, E. M. et al. 1987) following the general procedure reported at **pag. 118**. Compound **45g** was purified by column chromatography using cyclohexane/ethyl acetate 5:1 as eluent.

Yield = 31%; oil. $\underline{^1\text{H-NMR}}$ (CDCl$_3$-d$_1$) δ 1.04-1.09 (m, 2H, CH$_2$ cC$_3$H$_5$), 1.10-1.15 (m, 2H, CH$_2$ cC$_3$H$_5$), 1.86 (s, 3H, C$_4$-CH$_3$), 2.38-2.44 (m, 1H, CH cC$_3$H$_5$), 7.36-7.41 (m, 2H, Ar), 7.43-7.48 (m, 3H, Ar). $\underline{^{13}\text{C-NMR}}$ (CDCl$_3$-d$_1$) δ 7.30

Material and methods

(CH$_3$), 10.55 (CH$_2$), 12.71 (CH), 104.82 (C), 127.78 (C), 128.21 (CH), 128.35 (CH), 128.51 (CH), 130.44 (CH), 154.89 (C), 168.03 (C), 168.99 (C). ESI-MS calcd. for C$_{14}$H$_{13}$NO$_3$, 243.26; found: *m/z* 244.09 [M+H]$^+$. Anal. C$_{14}$H$_{13}$NO$_3$ (C, H, N).

HSQC comp. 45g

HMBC comp. 45g
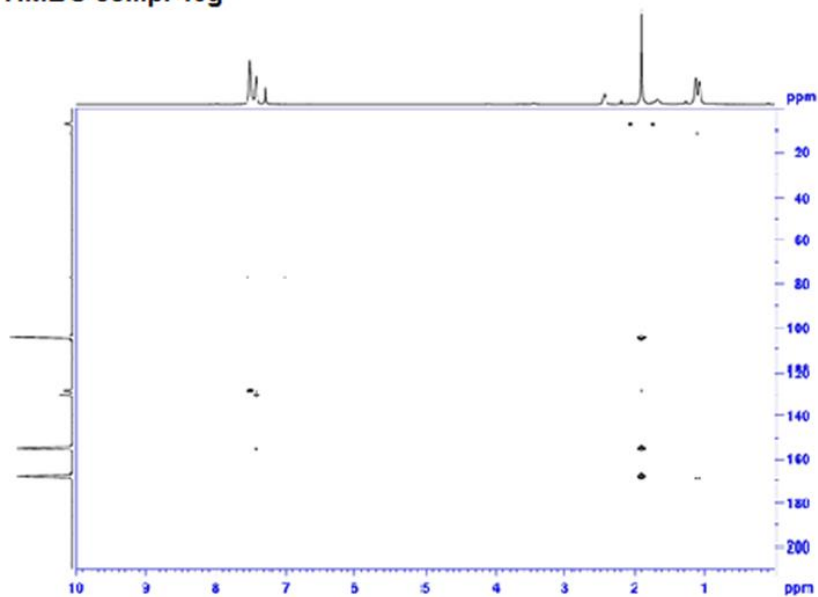
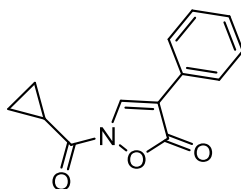**4-Methyl-2-(3-methylbenzoyl)-3-phenylisoxazol-5(*2H*)-one (45h)**
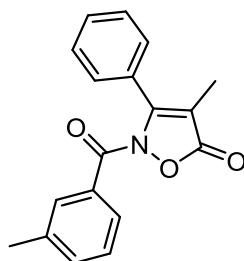
Obtained from compound **42i** (Beccalli, E. M. et al. 1987) following the general procedure reported at **pag. 118**. Compound **45h** was purified by column chromatography using cyclohexane/ethyl acetate 5:1 as eluent.

Yield = 27%; oil. $\underline{^1\text{H-NMR}}$ (CDCl$_3$-d$_1$) δ 1.96 (s, 3H, C$_4$-CH$_3$), 2.40 (s, 3H, m-*CH$_3$*-Ph), 7.32-7.40 (m, 2H, Ar), 7.44-7.50 (m, 5H, Ar), 7.70 (d, 2H, Ar, J = 6.8 Hz). $\underline{^{13}\text{C-NMR}}$ (CDCl$_3$-d$_1$) δ 7.57 (CH$_3$), 21.63 (CH$_3$), 105.74 (C), 127.37 (CH), 128.01 (CH), 128.33 (CH), 128.67 (CH), 128.82 (C), 130.51 (CH), 130.60 (CH), 131.07 (C), 134.31 (CH), 138.46 (C), 156.85 (C), 165.24 (C), 169.02 (C). ESI-MS calcd. for C$_{18}$H$_{15}$NO$_3$, 293.32; found: *m/z* 294.11 [M+H]$^+$. Anal. C$_{18}$H$_{15}$NO$_3$ (C, H, N).

2-(Cyclopropanecarbonyl)-3-phenylisoxazol-5(*2H*)-one (45i)
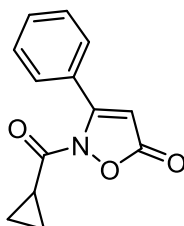
Obtained from compound **42j** (Maquestiau, A. et al. 1974) following the general procedure reported at **pag. 118**. Compound **45i** was purified by column chromatography using cyclohexane/ethyl acetate 5:1 as eluent.

Yield = 57%; oil. $\underline{^1\text{H-NMR}}$ (CDCl$_3$-d$_1$) δ 1.10-1.16 (m, 2H, CH$_2$ cC$_3$H$_5$), 1.23-1.28 (m, 2H, CH$_2$ cC$_3$H$_5$), 1.84-1.90 (m, 1H, CH cC$_3$H$_5$), 6.34 (s, 1H, CH), 7.42-7.47 (m, 3H, Ar), 7.74-7.79 (m, 2H, Ar). $\underline{^{13}\text{C-NMR}}$ (CDCl$_3$-d$_1$) δ 10.82 (CH$_2$), 12.71 (CH), 85.75 (CH), 126.55 (CH), 128.87 (CH), 129.27 (C), 130.26 (CH), 164.15 (C), 165.51 (C), 168.48 (C). ESI-MS calcd. for C$_{13}$H$_{11}$NO$_3$, 229.23; found: *m/z* 230.08 [M+H]$^+$. Anal. C$_{13}$H$_{11}$NO$_3$ (C, H, N).

2-(3-Methylbenzoyl)-3-phenylisoxazol-5(*2H*)-one (45j)

Obtained from compound **42j** (Maquestiau, A. et al. 1974) following the general procedure reported at **pag. 118**. Compound **45j** was purified by column chromatography using cyclohexane/ethyl acetate 5:1 as eluent.

Yield = 72%; oil. $\underline{^1\text{H-NMR}}$ (CDCl$_3$-d$_1$) δ 2.46 (s, 3H, m-*CH$_3$*-Ph), 6.54 (s, 1H, CH), 7.43-7.50 (m, 5H, Ar), 7.82-7.87 (m, 2H, Ar), 8.11-8.16 (m, 2H, Ar). $\underline{^{13}\text{C-NMR}}$ (CDCl$_3$-d$_1$) δ 21.24 (CH$_3$), 85.88 (CH), 126.76 (CH), 126.98 (C), 127.94 (CH), 129.04 (CH), 129.18 (C), 130.38 (CH), 131.23 (CH), 135.69 (CH), 139.06 (C), 160.47 (C), 164.26 (C), 165.70 (C). $\underline{\text{IR}}$ = 1600 cm^{-1} (CO amide), 1757 cm^{-1} (CO ester). ESI-MS calcd. for C$_{17}$H$_{13}$NO$_3$, 279.29; found: *m/z* 280.09 [M + H]$^+$. Anal. C$_{17}$H$_{13}$NO$_3$ (C, H, N).

2-(Cyclopropanecarbonyl)-3,4-diphenylisoxazol-5(*2H*)-one (45k)
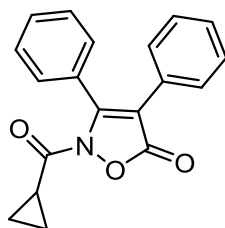
Obtained from compound **42k** (Breslow, T. et al. 1965) following the general procedure reported at **pag. 118**. Compound **45k** was purified by column chromatography using cyclohexane/ethyl acetate 6:1 as eluent.

Yield = 21%; mp = 100-103°C (EtOH). ^{1}H-NMR (CDCl$_3$-d$_1$) δ 1.06-1.11 (m, 2H, CH$_2$ cC$_3$H$_5$), 1.16-1.21 (m, 2H, CH$_2$ cC$_3$H$_5$), 1.80-1.86 (m, 1H, CH cC$_3$H$_5$), 7.17-7.22 (m, 2H, Ar), 7.31-7.40 (m, 5H, Ar), 7.39 (d, 1H, Ar, *J* = 7.2 Hz), 7.46 (d, 2H, Ar, *J* = 7.6 Hz). ^{13}C-NMR (CDCl$_3$-d$_1$) δ 10.39 (CH$_2$), 12.51 (CH), 103.59 (C), 128.03 (CH), 128.31 (CH), 128.37 (CH), 128.72 (CH), 129.16 (CH), 129.84 (CH), 134.92 (C), 142.60 (C), 170.20 (C), 180.73 (C). ESI-MS calcd. for C$_{19}$H$_{15}$NO$_3$, 305.33; found: *m/z* 306.11 [M+H]$^+$. Anal. C$_{19}$H$_{15}$NO$_3$ (C, H, N).

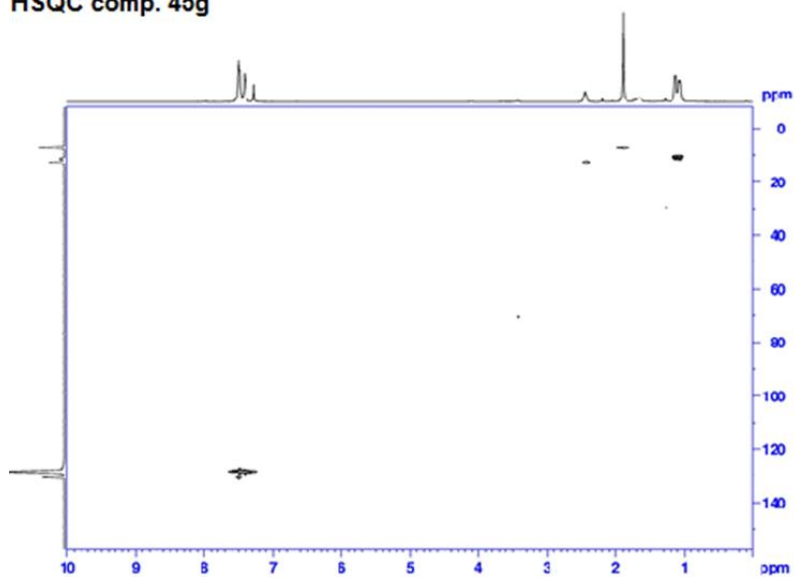**2-(3-Methylbenzoyl)-3,4-diphenylisoxazol-5(*2H*)-one (45l)**
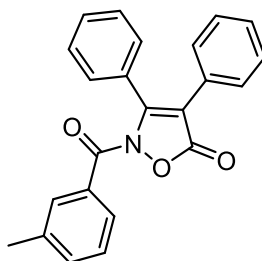
Obtained from compound **42k** (Breslow, T. et al. 1965) following the general procedure reported at **pag. 118**. Compound **45l** was purified by column chromatography using cyclohexane/ethyl acetate 5:1 as eluent.

Yield = 14%; mp = 160-163°C (EtOH). $\underline{^{1}\text{H-NMR}}$ (CDCl$_3$-d$_1$) δ 2.42 (s, 3H, m-*CH$_3$*-Ph), 7.26-7.32 (m, 5H, Ar), 7.37-7.48 (m, 7H, Ar), 7.72-7.77 (m, 2H, Ar). $\underline{^{13}\text{C-NMR}}$ (CDCl$_3$-d$_1$) δ 21.40 (CH$_3$), 101.40 (C), 127.48 (CH), 128.31 (CH), 128.46 (CH), 128.53 (CH), 128.83 (CH), 130.74 (CH), 132.49 (C), 132.63 (C), 134.21 (C), 134.52 (CH), 138.50 (C), 142.65 (C), 157.66 (C), 165.80 (C). ESI-MS calcd. for C$_{23}$H$_{17}$NO$_3$, 355.39; found: *m/z* 356.12 [M+H]$^+$. Anal. C$_{23}$H$_{17}$NO$_3$ (C, H, N).

2-(Cyclopropanecarbonyl)-3-(4-nitrophenyl)isoxazol-5(*2H*)-one (45m)
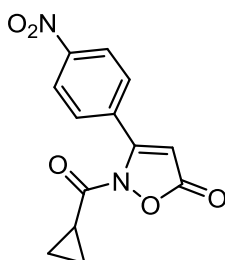
Obtained from compound **42l** (Maquestiau, A. et al. 1974) following the general procedure reported at **pag. 118**. Compound **45m** was purified by column chromatography using cyclohexane/ethyl acetate 4:1 as eluent.

Yield = 23%; mp = 160-163°C (EtOH). $\underline{^{1}\text{H-NMR}}$ (CDCl$_3$-d$_1$) δ 1.16-1.21 (m, 2H, CH$_2$ cC$_3$H$_5$), 1.27-1.32 (m, 2H, CH$_2$ cC$_3$H$_5$), 1.87-1.94 (m, 1H, CH cC$_3$H$_5$), 6.43 (s, 1H, CH), 7.96 (d, 2H, Ar, *J* = 8.8 Hz), 8.31 (d, 2H, Ar, *J* = 8.8 Hz). $\underline{^{13}\text{C-NMR}}$ (CDCl$_3$-d$_1$) δ 10.55 (CH$_2$), 12.71 (CH), 86.27 (CH), 121.42 (C), 124.67 (CH), 127.37 (CH), 135.22 (C), 148.74 (C), 162.53 (C), 168.75 (C). ESI-MS calcd. for C$_{13}$H$_{10}$N$_2$O$_5$, 274.23; found: *m/z* 275.06 [M+H]$^+$. Anal. C$_{13}$H$_{10}$N$_2$O$_5$ (C, H, N).

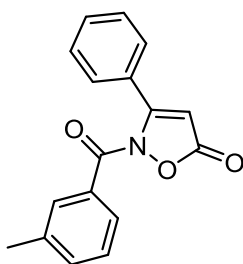**2-(3-Methylbenzoyl)-3-(4-nitrophenyl)isoxazol-5(*2H*)-one (45n)**
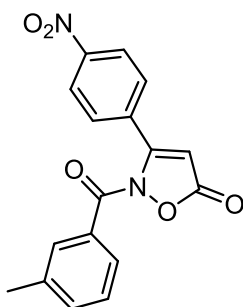
Obtained from compound **42l** (Maquestiau, A. et al. 1974) following the general procedure reported at **pag. 118**. Compound **45n** was purified by column chromatography using cyclohexane/ethyl acetate 5:1 as eluent.

Yield = 40%; mp = 177-180°C dec. (EtOH). ^{1}H-NMR (DMSO-d$_6$) δ 2.42 (s, 3H, m-*CH$_3$*-Ph), 7.13 (s, 1H, CH), 7.54 (t, 1H, Ar, *J* = 7.6 Hz), 7.64 (d, 1H, Ar, *J* = 7.6 Hz), 7.95-8.00 (m, 2H, Ar), 8.20 (d, 2H, Ar, *J* = 8.8 Hz), 8.36 (d, 2H, Ar, *J* = 8.8 Hz). ^{13}C-NMR (DMSO-d$_6$) δ 21.27 (CH$_3$), 124.60 (CH), 125.76 (C), 126.91 (CH), 127.99 (CH), 128.28 (CH), 128.91 (CH), 130.18 (CH), 131.20 (C), 133.90 (CH), 136.50 (C), 138.35 (C), 148.54 (C), 160.45 (C), 167.84 (C). ESI-MS calcd. for C$_{17}$H$_{12}$N$_2$O$_5$, 324.29; found: *m/z* 325.08 [M+H]$^+$. Anal. C$_{17}$H$_{12}$N$_2$O$_5$ (C, H, N).

N-(4-(2-(3-methylbenzoyl)-5-oxo-2,5-dihydroisoxazol-3-yl)phenyl)acetamide (45o)
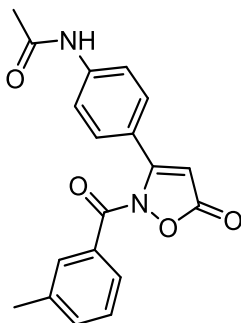
Obtained from compound **42m** (Belzecki, C. et al. 1958) following the general procedure reported at **pag. 118**. Compound **45o** was purified by column chromatography using cyclohexane/ethyl acetate 1:1 as eluent.

Yield = 21%; oil. ^{1}H-NMR (CDCl$_3$-d$_1$) δ 2.20 (s, 3H, CH$_3$CO), 2.45 (s, 3H, m-*CH$_3$*-Ph), 6.50 (s, 1H, CH), 7.42 (t, 1H, Ar, J = 7.8 Hz), 7.50 (d, 1H, Ar, J = 7.6 Hz), 7.56 (exch br s, 1H, NH), 7.62 (d, 2H, Ar, J = 8.0 Hz), 7.76 (d, 2H, Ar, J = 8.4 Hz), 7.98-8.13 (m, 2H, Ar). ^{13}C-NMR (CDCl$_3$-d$_1$) δ 21.30 (CH$_3$), 24.81 (CH$_3$), 85.70 (C), 119.72 (CH), 127.45 (CH), 127.93 (CH), 128.88 (CH), 129.65 (C), 131.17 (CH), 134.11 (C), 135.75 (CH), 138.99 (C), 139.73 (C), 156.05 (C), 157.65 (C), 167.14 (C), 168.90 (C). ESI-MS calcd. for C$_{19}$H$_{16}$N$_2$O$_4$, 336.34; found: *m/z* 337.11 [M+H]$^+$. Anal. C$_{19}$H$_{16}$N$_2$O$_4$ (C, H, N).

General procedure for compounds (46a-c). A mixture of the appropriate intermediates (**42a**, **42f**, **42g**) (0.63 mmol) (Krogsgaar-Laersen, P. et al. 1973) (Jacobsen, N. et al. 1984) (Beccalli, E. M. et al. 1987), K$_2$CO$_3$ (1.26 mmol), and 3-methyl benzyl chloride (0.95 mmol) in 2 mL of anhydrous acetonitrile was stirred at reflux for 2h. After cooling, the mixture was concentrated *under vacuum*, diluted with ice-cold water (10 mL), and extracted with ethyl acetate (3 x 15 mL). The organic phase was dried over sodium sulfate, and the solvent was evaporated *under vacuum* to obtain the final compounds **46a-c**, which

were purified by column chromatography using cyclohexane/ethyl acetate in different ratio as eluent (1:1 for **46a**, 2:1 for **46b** and **46c**).

3,4-Dimethyl-2-(3-methylbenzyl)isoxazol-5(2H)-one (46a)
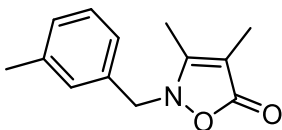
Yield = 26%; mp = 80-83°C (EtOH). ^{1}H-NMR (CDCl$_3$-d$_1$) δ 1.73 (s, 3H, C$_4$-CH$_3$), 2.13 (s, 3H, C$_3$-CH$_3$), 2.32 (s, 3H, *m-CH$_3$*-Ph), 4.59 (s, 2H, CH$_2$), 7.03-7.12 (m, 3H, Ar), 7.20 (t, 1H, Ar, *J* = 7.6 Hz). ^{13}C-NMR (CDCl$_3$-d$_1$) δ 6.75 (CH$_3$), 11.30 (CH$_3$), 29.70 (CH$_3$), 55.18 (CH$_2$), 100.16 (C), 125.42 (CH), 128.63 (CH), 129.10 (CH), 129.19 (CH), 133.40 (C), 138.50 (C), 160.32 (C), 171.85 (C). ESI-MS calcd. for C$_{13}$H$_{15}$NO$_2$, 217.26; found: *m/z* 218.11 [M+H]$^+$. Anal. C$_{13}$H$_{15}$NO$_2$ (C, H, N).

HSQC comp. 46a

Material and methods

HMBC comp. 46a
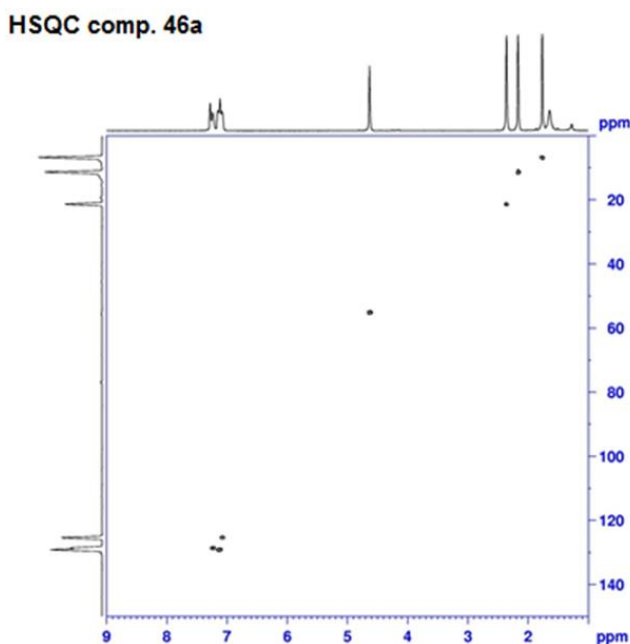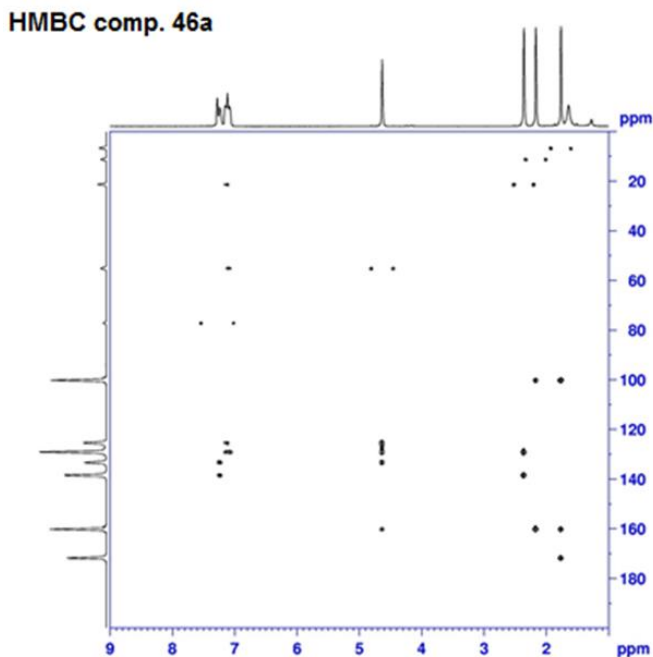
3-Isopropyl-2-(3-methylbenzyl)isoxazol-5(2H)-one (46b)
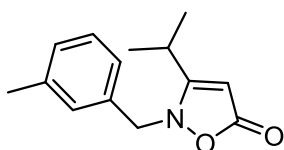
Yield = 14%; oil. $\underline{^1\text{H-NMR}}$ (CDCl$_3$-d$_1$) δ 1.24 (d, 6H, CH*(CH$_3$)$_2$*, J = 6.8 Hz), 2.33 (s, 3H, *m-CH$_3$*-Ph), 2.73-2.79 (m, 1H, *CH*(CH$_3$)$_2$), 4.74 (s, 2H, CH$_2$), 5.00 (s, 1H, CH), 7.02-7.07 (m, 2H, Ar), 7.12 (d, 1H, Ar, J = 7.6 Hz), 7.22 (t, 1H, Ar, J = 7.4 Hz). $\underline{^{13}\text{C-NMR}}$ (CDCl$_3$-d$_1$) δ 21.41 (CH$_3$), 21.60 (CH$_3$), 26.58 (CH), 56.00 (CH$_2$), 81.50 (CH), 124.93 (CH), 129.40 (CH), 133.87 (CH), 138.22 (C), 138.81 (CH), 141.50 (C), 171.51 (C), 174.09 (C). ESI-MS calcd. for C$_{14}$H$_{17}$NO$_2$, 231.29; found: m/z 232.13 [M+H]$^+$. Anal. C$_{14}$H$_{17}$NO$_2$ (C, H, N).

3-Methyl-2-(3-methylbenzyl)-4-phenylisoxazol-5(2H)-one (46c)
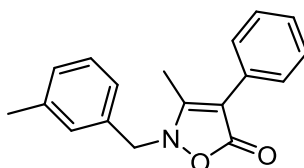
Yield = 57%; oil. ^{1}H-NMR (CDCl$_3$-d$_1$) δ 2.35 (s, 6H, 2 x CH$_3$), 4.79 (s, 2H, CH$_2$), 7.07-7.14 (m, 3H, Ar), 7.22-7.28 (m, 2H, Ar), 7.38 (t, 2H, Ar, J = 7.8 Hz), 7.45 (d, 2H, Ar, J = 7.2 Hz). ^{13}C-NMR (CDCl$_3$-d$_1$) δ 12.44 (CH$_3$), 21.63 (CH$_3$), 54.90 (CH$_2$), 103.58 (C), 125.16 (CH), 127.17 (CH), 128.21 (CH), 128.58 (CH), 128.82 (CH), 128.90 (CH), 129.40 (CH), 129.77 (C), 133.45 (C), 138.75 (C), 158.65 (C), 169.53 (C). ESI-MS calcd. for C$_{18}$H$_{17}$NO$_2$, 279.33; found: *m/z* 280.13 [M+H]$^+$. Anal. C$_{18}$H$_{17}$NO$_2$ (C, H, N).

General procedure for compounds (50a-c). To suspension of the substrate **49** (0.37 mmol) (Wierenga, W. et al. 1984) in *tert*-Butanol (3 mL), 0.41 mmol of K$_2$CO$_3$ and 0.74 mmol of the appropriate acyl chloride were added. The mixture was stirred at reflux for 3h. After evaporation of the solvent, the residue was mixed with ice-cold water (20 mL) and extracted with ethyl acetate (3 x 15 mL). The organic phase was dried over sodium sulfate, and the solvent was evaporated *under vacuum* to afford the final compounds **50a-c**, which were purified by column chromatography using cyclohexane/ethyl acetate (5:1) as eluent.

1-Propionylbenzo[c]isoxazol-3(1H)-one (50a)
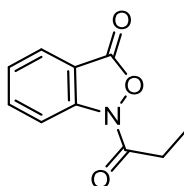
Yield = 10%; oil. $\underline{^1H\text{-NMR}}$ (CDCl$_3$-d$_1$) δ 1.28 (t, 3H, CH$_2$*CH$_3$*, J = 7.4 Hz), 2.83 (q, 2H, *CH$_2$*CH$_3$, J = 7.2 Hz), 7.38 (t, 1H, Ar, J = 7.6 Hz), 7.78 (t, 1H, Ar, J = 7.6 Hz), 7.89 (d, 1H, Ar, J = 8.0 Hz), 8.11 (d, 1H, Ar, J = 8.4 Hz). $\underline{^{13}C\text{-NMR}}$ (CDCl$_3$-d$_1$) δ 9.72 (CH$_3$), 20.70 (CH$_2$), 120.35 (CH), 122.50 (C), 124.09 (CH), 130.31 (CH), 133.90 (CH), 142.44 (C), 166.02 (C), 172.05 (C). ESI-MS calcd. for C$_{10}$H$_9$NO$_3$, 191.18; found: *m/z* 192.06 [M+H]$^+$. Anal. C$_{10}$H$_9$NO$_3$ (C, H, N).

1-Pentanoylbenzo[c]isoxazol-3(1H)-one (50b)
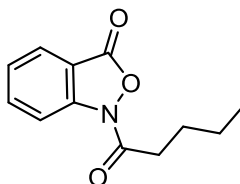
Yield = 12%; oil. $\underline{^1H\text{-NMR}}$ (CDCl$_3$-d$_1$) δ 0.87 (t, 3H, *CH$_3$*CH$_2$CH$_2$CH$_2$CO, J = 6.8 Hz), 1.53-1.58 (m, 2H, CH$_3$*CH$_2$*CH$_2$CH$_2$CO), 1.98-2.03 (m, 2H, CH$_3$CH$_2$*CH$_2$*CH$_2$CO), 3.63 (t, 2H, CH$_3$CH$_2$CH$_2$*CH$_2$*CO, J = 6.8 Hz), 7.22 (d, 1H, Ar, J = 8.4 Hz), 7.31 (t, 1H, Ar, J = 7.4 Hz), 7.68 (t, 1H, Ar, J = 7.6 Hz), 7.86 (d, 1H, Ar, J = 7.6 Hz). $\underline{^{13}C\text{-NMR}}$ (CDCl$_3$-d$_1$) δ 13.10 (CH$_3$), 22.15 (CH$_2$), 27.65 (CH$_2$), 28.21 (CH$_2$), 120.31 (CH), 122.49 (C), 124.00 (CH), 130.33 (CH), 133.90 (CH), 142.41 (C), 165.31 (C), 172.22 (C). ESI-MS calcd. for C$_{12}$H$_{13}$NO$_3$, 219.24; found: *m/z* 220.09 [M+H]$^+$. Anal. C$_{12}$H$_{13}$NO$_3$ (C, H, N).

1-(3-methylbenzoyl)benzo[c]isoxazol-3(1H)-one (50c)
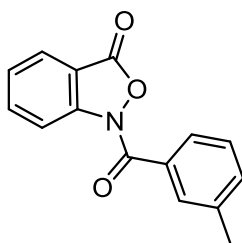
Yield = 53%; mp = 116-119°C (EtOH). $\underline{^1\text{H-NMR}}$ (CDCl$_3$-d$_1$) δ 2.44 (s, 3H, CH$_3$), 7.39-7.45 (m, 3H, Ar), 7.75-7.80 (m, 2H, Ar), 7.83 (t, 1H, Ar, J = 8.4 Hz), 7.92 (d, 1H, Ar, J = 8.0 Hz), 8.22 (d, 1H, Ar, J = 8.4 Hz). $\underline{^{13}\text{C-NMR}}$ (CDCl$_3$-d$_1$) δ 21.40 (CH$_3$), 115.83 (CH), 117.51 (C), 125.60 (CH), 126.03 (CH), 126.87 (CH), 128.34 (CH), 130.12 (CH), 133.40 (C), 133.81 (CH), 136.54 (CH), 137.80 (C), 151.60 (C), 158.51 (C), 172.03 (C). ESI-MS calcd. for C$_{15}$H$_{11}$NO$_3$, 253.25; found: *m/z* 254.08 [M+H]$^+$. Anal. C$_{15}$H$_{11}$NO$_3$ (C, H, N).

6.2 *BIOLOGY*

6.2.1 *HNE inhibition assay*

Compounds were dissolved in 100% DMSO at 5 mM stock concentrations. The final concentration of DMSO in the reactions was 1%, and this level of DMSO had no effect on enzyme activity. The HNE inhibition assay was performed in black flat-bottom 96-well microtiter plates. Briefly, a buffer solution containing 200 mM Tris–HCl, pH 7.5, 0.01% bovine serum albumin, 0.05% Tween-20, and 20 mU/mL of HNE (Calbiochem) was added to wells containing different concentrations of each compound. The reaction was initiated by addition of 25 μM elastase substrate (N-methylsuccinyl-Ala-Ala-Pro-Val-7-amino-4-methylcoumarin, Calbiochem) in a final reaction volume of 100 μL/well. Kinetic measurements were obtained every 30 s for 10 min at 25 °C using a Fluoroskan Ascent FL fluorescence microplate reader (Thermo Electron, MA) with excitation and emission wavelengths at 355 and 460 nm, respectively. For all compounds tested, the concentration of inhibitor that

caused 50% inhibition of the enzymatic reaction (IC_{50}) was calculated by plotting % inhibition versus logarithm of inhibitor concentration (at least six points). The data are presented as the mean values of at least three independent experiments with relative standard deviations of <15%.

6.2.2 *Analysis for compounds stability*

Spontaneous hydrolysis of selected derivatives was evaluated at 25 °C in 0.05 M phosphate buffer, pH 7.3. Kinetics of hydrolysis were monitored by measuring changes in absorbance spectra over time using a SpectraMax Plus microplate spectrophotometer (Molecular Devices, Sunnyvale, CA). Absorbance (A_t) at the characteristic absorption maxima of each compound was measured at the indicated times until no further absorbance decreases occurred (A_∞) (Forist, A. A. and Weber, D. J. 1973). Using these measurements, we created semi-logarithmic plots of log(A_t–A_∞) versus time, and k' values were determined from the slopes of these plots. Half-conversion times were calculated using $t_{1/2} = 0.693/k'$ (Crocetti, L. et al. 2011).

6.3 *MOLECULAR MODELING*

Initial structures of the compounds were generated with HyperChem 8.0 (Shimadzu Corporation, Kyoto, Japan) and optimized by the semi-empirical PM3 method. Docking of the molecules was performed using Molegro Virtual Docker (CLC Bio, København, Denmark) (MVD), version 4.2.0 (CLC Bio, København, Denmark) (Crocetti, L. et al. 2013). The structure of HNE complexed with a peptide chloromethyl ketone inhibitor (Navia, M. A. et al. 1989) was used for the docking study (1HNE entry of the Protein Data Bank). The search area for docking poses was defined as a sphere with a 10 Å radius centered at the nitrogen atom in the five-membered ring of the peptide chloromethyl ketone inhibitor. After removal of this peptide and co-crystallized water molecules from the program workspace, we set side chain flexibility for the 42 residues closest to the centre of the search area (Crocetti, L. et al. 2013). Fifteen docking runs were performed for each compound, with full

flexibility of a ligand around all rotatable bonds and side chain flexibility of the above-mentioned residues of the enzyme. Parameters used within Docking Wizard of the Molegro program were as described in our previous work (Crocetti, L. et al. 2013). The docking poses corresponding to the lowest-energy binding mode of each inhibitor were evaluated for the ability to form a Michaelis complex between the hydroxyl group of Ser195 and the carbonyl group in the amido moiety of an inhibitor. For this purpose, values of d_1 [distance O(Ser195)·C between the Ser195 hydroxyl oxygen atom and the inhibitor carbonyl carbon atom closest to O(Ser195)] and α [angle O(Ser195)···C=O, where C=O is the carbonyl group of an inhibitor closest to O(Ser195)] were determined for each docked compound (Peters, M. B. and Merz, K. M. 2006). In addition, we estimated the possibility of proton transfer from Ser195 to Asp102 through His57 (the key catalytic triad of serine proteases) by calculating distances d_2 between the NH hydrogen in His57 and carboxyl oxygen atoms in Asp102, as described in our previous work (Crocetti, L. et al. 2013). The distance between the hydroxyl proton in Ser195 and the pyridine-type nitrogen in His57 is also important for proton transfer. However, because of easy rotation of the hydroxyl about the C–O bond in Ser195, we measured distance d_3 between the oxygen in Ser195 and the basic nitrogen atom in His57. The effective length L of the channel for proton transfer was calculated as $L = d_3 + \min (d_2)$.

6.4 *CRYSTALLOGRAPHIC ANALYSIS*

The data were collected at 100(2)K on Xcalibur3 CCD 4-circle diffractometer using a graphite monochromator, Mo Ka radiation. A reference frame was monitored every 50 frames to control the stability of the crystal, and the system revealed no intensity decay. The data set was corrected for Lorentz, polarization effects, and absorption corrections were performed by the ABSPACK (CrysAlis RED Oxford Diffraction) multi-scan procedure of the CrysAlis data reduction package. The structure was solved using the direct method with SUPERFLIP (Palatinus, L. and Chapuis, G. 2007) software, and

the refinement was carried out using the SHELXL-2013 (Sheldrick, G. M. 1990) software package. All non-hydrogen atoms were located from the initial solution or from subsequent electron density difference maps during the initial course of the refinement. After locating the non-hydrogen atoms, the models were refined against F^2, first using isotropic and finally anisotropic thermal displacement parameters. Hydrogen atoms have been introduced as "riding hydrogens". Programs used in the crystallographic calculations included WinGX4 (Farrugia, L. J. 2012) and Mercury (Mercury CSD 3.6, Copyright CCDC 2001-2015) for graphics.
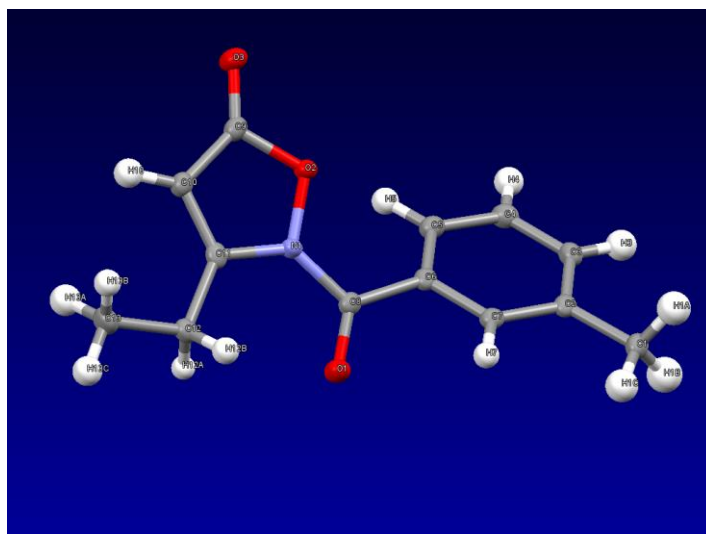
Fig. 28: X-ray structure for compound **43j**

Table 9: Crystal data and structure refinement for **43j**.

<u>Empirical formula</u>	$C_{13}H_{13}NO_3$
<u>Formula weight</u>	231.24
<u>Temperature</u>	298(2) K
<u>Wavelength</u>	1.54184Å
<u>Crystal system</u>	Monoclinic
<u>Space group</u>	P 21/c
<u>Unit cell dimensions</u>	a = 9.7480(2) Å alpha = 90°.
	b = 14.0846(3) Å beta = 91.372(2)°.
	c = 8.10170(10) Å gamma = 90°.
<u>Volume</u>	1112.02(4) Å^3
<u>Z</u>	4
<u>Calculated density</u>	1.381 Mg/m^3
<u>Absorption coefficient</u>	0.814 mm^{-1}
<u>F(000)</u>	488
<u>Crystal size</u>	0.35 x0.25x0.22mm
<u>Theta range for data collection</u>	5.520 to 72.227 deg.
<u>Limiting indices</u>	-11<=h<=11, -16<=k<=16, -9<=l<=7
<u>Reflections collected / unique</u>	6174 / 2114 [R(int) = 0.0276]
<u>Completeness to theta</u>	70.000 98.9 %
<u>Refinement method</u>	Full-matrix least-squares on F^2
<u>Data / restraints / parameters</u>	2114 / 0 / 206
<u>Goodness-of-fit on F^2</u>	1.100
<u>Final R indices [I>2sigma(I)]</u>	R1 = 0.0386, wR2 = 0.0937
<u>R indices (all data)</u>	R1 = 0.0498, wR2 = 0.1017
<u>Largest diff. peak and hole</u>	0.203 and -0.349 e.A$^-$

Material and methods
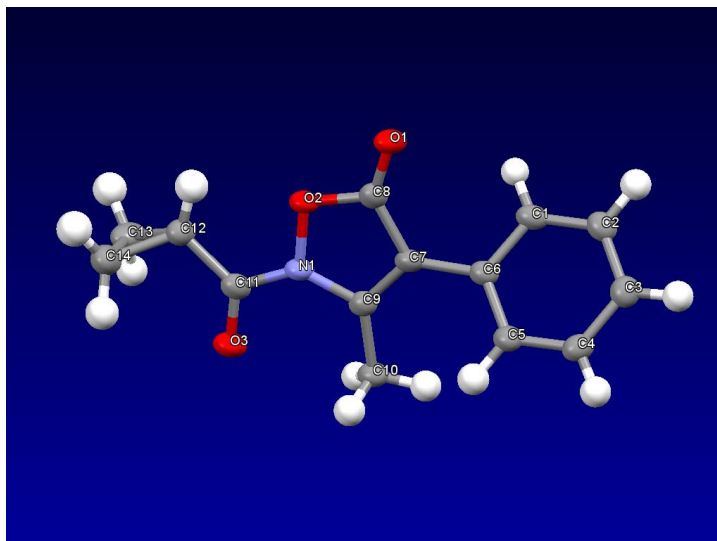
Fig. 29: X-ray structure for compound **45a**

Table 10: Crystal data and structure refinement for **45a**.

Empirical formula	C14 H13 N O3
Formula weight	243.25
Temperature	298(2) K
Wavelength	1.54184 Å
Crystal system	Orthorhombic
Space group	P 21 21 21
Unit cell dimensions	a = 7.4305(2) Å alpha = 90 deg.
	b = 10.6042(3) Å beta = 90 deg.
	c = 15.1154(4) Å gamma = 90 deg.
Volume	191.01(6) Å^3
Z	4
Calculated density	1.357 Mg/m^3
Absorption coefficient	0.790 mm^{-1}
F(000)	512
Crystal size	0.35 x 0.25 x 0.20 mm
Theta range for data collection	5.855 to 71.849 deg.
Limiting indices	-4<=h<=8, -8<=k<=12, -18<=l<=18

Reflections collected / unique	4302 / 2073 [R(int) = 0.0361]
Completeness to theta	70.000 97.7 %
Refinement method	Full-matrix least-squares on F^2
Data / restraints / parameters	2073 / 0 / 215
Goodness-of-fit on F^2	1.184
Final R indices [I>2sigma(I)]	R1 = 0.0392, wR2 = 0.0897
R indices (all data)	R1 = 0.0518, wR2 = 0.0976
Absolute structure parameter	0.1(2)
Largest diff. peak and hole	0.153 and -0.184 e. $Å^{-3}$

7. REFERENCES

- Adembri, G.; Tedeschi, P. Synthesis and properties of 5-haloisoxazoles. *Bull Sci Fac Chim Ind (Bologna)* **1965**, *2*, 203-222.

- Agraz-Cibriana, J. M.; Giraldob, D. M.; Maryc, F-M.; Urcuqui-Inchimab, S. Understanding the molecular mechanisms of NETs and their role in antiviral innate immunity. *Virus Res.* **2017**, *228*, 124-133.

- Ahrendt, K. A.; Buckmelter, A. J.; Grina, J.; Hanses, J. D.; Laird, E. R.; Moreno, D.; Newhouse, B.; Ren, L.; Wenglowsky, S. M.; Feng, B. N-pyrrolo[2,3-b]pyridinyl benzamide derivatives as Raif inhibitors and their preparation pharmaceutical compositions and use in the treatment of diseas. PCT Int. Appl., WO2009111278 A2 20090911, **2009**.

- Aikawa, N.; Ishizaka, A.; Hirasawa, H. Re-evaluation of the efficacy and safety of the neutrophil elastase inhibitor. Sivelestat, for the treatment of acute lung injury associated with systemic inflammatory response syndrome; a phase IV study. *Pulm. Pharmacol. Ther.* **2011**, *24 (5)*, 549-554.

- Alpha Therapeutic Corp: Alpha Therapeutic Corporation Receives FDA Approval for Aralast (TM) Alpha-1 Proteinase Inhibitor. *Press Release* **2003**, January 09.

- American Thoracic Society/ European Respiratory Society Statement. Standards for the diagnosis and management of individual with alpha-1-antitrypsi deficiency. *Am. J. Respir. Crit. Care Med.* **2003**, *168*, 819-900.

- Antonicelli, F.; Bellon, G.; Debelle, L.; Hornebeck, W. Elastin-elastases and inflamm-aging. *Curr. Top. Dev. Biol.* **2007**, *79*, 99-155.

- Armani, E.; Capaldi, C.; Sutton, J. M. Novel compounds. PCT int. Appl. US 201J/0353561A1, **2015**.

- Bahekar, R. H.; Jain, M. R.; Jadav, P. A.; Prajapati, V. M.; Patel, D. N.; Gupta, A. A.; Sherma, A.; Tom, R.; Bandyopadhya, D.; Modi, H.; Patel, P. R. Synthesis and antidiabetic activity of 2,5-disubstituted-3-imidazol-

2-yl-pyrrolo[2,3-b]pyridines and thieno[2,3-b]pyridines. *Bioorg. Med. Chem.* **2007**, *15(21)*, 6782-6795.

- Baltus, C. B.; Jorda, R.; Marat, C.; Berka, C.; Bazgier, V.; Krystal, V.; Priè, G.; Viad,-Massuard, M. C. Synthesis, biological evaluation and molecular modeling of a novel series of 7-azaindole based tri-heterocyclic compounds as potent CDK2/ cyclin E inhibitors. *Eur. J. Med. Chem.* **2016**, *108*, 701-719.

- Barnes, P.J.; Stockley, R. A. COPD: current therapeutic interventions and future approaches. *Eur. Respir. J.* **2005**, *25*, 1084-1106.

- Barret, A. J.; Salvesen, G. An introduction to the proteinases. In: Protease inhibitors. *Elsevier* **1986**, 1-22.

- Bayer Healthcare. Elastase Inhibitors. Ag. WO2004020410&WO2004020412. *Expert Opin. Ther. Pat.* **2004**, *14(10)*, 1511-1516.

- Beccalli, E. M.; Marchesini, A. The Vilsmeier-Haack reaction of isoxazoline-5-ones. Synthesis and reactivity of 2-(dialkylamino)-1,3-oxazin-6-ones. *J. Org. Chem.* **1987**, *52*, 3426-3434.

- Beccalli, E. M.; La Rosa, C.; Marchesini, A. Oxidation of 4-aryl-substituted isoxazoline-5-ones, a new synthesis of 2,5-diaryl-1,3-oxazin-6-ones. *J. Org. Chem.* **1984**, 49, 4290-4293.

- Belzecki, C.; Urbanski, T. New antituberculosis agents. XXXVII. Thiosemicarbazones of oxo acids. 2. Thiosemicarbazones of aroyl fatty acids. *Roczniki Chemii* **1958**, *32*, 769-778.

- Benarafa, C.; Cooley, J.; Zeng, W.; Bird, P. I.; O'Donnell, E. R. Characterization of four murine homologs of the human ov-serpin monocyte neutrophil elastase inhibitor MNEI (*SERPINB1*). *J. Biol. Chem.* **2002**, *277*, 42028-42033.

- Bieth, J. G. Elastases: catalityc and biological properties in regulation of matrix accumulation. *Academic Press* **1986**, 217-230.

References

- Boulton, A. J.; Katritzky, A. R. The tautomerism of heteroaromatic compounds with five-membered rings. I 5-hydroxyisoxazoles-isoxazol-5-ones. *Tetrahedron* **1961**, *12*, 41-50.

- Breslow, T.; Eicher, A.; Krebs, R. A.; Peterson, J.; Posner, J. Diphenylcyclopropenone. *J. Am. Chem. Soc.* **1965**, *87*, 1320-1325.

- Brinkmann, V.; Reichard, U.; Goosmann, C.; Fauler, B.; Uhlemann, Y.; Weiss, D. S. Neutrophil extracellular traps kill bacteria. *Science* **2004**, *303*, 1532-1535.

- Brown, R. S.; Hays, G. L.; Flaitz, C. M.; O'Neill, P. A.; Abramovitch, K.; White, R. R. A possible late onset variation of Papillon-Lefèvre syndrome: report of 3 cases. *J. Periodontol.* **1993**, *64*, 379-86.

- Buchanan, P. J.; Ernst, R. K.; Elborn, J. S.; Schock, B. Role of CFTR, Pseudomonas aeruginosa and Toll-like receptors in cystic fibrosis lung inflammation. *Biochem. Soc. Trans.* **2009**, *37*, 863-867.

- Capsoni, F.; Sarzi-Puttini, P.; Atzeni, F.; Minonzio, F.; Bonara, P.; Doria, A.; Carrabba, M. Effect of adalimumab on neutrophil function in patients with rheumatoid arthritis. *Arthritis Res. Ther.* **2005**, *7,* R250-R255.

- Carbone, A.; Parrino, B.; Di Vita, G.; Attanzio, A.; Spano, V.; Montalbano, A.; Baraja, P.; Tesoriere, L.; Livrea, M. A.; Diana, P.; Cirrincione, G. Synthesis and antiproliferative activity of thiazolyl-bis-pyrolo[2,3-c]piridine, nortopsentin analogues. *Marine Drugs* **2015**, *13(1),* 460-492.

- Cepinskas, G.; Sanding, M.; Kvietys, P. R. PAF-induced elastase-dependent neutrophil transendothelial migration is associated with the mobilization of the elastase to the neutrophil surface and localization to the migrating front. *J. Cell. Sci.* **1999**, *112*, 1937-1945.

- Chavan, N. L.; Nayak, S. K.; Kusurkar, R. S. A rapid method toward the synthesis of new substituted tetrahydro-α-carbolines and α-carboline. *Tetrahedron* **2010**, *66(10)*, 1827-1831.

- Coussens, L. M.; Werb, Z. Inflammation and cancer. *Nature* **2002**, *420*, 860–867.

- Crocetti, L.; Giovannoni, M. P.; Schepetkin, I. A.; Quinn, M. T.; Khlebnikov, A. I.; Cilibrizzi, A.; Dal Piaz, V.; Graziano, A.; Vergelli, C. Design, synthesis and evaluation of N-benzoylindazole derivatives and analogues as inhibitors of human neutrophil elastase. *Bioorg. Med. Chem*. **2011**, *19*, 4460-4472.

- Crocetti, L.; Schepetkin, I. A.; Ciciani, G.; Giovannoni, M. P.; Guerrini, G.; Iacovone, A.; Khlebnikow, A. I.; Kirpotina, L. N.; Quinn, M. T. Synthesis and farmacological evaluation of indole derivatives as deaza analogues of potent human neutrophil elastase inhibitors. *Drug Dev. Res.* **2016**, *77 (6)*, 285-289.

- Crocetti, L.; Schepetkin, I. A.; Cilibrizzi, A.; Graziano, A.; Vergelli, C.; Giomi, D.; Khlebnikov, A. I.; Quinn, M. T.; Giovannoni, M. P. Optimization of N-benzoylindazole derivatives as inhibitors of human neutrophil elastase. *J. Med. Chem*. **2013**, *56*, 6259-6272.

- CrysAlis RED Oxford Diffraction (version 171.34.41). Abingdon, Oxfordshire, UK: Oxford Diffraction Ltd.

- Demaria, S.; Pikarsky, E.; Karin, M.; Coussens, L. M.; Chen, Y. C.; El-Omar, E. M.; Trinchieri, G.; Dubinett, S. M.; Mao, J. T.; Szabo, E.; Krieg, A.; Weiner, G. J.; Fox, B. A.; Coukos, G.; Wang, E.; Abraham, R. T.; Carbone, M.; Lotze, M. T. Cancer and inflammation: promise for biologic therapy. *J. Immunother.* **2010**, *33,* 335-351.

- Devaney, J. M.; Greene, C. M.; Taggart, C. C.; Carroll, T. P.; O'Neill, S. J.; Mc Elvaney, N. G. Neutrophil elastase up-regulates interleukin-8 via toll-like receptor 4. *FEBS Lett.* **2003**, *544*, 129-132.

- Dhanrajani, P.J. Papillon-Lefevre syndrome: clinical presentation and a brief review. *Oral. Surg. Oral. Med. Oral. Pathol. Oral. Radiol. Endod.* **2009**, *108,* 1-7.

References

- Di Cesare Mannelli, L.; Micheli, L.; Cinci, L.; Maresca, M.; Vergelli, C.; Pacini, A.; Quinn, M. T.; Giovannoni, M. P.; Ghelardini, C. Effects of the neutrophil elastase inhibitor EL17 in rat adjuvant-induced arthritis. *Rheumatology (Oxford)* **2016**, *55(7)*, 1285-1294.

- Dollery, C. M.; Owen, C. A.; Sukhova, G. K.; Krettek, A.; Shapiro, S. D.; Libby, P. Neutrophil elastase in human atherosclerotic plaques: production by macrophages. *Circulation* **2003**, *107,* 2829-2836.

- Edwards, P. D.; Andisik, D. W.; Strimpler, A. M.; Gomes, B.; Tuthill, P. A. Non-peptidic inhibitors of human neutrophil elastase. 7. Design, synthesis, and in vitro activity of a series of pyridopyrimidine trifluoromethyl ketones. *J. Med. Chem*. **1996**, *39*, 1112-1124.

- Ekeowa, U. I.; Gooptu, B.; Belorgey, D.; Hägglöf, P.; Karlsson-Li, S.; Miranda, E.; Pérez, J.; MacLeod, I.; Kroger, H.; Marciniak, S. J.; Crowther, D. C.; Lomas, D. A. Alpha1-Antitrypsin deficiency, chronic obstructive pulmonary disease and the serpinopathies. *Clin. Sci.* **2009**, *116,* 837-850.

- Farrugia, L. J. WinGX: an update. *J. Appl. Crystallogr.* **2012**, *45*, 849–54.

- Faurschou, M.; Borregaard N. Neutrophil granules and secretory vesicles in inflammation. *Microbes Infec.* **2003**, *5*, 1317-1327.

- Forist, A. A.; Weber, D. J. Kinetics of hydrolysis of hypoglycemic 1-acyl 3,5-dimethylpyrazoles. *J. Pharm. Sci.* **1973**, *62*, 318-19.

- Fregonese, L.; Stolk, J. Hereditary alpha-1-antitrypsin deficiency and its clinical consequences. *Orphanet J. Rare Dis.* **2008**, *3*, 16-24.

- Frolund, B.; Jensen, L. S.; Guandalini, L.; Canillo, C.; Vestergaard, H. T.; Kristiansen, U.; Nielsen, B.; Stensbol, T. B.; Madsen, C.; Krogsgaard-Larsen, P.; Liljefors, T. Potent 4-Aryl- or 4-arylalkyl-substituted 3-isoxazolol GABA$_A$ antagonists: synthesis, pharmacology, and molecular modeling. *J. Med. Chem.* **2005**, *48*, 427-439.

- Fujii, M.; Miyagi, Y.; Bessho, R.; Nitta, T.; Ochi, M.; Shimizu, K. Effect of a neutrophil elastase inhibitor on acute lung injury after

cardiopulmonary bypass. *Interact. Cardiov. Thor. Surg.* **2010**, *10*, 859-862.

- Fujinaga, M.; Chernaiaa, M. M.; Halenbeck, R.; Koths, K.; James M. N. G. The Crystal Structure of PR3, a neutrophil serine proteinase antigen of Wegener's granulomatosis antibodies. *J. Mol. Biol.* **1996**, *261*, 267-278.

- Garcia-Touchard, A.; Henry, T. D.; Sangiorgi, G.; Spagnoli, L. G.; Mauriello, A.; Conover, C.; Schwartz, R. S. Extracellular proteases in atherosclerosis and restenosis. *Arterioscler. Thromb. Vasc. Biol.* **2005**, *25*, 1119-1127.

- Geraghty, P.; Rogan, M. P.; Greene, C. M.; Boxio, R. M. M.; Poiriert, T.; O'Mahony, M.; Belaaouaj, A.; O'Neill, S. J.; Taggart, C. C.; Mc Elvaney, N. G. Neutrophil elastase up-regulates cathepsin B and matrix metalloprotease-2 expression. *J. Immunol.* **2007**, *178,* 5871-5878.

- Giovannoni, M. P.; Schepetkin, I. A.; Crocetti, L.; Ciciani, G.; Cilibrizzi, A.; Guerrini, G.; Khelebnikov, A. I.; Quinn, M. I.; Vergelli, C. Cinnoline derivatives as human neutrophil elastase inhibitors. *J. Enz. Inhib. Med. Chem.* **2016**, *31(4)*, 628-639.

- Gipson, T. S.; Bless, N. M.; Shanley, T. P.; Crouch, L. D.; Bleavins, M. R.; Younkin, E. M.; Sarma, V.; Gibbs, D. F.; Tefera, W.; McConnell, P. C.; Mueller, W. T.; Johnson, K. J.; Ward, P. A regulatory effects of endogenous protease inhibitors in acute lung inflammatory injury. *J. Immunol.* **1999**, *162,* 3653-3662.

- Griese, M.; Kappler, M.; Gaggar, A.; Hartl, D. Inhibition of airway proteases in cystic fibrosis lung disease. *Eur. Respir. J.* **2008**, *32*, 783-95.

- Groutas, W. C.; Dou, D.; Alliston, K. R. Neutrophil elastase inhibitors. *Expert Opin Ther Pat.* **2011**, *21*, 339-354.

- Gunawardena, K.; Gullstrand, H.; Perret, J. Safety, tolerability and pharmacokinetics of AZD9668, an oral neutrophil elastase inhibitor, in healthy subjects and patients with COPD. *Eur. Resp. J.* **2010**, 203s.

References

- Guyot, N.; Butler, M. W.; Mc Nally, P.; Weldon, S.; Greene, C. M.; Levine, R. L.; O'Neill, S. J.; Taggart, C. C.; Mc Elvaney, N. G. Elafin, an elastase-specific inhibitor, is cleaved by its cognate enzyme neutrophil elastase in sputum from individuals with cystic fibrosis. *J. Biol. Chem.* **2008**, *283*, 32377-32385.

- Hajjar, E.; Broemstrup, T.; Kantari, C.; Witko-Sarsat, V.; Reuter, N. Structures of human proteinase 3 and neutrophil elastase – so similar yet so different. *Febs J.* **2010**, 277, 2238-2254.

- Hansen, G.; Gielen-Hartwig, H.; Reinemer, P.; Schomburg, D.; Harrenga, A.; Nie find, K. Unexpected active-site flexibility in the structure of human neutrophil elastase in complex with a new dihydropyrimidone inhibitors. *J. Mol. Bio.* **2011**, *409*, 681-691.

- Hartwig, H.; Silvestre Roig, C.; Daemen, M.; Lutgens, E.; Soehnlein, O. Neutrophils in atherosclerosis. A brief overview. *Hämostaseologie* **2015**, *35,* 121-127.

- Havemann, K.; Janoff, A. Neutral proteases of human polymorphonuclear leukocytes. *Urban & Schwarzenberg* **1978**.

- Henriksen, P. A.; Sallenave, J. M. Human neutrophil elastase: mediator and therapeutic target in atherosclerosis. *Int. J. Biochem. Cell. Biol.* **2008**, *40,* 1095-100.

- Hermant, B.; Bibert, S.; Concord, E.; Dublet, B.; Wiedenhaup, M.; Vernet, T.; Gulino-Debrac, D. Identification of proteases involved in the proteolysis of vascular endothelium cadherin during neutrophil transmigration. *J. Biol. Chem.* **2003**, *278*, 14002-14012.

- Heutinck, K. M.; ten Berge I. J. M.; Hack, C. E.; Hamann, J.; Rowshani, A. T. Serine proteases of the human immune system in health and disease. *Mol. Immunol.* **2010**, *47*, 1943-1955.

- Hoenderdos, K.; Condliffe, A. The neutrophil in chronic obstructive pulmonary disease. Too little, too late or too much, too soon? *Am. J. Respir. Cell. Mol. Biol.* **2013**, *48,* 531-539.

- Hornebeck, W.; Robinet, A.; Duca, L.; Antonicelli, F.; Wallach, J.; Bellon, G. The elastin connection and melanoma progression. *Anticancer Res.* **2005**, *25,* 2617-2625.

- Houghton, A. M.; Quintero, P. A.; Perkins, D. L.; Kobayashi, D. K.; Kelley, D. G.; Marconcini, L. A.; Mecham, R. P.; Senior, R. M.; Shapiro, S. D. Elastin fragments drive disease progression in a murine model of emphysema. *J. Clin. Invest.* **2006**, *116*, 753-759.

- Ibrahim, P. N.; Artis, D. R.; Bremer, R.; Habets, G.; Momo, S.; Nespi, M.; Zhang, J.; Zhang, J.; Zhu, Y. L.; Zuckerman, R. Pyrrolo[2,3-b]pyridine derivatives as protein kinase inhibitors and their preparation, pharmaceutical compositions and use in the treatment of diseases. PCT Int. Appl., WO2007002433 A1 20070104; **2007**.

- Inoue, N.; Oka, N.; Kitamura, T.; Shibata, K.; Itatani, K.; Tomoyasu, T.; Miyaji, K. Neutrophil elastase inhibitor Sivelestat attenuates perioperative inflammatory response in pediatric heart surgery with cardiopulmonary bypass. A prospective randomized study. *Int. Heart J.* **2013**, *37*, 1027-1033.

- Jacobsen, N.; Kolind-Andersen, H. 3-Hydroxyisoxazoles. PCT Int. Appl., WO8401774 A1 19840510, **1984**.

- Janciauskiene, S. M.; Bals, R.; Koczulla, R.; Vogelmeier, C.; Köhnlein, T.; Welte, T. The discovery of α1-antitrypsin and its role in health and disease. *Resp. Med.* **2011**, *105*, 1129-1139.

- Jia, H.; Dai, G.; Weng, J.; Zhang, Z.; Weng, Q.; Zhan, F.; Jiao, L.; Cui, J.; Ren, Y.; Fan, S. Discovery of (S)-1-(1-(Imidazo [1,2-a]pyridine-6-yl-)ethyl)-6-(1-methyl-1H-pyrazol-4-yl)-1H-[1,2,3]triazolo[4,5-b]pyrazine (Volitinib) as a highly potent and selective Mesenchymal-Epithelial Transition Factor (c-Met) inhibitor in clinical development for treatment of cancer. *J. Med. Chem.* **2014**, *57(18)*, 7577-7589.

- Jiang, J. H.; Liu, X. F.; Zhen, C. H.; Zhou, Y. J.; Zho, J.; Lv, J. G.; Sheng, C. Q. Acrosin structure –based design, synthesis and biological

References

activities of 7-azaindol derivatives as new acrosin inhibitors. *Chinese Chem. Lett.* **2011**, *22(3)*, 272-275.

- Kalaitzakis, D.; Kambourakis, S.; Rozzel, D. J.; Smonou, I. Stereoselective chemoenzymatic synthesis of sitophilate: a natural pheromone. *Thetrahedron Asymmetry* **2007**, *18*, 2418-2426.

- Katritzky, A. R.; Barczynsky, P.; Ostercamp, D. L.; Yousaf, T. I. Mechanisms of heterocyclic ring formations. 4. A 13C-NMR study of the reaction of β-keto esters with hydroxylamine. *J. Org. Chem.* **1986**, *51*, 4037-4042.

- Kawabata, K.; Hagio, T.; Matsuoka, S. The role of neutrophil elastase in acute lung injury. *Eur. J. Pharmacol.* **2002**, *451,* 1-10.

- Kelly, E.; Greene, C.M.; McElvaney, N.G. Targeting neutrophil elastase in cystic fibrosis. *Expert Opin. Ther. Targets* **2008**, *12*, 145-157.

- Khlebnikov, A. I.; Schepetkin, I. A.; Quinn, M. T. Structure-activity relationship analysis of N-benzoylpyrazoles for elastase inhibitory activity: A simplified approach using atom pair descriptors. *Bioorg. Med. Chem.* **2008***, 16*, 2791-2802.

- Kohnlein, T.; Welte, T. Alpha-1-antitrypsin deficiency: pathogenesis, clinical presentation, diagnosis and treatment. *Am. J. Med.* **2008**, *121*, 3-9.

- Korkmaz, B.; Horwitz, M. S.; Jenne, D. E.; Gauthier, F. Neutrophil elastase, proteinase 3, and cathepsin G as therapeutic targets in human diseases. *Pharmacol. Rev.* **2010**, *62*, 726-759.

- Korkmaz, B.; Moreau, T.; Gauthier, F. Neutrophil elastase, proteinase 3 and cathepsin G: physicochemical properties, activity and physiopathological functions. *Biochimie* **2008**, *90*, 227-242.

- Krogsgaard-Laersen, P.; Brogger Christensen, S.; Hjeds H. Organic hydroxylamine derivatives. VII. Isoxazolyn-5-ones. Reaction sequence previously stated to give 3-hydroxyisoxazoles. *Acta Chem. Scand.* **1973**, *27*, 2802-2812.

- Lape, H. E.; Hoppe, J. O.; Bell, M. R.; Wood, D.; Selberis, W. H.; Arnold, A. Antihypertensive properties of a series of indole and azaindole amidoximes with particular reference to 7-azaindole-3-acetamidoxime and indole-1-acetamidoxime. *Arch. Int. Pharmacodyn. Ter.* **1968**, *172(2)*, 394-414.

- Laufer, S. A.; Margutti, S. Isoxazolone based inhibitors of p38 MAP kinases. *J. Med. Chem.* **2008**, *51*, 2580-2584.

- Leavell, K. J.; Peterson, M. W.; Gross, T. J. The role of fibrin degradation products in neutrophil recruitment to the lung. *Am. J. Respir. Cell. Mol. Biol.* **1996**, *14*, 53-60.

- Lee, W. L.; Downey, G. P. Leukocyte elastase: physiological functions and role in acute lung injury. *Am. J. Respir. Crit. Care Med.* **2001**, *164*, 896-904.

- Li, L.; Ding, H.; Wang, B.; Yu, S.; Zou, Y.; Chai, X.; Wu, Q. Synthesis and evaluation of novel azoles as potent antifungal agents. *Bioorg. Med. Chem. Lett.* **2014**, *24(1)*, 192-194.

- Lind, K. E.; Cao, K.; Lin, E. Y. S.; Nguyen, T. B.; Tangonon, B. T.; Lee, W. C.; Sun, L. Preparation of pyridinonyl PDK1 inhibitors. PCT Int. Appl., WO2008005457 A2 20080110, **2008**.

- Lomas, D. A.; Parfrey, H. α1-Antitrypsin deficiency. 4: Molecular pathophysiology. *Thorax* **2004**, *4,* 354-357.

- Lu, P.; Weaver, V. M.; Werb, Z. The extracellular matrix: a dynamic niche in cancer progression. *J. Cell. Biol.* **2012**, *196,* 395-406.

- Lucas, S. D.; Costa, E.; Guedes, R. C.; Moreira, R. Targeting COPD: advances on low-molecular-weight inhibitors of human neutrophil elastase. *Med. Res. Rev.* **2011**, *33*, E73-E101.

- Maquestiau, A.; Van Haverbeke, Y.; Muller, R. N. Prototropic equilibrium of aryl- and alkylisoxazolin-5-ones. Effect of the basicity of the aprotic medium. *Bulletin des Societes Chimiques Belges* **1974***, 83(7-8)*, 263-269.

References

- Matera, M. G.; Calzetta, L.; Segreti, A.; Cazzola, M. Emerging drugs for chronic obstructive pulmonary disease. *Exp. Opin. Emer. Drugs* **2012**, *17,* 61-82.
- Mercury CSD 3.6 (Build RC6), Copyright CCDC 2001–2015. All rights reserved.
- Minakata, S.; Hamada, T.; Kamatsu, M. Synthesis and biological evaluation of 1H-pyrrolo [2,3-b]pyridine derivatives: correlation between inhibitory activity against the fungus causing rice blast and ionization potential. *J. Agric. Food Chem.* **1997**, *45*, 2345-2348.
- Mulchande, J.; Oliveira, R.; Carrasco, M.; Gouveia, L.; Guedes, R. C.; Iley, J.; Moreira, R. 4-Oxo-beta-lactams (Azetidine-2,4-diones) are potent and selective inhibitors of human leukocyte elastase. *J. Med. Chem.* **2010**, *53*, 241-253.
- Naruko, T.; Ueda, M.; Haze, K.; Van der Wal, A. C.; Van der Loos, C. M.; Itoh, A.; Komatsu, R.; Ikura, Y.; Ogami, M.; Shimada, Y.; Ehara, S.; Yoshiyama, M.; Takeuchi, K.; Yoshikawa, J.; Becker, A. E. Neutrophil infiltration of culprit lesions in acute coronary syndromes. *Circulation* **2002**, *106*, 2894-2900.
- Nauseef, W. M. How human neutrophils kill and degrade microbes: an integrated view. *Immunol. Rev.* **2007**, *219*, 88-102.
- Navia, M. A.; McKeever, B. M.; Springer, J. P. Structure of human neutrophil elastase in complex with a peptide chloromethyl ketone inhibitor at 1.84-A resolution. *Proc. Natl. Acad. Sci. USA* **1989**, *86*, 7-11.
- Nichols, D. P.; Chmiel, J. F. Inflammation and its genesis in cystic fibrosis. *Pediatr. Pulmonol.* **2015**, *40*, 39-56.
- Nobar, S. M.; Zani, M. L.; Boudier, C.; Moreau, T.; Bieth, J. G. Oxidized elafin and trappin poorly inhibit the elastolytic activity of neutrophil elastase and proteinase 3. *FEBS J.* **2005**, *272,* 5883-5893.
- Ohbayashi, H. Current synthetic inhibitors of human neutrophil elastase in 2005. *Expert Opin. Ther. Pat.* **2005**, *15*, 759-771.

- Padrines, M.; Wolf, M.; Walz, A.; Baggiolini, M. Interleukin-8 processing by neutrophil elastase, cathepsin G and proteinase-3. *FEBS Lett.* **1994**, *352*, 231-235.

- Palatinus, L.; Chapuis, G. Superflip – a computer program for the solution of crystal structures by charge flipping in arbitrary dimensions. *J. Appl. Cryst.* **2007**, *40*, 786-90.

- Perera, C. N.; Wiesmüller, K.; Larsen, M. T.; Schacher, B.; Eickholz, P.; Borregaard, N.; Jenne, D. E. NSP4 Is Stored in Azurophil Granules and Released by Activated Neutrophils as Active Endoprotease with Restricted Specificity. *J. Immunol.* **2013**, *191*, 2700-2707.

- Peters, M. B.; Merz, K. M. Semi-empirical comparative binding energy analysis (SE-COMBINE) of a series of trypsin inhibitors. *J. Chem. Theory Comput.* **2006**, *2*, 383-99.

- Petersen, C. M. Alpha 2-macroglobulin and pregnancy zone protein. Serum levels, alpha 2-macroglobulin receptors, cellular synthesis and aspects of function in relation to immunology. *Dan. Med. Bull.* **1993**, *40,* 409-46.

- Pfundt, R.; Wingens, M.; Bergers, M.; Zweers, M.; Frenken, M.; Schalkwijk, J. TNF-alpha and serum induce SKALP/elafin gene expression in human keratinocytes by a p38 MAP kinase-dependent pathway. *Arch. Dermatol. Res.* **2000**, *292*, 2370-2378.

- Pham, C.T. Neutrophil serine proteases: specific regulators of inflammation. *Nat. Rev. Immunol.* **2006**, *6,* 541-550.

- Pires, M. J. D.; Palira, D. L.; Purificacao, S. I.; Marques, M. M. D. Synthesis of substituted 4-, 5-, 6- and 7-azaindoles from aminopyridines via a cascade C-N cross-coupling/ Heck reaction. *Org. Lett.* **2016**, *18(13)*, 3250-3253.

- Quabius, E. S.; Görögh, T.; Fischer, G. S.; Hoffmann, A. S.; Gebhard, M.; Evert, M.; Beule, A.; Maune, S.; Knecht, R.; Óvári, A.; Durisin, M.; Hoppe, F.; Röcken, C.; Hedderich, J.; Ambrosch, P.; Hoffmanna, M. The antileukoprotease secretory leukocyte protease

References

inhibitor (SLPI) and its role in the prevention of HPV-infections in head and neck squamous cell carcinoma. *Canc. Lett.* **2015**, *357*, 339-345.

- Radhakrishnan, R.; Presta, L. G.; Meyer, E. F.; Wildonger, R. Crystal-structures of the complex of porcine pancreatic elastase with 2 valine-derived benzoxazinone inhibitors. *J. Mol. Biol.* **1987**, *198*, 417-424.

- Raeppel, F.; Raeppel, S. L.; Therrien, E. Design, synthesis and RON receptor tyrosine kinase inhibitory activity of new head groups analogs of LCRF-004. *Bioorg. Med. Chem. Lett.* **2015**, *25(18)*, 3810-3815.

- Rao, R. M.; Betz, T. V.; Lamont, D. J.; Kim, M. B.; Shaw, S. K.; Froio, R. M.; Baleux, F.; Arenzana-Seisdedos, F.; Alon, R.; Luscinskas, F. W. Elastase release by transmigrating neutrophils deactivates endothelial-boundSDF-1α and attenuates subsequent T lymphocyte transendothelial migration. *J. Exp. Med.* **2004**, *200*, 713-724.

- Robinson, M. M.; Robinson, B. L.; Butler, F. P. 7-azaindole VI: preparation of 5- and 6-substituted 7-azaindoles. *J. Am. Chem. Soc.* **1959**, *81*, 743-747.

- Ryu, O. H.; Choi, S. J.; Firatli, E.; Choi. S. W.; Hart, P. S.; Shen, R. F.; Wang, G.; Wu, W. W.; Hart, T. C. Proteolysis of macrophage inflammatory protein-1α isoforms LD78β and LD78α by neutrophil-derived serine proteases. *J. Biol. Chem.* **2005**, *280*, 17415-17421.

- Sallenave J. M. Secretory leukocyte protease inhibitor and elafin/trappin-2: versatile mucosal antimicrobials and regulators of immunity. *Am. J. Respir. Cell. Mol. Biol.* **2010**, *42*, 635-643.

- Sallenave, J. M. Antimicrobial activity of antiproteinases. *Biochem. Soc.* **2002**, *30,* 111-115.

- Sallenave, J. M. The role of secretory leukocyte proteinase inhibitor and elafin (elastase-specific inhibitor/skin-derived antileukoprotease) as alarm antiproteinases in inflammatory lung disease. *Respir. Res.* **2000**, *1,* 87–92.

- Sandham, D. A.; Adcock, C.; Bala, K.; Barker, L.; Brown, Z.; Dubois, G.; Budd, D.; Cox, B.; Fairhust, R. A.; Furegati, M.; Leblanc, C.; Manini,

J.; Profit, R.; Reilly, J.; Stringer, R.; Shmidt, A.; Turner, K. L.; Watson, S. J.; Willis, J.; Williams, J.; Wilson, C. 7-azaindole-3-acetic acid derivatives: potent and selective CRTh2 receptor antagonists. *Bioorg. Med. Chem.* **2009**, *19*, 4794-4798.

- Sato, K.; Sugai, S.; Tomita, K. Synthesis of 3-hydroxyisoxazoles from b-ketoesters and hydroxylamine. *Agric. Biol. Chem.* **1986**, *50*, 1831-1837.

- Sato, T.; Takahashi, S.; Mizumoto, T.; Harao, M.; Akizuki, M.; Takasugi, M.; Fukutomi, T.; Yamashita, J. Neutrophil elastase and cancer. *Surg. Oncol.* **2006**, *51*, 5054-5059.

- Schepetkin, I. A.; Khlebnikov, A. I.; Quinn, M. T. *N*-benzoylpyrazoles are novel small-molecule inhibitors of human neutrophil elastase. *J. Med. Chem.* **2007**, *50,* 4928-4938.

- Scott, A.; Weldon, S.; Taggart, C. C. SLPI and elafin: multifunctional antiproteases of the WFDC family. *Biochem. Soc.* **2011**, *39,* 1437-1440.

- Sheldrick, G. M. Phase annealing in SHELX-90: direct methods for larger structures. *Acta Crystalogr. A* **1990**, *46*, 467-73.

- Shneider, P.; Pisarevsky, E.; Fristrup, P.; Szpilman, A. M. Oxidative umpolung α-alkylation of ketones. *Org. Lett.* **2009**, *17(2)*, 282-285.

- Shreder, K. R.; Cajica, J.; Du, L. L.; Fraser, A.; Hu, Y.; Kohno, Y.; Lin, E. C. K.; Liu, S. J.; Okerberg, E.; Pham, L.; Wu, J. Y.; Kozarich, J. W. Synthesis and optimization of 2-pyridin-3-yl-benzo[d][1,3]oxazin-4-one based inhibitors of human neutrophil elastase. *Bioorg. Med. Chem. Lett.* **2009**, *1,* 4743-4746.

- Shu, Z.; Zhang, J.; Zhang, Y.; Wang, J. Palladium-catalized cross-coupling of aryl iodides with β-trimethylsiloxy-α-diazoesters. A novel approach toward β-keto-α-arylesters. *Chem. Lett.* **2011**, *40(9),* 1009-1011.

References

- Singla, P.; Luxami, V.; Paul, K. Pyrrolo[2,3-b]pyridine derivatives: synthesis and preliminary evaluation of their Calf Thymus DNA binding properties. *Chemistry Select*. **2016**, *1(15)*, 4772-4777.

- Sottrup-Jensen, L. Alpha-macroglobulins: structure, shape, and mechanism of proteinase complex formation. *J. Biol. Chem.* **1989**, *264*, 11539-11542.

- Stevens, T.; Ekholm, K.; Granse, M.; Lindahl, M.; Kozma, V.; Jungar, C. AZD9668: pharmacological characterization of a novel oral inhibitor of neutrophil elastase. *J. Pharmacol. Exp. Ther*. **2011**, *339*, 313-320.

- Stockley, R.; De Soyza, A.; Gunawardena, K.; Perret, J.; Forsman-Semb, K.; Entwistle, N.; Snell, N. Phase II study of a neutrophil elastase inhibitor (AZD9668) in patients with bronchiectasis. *Resp. Med*. **2013**, *107*, 524-533.

- Stocks, J. M.; Brantly, M. L.; Wang-Smith, L.; Campos, M. A.; Chapman, K. R.; Kueppers, F.; Sandhaus, R. A.; Strange, C.; Turino, G. Pharmacokinetic comparability of Prolastin®-C to Prolastin® in alpha1-antitrypsin deficiency: a randomized study. *BMC Pharmacol.* **2010**, *10*, 1-11.

- Stoller, J. K.; Rouhani, F.; Brantly, M.; Shahin, S.; Dweik, R. A.; Stocks, J. M.; Clausen, J.; Campbell, E.; Norton, F. Biochemical efficacy and safety of a new pooled human plasma alpha(1)-antitrypsin. *Chest*. **2002**, *122*, 66-74.

- Taggart, C. C.; Lowe, G. J.; Greene, C. M.; Mulgrew, A. T.; O'Neill, S. J.; Levine, R. L.; Mc Elvaney, N. G. Cathepsin B, L, and S cleave and inactivate secretory leucoprotease inhibitor. *J. Biol. Chem.* **2001**, *276,* 33345-33352.

- Tamakuma, S.; Ogawa, M.; Aikawa, N. Relationship between neutrophil elastase and acute lung injury in humans. *Pulm. Pharmacol. Ther*. **2004**, *17 (5)*, 271-279.

- Tebbutt, S. J. Technology evaluation: transgenic alpha-1-antitrypsin (AAT), PPL therapeutics. *Curr. Opin. Mol. Ther.* **2000**, *2*, 199-204.

- Teshima, T.; Griffin, J. C.; Powers, J. C. A new class of heterocyclic serine protease inhibitors. Inhibition of human-leukocyte elastase, porcine pancreatic elastase, cathepsin-g, and bovine chymotrypsin-a-alpha with substituited benzoxazinones, quinazolines, and anthranilates. *J. Biol. Chem.* **1982**, 257, 5085-5091.

- Thompson, R. C.; Ohlsson, K. Isolation, properties, and complete amino acid sequence of human secretory leukocyte protease inhibitor, a potent inhibitor of leukocyte elastase. *Proc. Natl. Acad. Sci. USA* **1986**, *83*, 6692-6696.

- Tizzano, E. F.; Buchwald, M. Cystic fibrosis: beyond the gene to therapy. *J. Pediatr.* **1992**, *120*, 337-349.

- Travis, J.; Salvesen, G. S. Human plasma proteinase inhibitors. *Ann. Rev. Biochem.* **1983**, *52*, 655-709.

- Tsushima, K.; King, L. S.; Aggarwal, N. R.; De Gorordo, A.; D'Alessio, F. R.; Kubo, K. Acute lung injury review. *Intern. Med.* **2009**, *48*, 621-630.

- Turk, V.; Stoka, V.; Vasiljeva, O.; Renko, M.; Sun, T.; Turk, B.; Turk, D. Cysteine cathepsin: from structure, funtion and regulation to the new frontiers. *Biochim. Biophys. Acta* **2012**, *1824(1)*, 68-88.

- Turk, V.; Stoka, V.; Turk, D. Cystatins: biochemical and structural properties, and medical relevance. *Front. Biosci.* **2008**, *13*, 5406-5420.

- Van den Steen, P. E.; Proost, P.; Wuyts, A.; Van Damme, J.; Opdenakker, G. Neutrophil gelatinase B potentiates interleukin-8 tenfold by aminoterminal processing, whereas it degrades CTAP-III, PF-4, and GRO-α and leaves RANTES and MCP-2 intact. *Blood* **2000**, *96(8)*, 2673-2681.

- Vergelli, C.; Schepetkin, I. A.; Crocetti, L.; Iacovone, A.; Giovannoni, M. P.; Guerrini, G.; Khlebnikow, A. I.; Ciattini, S.; Ciciani, G.; Quinn, M. T. Isoxazol-5(2H)-one: a new scaffold for potent human neutrophil elastase (HNE) inhibitors. *J. Enz. Inhib. Med. Chem.* **2017**, *32 (1)*, 821-831.

References

- Vergely, I.; Laugaa, P.; Reboud-Ravaux, M. Interaction of human leukocyte elastase with a N-aryl azetidinone suicide substrate: conformational analyses based on the mechanism of action of serine proteinases. *J. Mol. Graph.* **1996**, *14*, 158-67.

- Von Nussbaum, F.; Li, V. M. J. Neutrophil elastase inhibitors for the treatment of (cardio)pulmonary diseases: Into clinical testing with pre-adaptive pharmacophores. *Bioorg. Med. Chem. Lett.* **2015a**, *25*, 4370-4381.

- Von Nussbaum, F.; Li, V. M. J.; Allerheiligen, S.; Anlauf, S.; Bärfacker, L.; Beckem, M.; Delbeck, M.; Fitzgerald M. F.; Gerisch, M.; Gielen-Haertwig, H.; Haning, H.; Karthaus, D.; Lang, D.; Klemens, L.; Meibom, D.; Mittendorf, J.; Rosentreter, U.; Schäfer, M.; Schäfer, S.; Schamberger, J.; Telan, L. A.; Tersteegen, A. Freezing the bioactive conformation to boost potency: the identification of BAY 85-8501, a selective and potent inhibitor of human neutrophil elastase for pulmonary diseases. *Chem. Med. Chem.* **2015b**, *10*, 1163-1173.

- Von Nussbaum, F.; Li, V. M. J.; Daniel Meibom, D.; Anlauf, S.; Bechem, M.; Delbeck, M.; Gerisch, M.; Harrenga, A.; Karthaus, D.; Lang, D.; Lustig, K.; Mittendorf, J.; Schäfer, M.; Schäfer, S.; Schamberger, J. Potent and selective human neutrophil elastase inhibitors with novel equatorial ring topology: in vivo efficacy of the polar pyrimidopyridazine BAY-8040 in a pulmonary arterial hypertension rat model. *Chem. Med. Chem.* **2016**, *11*, 199-206.

- Voynow, J. A.; Fischer, B. M.; Zheng, S. Proteases and cystic fibrosis. *Int. J. Biochem. Cell. Biol.* **2008**, *40*, 1238-1245.

- Wagner, C. J.; Schultz, C.; Mall, M. A. Neutrophil elastase and matrix metalloproteinase 12 in cystic fibrosis lung disease. *Mol. Cell. Pediatr.* **2016**, *3*, 25.

- Walsh, D. E.; Greene, C. M.; Carrol, T. P.; Taggart, C. C.; Gallagher, P. M.; O'Neill, S. J.; McElvaney, N. G. Interleukin-8 Up-regulation by

Neutrophil Elastase Is Mediated by MyD88/IRAK/TRAF-6 in Human Bronchial Epithelium. *J. Biol. Chem.* **2001**, *276*, 35494-35499.

- Wang, Z.; Chen, F.; Zhai, R.; Zhang, L.; Su, L.; Lin, X.; Thompson, T.; Christiani, D. C. Plasma neutrophil elastase and elafin imbalance is associated with acute respiratory distress syndrome (ARDS) development. *Plos One* **2009**. *4*, e4380.

- Weinrauch, Y.; Drujan, D.; Shapiro, S. D.; Weiss, J.; Zychlinsky, A. Neutrophil elastase targets virulence factor of enterobacteria. *Nature* **2002**, *417*, 91-94.

- Wetzel, A.; Wetzig, T.; Haustein, U. F.; Sticherling, M.; Anderegg, U.; Simon, J. C.; Saalbach, A. Increased neutrophil adherence in psoriasis: role of the human endothelial cell receptor Thy-1 (CD90). *J. Invest. Dermatol.* **2006**, *126*, 441-52.

- Wewers, M. D.; Casolaro, M. A.; Sellers, S. E.; Swayze, S. C.; Mc Phaul, K. M.; Wittes, J. T.; Crystal, R. G. Replacement therapy for alpha1-antitrypsin deficiency associated with emphysema *N. Engl. J. Med.* **1987**, *316*, 1055-1062.

- Wiedow, O.; Schroderj, J.-M.; Gregory, H.; Young, J. A.; Christophers, E. Elafin: an elastase-specific inhibitor of human skin. Purification, characterization, and complete amino acid sequence. *J. Biol. Chem.* **1990**, *265,* 14791-14795.

- Wiedow, O.; Wiese, F.; Streit, V.; Kalm, C.; Christophers, E. Lesional elastase activity in psoriasis, contact dermatitis, and atopic dermatitis. *J. Invest. Dermatol.* **1992**, *99,* 306-309.

- Wierenga, W.; Evans, B. R.; Zurenko, G. E. Benzoisoxazolones: antimicrobial and antileukemic activity. *J. Med. Chem.* **1984**, *27*, 1212-1215.

- Wittamer, V.; Bondue, B.; Guillabert, A.; Vassart, G.; Parmentier, M.; Communi, D. Neutrophil-Mediated Maturation of Chemerin: A Link between Innate and Adaptive Immunity. *J. Immunol.* **2005**, *175*, 487-493.

References

- Yamaguchi, M.; Takiguchi, O.; Tsukase, M.; Ishiwata, Y. Hair dyecomposition comprising azo dye. PCT Int. Appl., WO2009005139 A2 20090108, **2009**.

- Zani, M. Z.; Nobar, S. M.; Lacour, S. A.; Lemoine, S.; Boudier, C.; Bieth, J. G.; Moreau, T. Kinetics of the inhibition of neutrophil proteinases by recombinant elafin and pre-elafin (trappin-2) expressed in _Pichia pastoris. FEBS J. **2004**, 271_, 2370–2378.

- Zeiher, B. G.; Artigas, A.; Vincent, J. L. Neutrophil elastase inhibition in acute lung injury: results of the STRIVE study. _Crit. Care Med._ **2004**, _32 (8)_, 1695-1702.

- Zhang, J.; Ibrahim, P. N.; Bremer, R.; Spevak, W.; Cho, H. Preparation of azaindole compounds and methods for kinase modulation and indication therefore. PCT Int. Appl. WO2011057022 A1 20110512, **2011**.

- Zhong, Q. Q.; Wang, X.; Li, Y. F.; Peng, L. J.; Jiang, Z. S. Secretory leukocyte protease inhibitor promising protective roles in obesity-associated atherosclerosis. _Exp. Biol. Med._ **2017**, _242(3)_, 250-257.

SOLID PHASE PEPTIDE SYNTHESIS OF SMALL PEPTIDE-BASED METAL CHELATORS

SUPERVISOR: Prof. Robert Hider

TABLE OF CONTENTS

1. INTRODUCTION

1.1 *Iron overload and iron chelators*

Iron is an essential metal in all living organisms, but it can become toxic when present in excess because there is no physiologic excretory pathway for this essential element. In the presence of molecular oxygen, "loosely-bound" iron undergoes to redox cycle between the two most stable oxidation states thereby generating oxygen-derived free radicals, such as the hydroxyl radical (Halliwell, B. et al. 1998). This last one is highly reactive and it is able to interact with most types of biological molecules including sugars, lipid, proteins and nucleic acids, resulting in peroxidative tissue damage. The uncontrolled production of these highly reactive species is undesirable, thus cells adopted a number of protective strategies to prevent their formation and following tissue damage. These cellular mechanisms include the efficient control of iron storage, transport and distribution (Crichton, R. R. 1991).

In healthy individuals, iron levels are under extremely tight control and rarely iron-catalyzed free radical generating reactions occur (Zhou, T. et al. 2011). However, in some cases the iron status can change, either locally as in ischemic tissue, or systematically due to genetic hemochromatosis or transfusion-induced iron overload (e.g. β-thalassemia major and sickle cell anemia). In patients affected by β-thalassemia major, regular blood transfusions lead to elevated body iron levels due to inability to excrete iron. Each unit of blood (400 mL) contains approximately 250 mg of iron and thus if received more than twice per annum, the patient will begin to rapidly accumulate iron. Excess of iron is mainly located in the liver and the spleen but its levels gradually increase in the heart and endocrine tissue over a period of years (Ma, Y. et al. 2012). In these cases, the elevated levels of iron ultimately lead to free radical-mediated tissue damage and eventually death (Brittenham, G. M. 1991). Although excess of iron can be removed by venesection where an adequate erythropoietic reserve exists, iron chelation

is the only effective way to relieve iron overload in transfusion-dependent patients. In this view, the design of an orally active iron chelator has been a major research objective resulting in the development of a large number of iron chelators (Hider, R. C. and Zhou, T. 2005). In the design of iron chelators for clinical applications, it is necessary to evaluate the efficacy of the iron chelator by measuring the amount of iron eliminated during use of the chelator and comparing that with the amount of iron input. However, efficacy assessment may be somewhat more complicated, because one is concerned not only in achieving a negative iron balance, but also in minimizing iron-induced organ toxicity. Since some chelators may be more effective in removing iron from some tissues/organs than others, in part based upon their ability to access these sites, organ-specific iron removal is another key factor in the assessment of efficacy (Galanello, R. 2007). In addition to the efficacy, other important parameters that must be considered in the design of an ideal iron chelator are metal selectivity and affinity, kinetic stability of the complex, iron-binding capacity, bioavailability and toxicity (Zhou, T. et al. 2011).

Many examples of iron chelators are reported in the literature and numerous compound are currently approved for clinical use in the treatment of the pathologies characterized by iron overload. Below are reported two important examples of compounds that have been commonly used in therapy as iron chelators: Desferrioxamine and Deferiprone (Ma, Y. et al. 2012).

Desferrioxamine (DFO) (**Fig. 1**) is a natural hexadentate chelator produced by the microorganism *Streptomyces pilosus*. It is used to treat diseases characterized by iron overload and it shows a high lipophilicity, being able to interact with iron in the hepatocytes both at the intracellular and extracellular levels; it promotes iron excretion through the urinary tract and bile ducts and it shows a good selectivity for Iron(III). Despite this, Desferrioxamine is not considered a good therapeutic agent due to oral inefficiency and rapid kidney clearance (plasma half-life 5-10 minutes) (Summers, M. R. et al. 1979), allowing only parenteral administration, typically as an 8- to 12-hour nightly

infusion for 5–7 nights a week (Pippard, M. J. et al. 1978). Although, DFO showed a safe drug for the treatment of elevated iron burden in the body, intensive therapy in young patients with lower body iron stores may results in serious neurotoxicity and additional adverse effects (Porter, J. B. et al. 1989) (Olivieri, N. F. et al. 1986).
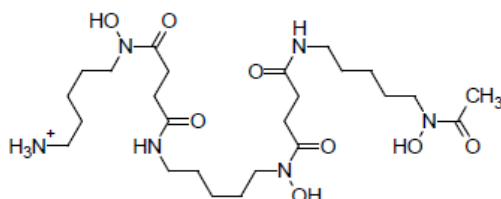
Fig. 1: Desferrioxamine

Deferiprone (DFP, Ferriprox™, Kelfer™) (**Fig. 2**) belong to a series of hydroxypyridinone-based iron chelators synthesized in the early 80s in the laboratory of Professor R. Hider in London (Dobbin, P. S. et al. 1993). DFP was licensed for use in India in 1994 and in Europe in 1999, receiving full marketing authorization in 2002 and FDA approval in 2011.
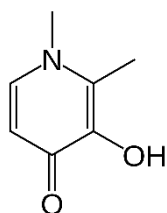
Fig. 2: Deferiprone

A particularly important feature of Deferiprone is the ability to penetrate into the cells, and form a neutral complex by coordinating iron, which is also able to permeate cell membranes. Thus, iron can be readily removed from iron-loaded cells including those of cardiac tissue (**Fig. 3**) (Glickstein, H. et al. 2006) (Ma, Y. et al. 2012). This ability extends to clinical applications (Pennel,

Introduction

D. J. et al. 2006) (Hershko, C. et al. 2004), where it has been directly demonstrated that Deferiprone therapy is associated with significantly greater cardiac protection than Desferrioxamine in patients with thalassemia major (Borgna-Pignatti, C. et al. 2006) (Pepe, A. et al. 2011). DFP is rapidly and completely absorbed after oral administration, with a plasma peak level typically occurring about 1 hour after administration. In addition, DFP is rapidly eliminated from the body (i.e. half-life of about 2 hours) due to hepatic biotransformation, with glucuronidation accounting for almost all the metabolism (i.e. about 90% of the drug is excreted in the urine as the glucuronide). Long-term therapy with Deferiprone is associated with the occurrence of transient gastrointestinal symptoms (GI) such as nausea, vomiting, and abdominal pain, which are the most frequently reported adverse symptoms for DFP (Galanello, R. 2007), although also a low incidence of reversible agranulocytosis has been occasionally found (Ceci, A. et al. 2002).
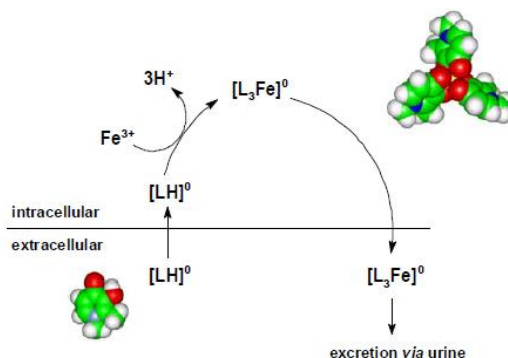
Fig. 3: Schematic representation of the Deferiprone penetration $[LH]_0$ through the plasma membrane

1.2 *Prostate cancer and gallium chelators*

Prostate cancer is the most common malignancy in men and a major cause of cancer death. It is classified as an adenocarcinoma that begins when normal semen-secreting prostate gland cells mutate into cancer cells. Aside from age and race, the only established risk factor for prostate cancer is a family history of the disease. The risk for first-degree relatives of men with

prostate cancer is about twice that for men in the general population (Goldgar, D. E. et al. 1994) (Schaid, D. J. 2004). This familial risk is more than four times higher than in the general population for first-degree relatives of men with prostate cancer diagnosed younger than 60 years (Johns, L. E. and Houlston, R. S. 2003). Its incidence differs between countries due to coverage of prostate-specific antigen (PSA) screening, but in both populations with and without PSA screening, prostate cancer is the cause of 1–2% of death in men (Cancer Research UK, 2011). It was estimated that in 2012 there would be 241,740 new cases of prostate cancer diagnosed in the United States and that 28,170 men would die of the disease. When detected early, and when disease is only localized in the prostate gland, the 5-years survival rate is nearly 100%. However, once the cancer has spread beyond the prostate, survival rates fall dramatically. Hence, the primary clinical goal is to define the anatomic extent of the tumor and to distinguish patients with organ-confined, locally invasive, or metastatic disease. As accurate detection is critical to determining appropriate patient management, it follows that sensitive and specific localization of disease should be a vital component of staging (American Cancer Society, 2012).

In this view, effective diagnosis and treatment response in prostate cancer are major challenges commonly faced by oncologists and radiologists, since both PSA level determination and radiological imaging have limitations with respect to diagnosis, staging, and prognosis, showing high false positives during screening in relation to benign prostatic hyperplasia and prostatitis (Chappell, B. and Mc Loughlin, J. 2005).

Positron emission tomography (PET) is a whole body diagnostic three-dimensional molecular imaging modality used in nuclear medicine that detects radiation arising from the decay of unstable positron-emitting radioisotopes (Cusnir, R. et al. 2017). With the advent of PET, several radiotracers such as ^{11}C-Acetate, ^{18}F-Choline, and ^{11}C-Choline have been used for prostate cancer imaging. ^{11}C acetate is not a sensitive marker for detection of prostate cancer, due to the age that causes physiological accumulation of ^{11}C-Acetate and

therefore careful interpretation of images is necessary (Kato, T. et al. 2002). Moreover, ^{11}C-Acetate uptake is also present in other tissues such as liver, cardiac and bladder, thereby being nonspecific for prostate cancer (Kallur, K. G. et al. 2017).

Additionally, PSA values show a lot of inter and intra-individual variations with time due to manipulations of the prostate and they are less reliable as a standalone marker. For all these reasons, it was necessary to identify more robust surface biomarkers in prostate cancer. One of these molecules is *Prostate-Specific Membrane Antigen* (PSMA) also known as folate hydrolase I or glutamate carboxypeptidase I. PSMA is a cell surface protein with a significantly increased expression in prostate cancer cells when compared to other PSMA-expressing tissues such as kidney, proximal small intestine or salivary glands (Sweat, S. D. et al. 1998) (Mannweiler, S. et al. 2009) (Schuhmacher, J. and Maier-Borst, W. 1981). An additional advantage of PSMA detection is the transmembrane location with a large extracellular domain that allows for internalization of the receptor after ligand binding, providing an accurate target for prostate carcinoma specific imaging and therapy (Ghosh, A. and Heston, W. D. 2004). Consequently, there is a need for the development of high-resolution PET imaging methods using the extracellular domain of PSMA (Afshar-Oromieh, A. et al. 2013). Recently, methods have been developed to label PSMA ligands with ^{68}Ga, ^{99m}Tc, [123/124/131]I enabling their use for PET imaging, more scintigraphy options and radio ligand therapy (Hillier, S. M. et al. 2009) (Eder, M. et al. 2012). Earlier observations with ^{68}Ga-PSMA suggests that this novel tracer can detect prostate carcinoma relapses and metastases with high contrast by targeting the extracellular domain of PSMA (Afshar-Oromieh, A. et al. 2013).

In this context, hexadentate tris(3,4-hydroxypyridinone) ligands (THP) that show complex high affinities for oxophilic trivalent metal ions (e.g. Fe^{3+}) demonstrated to be good candidate for the development of $^{68}Ga^{3+}$ bifunctional chelators, the positron emitting radio metal which is clinically used for molecular imaging in positron emission tomography (PET). THP-peptide bio-

conjugates rapidly and quantitatively complex $^{68}Ga^{3+}$ at room temperature, neutral pH and micromolar concentrations of ligand, making them amenable to kit-based radio synthesis of ^{68}Ga-PET radiopharmaceuticals. ^{68}Ga-labelled THP-peptides accumulate at target tissue in vivo, and are excreted largely via a renal pathway, providing high quality PET images (Cusnir, R. et al. 2017).

The research group of Professor R. Hider at King's College London, where I performed my PhD visiting period, has been involved for many years in the design and synthesis of new metal chelators (e.g. Deferiprone, the small-molecule iron chelator reported above). More recently, a new research project has been started by the group focused on the development of peptide-based ligands for both iron and gallium.

In this context, my project focused on the solid-phase synthesis of tripeptide (Lys-Lys-Lys) and tetrapeptide (Lys-Lys-Lys-Lys) derivatives bearing 3,4-dihydroxy picolinic acid and the 3-(3-hydroxy-2-methyl-4-oxopyridin-1(4H)-yl)propionic acid (as chelating groups) on the amino groups of the side chains . All final compounds will be tested in the near future as iron and gallium chelators for biological and clinical applications. In particular, as regard the iron chelators, all the final products will be subjected to spectrophotometric titration in order to determine the pka values and the affinity costants for iron(III). These compounds will also be tested in cell culture, in order to investigate their ability to remove iron from cells.

2. CHEMISTRY

The synthetic pathway followed to obtain the final compounds **12a**,**b** and **20a**,**b** are reported in the **Schemes 1** and **2**.

Scheme 1
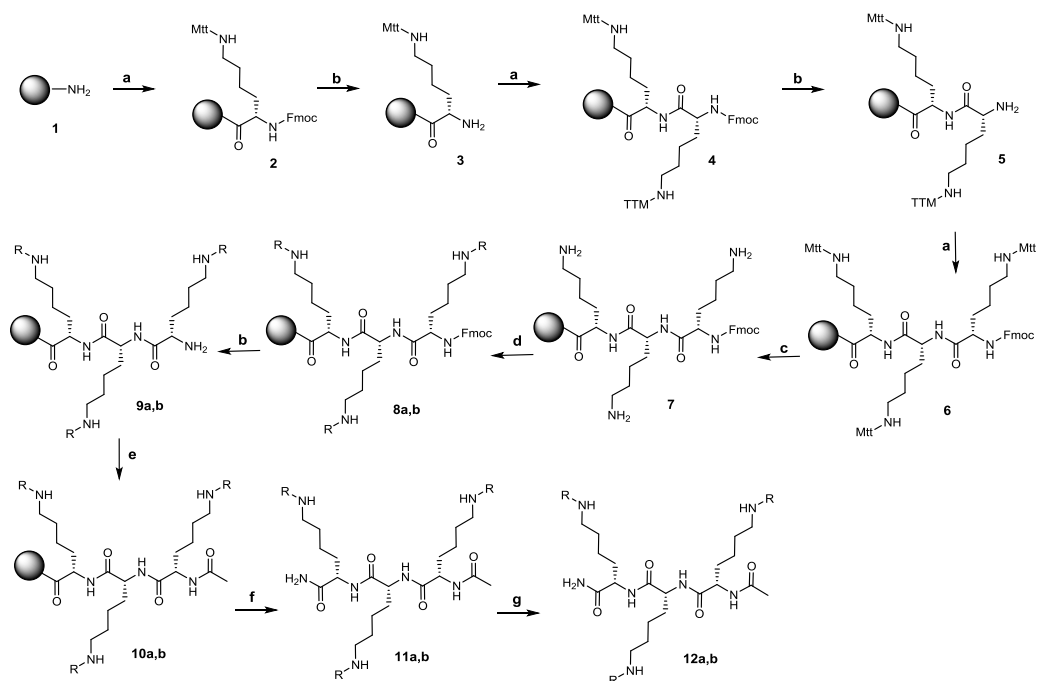
Reagents and conditions:

a) Fmoc-Lys-Mtt, ethyl (hydroxyimino)cyanoacetate, DIC, dry DMF.

b) Piperidine-DMF (2:8, v/v).

c) TFA (2% v/v), TIPS (2% v/v), DCM (96% v/v).

d) R-COOH, PyOxP, DIPEA, dry DMF.

e) $(CH_3CO)_2O$, DIPEA.

f) TFA (90% v/v), phenol (5% w/v), TIPS (5% v/v), H_2O (5% v/v).

g) BCl_3, dry DCM.

Scheme 2
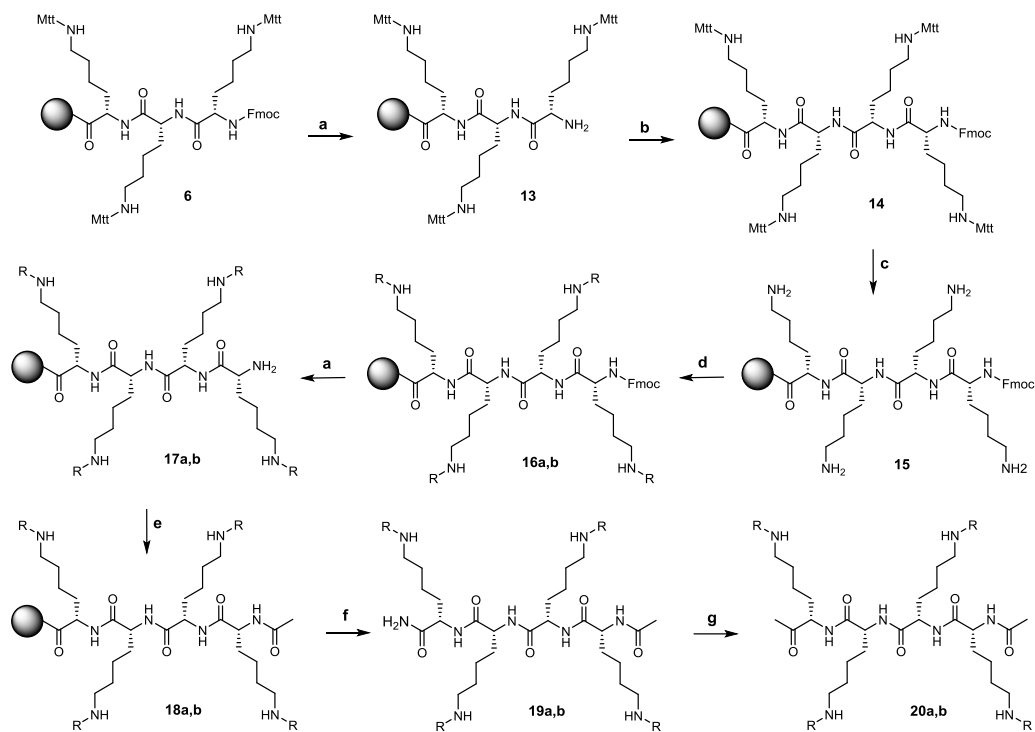
Reagents and conditions:

a) Fmoc-Lys-Mtt, ethyl (hydroxyimino)cyanoacetate, DIC, dry DMF.

b) Piperidine-DMF (2:8, v/v).

c) TFA (2% v/v), TIPS (2% v/v), DCM (96% v/v).

d) R-COOH, PyOxP, DIPEA, dry DMF.

e) $(CH_3CO)_2O$, DIPEA.

f) TFA (90% v/v), phenol (5% w/v), TIPS (5% v/v), H_2O (5% v/v).

g) BCl_3, dry DCM.

8-11, 16-19	R
a	BnO, BnO pyridine ring with C(=O)
b	pyridinone ring with OBn, N-propanoyl

12, 20	R
a	HO, HO pyridine ring with C(=O)
b	pyridinone ring with OH, N-propanoyl

Chemistry

For solid-phase synthesis we used NovaPeg Rink Amide Resin, consisting of only PEG units. This unique composition confers excellent swelling and mechanical properties on the polymer. Furthermore, in contrast to polystyrene and other commonly used supports, NovaPeg resin appears not to suffer from osmotic shock when solvent is exchanged from hydrophobic to hydrophilic and it shows an excellent chemical stability, particularly towards strong acids and bases (Garcia-Martin, F. et al. 2006). The Fmoc/Mtt solid-phase strategy involved the use of the base labile Fmoc protecting group for α-amino protection and Mtt protecting groups for side chain ε-amino protection of Lysine. Mtt-based protecting groups are highly convenient because they are removed with 2% of TFA in dichloromethane, being stable to piperidine used to remove the Fmoc group (Palomo, J. M. 2014). The amino acid couplings (compounds **2**, **4**, **6** and **14**) were performed using DIPEA as a base, DIC to activate the carboxylic groups and ethyl (hydroxyimino)cyanoacetate as an agent to minimize epimerization.

The picryl sulfonic acid test for detection of primary amines was performed after each coupling to confirm the coupling completion (Cayot, P. et al. 1997). When the test was negative (absence of free amines) the Fmoc group was removed with piperidine-DMF (2:8 v/v) and we coupled the next amino acid. Once the Mtt protecting peptides were obtained (compounds **6** and **14**) we remove the protecting groups using 2% of TFA in dichloromethane (compounds **7** and **15**) and we performed the coupling with two different chelating groups (3,4-dihydroxy picolinic acid and the 3-(3-hydroxy-2-methyl-4-oxopyridin-1(4H)-yl)propionic acid) (Gaeta A. et al. 2011) (Dobbin, P. S. et al. 1993). These coupling reactions (for compounds **8a**, **8b**, **16a** and **16b**) were carried out using the appropriate acid, PyOxP and DIPEA.

PyOxP (O-[(1-cyano-2-ethoxy-2-oxoethylidene) amino]-oxytri(pyrrolidin-1-yl)phosphonium hexafluoro phosphate) is a new coupling reagent that exhibited higher capacity to suppress racemization in various peptide models and enhanced solubility in DMF and DCM than benzotriazole-based reagents (Subiròs-Funosas, R. et al. 2010). This is the most difficult step of the

synthesis because we had to be sure that the coupling had occurred on all the amino groups. Therefore, we worked with particular reaction conditions modulating the stoichiometric ratios and the reaction times depending on whether the coupling was carried out on the tripeptide or the tetrapeptide. Also in this case, after the coupling, we performed the picryl sulfonic acid test as previously described. After the last Fmoc removal (compounds **9a**, **9b**, **17a** and **17b**), we performed the acetic capping using acetic anhydride and DIPEA in large excess and we obtained compounds **10a**, **10b**, **18a** and **18b**. Washings after every coupling and every deprotection were performed with DMF, methanol and dichloromethane. Then we carried out the cleavage from the resin with TFA in presence of phenol (5% w/v), water (5% v/v) and triisopropylsilane (5% v/v) as scavengers (compound **11a**, **11b**, **19a** and **19c**). The last step of the synthesis was performed in solution using BCl_3 in dry dichloromethane at room temperature, in order to remove benzyl protections on OH groups and obtain the final compounds **12a**, **12b**, **20a** and **20b**.

3. MATERIAL AND METHODS

^{1}H-NMR, ^{13}C-NMR, COSY and HSQC spectra were recorded on an Avance 400 instrument (Bruker AscendTM 400). Chemical shifts (δ) are reported in ppm to the nearest 0.01 ppm using the solvent as an internal standard. Coupling constants (*J* values) are given in Hz (rounded to the nearest 0.1 Hz) and were calculated using TopSpin 3.5 pl software (Nicolet Instrument Corp., Madison, WI) . *HPLC-DAD*: HP 1050 series equipped with quaternary pump, auto-sampler, diode array detector (DAD) and Kontron DEG 104 degasser. Mass spectra were recorded on Agilent 1100 series coupled to LCQDECAXP (from Thermo Finnigan) and reported mass values are within the error limits of ±5 ppm mass unists. Preparative HPLC was performed on MicromassXQ (Waters). A C8 Kinetex® column (Phenomenex Inc.) 100×2.1 mm i.d., particle size 5 µm was used for analytical characterizations. HPLC mobile phases A and B consisted of 0.1% v/v TFA in water and acetonitrile, respectively. The gradient was 0% B ramping to 90% B within 30 minute. The flow rate was set at 0.2 mL/min and the injection volume was 5-20 µL.

H-Lys-(Mtt)-NovaPeg resin (2)

NovaPeg Rink amide resin (2.0 g equivalent to a loading of 0.98 mmol) was placed in a 60.0 mL polypropylene syringe fitted with a polyethylene filter disk and it was conditioned with DMF for 30 minutes. A solution of Fmoc-Lys-Mtt-OH (1.84 g, 2.94 mmol, 3.0 eq), ethyl (hydroxyimino)cyanoacetate (0.42 g, 2.94 mmol, 3.0 eq) and *N,N'*-diisopropylcarbodiimide (DIC, 0.43 mL, 2.94 mmol, 3.0 eq) in dry DMF was added. After stirring overnight, the resin was washed with DMF (3 x 0.5 min), MeOH (3 x 0.5 min), DCM (3 x 0.5 min) and subsequently treated with acetic anhydride and DIPEA for 30 minutes. Thereafter the resin was washed again (DMF/MeOH/DCM) and finally dried under vacuum to perform the picryl sulfonic acid test (Cayot, P. et al. 1997) that resulted negative (no free amine). The Fmoc group was removed as

indicated in the following General procedure for Fmoc-removal producing resin-bound compound **3**.

General procedure for Fmoc-removal: the Fmoc protecting-group was removed with piperidine/DMF (2:8 v/v) (3 x 20 min). Washing between deprotection, coupling and again deprotection steps was performed with DMF (3 X 0.5 min), MeOH (3 x 0.5 min), DCM (3 x 0.5 min) using 20 mL solvent/resin each time.

General procedure for compounds 4, 6 and 13: Fmoc-Lys-Mtt-OH (1.22 g, 1.96 mmol, 2.0 eq), ethyl (hydroxyimino)cyanoacetate (0.28 g, 1.96 mmol, 2.0 eq) and *N*,*N'*-diisopropylcarbodiimide (DIC, 0.30 mL, 1.96 mmol, 2.0 eq) in dry DMF were added to the appropriate substrate. After one night, the picryl sulfonic acid test (Cayot, P. et al. 1997) was negative for all the couplings. Then, the peptidyl-resin was subjected to Fmoc-removal and washing treatment as described in the General procedure for Fmoc-removal previously described.

General procedures for cleavage from the resin: the peptidyl-resin was treated with TFA (90% v/v) for 2 hours at room temperature in the presence of phenol (5% w/v), water (5% v/v), water (5% v/v) and TIPS (2% v/v) as scavengers. The filtrate was collected and the resin washed with TFA. The solution was concentrated to <0.5 mL at 40°C under a gentle stream of nitrogen. Ice-cold diethyl ether was added to precipitate the compound. The suspension was centrifuged and the supernatant removed. The precipitate was washed with diethyl ether and finally dried in the desiccator under vacuum.

H-Lys-(Mtt)-Lys-(Mtt)-Lys-(Mtt)-NovaPeg Resin (6)

A small aliquot of the peptidyl-resin was subjected to the "small cleavage" following the general procedure for cleavage from the resin as reported above.

During the "small cleavage" for the check of the tripeptide 6 we also lost the acid labile Mtt protecting-group. The HPLC-DAD analysis (t_R = 10.02 min) of the crude showed a purity of >90%. LC-MS: calcd. for $C_{33}H_{49}N_7O_5$, 623.4 Found: *m/z* 624.4 $[M+H]^+$, 312.7 $[M+2H]^{2+}$.

H-Lys-(Mtt)-Lys-(Mtt)-Lys-(Mtt)-Lys-(Mtt)-NovaPeg Resin (13)

A small aliquot of the peptidyl-resin was subjected to the "small cleavage" following the general procedure for cleavage from the resin as above reported. During the "small cleavage" for the check of the tetrapeptide **13** we also lost the acid labile Mtt protecting-group. The HPLC-DAD analysis (t_R = 9.85 min) of the crude showed a purity of >90%. (LC-MS): calcd. For $C_{39}H_{61}N_9O_6$, 751.5. Found: *m/z* 752.5 $[M+H]^+$, 376.7 $[M+2H]^{2+}$.

General procedure for Mtt removal (compounds 7 and 15): the Mtt protecting group was removed using TFA (2% v/v), TIPS (2% v/v) as scavenger and DCM (96% v/v) (5 x 15 min). Washing after deprotection was performed with DMF (3 x 0.5 min), MeOH (3 x 0.5 min), DCM (3 x 0.5 min) using 20 mL solvent/resin each time.

General procedure for compounds 9a and 9b: the appropriate acid (2.94 mmol, 6.0 eq) and PyOxP (0.775 g, 2.94 mmol, 6.0 eq) (Subiròs-Funosas, R. et al. 2010) were dissolved in DMF dry and then DIPEA (0.51 mL, 5.88 mmol, 12.0 eq) was added. The mixture was added to the peptidyl-resin **7** (0.49 mmol). After three days of coupling, the picryl sulfonic acid test (Cayot, P. et al. 1997) was negative for both compounds **8a** and **8b**. Then, the peptidyl-resin was subjected to Fmoc-removal and washing treatment as described in the General procedure for Fmoc-removal reported above.

Compound 9a

A small aliquot of the peptidyl-resin was subjected to the "small cleavage" following the General procedure for cleavage from the resin as above

reported. (LC-MS): calcd. For $C_{78}H_{84}N_{10}O_{12}$, 1353.6. Found: *m/z* 1354.4 [M+H]$^+$, 677.8 [M+2H]$^{2+}$, 452.2 [M+3H]$^{3+}$.

Compound 9b

A small aliquot of the peptidyl-resin was subjected to the "small cleavage" following the General procedure for cleavage from the resin as above reported. (LC-MS): calcd. For $C_{66}H_{84}N_{10}O_{12}$, 1208.6. Found: *m/z* 1209.5 [M+H]$^+$, 605.7 [M+2H]$^{2+}$, 404.3 [M+3H]$^{3+}$.

General procedure for compound 17a and 17b: the appropriate acid (3.92 mmol, 8.0 eq) and PyOxP (1.034 g, 3.92 mmol, 8.0 eq) (Subiròs-Funosas, R. et al. 2010) were dissolved in DMF dry and then DIPEA (0.68 mL, 7.84 mmol, 16.0 eq) was added. The mixture was added to the peptidyl-resin **15** (0.49 mmol). After four days of coupling, the picryl sulfonic acid test (Cayot, P. et al. 1997) was negative for both compounds **16a** and **16b**. Then, the peptidyl-resin was subjected to Fmoc-removal and washing treatment as described in the General procedure for Fmoc-removal reported above.

Compound 17a

A small aliquot of the peptidyl-resin was subjected to the "small cleavage" following the General procedure for cleavage from the resin as reported above. (LC-MS): calcd. For $C_{104}H_{111}N_{13}O_{16}$, 1797.8. Found: *m/z* 899.5 [M+2H]$^{2+}$, 600.3 [M+3H]$^{3+}$.

Compound 17b

A small aliquot of the peptidyl-resin was subjected to the "small cleavage" following the General procedure for cleavage from the resin as reported above. (LC-MS): calcd. For $C_{88}H_{111}N_{13}O_{16}$, 1605.8 Found: *m/z* 803.5 [M+2H]$^{2+}$, 536.3 [M+3H]$^{3+}$.

General procedure for "acetic capping" (compound 10a, 10b, 18a and 18b): the appropriate peptidyl-resin was treated with acetic anhydride (10.0 eq) and DIPEA (20.0 eq). After stirring for 50 minutes, the resin was washed with DMF/MeOH/DCM and finally dried under vacuum to perform the picryl sulfonic acid test (Cayot, P. et al. 1997) that resulted negative (no free amine). After the acetic capping, the peptidyl-resins were subjected to the cleavage from the resin following the General procedure for cleavage from the resin as reported above, obtaining respectively compounds **11a**, **11b**, **19a** and **19b**.

General procedure to obtain compounds 12a, 12b, 20a and 20b: the appropriate substrate was dissolved in dry DCM under N_2 and the solution was cooled at 0°C. Then, a large excess of BCl_3 (i.e. 1 M solution of BCl_3 in anhydrous dichloromethane, ca. 3 mL of solution for 10 mg of substrate) was added and the reaction mixture was stirred at room temperature overnight. After quenching with MeOH, the solvent was evaporated and ice-cold diethyl ether was added to precipitate the compound. The suspension was centrifuged and the supernatant removed. The precipitate was washed with diethyl ether and finally dried in the desiccator under vacuum. After preparative HPLC purification, the residues were lyophilized and the final products were obtained as white solids.
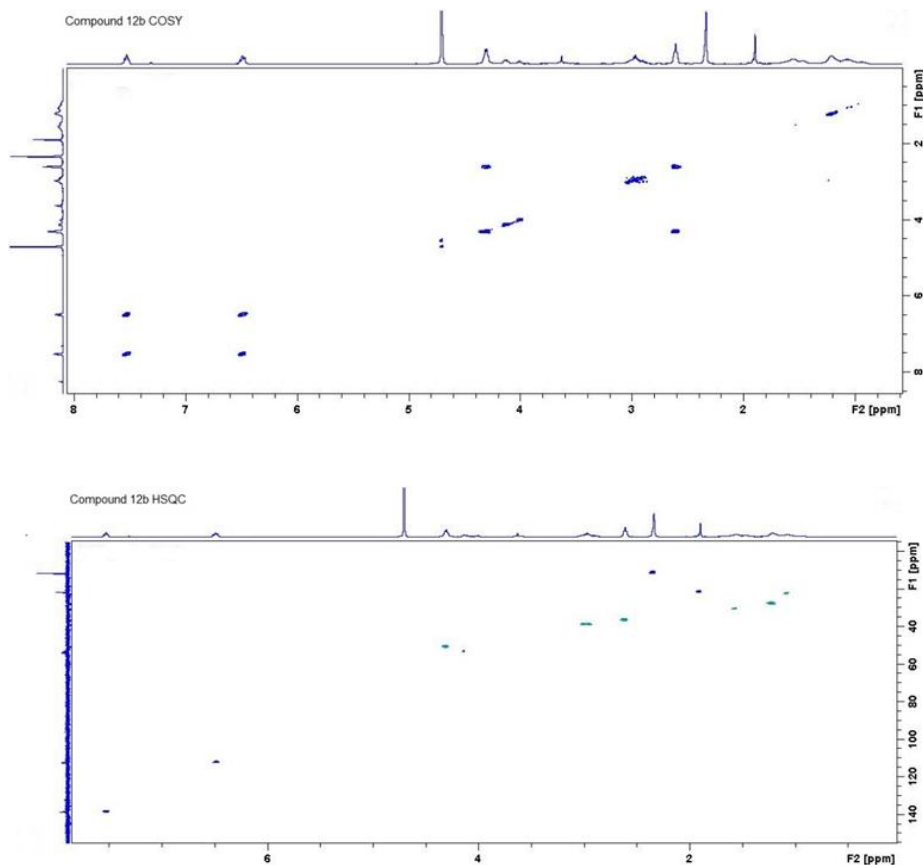
Compound 12a

Yield: 10%; <u>^{1}H-NMR</u> (MeOH-d_4) δ 1.20-1.39 (m, 8H, 4 x CH_2, side chain), 1.59-1.77 (m, 10H, 5 x CH_2, side chain), 1.93 (s, 3H, NHCO*CH_3*), 3.37-3.45 (m, 6H, 3 x NH*CH_2*), 4.21-4.27 (m, 3H, 3 x NH*CH*CH_2), 7.27 (d, 3H, Ar, *J* = 8.0 Hz), 8.11 (d, 3H, Ar, *J* = 8.0 Hz). <u>^{13}C-NMR</u> (MeOH-d_4) δ 20.74 (CH_3), 22.71 (CH_2), 28.35 (CH_2), 39.61 (CH_2), 47.93 (CH), 112.39 (CH), 127.68 (C), 135.56 (CH), 145.58 (C), 158.85 (C), 162.82 (C). The HPLC-DAD analysis (t_R = 8.13 min) showed a purity of 90%. (LC-MS): calcd. For $C_{38}H_{50}N_{10}O_{13}$, 854.4 Found: *m/z* 855.3 [M+H]$^+$, 428.3 [M+2H]$^{2+}$.

Compound 12a COSY

Compound 12a HSQC
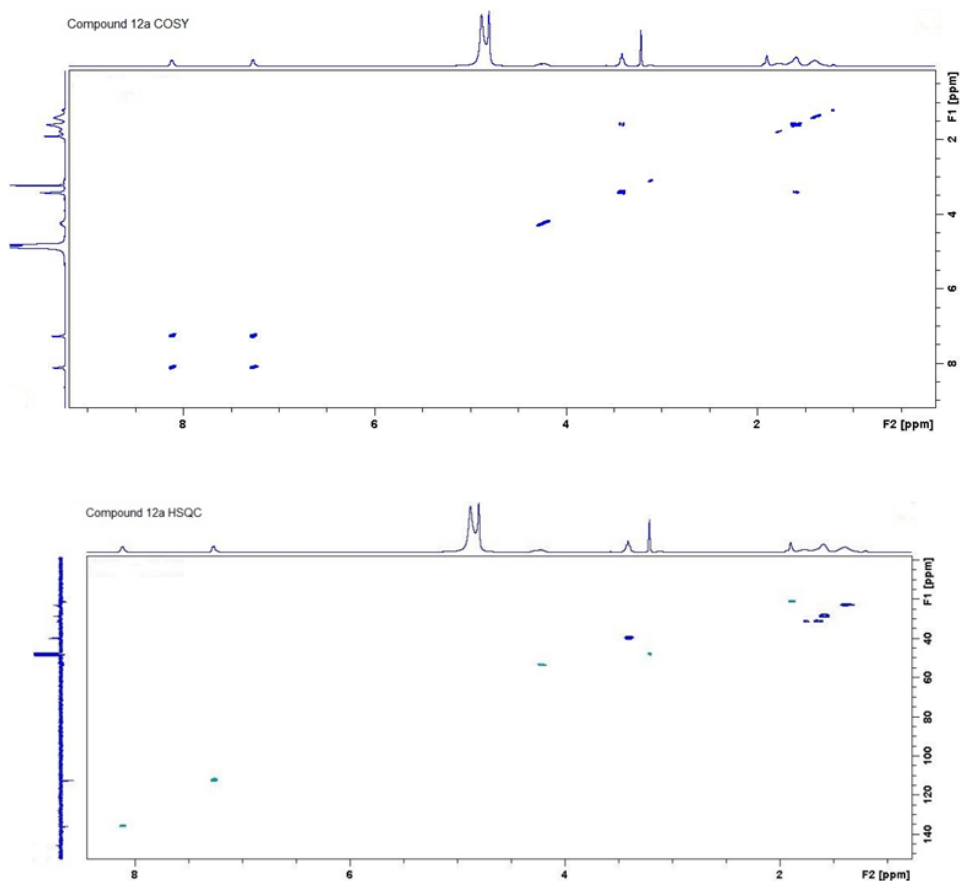
Compound 12b

Yield: 22%; <u>^{1}H-NMR</u> (MeOH-d$_4$) δ 1.07-1.22 (m, 10H, 5 x CH$_2$, side chain), 1.46-1.55 (m, 8H, 4 x CH$_2$, side chain), 1.89 (s, 3H, NHCO*CH$_3$*), 2.33 (s, 9H, 3 x *CH$_3$*-C), 2.57-2.63 (m, 6H, 3 x NCH$_2$*CH$_2$*CO), 2.85-3.04 (m, 6H, 3 x NH*CH$_2$*), 3.99-4.07 (m, 1H, NH*CH*CH$_2$), 4.08-4.13 (m, 2H, 2 x NH*CH*CH$_2$), 4.26-4.35 (m, 6H, 3 x N*CH$_2$*CH$_2$CO), 6.46-6.51 (m, 3H, Ar), 7.48-7.54 (m, 3H, Ar). <u>^{13}C-NMR</u> (MeOH-d$_4$) δ 11.40 (CH$_3$), 21.19 (CH$_3$), 22.25 (CH$_2$), 27.83 (CH$_2$), 30.69 (CH$_2$), 36.27 (CH$_2$), 38.99 (CH$_2$), 50.77 (CH$_2$), 50.96 (CH$_2$), 53.14 (CH), 53.38 (CH), 53.80 (CH), 112.15 (CH), 138.82 (CH), 144.39 (C), 167.48 (C), 172.04 (C), 174.13 (C). The HPLC-DAD analysis (t_R = 7.49 min) showed a purity of 91%. (LC-MS): calcd. For C$_{47}$H$_{68}$N$_{10}$O$_{13}$, 980.5 Found: *m/z* 981.5 [M+H]$^+$, 491.4 [M+2H]$^{2+}$, 328.1 [M+3H]$^{3+}$.

Compound 12b COSY

Compound 12b HSQC

Compound 20a

Yield: 10%; <u>1H-NMR</u> (MeOH-d$_4$) δ 1.35-1.52 (m, 8H, 4 x CH$_2$, side chain), 1.64-1.78 (m, 10H, 5 x CH$_2$, side chain), 1.84-1.97 (m, 6H, 3 x CH$_2$, side chain), 2.02 (s, 3H, NHCO*CH$_3$*), 3.45-3.56 (m, 8H, 4 x NH*CH$_2$*), 4.28-4.39 (m, 4H, 4 x NH*CH*CH$_2$), 7.34-7.42 (m, 4H, Ar), 8.19-8.28 (m, 4H, Ar). <u>13C-NMR</u> (MeOH-d$_4$) δ 21.07 (CH$_3$), 22.70 (CH$_2$), 28.36 (CH$_2$), 30.98 (CH$_2$), 39.64 (CH$_2$), 49.96 (CH), 112.39 (CH), 135.58 (CH), 142.22 (C), 158.55 (C), 162.80 (C). The HPLC-DAD analysis (t_R = 8.26 min) showed a purity of 91%. MS (LC-MS): calcd. For C$_{50}$H$_{65}$N$_{13}$O$_{17}$, 1119.5 Found: *m/z* 1120.4 [M+H]$^+$, 560.9 [M+2H]$^{2+}$.

Compound 20a COSY

Compound 20a HSQC
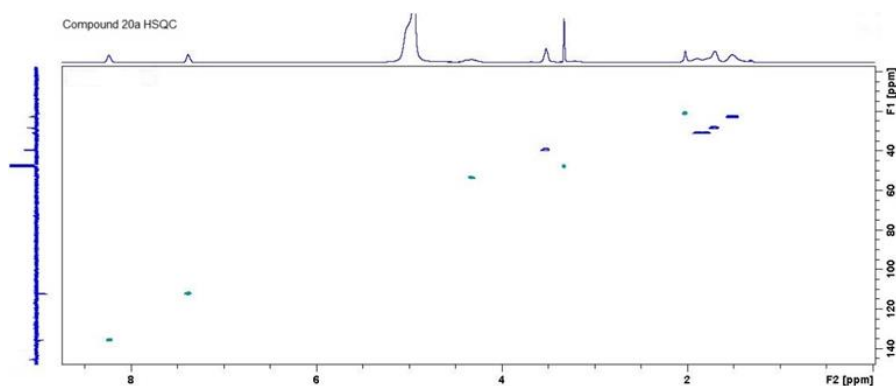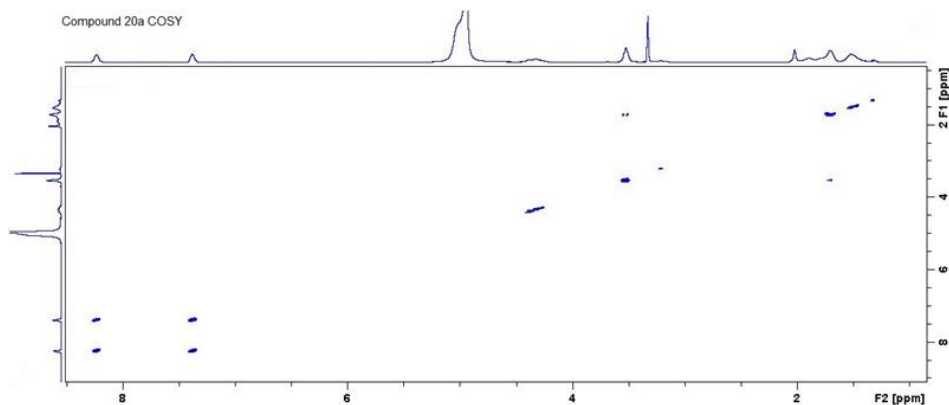
Compound 20b

Yield: 21%; ^{1}H-NMR (MeOH-d$_4$) δ 1.08-1.47 (m, 16H, 8 X CH$_2$, side chain), 1.59-1.82 (m, 8H, 4 X CH$_2$, side chain), 1.98 (s, 3H, NHCO*CH$_3$*), 2.46 (s, 12H, 4 X *CH$_3$*-C), 2.93-3.26 (m, 8H, 4 X NCH$_2$*CH$_2$*CO), 3.28-3.37 (m, 8H, 4 X NH*CH$_2$*), 4.21-4.44 (m, 12H, 4 X NH*CH*CH$_2$, 4 X N*CH$_2$*CH$_2$CO), 6.37-6.45 (m, 4H, Ar), 7.53-7.60 (m, 4H, Ar). ^{13}C-NMR (MeOH-d$_4$) δ 10.43 (CH$_3$), 20.37 (CH$_3$), 22.88 (CH$_2$), 22.99 (CH$_2$), 23.11 (CH$_2$), 28.36 (CH$_2$), 28.68 (CH$_2$), 31.46 (CH$_2$), 31.63 (CH$_2$), 49.66 (CH$_2$), 50.06 (CH$_2$), 52.92 (CH), 58.33 (CH), 53.62 (CH), 111.57 (CH), 131.70 (C), 137.72 (CH), 145.81 (C), 169.06 (C), 170.20 (C), 171.91 (C), 172.82 (C), 173.00 (C), 173.18 (C), 175.40 (C). The HPLC-DAD analysis (t_R = 8.07 min) showed a purity of 90%. (LC-MS): calcd. For C$_{62}$H$_{89}$N$_{13}$O$_{17}$, 1287.6 Found: *m/z* 1288.6 [M+H]$^+$, 645.1 [M+2H]$^{2+}$, 430.6 [M+3H]$^{3+}$.

Compound 20b COSY

Compound 20b HSQC
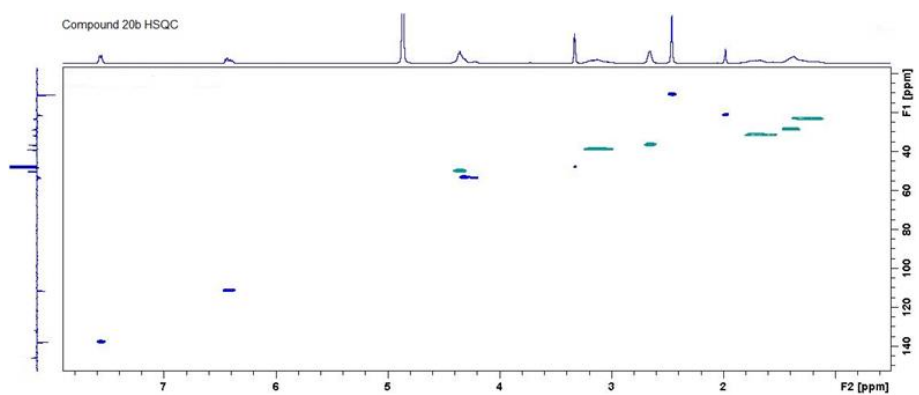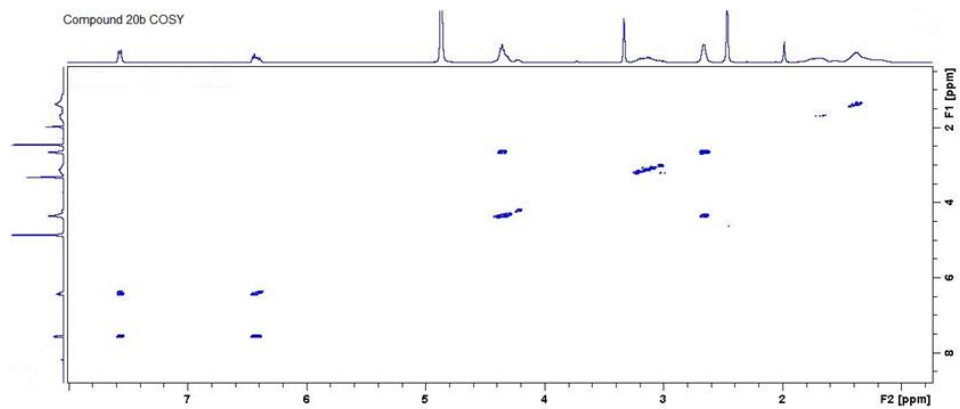
4. REFERENCES

- Afshar-Oromieh, A.; Malcher, A.; Eder, M.; Eisenhut, M.; Linhart, H. G.; Hadaschik, B. A.; Holland-Letz, T.; Giesel, F. L.; Kratochwil, C.; Haufe, S.; Haberkorn, U.; Zechmann, C. M. PET imaging with a (68Ga) gallium-labelled PSMA ligand for the diagnosis of prostate cancer: bio distribution in humans and first evaluation of tumor lesions. *Eur. J. Nucl. Med. Mol. Imaging* **2013**, *40*, 486-495.

- American Cancer Society Web site. Cancer facts and figures. http://www.cancer.org/Research/CancerFactsFigures/index, **2012**.

- Borgna-Pignatti, C.; Cappellini, M. D.; De Stefano, P.; Del Vecchio, G. C.; Forni, G. L.; Gamberini, M. R.; Ghilardi, R.; Piga, A.; Romeo, M. A.; Zhao, H. Cardiac morbidity and mortality in deferoxamine- or deferiprone treat patients with thalassemia major. *Blood* **2006**, *107*, 3733-3737.

- Brittenham, G. M. Disorders of iron metabolism: deficiency and overload. In: Hoffman R et al, ed. *Hematology: Basic Principles and Practice*. NewYork: Churchill Livingstone, **1991** 327-349.

- Cancer Research UK. Cancer risk. July 27, 2011.

- Cayot, P.; Tainturier, G. The quantification of protein amino groups by the trinitro benzene sulfonic acid method: a re-examination. *Anal. Biochem.* **1997**, *249(2)*, 184-200.

- Ceci, A.; Baiardi, P.; Felisi, M.; Cappellini, M. D.; Carnelli, V.; De Sanctis, V.; Galanello, R.; Maggio, A.; Mosera, G.; Piga, A.; Schettini, F.; Stefano, I.; Tricta, F. The Safety and Effectiveness of Deferiprone in a Large-scale 3-year Study in Italian Patients. *Br. J. Haematol.* **2002**, *118*, 330-336.

- Chappell, B.; Mc Loughlin J. Technical considerations when obtaining and interpreting prostatic biopsies from men with suspicion of early prostate cancer: *Part I. BJU Int.* **2005**, *95*, 1135-40.

References

- Crichton R. R. Inorganic Biochemistry of Iron Metabolism. *New York; London: Ellis Harwood*, **1991**.

- Cusnir, R.; Imberti, C.; Hider, R. C.; Blower, P. J.; Ma, M. T. Hydroxypyridinone chelators: from iron scavenging to radiopharmaceuticals for PET imaging with Gallium-68. *Int. J. Mol. Sci.* **2017**, *18*, 116.

- Dobbin, P. S.; Hider, R. C.; Hall, A. D.; Taylor, P. D.; Sarpong, P.; Porter, J. B.; Xiao, G.; Van der Helm, D. Synthesis, physical-chemical properties and biological evaluation of N-substituted 2-alkyl-3-hydroxy-4(1H)-pyridinones: orally active iron chelators with clinical potential. *J. Med. Chem.* **1993**, *36(17)*, 244-258.

- Eder, M.; Schäfer, M.; Bauder-Wüst, U.; Hull, W. E.; Wangler, C.; Mier, W. (68)Ga-complex lipophilicity and the targeting property of a urea-based PSMA inhibitor for PET imaging. *Bioconjug. Chem.* **2012**, *23*, 688-97.

- Gaeta, A.; Holgado-Molina, F.; Kong, X. L.; Salvage, S.; Francis, P. T.; Williams, R. J.; Hider, R. C. Synthesis, physical-chemical characterization and biological evaluation of novel 2-amido-3-hydroxypyridin-4(1H)-ones: iron chelators with the potential for the treating Alzheimer's disease. *Bioorg. Med. Chem.* **2011**, *19(3)*, 1285-1297.

- Galanello, R. Deferiprone in the treatment of transfusion-dependent thalassemia: a review and prospective. *Ther. Clin. Risk Menag.* **2007**, *3(5)*, 795-805.

- Garcia-Martin, F.; Quintanar-Audelo, M.; Garcia-Ramos, Y.; Cruz, L. J.; Gravel, C.; Furic, R.; Côté, S.; Tulla-Puche, J.; Albericio, F. ChemMatrix, a Poly(ethylene glycol)-based support for the solid-phase synthesis of complex peptides. *J. Comb. Chem.* **2006**, *8(2)*, 213-220.

- Ghosh, A.; Heston, W. D. Tumor target prostate specific membrane antigen (PSMA) and its regulation in prostate cancer. *J. Cell. Biochem.* **2004**, *91*, 528-39.

- Glickstein, H.; Ben El, R.; Link, G.; Breuer, W.; Konijn, A. M.; Hershko, C.; Nick, H.; Cabantchik, Z. I. Action of chelators in iron-loaded cardiac cells: accessibility to intracellular labile iron and functional consequences. *Blood* **2006**, *108*, 3195-3203.

- Goldgar, D. E.; Easton, D. F.; Cannon-Albright L. A.; Skolnick, M. H. Systematic population-based assessment of cancer risk in first-degree relatives of cancer probands. *J. Natl. Cancer Inst.* **1994**, *86*, 1600-1608.

- Halliwell, B.; Gutteridge, J. M. C. *Free Radicals in Biology and Medicine, third ed.*, Oxford University press, Oxford, **1998**.

- Hershko, C.; Cappellini, M. D.; Galanello, R.; Piga, A.; Tognoni, G.; Masera, G. Purging iron from heart. *Br. J. Haematol.* **2004**, *125*, 545-551.

- Hershko, C.; Grady, R. W. Mechanism of iron chelation in the hyper transfused rat: definition of two alternative pathways of iron mobilization. *J. Lab. Clin. Med.* **1978**, *92*, 144-151.

- Hider R. C.; Zhou T. The design of orally active iron chelators. *Ann. N. Y. Acad. Sci.* **2005**, *1054*, 141-154.

- Hillier, S. M.; Maresca, K. P.; Femia, F. J.; Marquis, J. C.; Foss, C. A.; Nguyen, N. Preclinical evaluation of novel glutamate-urea-lysine analogues that target prostate-specific membrane antigen as molecular imaging pharmaceuticals for prostate cancer. *Cancer. Res.* **2009**, *69(17)*, 6932-40.

- Johns, L. E.; Houlston, R. S. A systematic review and meta-analysis of familial prostate cancer risk. *BJU Int.* **2003**, *91*, 789-94.

- Kallur, K. G.; Ramachandra, P. G.; Rajkumar, K.; Swamy, S. S.; Desai, I.; Rao, R. M.; Patil, S. G.; Sridhar, P. S.; Madhusudhan, N.;

References

Krishnappa, R. S.; Bhadrasetty, V.; Kumara, H. M.; Santosh, S. D.; Ajaikumar, B. Clinical utility of Gallium-68 PSMA PET/CT Scan for prostate cancer. *Indian. J. Nucl. Med.* **2017**, *32(2)*, 110-117.

- Kato, T.; Tsukamoto, E.; Kuge, Y.; Takei, T.; Shiga, T.; Shinohara, N. Accumulation of [^{11}C] acetate in normal prostate and benign prostatic hyperplasia: comparison with prostate cancer. *Eur. J. Nucl. Med. Mol. Imag.* **2002**, *29*, 1492-5.

- Ma, Y.; Zhou, T.; Kong, X.; Hider, R. C. Chelating agents for the treatment of systemic iron overload. *Curr. Med. Chem.* **2012**, *19*, 2816-2827.

- Mannweiler, S.; Amersdorfer, P.; Trajanoski, S.; Terrett, J. A.; King, D.; Mehes, G. Heterogeneity of prostate-specific membrane antigen (PSMA) expression in prostate carcinoma with distant metastasis. *Pathol. Oncol. Res.* **2009**, *15 (2)*, 167-72.

- Olivieri, N. F.; Buncic, J. R.; Chew, E.; Gallant, T.; Harrison, R. V.; Keenan, N.; Logan, W.; Mitchell, D.; Ricci, G.; Skarf, B. Visual and Auditory Neurotoxicity in Patients Receiving Subcutaneous Deferoxamine Infusions. *New Engl. J. Med.* **1986**, *314*, 869-873.

- Palomo, J. M. Solid-phase peptide synthesis: an overview focused on the preparation of biologically relevant peptides. *RSC Adv.* **2014**, *4*, 32658-32672.

- Pennell, D. J.; Berdoukas, V.; Karagiorga, M.; Ladis, V.; Piga, A.; Aessopos, A.; Gotsis, E. D.; Tanner, M. A.; Smith, G. C.; Westwood, M. A.; Wonke B.; Galanello, R. Randomized controlled trial of deferiprone or deferoxamine in beta-thalassemia major patients with asymptomatic myocardial siderosis. *Blood* **2006**, *107*, 3738-3744.

- Pepe, A.; Meloni, A.; Capra, M.; Cianciulli, P.; Prossomariti, L.; Deferasirox, deferiprone and desferrioxamine treatment in thalassemia major patients: cardiac iron and function comparison

determined by quantitative magnetic resonance imaging. *Haematol.* **2011**, *96*, 41-47.

- Pippard, M. J.; Callender, S. T.; Weatherall, D. J. Intensive iron-chelation therapy with desferrioxamine in iron-loading anaemias. *Clin. Sci. Mol. Med.* **1978**, *54*, 99-106.

- Porter, J. B.; Jawson, M. C.; Huehns, E. R.; East, C. A.; Hazell, J. W. P. Desferrioxamine toxicity: evaluation of risk factors in thalassaemic patients and guidelines for safe dosage. *Br. J. Haematol.* **1989**, *73*, 403-409.

- Schaid, D. J. The complex genetic epidemiology of prostate cancer. *Hum. Mol. Genet.* **2004**, *13 (suppl 1)*, R103-121.

- Schuhmacher, J.; Maier-Borst, W. A new 68Ge/68Ga radioisotope generator system for production of 68Ga in dilute HCl. *Int. J. Appl. Radiat. Isot.* **1981**, *32*, 31–6.

- Subiròs-Funosas, R.; El-Faham, A.; Albericio, F. PyOxP and PyOxB: the oxyma-based novel family of phosphonium salts. *Org. Biomol. Chem.* **2010**, *8*, 3655-3673.

- Summers, M. R.; Jacobs, A.; Tudway, D.; Perera, P.; Ricketts, C. Studies in desferrioxamine and ferrioxamine metabolism in normal and iron-loaded subjects. *Br. J. Haematol.* **1979**, *42*, 547-555.

- Sweat, S. D.; Pacelli, A.; Murphy, G. P.; Bostwick, D. G. Prostate-specific membrane antigen expression is greatest in prostate adenocarcinoma and lymph node metastases. *Urology* **1998**, *52(4)*, 637-640.

- Zhou, T.; Winkelmann, G.; Dai, Z. Y.; Hider, R. C. Design of clinically useful macromolecular iron chelators. *J. Pharm. Pharmacol.* **2011**, *63*, 893-903.